The chemotherapeutic potential of *Boswellia carterii* oleoresins

Matthew Allan Jones

School of Science, Engineering and Environment

University of Salford

Supervisor: Dr David Greensmith

Submitted in partial fulfilment of the requirements of the Degree of Doctor of Philosophy

2021

List of contents

List of figures

List of tables

List of equations

Acknowledgements

I am grateful for all of the support and guidance provided by my supervisor, Dr David Greensmith.

I would further like to thank Steven Holmes and Peter Cobain for providing the *Boswellia carterii* oleoresins used for this study and supporting my PhD studentship.

I would like to thank my brother Andrew Worthington, and my grandparents, Allan and Barbara Jones for their constant love and support.

Lastly, I would like to thank my mum, Caroline Hayton-Jones, for always being there for me, through the good and the bad, and for always being supportive and caring throughout my whole academic journey so far.

Confirmation of Ethical approval

University of Salford MANCHESTER

Research, Innovation and Academic Engagement Ethical Approval Panel

Research Centres Support Team
G0.3 Joule House
University of Salford
M5 4WT

T +44(0)161 295 5278

www.salford.ac.uk/

26 March 2018

Matthew Jones

Dear Matthew,

RE: ETHICS APPLICATION STR1718-35: The pharmacological potential of frankincense distillation by-products; identification of active compounds and characterisation of their biological effects in cancer and cardiac cell lines

Based on the information you provided, I am pleased to inform you that your application STR1718-35 has been approved.

If there are any changes to the project and/ or its methodology, please inform the Panel as soon as possible by contacting S&T-ResearchEthics@salford.ac.uk

Yours sincerely,

APHigham.

Dr Anthony Higham
Chair of the Science & Technology Research Ethics Panel

List of abbreviations

5-HPETE - Arachidonic acid 5-hydroperoxide

5-LO - Arachidonate 5-lipoxygenase

AJS - Agilent Jet Stream

AKBA - Acetyl-11-keto-β-boswellic acid

AKT - protein kinase B

ALL - Acute lymphoblastic leukaemia

ANOVA - Analysis of variance

Apaf-1 - Apoptotic protease activating factor 1

ATM - Ataxia-telangiectasia mutated protein kinase

ATR - Ataxia telangiectasia and Rad3 related protein

AV - Annexin V

BAD – BCL-2 associated agonist of cell death protein

BAK - BCL-2 homologous antagonist killer protein

BAX - BCL-2-associated X protein

BCL-xL - B-cell lymphoma-extra-large protein

BD - Becton Dickinson

BID - BH3 interacting-domain death agonist

BIM - BCL-2-like protein 11

BSA - Bovine serum albumin

CA 125 - Cancer antigen 125

Cdc25c - M-phase inducer phosphatase 3

CDK - Cyclin dependent kinase

CML - Chronic myeloid leukaemia

CNS - Central nervous system

CO_2 - Carbon dioxide

CSC's - Cancer stem cells

CT - Computed tomography

DAMP - Damage associated molecular patterns

dH_2O - Distilled water

DIABLO - Direct IAP-binding protein with low pI.

DISC - death-inducing signalling complex

DMEM - Dulbecco modified Eagles media

DMSO - Dimethyl Sulphoxide

DNA - Deoxyribonucleic acid

DR4 - Death receptor 4

DR5 - Death receptor 5

DTT - Dithiothreitol

E2F - E2 Transcription Factor

ECM - Extracellular matrix

ER - Endoplasmic reticulum

ERK - Extracellular signal-regulated kinase

ESI - Electrospray ionisation

FADD - Fas Associated Via Death Domain protein

Fas - Fas Cell Surface

FasR - Fas Cell Surface Death Receptor

FBS - Foetal Bovine serum

FTIR - Fourier-transform infrared spectroscopy

G_0 - Gap 0

G_1 - Gap 1

G_2 - Gap 2

GAPDH - Glyceraldehyde 3-phosphate dehydrogenase

GC - Gas chromatography

hCG - Human chorionic gonadotropin

hERG - Human Ether-à-go-go-Related Gene

HPLC - High-performance liquid chromatography

HRMS - High resolution mass spectrometry

HRP - Horseradish peroxidase

IFN-γ - Interferon-gamma

IKK - Inhibitor of nuclear factor-κB (IκB) kinase

IL-1 - Interleukin-1

IL-10 - Interleukin-10

IL-6 - Interleukin-6

IR - Infrared

JNK - c-Jun N-terminal kinases

KBA - 11-keto-β-Boswellic acid

LC - Liquid chromatography

LDS - Lithium dodecyl sulphate

M - Mitosis

m/z - Mass to charge ratio

mAb - Monoclonal antibody

MAPK - Mitogen-activated protein kinase

mAU - Mean arbitrary units

MCM - Minichromosome maintenance complex

MIC - Minimum inhibitory concentration

MPF - Maturation-promoting factor

MRI - Magnetic resonance imaging

MS - Mass spectrometry

mTOR - Mechanistic target of rapamycin

MTT - 3-(4,5-Dimethylthiazol-2-yl)-2,5-Diphenyltetrazolium Bromide

NEMO - NF-kappa-B essential modulator

NF-κB - Nuclear factor-κB

NMR - Nuclear magnetic resonance

Numa - Nuclear mitotic apparatus protein 1

PARP - Poly-ADP ribose polymerase

PBMC - Peripheral blood mononuclear cells

PBS - Phosphate buffered saline

PCNA - Proliferating cell nuclear antigen

PES - Polyethersulfone

PET - Positron emission tomography

PI - Propidium Iodide

PIK1 - 1-phosphatidylinositol 4-kinase

Plk1 - Polo-like kinase 1

ppm - Parts per million

pRB - Retinoblastoma protein

PRR - Pattern recognition receptors

PSA - Prostate specific antigen

PUMA - p53 upregulated modulator of apoptosis

PVDF - Polyvinylidene difluoride

RIPA - Radioimmunoprecipitation

RNA - Ribonucleic acid

ROS - Reactive oxygen species

RPMI - Roswell Park Memorial Institute

SDS - Sodium dodecyl sulphate

SDS-PAGE - Sodium dodecyl-sulphate polyacrylamide gel electrophoresis

SFE - Super fluid extraction

SMAC - Second mitochondria-derived activator of caspase

T_{25} - 25cm^2 cell culture flask

T_{75} - 75cm^2 cell culture flask

TBST - Tris buffered saline with 0.1 % Tween 20

TEA - Triethanolamine

TNFR1 - Tumour necrosis factor receptor 1

TNFα - Tumour necrosis factor alpha

TOF - Time of flight

TRADD - Tumour necrosis factor receptor type 1-associated DEATH domain protein

TRAILR - TNF-related apoptosis-inducing ligand receptor

UAE - Ultrasound assisted extraction

UHD - Ultra high definition

USFDA - United States Food and Drug Administration

UV - Ultraviolet

VEGF - Vascular endothelial growth factor

WHO - World Health Organisation

XIAP - X-linked inhibitor of apoptosis protein

Abstract

Cancer is a leading cause of death worldwide. Though effective treatments are available and reduce mortality, issues such as debilitating side-effects and drug resistance necessitate a need to develop alternatives. Natural products are a key and diverse source of novel drugs, though many plants remain therapeutically unexplored. Oleoresins from certain species of plants within the genus *Boswellia* are known to exhibit anti-microbial and anti-inflammatory activity; attributed to a group of compounds known as boswellic acids. Previous studies suggest certain species of *Boswellia* also exhibit anti-cancer activity and may be a potential chemotherapeutic source. However, research on one species; *Boswellia carterii* is comparatively limited. Given the chemical profile of *Boswellia* varies considerably across species, *B. carterii* may be an underexploited therapeutic source. Therefore, this study aimed to evaluate the anti-cancer potential and chemical profile of *B. carterii* oleoresin.

A methanolic extraction method was optimised to solubilise compounds from *B. carterii* oleoresin. Subsequently, MTT assay was used to evaluate cytotoxicity, against several cancer cell lines. Equivalent normal cell lines were used to ascertain specificity of action. Flow cytometry was used to measure relative levels of apoptosis and necrosis and for cell cycle analysis. Western blotting was then used to elucidate detailed molecular mechanisms. The chemical composition of the *B. carterii* oleoresin was analysed using high-performance liquid-chromatography mass spectrometry (HPLC-MS).

Methanolic extracts of the *B. carterii* oleoresin were cytotoxic to all cancer cell types used in the study. This cytotoxicity was time and concentration dependent with IC_{50} values between 33.34 and 106.34 µg/ml. IC_{50} values were higher in equivalent normal cell lines, with selectivity indices ranging between 1.75 and 2.68. Propidium iodide and annexin V fluorescence was significantly increased in cancer cells exposed to *B. carterii* extracts while western blotting revealed significant cleavage of caspases -3, -7, -9, and PARP. Flow-cytometric analysis of cell cycle showed the proportion of cells in sub G_1 and G_1 phases were significantly increased in all cancer cell types examined. This was associated with downregulation of cyclin D3 and CDK's 2, 4 and 6. p27 was upregulated. Chemical analysis confirmed the presence

of 3-acetyl-11-keto-β-boswellic acid, 3-*O*-acetyl-α-boswellic acid, 11-keto-β-boswellic acid and α or β-boswellic acid. 82 uncharacterised compounds were also revealed.

These data show methanolic extracts of *B. carterii* oleoresin are specifically cytotoxic to a diverse range of cancer cell types. Cytotoxicity is produced by activation of the intrinsic pathway of apoptosis. Furthermore, altered expression of cell cycle regulatory proteins leads to a G_1 cell cycle arrest and cessation of cancer cell division. Boswellic acids likely produce this biological activity, though other, previously unprofiled compounds may contribute.

These findings suggest that *B. carterii* oleoresin is a potential source of novel chemotherapeutics. Furthermore, given the chemical complexity of *B. carterii* it is likely the entire genus is therapeutically underexploited. Combined, further investigation towards potential novel drug development is justified.

Chapter 1

General Introduction

1.1 Relevant fundamental cell biology

To understand cancer pathogenesis and to elucidate the mechanism of action of the compounds tested in this thesis, we must first consider some fundamental cell biology.

1.1.1 The cell cycle

Within the human body, most cells reach a state of terminal differentiation at which point active cell division ceases. In the majority of tissues this cessation is permanent. In others such as stem cells and white blood cells where cell population renewal is essential, controlled division may recommence in response to external stimuli (Williams & Stoeber, 2012).

For any cell to undergo the process of cell division they must pass through the cell cycle. This cycle is a series of four key and tightly regulated steps, summarised in figure 1-1. Crucially, it is the cell cycle that allows cells to divide in a regulated way, ensuring that cells are checked for dysfunction or DNA damage, and ensuring that any damage is repaired before they are allowed to complete the process of cell division (Sherr & Bartek, 2017; Wenzel & Singh, 2018).

The four stages are; Gap 1 (G_1), S phase, Gap 2 (G_2) and mitosis (Bertoli, Skotheim, & De Bruin, 2013; Eymin & Gazzeri, 2010; Morgan, 2007; Salazar-Roa & Malumbres, 2017). The most important of these stages is the S phase, in which cells actively replicate DNA, and in mitosis, where the cell actively splits into two daughter cells (Williams & Stoeber, 2012). However, the two gap stages also play crucial roles in the cell cycle. The G_1 phase acts as a preparatory stage, where the cell begins to synthesise the machinery and proteins required for the process of cell division (Eymin & Gazzeri, 2010). Whilst in G_2, the replicated DNA is separated and organised through the mitotic spindle (Salazar-Roa & Malumbres, 2017).

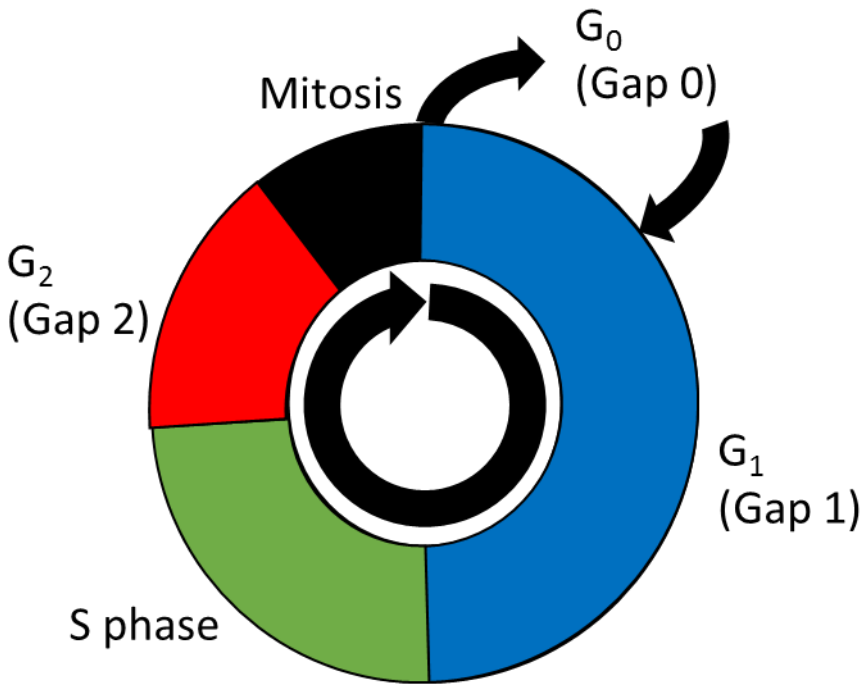

Figure 1-1. A summary of the key steps involved in progressing through the cell cycle.

Cells enter the cell cycle at the G_1 stage and progress either reversibly into quiescence (G_0) or advance to DNA replication in S phase. Once DNA is replicated, the cell enters the G_2 stage before undergoing mitosis. This cycle then repeats if more cells are required or is inhibited via physiological signalling mechanisms and cells enter quiescence (G_0) until required to renter the cell cycle.

Under certain circumstances, cells may remove themselves from the cell division cycle through the process of quiescence, also termed entering the gap 0 (G_0) phase (Hustedt & Durocher, 2017). While cells in G_0 phase are no longer actively dividing, they maintain their potential to proliferate (Bai, Li, & Zhang, 2017). This reversible state of dormancy allows cells to return to the cell cycle if given specific mitogenic stimuli such as growth factors (Bai *et al.*, 2017; Hustedt & Durocher, 2017; Williams & Stoeber, 2012). As such, the majority of stable non-dividing cells exist within the G_0 phase of the cell cycle (Bai *et al.*, 2017).

To ensure that cells entering and progressing through the cell cycle do not contain genetic defects or abnormalities, the process is highly regulated by checkpoints at each stage (Bai *et al.*, 2017; Foster, 2008). These checkpoints are present to ensure that a faithful copy of the cell is maintained and to repair any cellular damage arising

through the cell cycle (Bai *et al.*, 2017; Foster, 2008; Sherr & Bartek, 2017; Thu, Soria-Bretones, Mak, & Cescon, 2018).

The checkpoints between the G_1 and S phases are most critical and are therefore the most tightly regulated (Bendris, Lemmers, & Blanchard, 2015; Wiman & Zhivotovsky, 2017). This G_1/S checkpoint is significant as once cells have entered the S phase they are committed to the remainder of the cell cycle (Bendris *et al.*, 2015; Sherr & Bartek, 2017; Wiman & Zhivotovsky, 2017).

1.1.2 Molecular control of the cell cycle

The progression through the cell cycle is controlled by cyclin dependent serine/threonine kinases (CDK's) through regulatory processes including their phosphorylation, their interaction with cyclin proteins and their subsequent dephosphorylation and degradation (Bai *et al.*, 2017). Other key molecules involved in the progression through the cell cycle are p53, retinoblastoma protein (pRb) and E2F *(*García-Reyes *et al.*, 2018; Lopez-Mejia & Fajas, 2015).

Progression through the cell cycle is driven by the formation of cyclin/CDK complexes, via upstream signalling pathways, enabling the control of cell cycle regulation and the phosphorylation of downstream protein targets (Thu *et al.*, 2018). The key cyclins involved in cell cycle progression within humans are cyclins A, B, D and E, which generate complexes with multiple CDK's including CDK1, CDK2, CDK4 and CDK6 (Malumbres & Barbacid, 2006; Wiman & Zhivotovsky, 2017).

In addition to driving progression through the cell cycle, the formation of cyclin/CDK complexes have been shown to further regulate movement through the cell cycle through their ability to induce extracellular changes including the upregulation of growth factor signalling and increasing the presence of nutrients to the cell (Lapenna & Giordano, 2009). The activity of CDK's are tightly regulated to ensure that aberrant progression through the cell cycle is mitigated (Lopez-Mejia & Fajas, 2015; Wiman & Zhivotovsky, 2017). This regulation occurs via cyclical expression of the complexing cyclins, with cyclins only being expressed when required, or by their interaction with CDK inhibitory proteins (CKI's) (Lopez-Mejia & Fajas, 2015).

The transition between each stage of the cell cycle is regulated by the formation specific cyclin-CDK complexes. These complexes, summarised in figure 1-2, induce

downstream effects allowing cells to advance to the next stage of the cell cycle, before being inactivated (Williams & Stoeber, 2012).

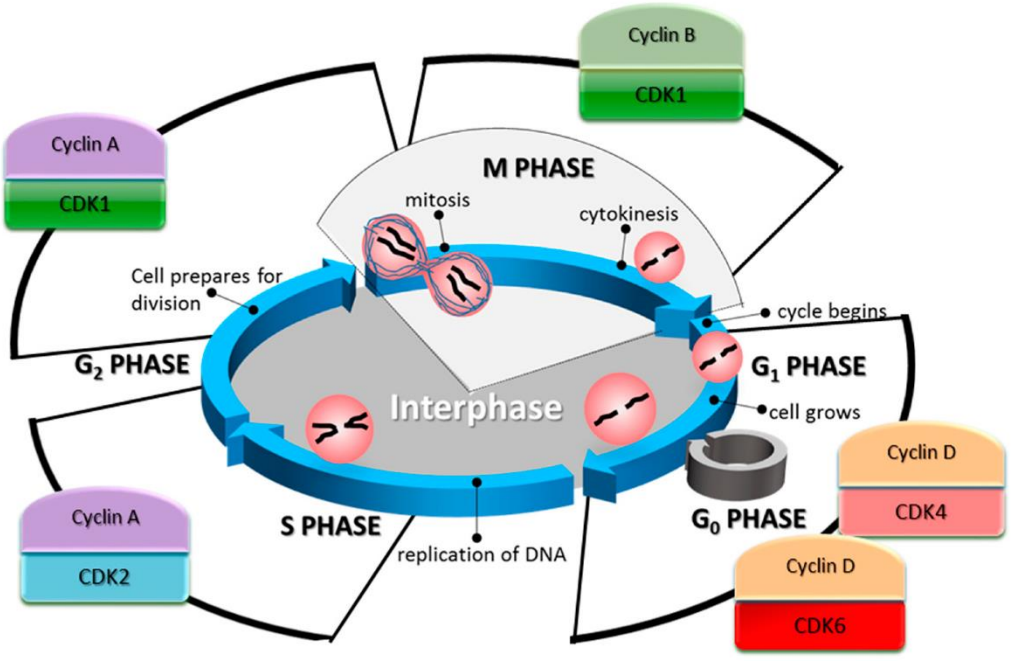

Figure 1-2. Cyclin and CDK regulation of cell cycle control at each stage of the cell cycle.

Many cyclin/CDK complexes are involved in the transition of cells through the cell cycle. Cyclin/CDK complexes have been shown to be involved at the transition between each stage of the cell cycle. These include cyclin D/CDK4 and cyclin D/CDK6 formed during the G_1 transition to S phase, cyclin A/CDK2 complexes formed in the transition between S phase and G_2, along with the formation of cyclin A/CDK1 complexes formed in the G_2 to mitosis transition. The formation of these complexes initiates downstream effects which trigger cells to progress to the next stage of the cell cycle. Figure adapted from Garcia-Reyes *et al.*, 2018.

Specifically, the formation of cyclin D/CDK4, cyclin D/CDK6 and cyclin E/CDK2 complexes direct G_1 progression through the G_1/S restriction checkpoint. S phase progression is initiated by the formation of cyclin A/CDK2, whist the development of cyclin A/CDK1 and cyclin B/CDK1 complexes regulate the progression through G_2 and the cells entry into mitosis (Malumbres & Barbacid, 2006; Nigg, 2001; Planas-Silva & Weinberg, 1997; Williams & Stoeber, 2012).

In response to the detection of DNA damage, extracellular factors and abnormal cell size, progression through the cell cycle can be halted via the activation of cell cycle checkpoints. This can happen during G_1 phase, S phase and at the G_2/M transition. These checkpoints prevent progression through the cell cycle until the abnormalities

have been resolved or cell death has been induced (Wiman & Zhivotovsky, 2017). The specific molecular mechanisms associated with each of these checkpoints are described in sections 1.1.2.1 - 1.1.2.3.

1.1.2.1 Molecular control of the G_1/S checkpoint

The G_1 to S phase transition is the first point of defence and protects cells from progressing through the cell cycle if they contain cellular defects such as DNA damage (Wenzel & Singh, 2018). Mitogenic signalling pathways such as Myc or the binding of extracellular growth factors activate cyclins and CDKs. This activation allows cells to begin the transition through the cell cycle, shown in figure 1-3 (Wiman & Zhivotovsky, 2017). These stimuli activate D cyclin expression, increasing their abundance within the cell, and allowing them to form complexes with CDK4 and CDK6 (Hustedt & Durocher, 2017; Wiman & Zhivotovsky, 2017). The formation of these cyclin D/CDK4 and cyclin D/CDK6 complexes catalyse the phosphorylation of pRb, resulting in the liberation of E2F from its complex with pRB. The liberation of E2F from this complex leads to its activation and allows E2F to bind to DNA and promote the expression of genes required for cell cycle progression and entry into the S phase of the cell cycle (Bendris *et al.*, 2015; Lopez-Mejia & Fajas, 2015).

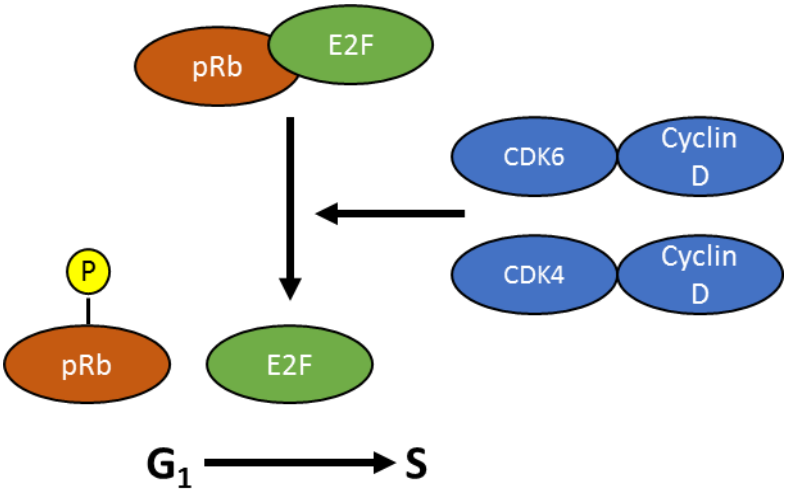

Figure 1-3. The cyclin/CDK regulation of G_1/S phase transition by cyclin D/CDK4 and cyclin D/CDK6.

The transition between the G_1 and s phases of the cell cycle is regulated by the formation and activity of cyclin D and CDK4/6 dimers. The formation of these dimers phosphorylates pRb on the inactive pRb/E2F complex. This phosphorylation liberates pRb from the complex, liberating E2F. E2F then acts downstream to increase the expression of genes required for further cell cycle progression and allow cells to enter the S phase of the cell cycle.

The initial activation of CDK's within the G_1 phase of the cell cycle can provide positive feedback for later stages of the cell cycle through the induction of genome wide changes to the cell. These changes result in further CDK expression as well as upregulating the expression of other proteins required later in the cell cycle (Bertoli *et al.*, 2013). This increased CDK expression also allows for further activation of downstream signalling pathways, in addition to diminishing the mechanisms impeding cell cycle progression (Hustedt & Durocher, 2017).

Regulation at this checkpoint ensures that abnormal cells do not progress through the cell cycle until any abnormalities have been resolved. A key mechanism involved in this regulation is p53. p53 is a transcription factor protein that acts as a tumour suppressor by regulating target genes involved in multiple processes including cell cycle arrest, apoptosis, autophagy and cellular senescence (T. Riley, Sontag, Chen, & Levine, 2008; Zilfou & Lowe, 2009). Under normal conditions p53 is expressed at low levels. However, once cells become stressed or damage is detected via ataxia telangiectasia mutated kinase (ATM), p53 expression becomes upregulated, and induces downstream tumour suppressive effects (Chen, 2016; Di Rora, Iacobucci, & Martinelli, 2017; Ozaki & Nakagawara, 2011; Wiman & Zhivotovsky, 2017). One of

these suppressive effects is the inducement of a G_1 cell cycle arrest and preventing dividing cells from progressing further.

Activation of p53, leads to activation the CDK inhibitor protein p21 (Chen, 2016). p21 binds to the cyclin D/CDK4 and cyclin D/CDK6 complexes, resulting in their inhibition (Abbas & Dutta, 2009; Chen, 2016). This blocks the phosphorylation of pRb, preventing the release of E2F and ultimately inhibiting progression through the G_1/S checkpoint (Wenzel & Singh, 2018).

1.1.2.2 Molecular control of S phase progression

Progression through S phase is the least tightly regulated of all stages in the cell cycle, as abnormal cells are typically identified at the G_1/S checkpoint and prevented from progressing into S phase (Grant & Cook, 2017). However, increased expression of CDK's following the G_1 phase regulates the replication processes during S phase, allowing the completion of bulk DNA synthesis (Ovejero, Bueno, & Sacristán, 2020).

Within S phase, the formation of complexes composed of cyclin E with CDK2, phosphorylate the DNA replication factors Sld2 and Sld3, allowing them to bind to Dpb11 and form the minichromosome maintenance (MCM) complex (Bertoli *et al.*, 2013; Grant & Cook, 2017; Muramatsu, Hirai, Tak, Kamimura, & Araki, 2010). This complex can then interact with the proteins associated with DNA replication, namely DNA polymerases (Muramatsu *et al.*, 2010). Additionally, the cyclin E/CDK2 complex can further liberate E2F, increasing the expression of the cyclins and CDK's required for further progression through the cell cycle, shown in figure 1-4 (Ding *et al.*, 2020). Following the replication of DNA, at the end of S phase the formation of cyclin A/CDK2 complexes allow cells to begin to transition out of S phase and in to the G_2 phase of the cell cycle (Bertoli *et al.*, 2013).

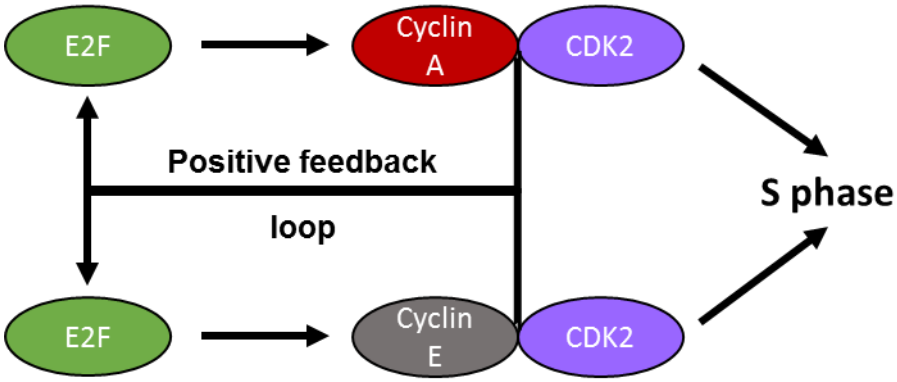

Figure 1-4. Molecular control of S phase progression via cyclin A/CDK2 and cyclin E/CDK2.

Liberated E2F (mechanism described in section 1.1.3.2.1) induces the expression of cyclins A and E in addition to CDK2. These cyclins and CDK's form complexes (cyclin A/CDK2 and cyclin E/CDK2) which promote DNA replication in S phase and allow cells to transition out of S phase into G_2 phase. The formation of these complexes also acts as a positive feedback loop, further stimulating the liberation of E2F, further increasing cyclin and CDK expression.

However, p53 via the expression of p21 has been described to inhibit DNA replication. In addition to preventing cell cycle progression at the G_1/S checkpoint, p21 can also interact with proliferating cell nuclear antigen (PCNA), inhibiting DNA replication, and resulting in the inhibition of cell cycle progression (Cazzalini *et al.*, 2008; Mansilla, De La Vega, Calzetta, Siri, & Gottifredi, 2020; Prives & Gottifredi, 2008).

1.1.2.3 Molecular control of G_2/M phase transition

The cell cycle checkpoint between the G_2 and M phases of the cell cycle is the most tightly regulated of all cell cycle checkpoints (Chao *et al.*, 2017). After the completion of DNA synthesis, CDK1, CDK2 and polo-like kinase 1 (Plk1) become activated at the S/G_2 transition, resulting in progression into G_2 and preparing the cell to undergo mitosis (Thu *et al.*, 2018).

When cells enter G_2, cyclin A expression is upregulated, allowing it to form complexes with CDK2 and activate E2F (Lee & Berger, 2019). This occurs by through phosphorylation of E2F, activating the DNA binding activity of E2F and inducing expression of proteins required for mitosis (Yang *et al.*, 1999; Zhu, Giangrande, & Nevins, 2004). Following the activation of E2F, cyclin A/CDK2 complexes become inactivated resulting in the phosphorylation of M-phase inducer phosphatase 3 (Cdc25C) (Lee *et al.*, 2019; Zhao *et al.*, 2008). The phosphorylation of Cdc25C induces

the formation and activation of cyclin B/CDK1 complexes, known as maturation promoting factor (MPF), which allow cells to progress out of G_2 and into mitosis (Shangguan, Li, & Zhang, 2014; Thu *et al.*, 2018).

The activity of MPF is pivotal in the regulation of the transition from G_2 to mitosis (Ovejero *et al.*, 2020). As the cell progresses towards mitosis, the concentration of MPF in the cells rises. Once this concentration reaches a specific threshold, cells enter mitosis (Shangguan *et al.*, 2014). Upon completion of mitosis, the mitotic cyclins are degraded, resulting in the inactivation of MPF. This inactivation causes cells to exit mitosis and re-enter the cell cycle at the G_1 phase (Ovejero *et al.*, 2020; Shangguan *et al.*, 2014).

In addition to cyclin/CDK regulation of cell cycle progression, regulatory enzymes play a significant role in the G_2/M transition (Thu *et al.*, 2018). A key enzyme involved in G_2/M progression is polo-like kinase 1 (Plk1). Plk1 mediates multiple mitotic processes such as the formation of bipolar spindles, the phosphorylation of Cdc25C, centrosome maturation and promotion of the anaphase promoting complex (Zhao *et al.*, 2008).

The G_2/M transition can be inhibited if errors in DNA replication, DNA damage or other cellular abnormalities are detected at the G_2 checkpoint (Bartek & Lukas, 2003; Moiseeva *et al.*, 2019). The detection of DNA damage activates ATM and Rad3-related kinase (ATR) with the aim of resolving any damage (Kastan & Lim, 2000; Yang *et al.*, 2004). Activated ATM and ATR interact with p53, inducing its activation, which causes a cell cycle arrest at the G_2/M checkpoint (Moiseeva *et al.*, 2019). Activated p53 mediates the inhibition to cyclin A/CDK2 complexes and preventing cells from progressing through the cell cycle (Foster, 2008). In addition, the presence of DNA damage in cells can activate the serine/threonine kinases Chk1 and Chk2 (Bartek & Lukas, 2003; Moiseeva *et al.*, 2019; Y. Zhang & Hunter, 2014). Activation of Chk1 and Chk2 inactivates Cdc25C, causing inhibition of MPF and arresting cell cycle progression at the G_2/M checkpoint (DiPaola, 2002; Moiseeva *et al.*, 2019; Niida, Katsuno, Banerjee, Hande, & Nakanishi, 2007; Y. Zhang & Hunter, 2014).

1.1.3 Necrosis

The ability to induce cell death is a vital process for normal human development, ageing and cell population homeostasis within organs (Elmore, 2007). The process of cell death can be classified as either controlled or uncontrolled. Controlled cell death,

known as apoptosis (see 1.1.4), is the tightly regulated mechanism of removing cells from the body that are no longer required, damaged or mutated without eliciting an adverse immune response (Rock, Lai, & Kono, 2011). However, certain conditions can induce an uncontrolled form of cell death, known as necrosis.

Necrosis is a form of cell death that is almost always associated with pathological processes. Unlike apoptosis, necrosis is an largely uncontrolled and passive process affecting large areas of cells (Tonnus *et al.*, 2019). However, recent studies have shown that there is an extent of regulation of the necrotic process including the regulation of mitochondrial dysfunction, enhanced reactive oxygen species (ROS) generation, increased proteolysis and induction of early plasma membrane rupture (Golstein & Kroemer, 2007; Tonnus *et al.*, 2019). These specific forms of regulated necrosis are termed necroptosis, pyroptosis, and ferroptosis (Tonnus *et al.*, 2019).

Traditional necrotic injury occurs via one of two mechanisms; (1) interference with the cellular energy supply or (2) by direct damage to cellular membranes (Fink & Cookson, 2005; Hou *et al.*, 2016; Van Cruchten & Van Den Broeck, 2002). Necrotic cell injury commonly occurs through ischemia, which prevents the supply of oxygen and glucose to the area surrounding the ischemic site (Kalogeris, Baines, Krenz, & Korthuis, 2012) or by mechanical injury damaging cellular membranes (Zong & Thompson, 2006).

Necrosis is morphologically described by the swelling of cellular organelles, loss of plasma membrane integrity and the development of electron-lucent cytoplasm (Zong & Thompson, 2006). Other morphological changes in necrosis, shown in figure 1-5, include the formation of cytoplasmic vacuoles, disrupted organelle membranes, ruptured and swollen mitochondria, detachment of ribosomes, ruptured lysosomes, and cytoplasmic blebbing (Elmore, 2007; Fink & Cookson, 2005; Golstein & Kroemer, 2007; Van Cruchten & Van Den Broeck, 2002).

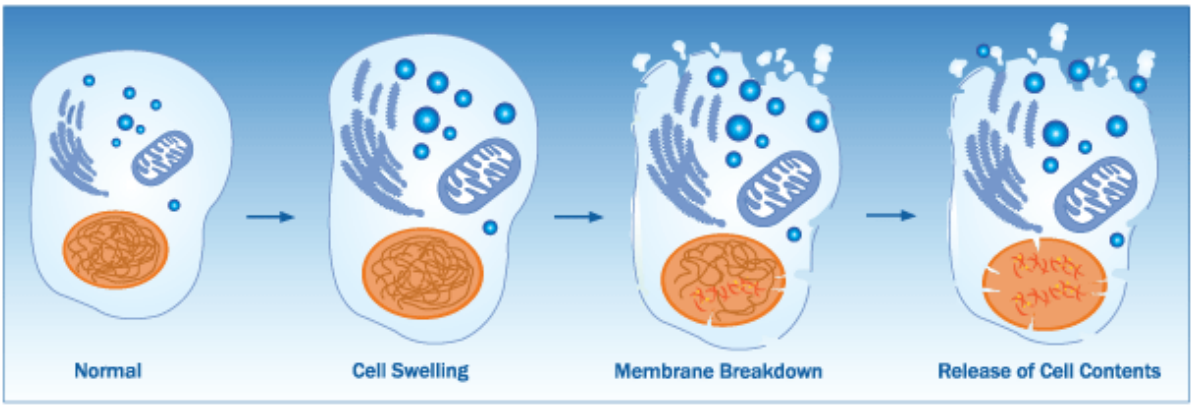

Figure 1-5. The key cellular morphological features associated with necrotic cell death.

Multiple key morphological changes have been shown to be associated with necrotic cell death. The morphological changes happen sequentially, following the initiation of necrosis. These changes include the swelling of the cell and its intracellular organelles, the breakdown of cellular membranes and as a result the release of intracellular contents into the extracellular environment. Adapted from Novus Biologicals (2021).

These morphological changes associated with necrosis have been shown to induce a significant inflammatory response in the region surrounding the necrotic area (Wallach & Kovalenko, 2014), induced by the release of intracellular contents into the extracellular environment via the loss of plasma membrane integrity (Rock & Kono, 2008).

These liberated cellular contents act as damage associated molecular patterns (DAMPS), which elicit an immune response and induce sterile inflammation within the necrotic region (Rock & Kono, 2008; Yang, Jiang, Zhang, & Fan, 2015). Multiple molecules within cells have been shown to act as DAMPs. These include: defensins, adenosine triphosphate, mitochondrial peptides, high-mobility group box 1, DNA and heat shock proteins (Rock & Kono, 2008). DAMPS interact with pattern recognition receptors (PRRs) to activate the innate immune system (Roh & Sohn, 2018). Subsequent production of pro-inflammatory cytokines elicits the inflammatory response associated with necrotic cell death (Rock *et al.*, 2011).

This inflammatory response means activation of necrosis is an undesirable property of chemotherapeutic agents given the far reaching and largely indiscriminate cellular side effects. Therefore, rather than promote necrosis, chemotherapeutics aim to induce apoptosis to both limit excessive inflammation and allow the rapid immune clearance

of eradicated cancer cells. To understand this, we must now consider apoptosis in detail.

1.1.4 Apoptosis

1.1.4.1 Overview

Apoptosis is a physiological mechanism and essential for development, the maintenance of homeostasis and the prevention of cancer (Singh, Letai, & Sarosiek, 2019). Furthermore, apoptosis can be triggered by the immune system in response to cellular damage, cellular dysfunction or as a result of toxic agents (Elmore, 2007) thus acting as a defence mechanism. Unlike necrosis, apoptosis is an active process, and following apoptotic stimuli requires input of energy (Singh *et al.*, 2019), which is required for cells to synthesise apoptotic proteins and undertake the intracellular mechanisms associated with apoptotic cell death.

The process of apoptosis is a more contained mechanism of cell death as it produces essentially no inflammatory response. This is because apoptotic cells do not release their intracellular contents into the extracellular environment. Rather, apoptotic cells are rapidly phagocytosed by immune cells in order to not produce a pro-inflammatory response (Elmore, 2007; Kurosaka, Takahashi, Watanabe, & Kobayashi, 2003; Savill & Fadok, 2000; Ziegler & Groscurth, 2004).

1.1.4.2 Apoptotic morphological changes

For cells to avoid inducing an inflammatory response, key cellular morphological changes are required. These include; cell shrinkage, plasma membrane blebbing, pyknosis (nuclear condensation), karyorrhexis (nuclear fragmentation), karyolysis (nuclear dissolution) and the formation of apoptotic bodies (Brauchle, Thude, Brucker, & Schenke-Layland, 2014). Crucially, these morphological changes occur in a specific order (see figure 1-6) to ensure that no intracellular contents are released from the cell, thus avoiding an inflammatory response (Kerr, Wyllie, & Currie, 1972; Ziegler & Groscurth, 2004).

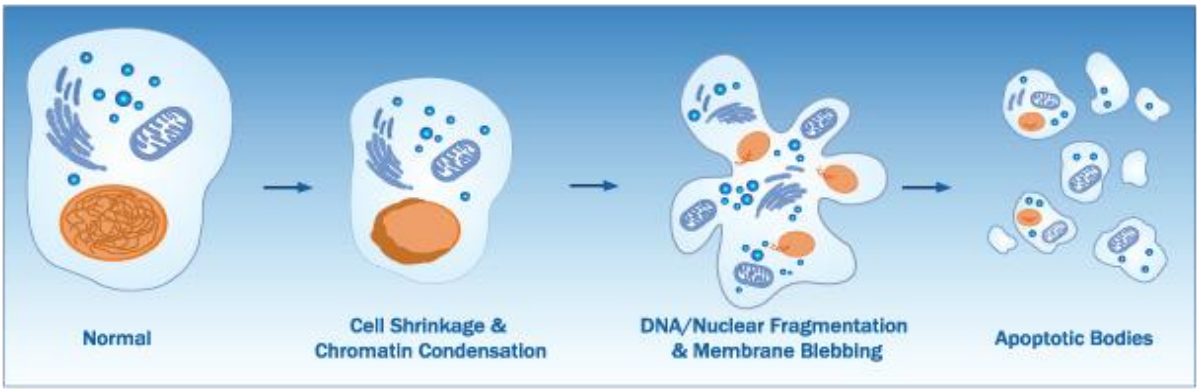

Figure 1-6. The cellular morphological changes associated with apoptotic cell death.

Apoptosis is a key form of cell death, commonly utilised in the physiological removal of damaged cells. In apoptosis, cells undergo multiple morphological changes to allow them to be removed by immune phagocytic cells. Initially cells and their intracellular organelles shrink, before the chromatin condenses. This condensation leads to the nucleus fragmenting, whilst simultaneously the cellular membrane begins to form protrusions, known as apoptotic blebs. Finally, the cell breaks apart via budding, resulting in the production of membrane bound structures known as apoptotic bodies. These apoptotic bodies can then be rapidly cleared by immune phagocytic cells. Adapted from Novus Biologicals (2021).

In the early stages of apoptosis, cells begin to shrink via condensation of their cytoplasm and nuclear material (Häcker, 2000; Wong, 2011). Following this, cells begin to form extracellular membrane blebs and cellular organelles begin to disintegrate (Ziegler & Groscurth, 2004). Finally, membrane blebbing becomes extensive and karyorrhexis occurs, leading to the formation of apoptotic bodies via a process known as budding (Saraste & Pulkki, 2000). These apoptotic bodies contain cytoplasm, tightly packed organelles and may contain nuclear material (Elmore, 2007; Häcker, 2000; Ziegler & Groscurth, 2004). It is the formation of these apoptotic bodies that attracts phagocytic cells such as macrophages and dendritic cells before ultimately being degraded by phagolysosomes (Elmore, 2007). To avoid secondary necrosis, this must happen rapidly.

In order for phagocytic cells to recognise apoptotic bodies as targets for degradation, modification to the structure of the extracellular membrane occurs. The key modification is the externalisation of the protein phosphatidylserine from the internal membrane of the cell (Ziegler & Groscurth, 2004). This externalisation of phosphatidyl

serine acts as a signal to phagocytic cells to target cells undergoing apoptosis for degradation (Wong, 2011).

To trigger the morphological changes associated with apoptotic cell death, molecular cell signalling pathways are required to be activated. The activation of these pathways induces downstream signalling cascades and in turn induce the morphological changes associated with apoptotic cell death.

1.1.5 Molecular control of apoptosis

The process of apoptosis is tightly regulated via internal molecular mechanisms. There are two main mechanisms which can induce apoptosis, (1) an intrinsic pathway mediated by mitochondria or (2) the extrinsic pathway activated by death receptors (Elmore, 2007; Singh *et al.*, 2019). These two activation pathways have been shown to converge into a single execution pathway, which ultimately leads to apoptotic cell death, shown in figure 1-7 (Elmore, 2007; Igney & Krammer, 2002; Singh *et al.*, 2019).

Both pathways induce apoptosis mediated by a family of cysteine-aspartic proteases commonly known as caspases (Julien & Wells, 2017; McIlwain, Berger, & Mak, 2013). So far studies have identified 10 main members of the caspase family of proteins, these proteins have been broadly categorised into initiator caspases (caspases-2,-8,-9,-10), effector or executioner caspases (caspases-3,-6,-7) and inflammatory caspases (caspases-1,-4,-5) (Julien & Wells, 2017; McIlwain *et al.*, 2013; Rai, Tripathi, Sharma, & Shukla, 2005).

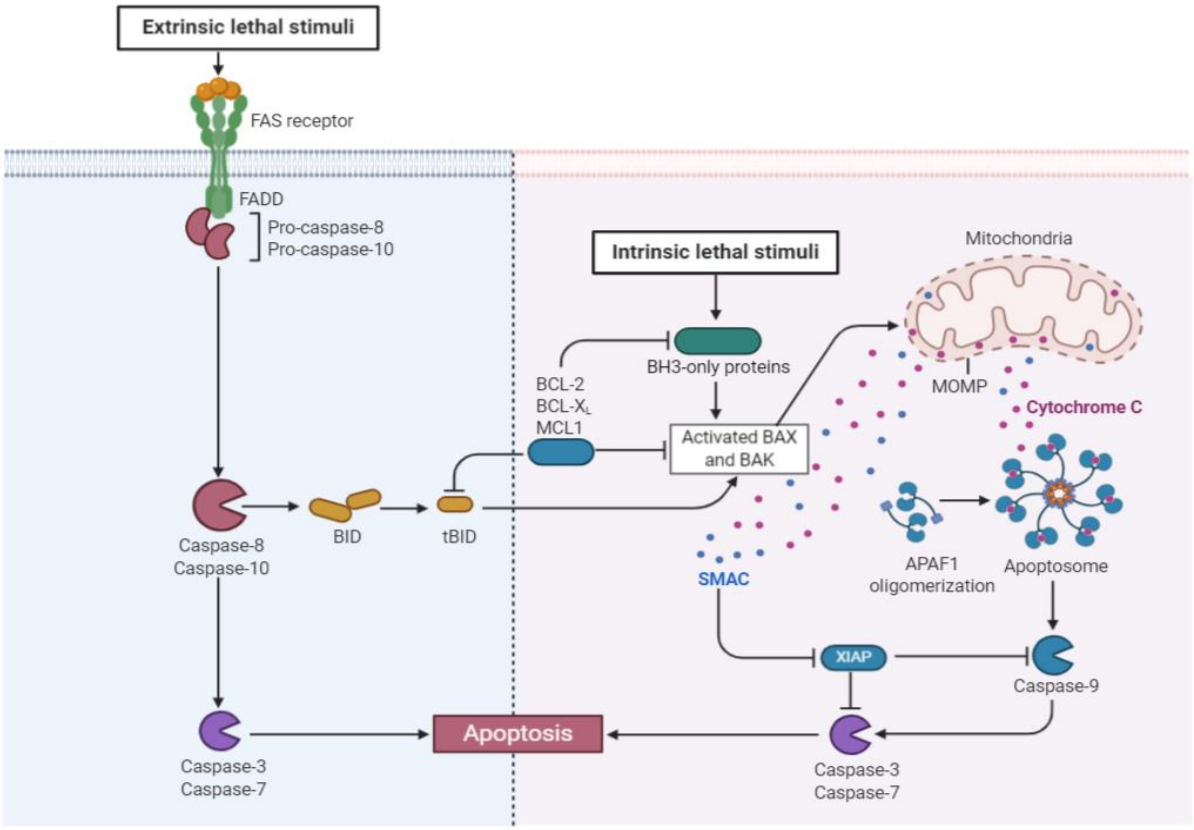

Figure 1-7. The molecular pathways that induce apoptotic cell death.

Apoptosis can occur through one of two main pathways, the extrinsic pathway resulting from external lethal stimuli binding to extracellular receptors or by the activation of the intrinsic pathway induced by internal lethal stimuli. The extrinsic pathway can also activate the intrinsic pathway, via the activation of BH3 interacting-domain death agonist (BID). Both pathways result in the activation of caspases-3 and 7 which mediate apoptotic cell death. Figure adapted from Biorender.com

Caspases are usually expressed in an inactive proenzyme form within most cells (Elmore, 2007). Once activated, these proenzymes further activate procaspases, inducing the initiation of a protease cascade (Li & Yuan, 2008). These procaspases also possess the capability to aggregate and further induce downstream effects (Lavrik, Golks, & Krammer, 2005; Tait, Ichim, & Green, 2014). The proteolytic cascade acts to amplify the apoptotic signalling pathway, evoking rapid cell death (Elmore, 2007).

1.1.5.1 The intrinsic pathway of apoptosis

The intrinsic pathway of apoptosis is initiated by a variety of microenvironmental stimuli including: growth factor withdrawal, DNA damage, endoplasmic reticulum (ER) stress, ROS overload, increased replication stress, microtubular alterations and defects in

mitosis (Galluzzi *et al.*, 2018; Tang, Kang, Berghe, Vandenabeele, & Kroemer, 2019). In response to these diverse stimuli, oncogenes become upregulated, including the increase in expression of p53 (Aubrey, Kelly, Janic, Herold, & Strasser, 2018).

Increased p53 expression activates several pathways which produce the molecules required for the intrinsic pathway of apoptosis. Specifically, p53 acts through the BCL-2-regulated pathway, which acts to control the intrinsic pathway, shown in figure 1-8 (Elmore, 2007; Fridman & Lowe, 2003; Hengartner, 2000). The key proteins of the BCL-2 pathway include BCL-2-like protein 4 (BAX), BCL-2 homologous antagonist killer (BAK), BCL-2-like protein 11 (BIM), BID, BCL-2 antagonist of cell death (BAD), BCL-2-modifying factor (BMF), and p53 upregulated modulator of apoptosis (PUMA) (Aubrey *et al.*, 2018; Letai, 2017; Nakano & Vousden, 2001). All of these proteins act together with the ultimate aim to permeabilise the outer mitochondrial membrane (Elmore, 2007; Kaufmann, 2007).

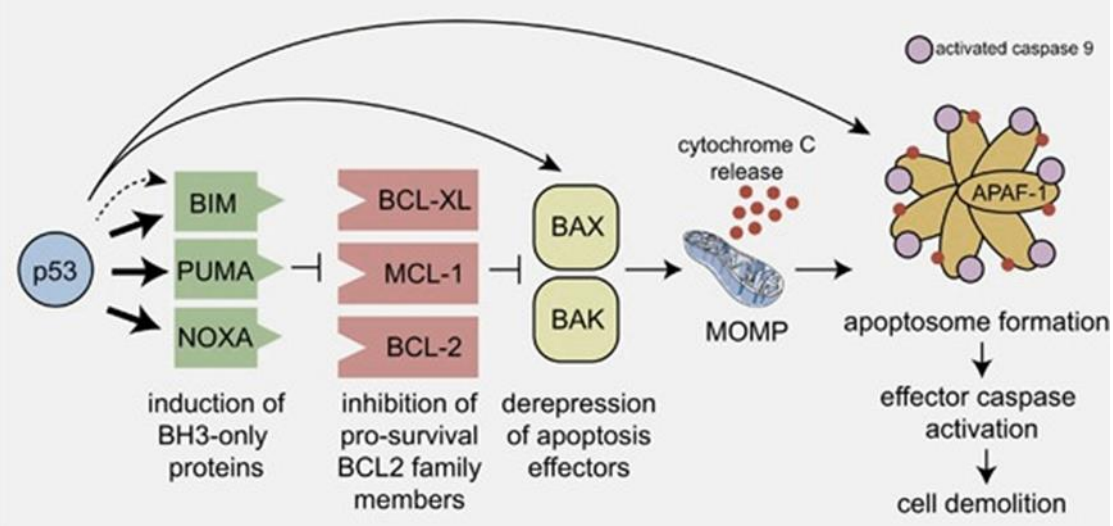

Figure 1-8. The p53 induced mediators of apoptosis.

Activated p53 induces the activation of multiple members if the BCL-2 family of proteins, evoking a pro-apoptotic response via the loss of mitochondrial membrane integrity, allowing the release of cytochrome C. Cytochrome C can then bind with activated caspase-9 and apoptotic protease activating factor 1 (Apaf-1) to form the apoptosome, which cleaves caspases into their active forms inducing apoptotic cell death. Figure adapted from Aubrey *et al.*, 2018.

The permeabilisation of the outer membrane occurs via the oligomerisation of BID, BAX and BAK into the mitochondrial outer membrane, shown in figure 1-9A (Montessuit *et al.*, 2010). This oligomerisation forms a membrane pore between the

inner and outer mitochondrial membrane, allowing the diffusion of the mitochondrial intermembrane compartment contents into the cytosol (Martinou & Youle, 2011). This loss of membrane integrity leads to the release of the pro-apoptotic factor cytochrome C (Kaufmann, 2007).

Once cytochrome C enters the cytosol, it can bind to Apaf-1 and procaspase-9, as shown in figure 1-9B (Dorstyn, Akey, & Kumar, 2018; Jin & El-Deiry, 2005). Apaf-1 and procaspase-9 are present in inactive forms within normal cells. However upon pro-apoptotic stimuli, these proteins become activated (Yuan & Akey, 2013). This activation initiates the assembly of a structure known as caspase-activation complex, also known as an apoptosome (Dorstyn *et al.*, 2018; Elmore, 2007; Jin & El-Deiry, 2005). Within the apoptosome, the activation of procaspase-9 occurs allowing the generation of additional apoptosomes further enhancing apoptosis whilst also possessing the ability to activate executioner caspases, which ultimately induces apoptosis (Jin & El-Deiry, 2005).

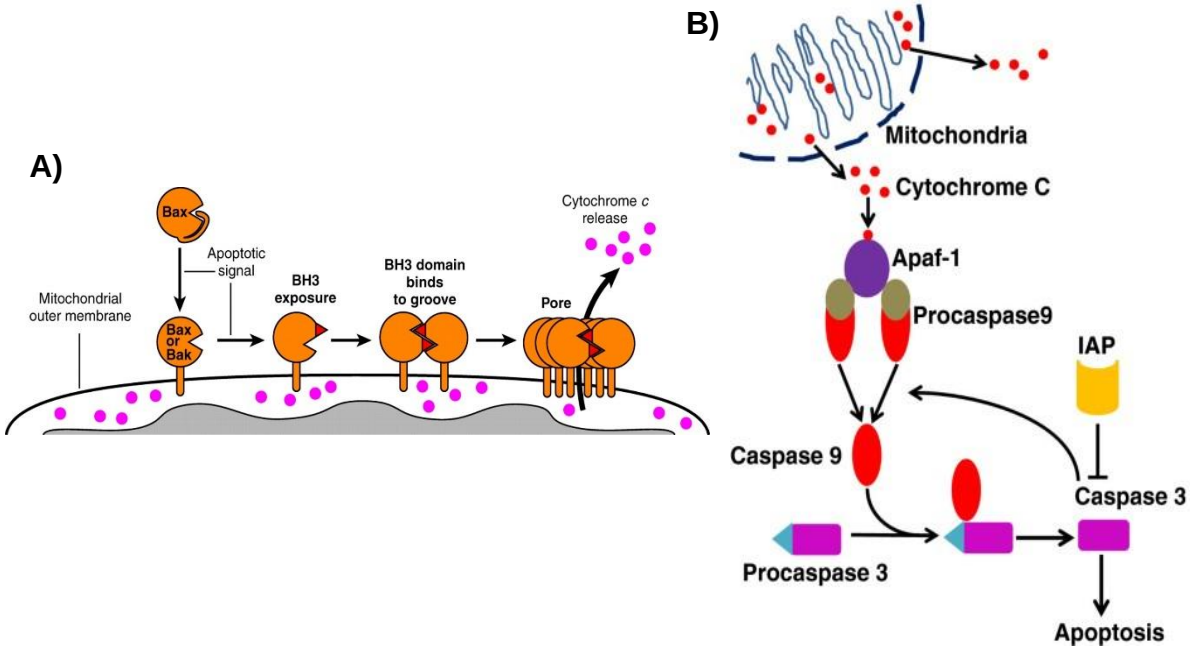

Figure 1-9. The mechanism of cytochrome C release and the downstream apoptosis signalling.

There are two key steps involved in the release of cytochrome C from mitochondria. **A)** The BAX and BAK dimerization, which induces the release of cytochrome C from the mitochondrial intermembrane compartment. **B)** The intrinsic pathway of apoptosis induced by the release of cytochrome C from the mitochondria intermembrane compartment. Figure adapted from Dewson and Kluck (2009).

The permeabilization of the mitochondrial membrane to release cytochrome C also results in the release of second mitochondria-derived activator of caspase/direct inhibitor of apoptosis-binding protein with low pI (SMAC/DIABLO) (Martinez-Ruiz, Maldonado, Ceballos-Cancino, Grajeda, & Melendez-Zajgla, 2008; Zhou, Zhou, Luo, & Chang, 2005). SMAC/DIABLO further induce apoptosis by the inhibition of X-linked inhibitor of apoptosis protein (XIAP) and survivin, which are key inhibitors of the caspase cascade and activators of the nuclear Factor kappa-light-chain-enhancer of activated B cells (NF-κB) pathway (Obexer & Ausserlechner, 2014; Qin *et al.*, 2016).

1.1.5.2 The Extrinsic pathway of apoptosis

The extrinsic pathway of apoptosis is evoked in response to external stimuli, mainly through the binding of ligands to the death receptors on the surface of cells, shown in figure 1-10 (Galluzzi *et al.*, 2018). Key examples of death receptors that can induce apoptosis include Fas receptor (FasR, CD95), TNF-related apoptosis-inducing ligand (TRAIL) receptor (TRAIL-R) and tumour necrosis factor receptor 1 (TNFR1) (Dai *et al.*, 2015; Peter *et al.*, 2015; Wajant & Siegmund, 2019). The binding of ligands to these receptors induces the formation of a multi-protein complex known as death-inducing signalling complex (DISC) (Fulda & Debatin, 2006; Kim, Choi, & Joe, 2000).

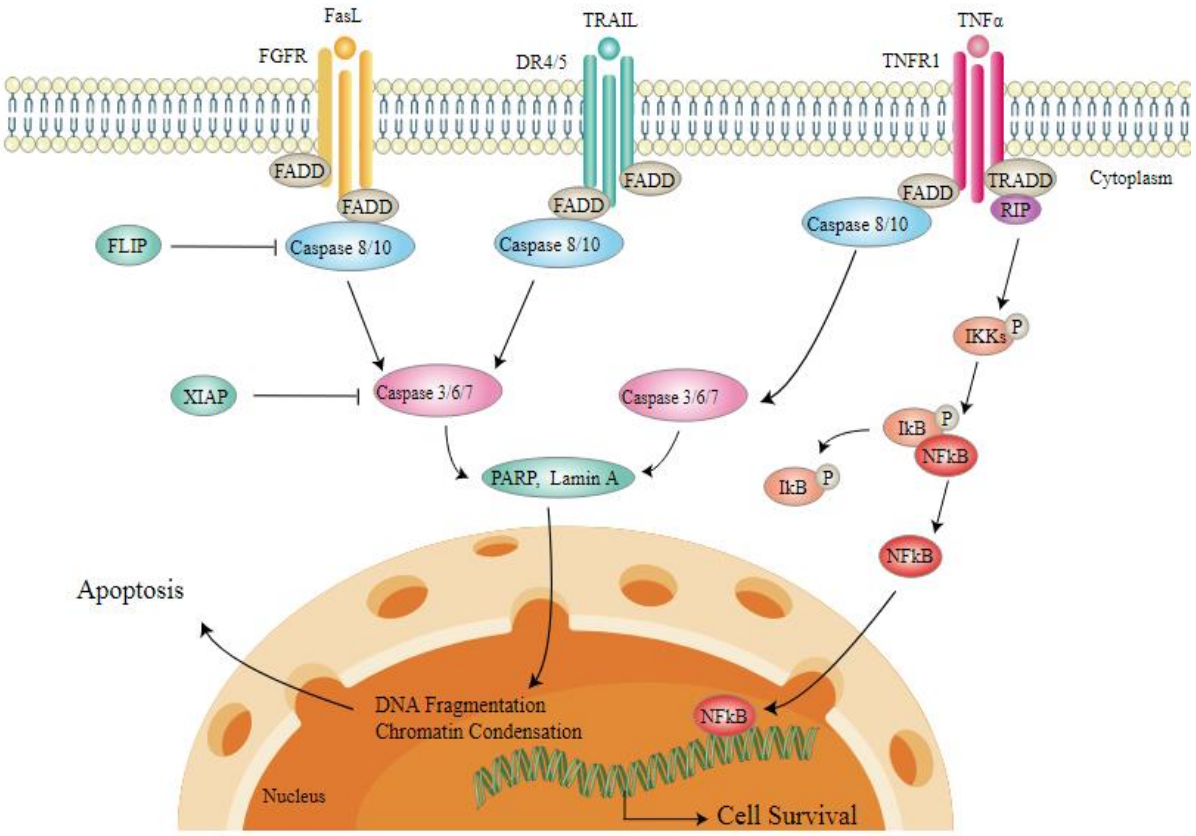

Figure 1-10. The extrinsic pathway of apoptosis.

The signalling pathways triggered by the activation of FAS, TRAIL and TNFR1 receptors, which lead to downstream activation of proapoptotic pathways and ultimately apoptotic cell death, following the binding of external death inducing stimuli. Adapted from www.creative-diagnostics.com/extrinsic-apoptosis-pathway.

The binding of ligands to death receptors induces the recruitment of the adaptor molecule FAS-associated protein with death domain (FADD) to the receptor site (Tourneur & Chiocchia, 2010). This recruitment of FADD causes further recruitment of procaspase-8 and procaspase-10 to the receptor site and completing the formation of active DISC (Dickens *et al.*, 2012; Oberst *et al.*, 2010). Once activated, DISC cleaves pro-caspase-8 and pro-caspase-10 into their active forms (caspase-8 and caspase-10), which mediate the direct downstream activation of executioner caspases. DISC can also activate caspases indirectly by interaction with the intrinsic pathway via the cleavage of BID into its active form (Dickens *et al.*, 2012; Galluzzi *et al.*, 2018).

The TNFR1 receptor induces apoptosis via a similar mechanism to that described in TRAIL receptors, however an additional adapter molecule can be recruited to the receptor (Pobezinskaya & Liu, 2012). This molecule known as tumour necrosis factor

receptor type 1-associated death domain protein (TRADD), which can bind to the TNFR1 receptor in place of FADD (Cao, Pobezinskaya, Morgan, & Liu, 2011).

The binding of TRADD to TNFR1 can induce dual functions, including the upregulation of apoptosis via inducement of a DISC complex, as well as the inhibition of apoptosis via activation of the NF-κB signalling pathway (Hoesel & Schmid, 2013; Kim *et al.*, 2011). Activation of TNFR1 with TRADD, leads to a signalling cascade inducing the activation of the inhibitor of NF-κB kinase (IKK), Extracellular signal-regulated kinase (ERK), NF-κB essential modulator (NEMO), p38, and the c-Jun N-terminal kinase (JNK) pathways (Cao *et al.*, 2011). The activation of NF-κB also upregulates the expression of survivin, BCL-2, B-cell lymphoma-extra-large protein (BCL-X_L), and XIAP resulting in the inhibition of apoptosis (Zheng, 2017).

1.1.5.3 The Execution pathway of apoptosis

Both the intrinsic and extrinsic apoptosis pathways merge at the activation of the executioner caspases. The activation of the executioner caspases occurs as a result of cleavage from their pro-form to their active form via the activity of caspases-8 and -10 from the extrinsic pathway or by caspase-9 from the intrinsic pathway (Cavalcante *et al.*, 2019; Elmore, 2007). The executioner caspases, namely caspases -3, -6, and -7 activate endonucleases and proteases, resulting in the morphological changes associated with apoptosis. Additionally, these executioner caspases cleave other substrates including cytokeratins, Poly (ADP-ribose) polymerase (PARP), alpha-fodrin and nuclear mitotic apparatus protein (NuMA) further inducing the morphological and biochemical modifications commonly associated with apoptosis (Cavalcante *et al.*, 2019; Elmore, 2007; Slee, Adrain, & Martin, 2001).

Within normal cells the process of apoptosis evokes the rapid clearance of dysfunction, damaged or no longer required cells to maintain homeostasis. However, cancer cells can manipulate this process to survive or avoid regulated cell death and continue proliferating.

1.2 Cancer

In cancer, previously healthy cells are triggered to grow and reproduce uncontrollably. The transformation of healthy cells to cancerous ones can occur in nearly all cells within the body, resulting in over one hundred different cancer types (Cooper & Hausman, 2019). These different cancer types vary in both their pathology and their response to treatment (Sarkar *et al.*, 2013).

There are two principle cancer subtypes; benign and malignant cancers. The key difference is the ability of the malignant cancers to migrate throughout the body, whilst benign tumours do not spread (Cooper & Hausman, 2019). The ability of malignant tumours to migrate is a result of the downregulation of the cell adhesion receptors necessary for tissue specific cell to cell attachment (Sarkar *et al.*, 2013). In addition, an upregulation of cell motility regulators and receptors is commonly observed in malignant cells, which are not observed in benign malignancies, which allows certain cancers to spread throughout the body (Sarkar *et al.*, 2013).

1.2.1 Incidence and epidemiology of cancer

Cancer is one of the leading causes of death worldwide, accounting for 28 % of all-cause mortality in the United Kingdom (CRUK, 2020b). Each year, globally, there are 18.1 million new cases of cancer and 9.6 million deaths (Bray *et al.*, 2018). In the United Kingdom alone, there are approximately 367,000 new cases of cancer each year and 165,000 deaths (CRUK, 2020b). The incidence of cancer continues to increase year on year, as shown in figure 1-11A, however, as a result of improved therapeutics and diagnostics cancer death rates have been declining over the past 25 years (figure 1-11B),worldwide, The transition of developing countries to a developed state may account for this increase (Bray *et al.*, 2018).

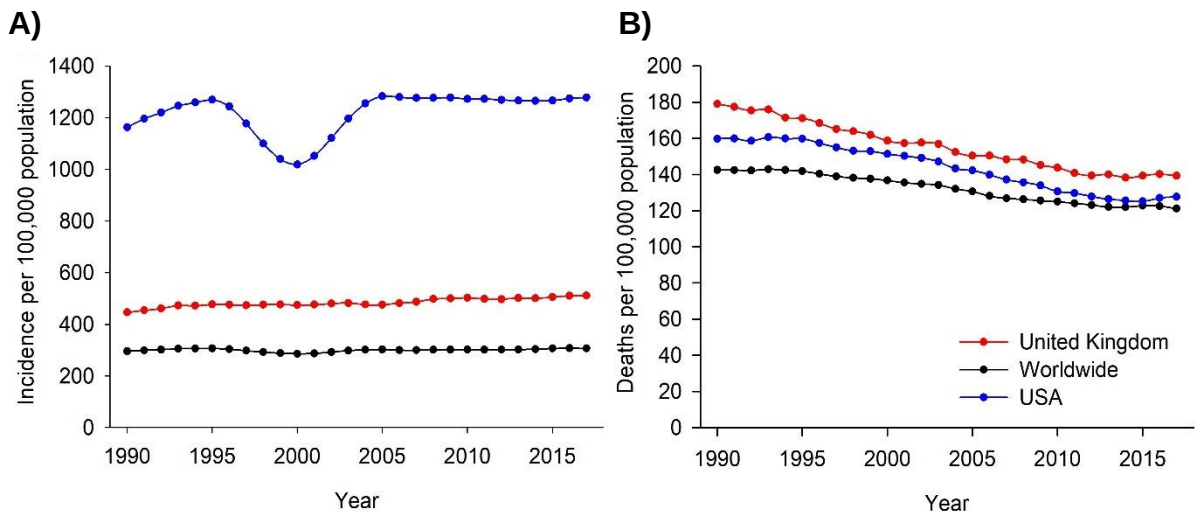

Figure 1-11. Comparisons of cancer incidence and mortality rates in the United Kingdom, the United states of America and Worldwide.

Comparisons were conducted between of the incidence and mortality rates of cancer globally (Black), the United States of America (USA) (Blue) and the United Kingdom (Red) between 1990 and 2017. **A)** The rate of incidence of cancer in the UK, USA and worldwide per 100,000 of the population between 1990 and 2017. **B)** The number of deaths per 100,000 of the population in the UK, USA and worldwide between 1990 and 2017. Figures adapted from data collected by the Global Burden of Disease Collaborative Network, Institute for Health Metrics and Evaluation, USA.

Cancer has been shown to affect people of any age (White *et al.*, 2014). However, it predominantly affects people later in life (figure 1-12), with 36 % of all cancer diagnoses in the UK being in people over the age of 75 years (CRUK, 2020c). The highest incidence rates are in populations aged between 85 and 89 years (CRUK, 2020a). A similar pattern is observed in other developed countries such as the USA and Australia (AIHW, 2019; Siegel, Miller, & Jemal, 2016; White *et al.*, 2014). Cancer has also been shown to be more prevalent in males compared to females (Meegan & O'Boyle, 2019), with one in five males compared to one in six females developing cancer in their lifetime (Meegan & O'Boyle, 2019). Of all males diagnosed with cancer, the most prevalent is lung cancer, whilst the most prevalent cancer type amongst women is breast cancer (Bray *et al.*, 2018).

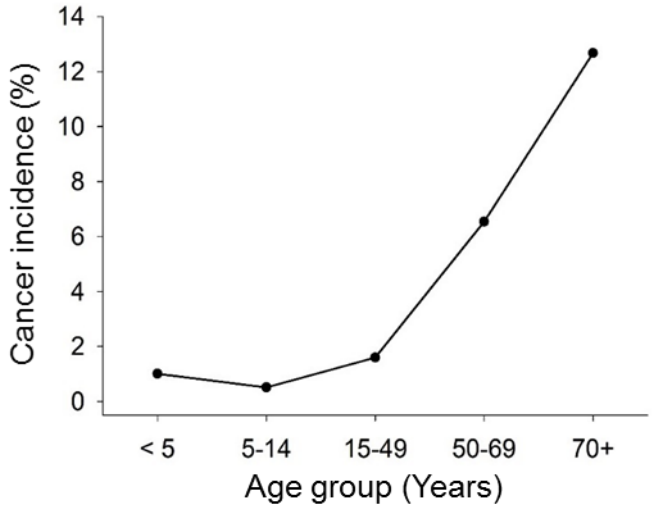

Figure 1-12.The association of cancer incidence with age in the United Kingdom. Populations aged greater than 50 years were found to have a substantially increased likelihood of having cancer compared to those aged less than 50 years. Figure reproduced from data collected by the Global Burden of Disease Collaborative Network, Institute for Health Metrics and Evaluation, USA.

Whilst this may be the general pattern of effect, certain cancer subtypes are more prevalent in younger populations compared to in elderly populations (White *et al.*, 2014). The most common types of cancer within children in the UK under the age of 14 are leukaemia's, brain cancers, non - Hodgkin's lymphoma and kidney cancer (ONS, 2018).

Cancer has historically been associated with developed countries (Bray *et al.*, 2018); however, it is becoming increasingly more prevalent in the developing world *(Bray et al.*, 2018). A study by Jemal, Center, DeSantis, and Ward (2010) determined that of all cancer cases worldwide, 56 % of cases and 64 % of deaths occurred within the economically developing world. The GLOBOCAN study conducted in 2018, showed that developed countries had a cancer incidence rate between two to three times higher than those of developing countries (Bray *et al.*, 2018). However, the death rate is generally the inverse, due to a higher level of medical infrastructure and diagnostic capabilities available in developed countries (Bray *et al.*, 2018). It is forecasted, that by 2030, cancer incidence rates will rise by 55 % worldwide as more countries begin to transition to a higher socioeconomic status (Ferlay, Wild, & Bray, 2016). This transition results in additional risks associated with an increased economic status.

Cancer survival rates vary worldwide and are commonly dependent on the socioeconomic status of the country in which the patient is diagnosed (Bouchardy, Verkooijen, & Fioretta, 2006). Within the UK, approximately 50 % of all cancer diagnoses result in a 10-year survival post diagnosis (CRUK, 2020b). However, this survival rate varies within populations of the of a country based on their ethnicity. Data from the Global Burden of Disease Network (IHME, 2018) shows that in the USA there is a 9.7 % lower survival rate in the Black population compared to the White population of the USA as of 2015, shown in figure 1-13. This is corroborated in studies by Kehm *et al.* (2018) and Ellis *et al.* (2018) who described that Black and Hispanic populations have between a 28 - 73 % lower survival rate compared to that of the white population. This difference in survival rate is probably attributable to systemic inequalities in access to health services as well as to optimal diagnostic and treatment services (Allemani *et al.*, 2015).

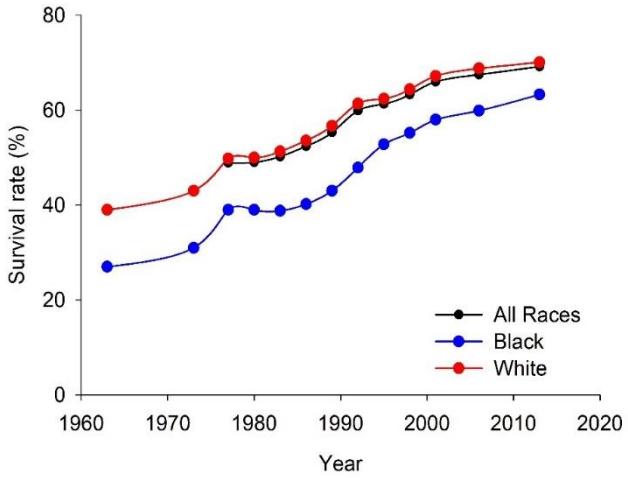

Figure 1-13. Comparisons of all cancer survival rates between ethnic groups in the USA between 1963 and 2013.

A graphical comparison of the cancer survival rates of all races (Black), Black (Blue) and White (Red) populations between 1963 and 2013. Figure adapted from data collected by Surveillance, Epidemiology and End Results Program (SEEAR), National Cancer Institute, USA.

The survival rates following cancer have also been found to significantly vary depending on the type of cancer and how early the cancer is detected. Diagnosis and treatment in the early stages of cancer development has been shown to significantly increase patient survival rates, with patients diagnosed earlier having significantly

smaller tumours and a significantly decreased likelihood of metastasis (Saadatmand, Bretveld, Siesling, & Tilanus-Linthorst, 2015).

Differences in survival rate also significantly differ between the type of cancer the patient develops. This difference can be observed in patients who develop pancreatic or testicular cancer; with patients who develop pancreatic cancer only having a 9 % 5 - year survival rate worldwide (Rawla, Sunkara, & Gaduputi, 2019), compared to a 98 % 5 - year survival rate for patients who develop testicular cancer (Park, Kim, Elghiaty, & Ham, 2018; Quaresma, Coleman, & Rachet, 2015). These differences in survival rate are due to the ability to diagnose patients early in the cancer development as well as the availability of effective treatment options. The ability to diagnose and treat cancer varies dependant on the type of cancer and the mechanism underpinning its development and transition from healthy cells to cancerous tissue.

1.2.2 Cancer aetiology

There are many factors that can increase the risk of a person developing cancer within their lifetime. The factors which can result in the development of cancerous cells are exhaustive and beyond the scope of this thesis. However, these factors can be broadly categorised into three main groups; (1) those caused by lifestyle, (2) those caused by chemicals, termed carcinogens and (3) those caused by biological agents.

There are many lifestyle factors that can contribute to the development of cancer. Of these, two of the most common causes include smoking and obesity (Arnold *et al.*, 2016; Islami *et al.*, 2018). Other lifestyle factors that have been described to be associated with the development of cancer include: low dietary fibre (Danaei *et al.*, 2005), physical inactivity (Brown *et al.*, 2018), smoking tobacco (Parkin, Boyd, & Walker, 2011), excessive alcohol consumption (Bagnardi *et al.*, 2015; Weiderpass, 2010), and being exposed to high levels of ultraviolet (UV) radiation (Rawla *et al.*, 2019).

The interaction of exogenous carcinogenic chemicals with cells can result in the formation of cancer. Key examples of chemicals which can induce carcinogenesis include: the chemicals within cigarette smoke, (Parkin *et al.*, 2011; Weiderpass, 2010) and the chemicals within urban air pollution (Danaei *et al.*, 2005; Parkin *et al.*, 2011), alongside many other chemicals which have been designated by the WHO

International Agency for Research on Cancer as potential carcinogens (Althouse, Huff, Tomatis, & Wilbourn, 1979; WHO, 2021).

The WHO have also designated numerous infectious agents to be potential carcinogens, due to their ability to damage cells and induce mutagenesis (Parkin, 2011; WHO, 2021). Of the bacterial and viral infections associated with carcinogenesis, key examples include; Hepatitis B, Hepatitis C, Human immunodeficiency virus, Epstein-Barr virus (Khan & Hashim, 2014), Human herpes virus type 8, *Helicobacter pylori* (Wroblewski, Peek, & Wilson, 2010) and Human papillomavirus (Saraiya *et al.*, 2015).

All of the factors stated above result in the modification and damage to normal cells. This damage leads to the development of genetic mutations and the pathogenesis of cancer further described in section 1.2.4.

1.2.3 Cancer diagnosis

The ability to diagnose cancer varies significantly depending on the type and location of the cancer within the body. Most cancers will ultimately become symptomatic as they progress, however many remain asymptomatic in their early stages making early detection difficult.

In patients who are symptomatic, initial diagnosis is usually made via laboratory tests or imaging techniques such as computerised tomography (CT), x-ray, ultrasound, positron emission tomography (PET) scans, nuclear or magnetic resonance imaging (MRI) (Barentsz *et al.*, 2006; Barkan *et al.*, 2018; Fass, 2008). These are commonly confirmed through biopsy of the tumour site (Egger *et al.*, 2003; Vaidyanathan, Soon, Zhang, Jiang, & Lim, 2019).

Certain cancers are actively screened for in the asymptomatic general population within the UK. This screening is commonly in place for members of the population have an increased likelihood of developing a particular type of cancer, based on their lifestyle factors or family history, in an attempt to diagnose patients before they begin to show symptoms (M. J. Duffy, 2013; Nagpal, Singh, Singh, Chauhan, & Zaidi, 2016). This commonly employs the use of imaging methods (for example breast cancer screening), cytology (for example the smear test for cervical cancer) or testing for the presence of genetic, protein or metabolite biomarkers which are elevated in certain cancers (M. J.

Duffy, 2013; Jain & Jain, 2010; Nagpal *et al.*, 2016). Common cancer markers routinely used for screening include: prostate specific antigen (PSA), cancer antigen 125 (CA 125), Human chronic gonadotrophins (hCG), bladder tumour antigen, α-fetoprotein and pepsinogen (Duffy, 2013; Jacobs & Bast Jr, 1989; Lilja, Ulmert, & Vickers, 2008; Mordente, Meucci, Martorana, & Silvestrini, 2015; Partheen, Kristjansdottir, & Sundfeldt, 2011; Stamey *et al.*, 1987). These commonly used screening biological markers are summarised in table 1-1.

Table 1-1. A summary of routinely evaluated biological markers used to screen and aid diagnose patients with specific cancer types.

Marker	Description
PSA	Prostate specific antigen is a routine screening marker for prostate cancer. It is an androgen-regulated serine protease produced by both prostate epithelial cells and prostate cancer. Serum total PSA levels are commonly elevated in prostate cancer patients compared to those without cancer (Balk, Ko, & Bubley, 2003).
CA 125	CA 125 is a common screening marker for ovarian cancer. CA125 is expressed as a membrane-bound protein at the surface of cells that undergo metaplastic differentiation into a Müllerian-type epithelium (Feeley & Wells, 2001; Scholler & Urban, 2007). CA 125 has been shown to be elevated in ovarian cancer as well as other cancer types (Scholler & Urban, 2007).
Human chronic gonadotrophins	hCG is expressed by both trophoblastic and non-trophoblastic human malignancies and plays a role in cell transformation, angiogenesis, metastasis, and immune evasion, all process key to cancer progression (Sisinni & Landriscina, 2015). hCG is commonly used as a screening marker for ovarian and testicular cancer, but concentrations are also elevated in liver, breast, lung, skin and stomach cancers (Sisinni & Landriscina, 2015).
α-Fetoprotein	Alpha fetoprotein is a screening marker used for liver carcinomas. It is a glycoprotein involved in foetal liver development, which drops off shortly after birth to normal adult serum concentrations of < 20ng/ml (Ersoy, 2005). In liver carcinomas this concentration rises to < 100 ng/ml allowing it to be used as a screening marker for liver carcinomas.
Pepsinogen	Serum pepsinogen is a screening marker for gastric cancers. Pepsinogen is a key gastric proenzyme secreted by gastric chief cells, which is converted to pepsin when secreted into stomach acid. In gastric cancers the presence of inflammation and metaplasia decrease the secretion of pepsinogen compared to healthy populations (Kim & Jung, 2010).
Bladder tumour antigen	Bladder tumour antigens are membrane proteins that are secreted into the urine when tumours invade into the bladder wall (Viola-Magni, 2017). Under normal conditions bladder tumour antigen is not present in urine, making it an ideal marker for detecting bladder carcinomas.

1.2.4 Pathogenesis of cancer

For cancers to develop, cells need to acquire six key properties, shown in figure 1-14. These properties include; the ability to proliferate self-sufficiently, unlimited replicative potential, anti-proliferative signal insensitivity, the evasion of controlled cell death (apoptosis), angiogenic capability and specifically for malignant tumour cells, the ability to invade and metastasise to other tissues and organs (Hanahan & Weinberg, 2000; Rakoff-Nahoum, 2006).

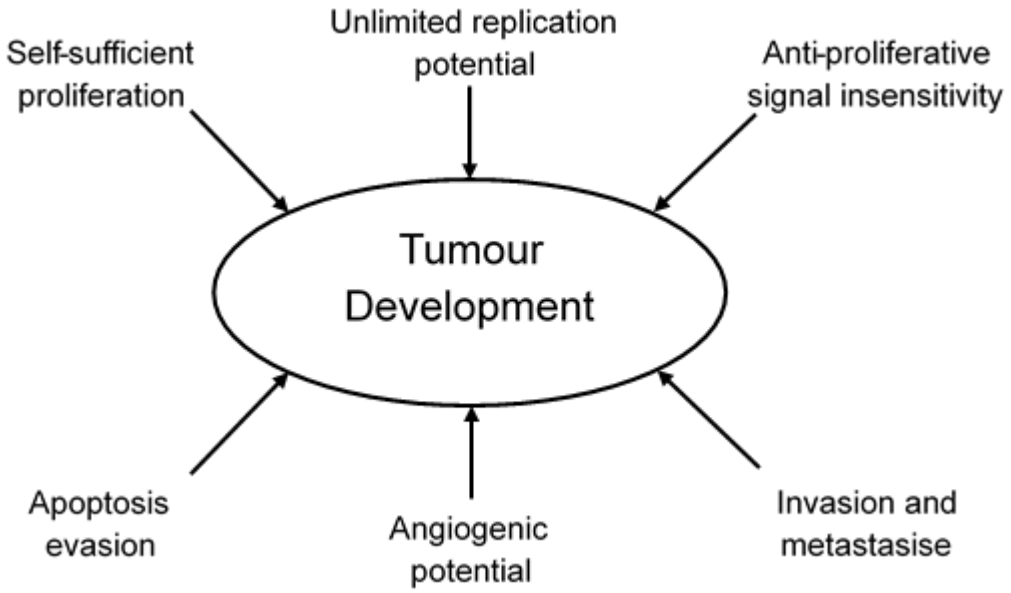

Figure 1-14. The six properties required for a normal healthy cell to become cancerous and tumours to develop.

Multiple key properties have been identified to play a significant role in the development of tumours. These include; the cancers ability to become insensitive to anti-proliferative signals, their ability to replicate to unlimited numbers, their ability to replicate without the necessity of external factors, their ability to actively and passively evade apoptosis and immune detection, cancers ability to generate new blood vessels to allow the delivery of nutrients to the growing tumour, and their ability to invade nearby tissues and organs, alongside their ability to metastasise to distant sites following their entry into the vasculature (Hanahan & Weinberg, 2011).

These properties arise from the development of genetic abnormalities within cells (Sarkar *et al.*, 2013). These genetic abnormalities can result in malignant transformation and include genetic mutation, chromosomal translocation, chromosomal deletion, dysregulation of protein expression, the dysfunction of signalling pathways, or a combination of all these mechanisms (Hanahan & Weinberg, 2000, 2011; Sarkar *et al.*, 2013). These genetic abnormalities can result in the

activation of proto-oncogenes to become oncogenes, key genes associated with the formation and development of cancer (Cooper & Hausman, 2019; Hassanpour & Dehghani, 2017).

Key genetic changes known to result in cancer formation via oncogene generation and genetic abnormalities are summarised in table 1-2. However, many other cancers are associated with genetic instability, which result in the formation of cancerous cells (Hassanpour & Dehghani, 2017).

Table 1-2. Key genetic changes associated with oncogene formation and cancer development.

Genetic change	Example of genetic change	Cancer associated with genetic change
Chromosomal translocation	Bcr-Abl	Chronic myeloid leukaemia
Point mutation	Ras	Colon cancer
Deletion	Erb-b	Breast cancer
Amplification	N-myc	Neuroblastoma
Insertion	C-myc	Acute lymphoblastic leukaemia

In addition to genetic abnormalities, cancer cells lose their necessity for external growth signals (Hanahan & Weinberg, 2011). In normal cells, it is usually the case that external growth signalling is required to induce cellular proliferation. However, in cancerous cells uncontrolled proliferation can be facilitated by expression of autocrine and paracrine signalling molecules, thus removing the influence of external regulation. Normal cells utilise these growth signals in order to move out of a quiescent state and begin to actively replicate (as per section 1.1.1). Tumour cells, however, no longer require these growth signals allowing them to avoid homeostatic mechanisms involved in maintaining proper cellular behaviour (Hanahan & Weinberg, 2000, 2011). Additionally, cancer cells, both benign and malignant, become insensitive to anti-growth signals allowing them to divide without regulation, resulting in their uncontrolled growth (Lazebnik, 2010).

During tumour formation, the tissue architecture and cellular microenvironment adapt to favour development. For example, the extracellular matrix (ECM) undergoes

substantial modifications, which aid in tumour progression and development (Walker, Mojares, & del Río Hernández, 2018). These modifications include: increased secretion of fibronectin and collagen, increased deposition of matrix proteins, increased integrin signalling and collagen and elastin crosslinking (Henke, Nandigama, & Ergün, 2020; Nallanthighal, Heiserman, & Cheon, 2019; Walker *et al.*, 2018). Combined, these changes result in increased ECM abundance and stiffness surrounding the tumour site (Walker *et al.*, 2018).

Further to this, an increase in integrin expression also occurs in cancer cells. These integrins have been shown to be activated as a result of the increased ECM stiffness surrounding cancer cells (Cox & Erler, 2011). These activated integrins promote cellular motility and allows the tumour to migrate through the basement membrane, significantly increasing the likelihood of the development of metastases (Cox & Erler, 2011; Desgrosellier & Cheresh, 2010; Walker *et al.*, 2018).

Cancer cells can also manipulate their microenvironment and induce chronic levels of inflammation, causing further corruption of the ECM composition, leading to enhancement of tumour growth and development (Coussens & Werb, 2002; Gonzalez, Hagerling, & Werb, 2018). This elevated inflammatory state acts as a promotor for tumour growth through the induction of increased neovascularisation, the direct upregulation of tumour-promoting signals and promoting pro-cancer functions onto cancer cells (Coussens & Werb, 2002; Greten & Grivennikov, 2019).

Many factors can mediate and stimulate this proinflammatory environment, including cytokines, chemokines, free radicals, reactive oxygen species, prostaglandins, growth factors and proteolytic enzymes (Aggarwal & Gehlot, 2009; Todoric, Antonucci, & Karin, 2016). These factors act directly on cancer cells, stimulating their proliferation and inhibiting their death. This inflammatory environment also promotes the accumulation of oncogenic mutations, further tumour development and extracellular matrix modifications (Todoric *et al.*, 2016).

Whilst these six properties initiate tumour development and progression, the ability of cancer cells to evade apoptotic cell death and to continue to proliferate unimpeded play a crucial role in the continuation of cancer progression and increased tumour volume.

1.2.4.1 Cell cycle dysregulation in cancer

With two of the hallmarks of cancer being a self-sufficiency in supply of growth signals and an insensitivity to anti-growth signals it is important to know what mechanisms have been modified to result in these characteristics (Hanahan & Weinberg, 2011). Research has shown that mutations and deficiencies in the regulation of the cell cycle result in the cancer cells ability to constantly divide, resulting in the formations of cancers (Wiman & Zhivotovsky, 2017). Of these mutations, those to proteins involved with the cell cycle restriction checkpoints - such as p53, pRb, CDK and cyclin pathways - are particularly associated with the a lack of cell cycle regulation in cancer (Wenzel & Singh, 2018).

Mutations to the p53 gene are one of the most common mutations found within cancers, being identified in over 50 % of all human malignancies (Perri, Pisconti, & Scarpati, 2016). In non-cancer cells, expression levels of p53 are low, due to the protein's short lifespan. However, mutations in the genes coding for the p53 protein, along with increased cellular stress signals, can stabilise p53 resulting in increased activation and increased protein lifespan (Hickman, Moroni, & Helin, 2002). The majority of these mutations result from missense, which inhibit the specific binding of p53 to DNA and activating transcription (Wiman & Zhivotovsky, 2017). As a result, a loss of cell cycle regulation through p53 is observed (Soussi & Wiman, 2015).

Mutation to p53 also causes a deficiency in the transcription of p21, resulting in a lack of cell cycle arrest at the G_1/S phase checkpoint (Greenblatt, 1994). This lack of cell cycle arrest allows cells with damaged or mutated DNA to progress through the cell cycle, avoiding DNA repair mechanisms, and result in the formation of daughter cells containing the same DNA damage found in the parent cell (Wenzel & Singh, 2018). However, other checkpoints still possess the capability to stop abnormal cells progressing through the cell cycle before daughter cells can be made, thus preventing abnormal cells from transitioning through the cell cycle (Wiman & Zhivotovsky, 2017).

Further to this, mutations to p53 also have many downstream effects, which further enhance cancer cell survival and tumour progression. These effects include inducing dysfunctional reactions to DNA lesions, oxidative stress, immune system interactions, metabolic imbalance and tumour microenvironment development (Mantovani, Collavin, & Del Sal, 2019). In addition to this, mutations to p53 also results in

dysfunctional activity of downstream signalling pathways further enhancing cancer cells capability to survive (Hickman *et al.*, 2002).

The expression of pRB, a signalling molecule downstream of p53, has been shown to play a major role in the G_1 cell cycle checkpoint, blocking cell division and preventing entry into the S phase of the cell cycle (Giacinti & Giordano, 2006). In non-cancerous cells, anti-proliferative signals activate pRb, causing it to become dephosphorylated, and block interaction between cyclin/CDK complexes and pRB. This dephosphorylation inhibits the in the blocking of progression through the cell cycle at the G_1/S checkpoint (Dyson, 2016; Engel, Cress, & Santiago-Cardona, 2015). However, in cancer cells the gene which codes for Rb is functionally inactivated, either by direct mutation or indirectly via modified expression of upstream or downstream regulatory signalling molecules (Dunn, Phillips, Becker, & Gallie, 1988; Giacinti & Giordano, 2006; H. Liu, Dibling, Spike, Dirlam, & Macleod, 2004).

Direct mutations to pRb function arise either by preventing expression of the protein or by causing the production of a non-functional protein (Engel *et al.*, 2015). The direct inactivation of the Rb gene via chromosomal mutation has been described to be one of the main reasons for the loss of pRb function in human cancers (Giacinti & Giordano, 2006). Indirect inactivation of pRb results from hyperphosphorylation of pRb, causing it to be persistently inactivated. Hyperphosphorylation of pRb results from aberrant upregulation of the cyclin and CDK family of proteins, which under normal conditions tightly regulate the phosphorylation of pRb and the cells transition into the S phase of the cell cycle (Dick & Rubin, 2013; Mittnacht, 1998; Rubin, 2013). However, mutations relating to the expression of these proteins have a downstream effect on pRb activity.

Cyclin's, CDK's and their associated complexes are key regulators of progression through the cell cycle. However, in cancers both cyclins and CDK's are found to have significantly upregulated expression (Bendris *et al.*, 2015; Casimiro, Crosariol, Loro, Li, & Pestell, 2012). Aberrant expression of multiple cyclins has been observed across multiple cancer types, with cyclins B, D and E all being shown to be overexpressed in Human cancers (Casimiro *et al.*, 2012; Wiman & Zhivotovsky, 2017). The overexpression of these cyclins as well as CDK4 and CDK6 have been shown to occur due to chromosomal translocations, or by abnormal gene amplification (Bendris *et al.*, 2015; Bortner & Rosenberg, 1997; Wiman & Zhivotovsky, 2017). This abnormal

increase in the expression of cyclins and CDK's result in significant effects on downstream signalling pathways. Increased expression of cyclins and CDK's increases the phosphorylation state of pRb to a hyperphosphorylated state, leading to inactivation of pRb, the activation of E2F and ultimately the dysfunction of the G_1/S cell cycle checkpoint (Du & Searle, 2009; Wiman & Zhivotovsky, 2017).

Whilst these mutations and dysfunction to the cancer cell cycle are important mechanisms by which cancer cells maintain their proliferative potential, other key mechanisms such as immune cell evasion and avoidance of cell death pathways are important in cancers progression and development.

1.2.4.2 Apoptosis evasion in cancer

Cancer cells have developed multiple mechanisms to avoid regulated cell death which ultimately avoids their clearance by the immune system. These mechanisms include the dysfunction of p53, upregulation of BCL-2 expression, downregulation of pro-apoptotic proteins, modifications to the death receptor pathway, the activation of pro-survival pathways and the development of decoy proteins (Chen, Jia, Song, & Zhang, 2018; Sharma, Boise, & Shanmugam, 2019; M. Wang *et al.*, 2017).

Over 50 % of all cancers possess p53 defects (Fernald & Kurokawa, 2013). The p53 protein regulates a number of processes that have a direct role in regulating cellular sensitivity to apoptosis via both the intrinsic and extrinsic apoptosis pathways (Kasibhatla & Tseng, 2003). In cancerous cells, a loss of p53 function or deletion of the p53 gene results in the downregulation of proapoptotic proteins BAX, BID, PUMA and NOXA, in addition to upregulating the anti-apoptotic protein BCL-2 (Fernald & Kurokawa, 2013; Sharma *et al.*, 2019; Zheng, 2017). These modifications to protein expression results in the inhibition of p53 mediated apoptosis due to BCL-2 supressing cytochrome C release from mitochondria via the inhibition of BAK, BAX and BID (Zheng, 2017).

Genetic abnormalities found in multiple cancer cell types are capable of generating novel or dysfunctional signalling proteins (Anderson *et al.*, 2011; Huang *et al.*, 2011; Moore, Beghelli, Zamboni, & Scarpa, 2003; Testa, Pelosi, & Castelli, 2018). A key example of this is the leukemic BCR-ABL genetic translocation, which produces an "always on" tyrosine kinase, resulting in the induction of uncontrollable cell division and inhibition of apoptosis (Kang *et al.*, 2016). BCR-ABL has been described to activate

the JAK-STAT, PI3K and RAS/MEK/ERK pathways, all of which increase cell survival, cell proliferation and the inhibition of apoptosis (Chen, Peng, Sullivan, Li, & Li, 2010; Cilloni & Saglio, 2012; Lovly & Shaw, 2014).

Cancer cells also exhibit a reduced response to death receptor pathways (Fulda, 2009). Defects include the downregulation of the Fas receptor on cancer cells inhibiting the activation of the extrinsic pathway of apoptosis (M. Wang *et al.*, 2017; X. Wang, Fu, Chen, & Liu, 2017). Additionally, cancer cells are capable of expressing non-functional Fas receptors or may secrete soluble Fas receptors, which sequester Fas ligands, preventing them from binding to cellular receptors (Kolben *et al.*, 2018; Owen-Schaub, 2001).

Additionally, defects to TRAIL receptors have also been described in multiple cancer cell types (Shin *et al.*, 2001; Voelkel-Johnson, 2011; Zhang & Fang, 2005; Zhang & Zhang, 2008). Abnormalities in the transport of TRAIL receptors to the extracellular membrane from the endoplasmic reticulum following their synthesis by cancer cells has been shown to confer resistance to apoptosis and inhibit TRAIL induced extrinsic apoptosis (Fulda, 2009; Jin, McDonald Iii, Dicker, & El-Deiry, 2004). Furthermore, cancer cells may also overexpress decoy receptor 3, which competitively binds to the ligands known to induce TRAIL mediated apoptosis thus inhibiting TRAIL induced apoptosis (Roth *et al.*, 2001; Wang *et al.*, 2013; Yuan *et al.*, 2018).

Cancer cells have also been described to dysregulate multiple anti-apoptotic and pro-survival pathways including: Protein kinase B (AKT), ERK and NF-κB to avoid undergoing apoptosis (Dolcet, Llobet, Pallares, & Matias-Guiu, 2005; A. H. Kim, Khursigara, Sun, Franke, & Chao, 2001; Samatar & Poulikakos, 2014; X. Zhang, Tang, Hadden, & Rishi, 2011). The abnormal activation of these pathways via hyperphosphorylation ensure that cancer cells downregulate pro-apoptotic signals whilst also upregulating pro-survival gene expression (Fernald & Kurokawa, 2013). The activation of NF-κB upregulates expression levels of Survivin, BCL-2, BCL-X_L and XIAP, which leads to mitigation of pro-apoptotic signals and enhancement of cell survival (Diping Wang *et al.*, 2009; Zheng, 2017).

These mechanisms allow cancer cells to avoid apoptotic processes and continue to proliferate and differentiate. However, these mechanisms offer key targets for

chemotherapeutic intervention to prevent cancer cell proliferation and induce apoptosis.

1.2.5 Cancer treatment strategies

Following diagnosis with cancer, multiple treatment options are available. These options include surgery, radiotherapy and chemotherapy (CRUK, 2021b). Treatment via surgery employs the use of surgical techniques to excise and remove cancerous tissue and cells from their site of growth (CRUK, 2021b). Surgical treatment is the primary option for solid tumour-based cancers, with it not being an option for circulating cancers such as blood-borne cancers. This treatment method however varies in effectiveness dependent on the cancer type, the size of the tumour, the stage of the cancer at the time of treatment, the presence of metastases and blood vessel involvement (CRUK, 2021a).

Radiotherapy utilises high doses of radiation to shrink tumour volumes and kill cancerous cells (Horn, Morild, & Dahl, 1990). Radiotherapy can be targeted towards the site of tumour growth, with the aim of only targeting cancerous cells with a minimal impact on heathy cells. Despite this, radiotherapy does have numerous side effects which may have a detrimental effect on the patient during and after treatment. Due to this radiotherapy is commonly employed alongside other treatment options including surgery and chemotherapy to limit patient exposure to radiation and increase the likelihood of complete cancer eradication.

Approximately 45 % of all patients undergo surgery as a part of their cancer treatment, whilst 27 % undergo radiotherapy (CRUK, 2021a). However, chemotherapeutic agents are employed for nearly all cancers during the course of treatment, irrespective of cancer type, in order to either shrink tumours, eradicate cancer cells, or target metastatic cancers.

1.2.6 Chemotherapeutic treatment of cancer

Chemotherapeutic therapies use chemical compounds to prevent cancer growth or kill cancerous cells (CRUK, 2021a). There are currently 150 chemotherapeutic drugs approved for clinical use by the US Food and Drug Administration (USFDA) (Kinch, 2014; Sun *et al.*, 2017). Of these 150 approved drugs, 40 % are classical cytotoxic drugs, whilst 60 % are target-based therapeutics (Sun *et al.*, 2017).

Classical cytotoxic drugs directly target the DNA of cells preventing cell division or inducing cell death (Malhotra & Perry, 2003). Whilst this class of chemotherapeutic drugs remains effective and in use today, these drugs can induce DNA mutations resulting in chemotherapeutic resistance (Meegan & O'Boyle, 2019). These drugs also cause severe long- and short-term side-effects, effecting the quality of life of patients and shortening cancer patient's lifespan following treatment. This led to the development of a new generation of anti-cancer drugs which target the proteins with abnormal expression inside the cancer cells, known as targeted chemotherapeutic agents (Meegan & O'Boyle, 2019).

Target-based agents block the growth and spread of cancer through interacting with specific molecular targets that are involved in the pathways relevant to cancer growth, progression, and spread (Tseng & He, 2013). Of these, 44 % target plasma membrane proteins, 26 % target cytoplasmic proteins, 23 % target nuclear proteins and 7 % target proteins within the extracellular space (Sun *et al.*, 2017). Plasma membrane targets account for the greatest number of the targeted chemotherapeutics. This is due to these proteins being more easily accessible chemical targets as these targets do not require the drugs internalisation into the cell (Meegan & O'Boyle, 2019). Amongst the 45 plasma membrane targets, 21 were tyrosine kinase receptors, 12 were other transmembrane receptors, five were tumour cell antigens, and five were G-protein coupled receptors (Sun *et al.*, 2017). This is not the case in the nuclear targets with the majority of targeted molecules being enzymes rather than receptors. Nuclear receptors do still account for a high proportion of the nuclear targets with 43 % of all approved nuclear targeted therapies being directed at receptors within the nucleus of cancerous cells (Meegan & O'Boyle, 2019).

Whilst targeted chemotherapies are successful in specific types of malignancies; their effectiveness has been limited by the development of drug resistance and side effects against normal tissues and cells, similar to that of classical chemotherapeutic agents (Meegan & O'Boyle, 2019). Despite these issues, numerous types of both classical and targeted chemotherapeutics are still utilised clinically in the treatment of cancer today.

1.2.6.1 Alkylating agents

The alkylating agents were the first nonhormonal drugs to be used effectively in the treatment of cancer (Chen *et al.*, 2018; Drabløs *et al.*, 2004; Kondo, Takahashi, Ono, & Ohnishi, 2010). There are multiple types of alkylating agents currently used as chemotherapeutic agents and include Nitrogen mustards, Oxazaphosphorines, Ethylene imines, Nitrosoureas, Alkyl alcane sulfonates, Triazenes and hydrazines along with platinum-based complexes (Drabløs *et al.*, 2004). Common alkylating agents used clinically, shown in figure 1-15, include; cisplatin, carboplatin, melphalan, cyclophosphamide, dacarbazine, mitomycin c, streptozotocin and chlorambucil (Fu, Calvo, & Samson, 2012).

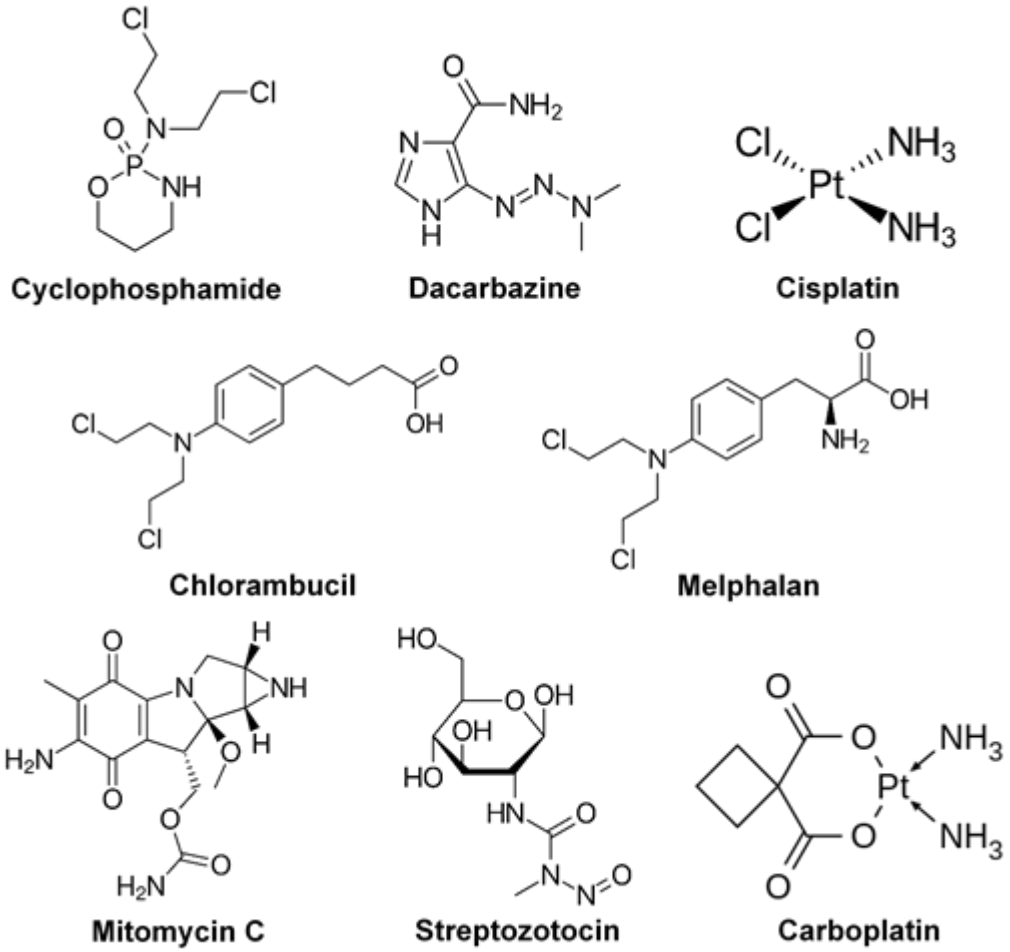

Figure 1-15. The chemical structures of alkylating agents commonly used as chemotherapeutic agents.

Alkylating agents irreversibly interact, either directly or through intermediaries, with several types of biological molecules, including amino acids, thiols, ribonucleic acid (RNA), and DNA (Middleton & Margison, 2003; Oronsky, Reid, Knox, & Scicinski,

2012). It is generally accepted that the cytotoxic effects of the alkylating agents are a result of their reactions with DNA (Oronsky *et al.*, 2012).

Alkylating agents behave as electrophilic entities that react with the nucleophilic regions of DNA or proteins causing the covalent transfer of an alkyl group (Gates, 2009; Puyo, Montaudon, & Pourquier, 2014). This is caused by the substitution of a hydrogen atom from the nucleophilic region of the biological molecule targeted with the alkyl group of the alkylating agent (Puyo *et al.*, 2014).

The alkylating class of anti-cancer agents can target cells in any stage of the cell cycle as well as being able to target resting cells and those that are actively dividing (Ralhan & Kaur, 2007). However, it has been shown that these drugs show increased activity against cells in the G_1 or S phases of the cell cycle (Ralhan & Kaur, 2007).

This covalent interaction of alkylating agents mediate cell death through interference with DNA structure and function via the formation of DNA crosslinks, inactivation of DNA repair enzymes, and cell membrane damage (Middleton & Margison, 2003; Oronsky *et al.*, 2012; Ralhan & Kaur, 2007). In addition, alkylating agents induce mutations in the genetic code of the DNA and the formation of mispaired nucleotides. This results in the formation of abnormal or non-functional proteins following transcription and translation (Puyo *et al.*, 2014) and ultimately result in cell death.

1.2.6.2 Intercalating agents

Intercalating agents target DNA within cells and insert themselves between the aromatic ring between base pairs of the DNA, as shown in figure 1-16 (Baguley, 1991; Lerman, 1961; Wheate, Brodie, Collins, Kemp, & Aldrich-Wright, 2007). For intercalation to occur, changes to the sugar phosphate structure of the DNA are required to allow the intercalating molecule to insert between the base pairs (Brana, Cacho, Gradillas, Pascual-Teresa, & Ramos, 2001). Following this structural change, the intercalating agent can insert within the minor groove of the DNA, where it is stabilised in position by an electrostatic interaction between the drug and the phosphate backbone of the DNA (Goftar, Kor, & Kor, 2014; Wheate *et al.*, 2007).

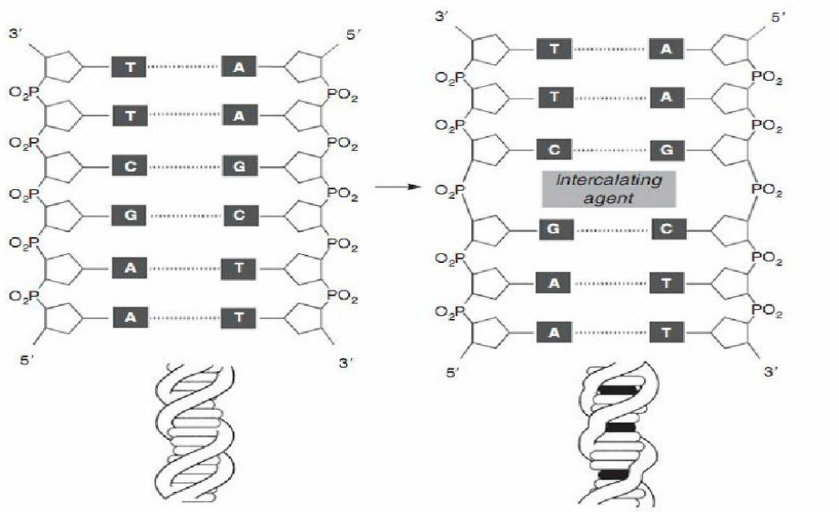

Figure 1-16. The mechanism by which intercalating agents interact with cellular DNA.

Intercalating agents bind between the base pairs of DNA and results in modifications to the DNA structure. **Left.** Shows the normal DNA structure. **Right**. Shows the changes to DNA structure following the introduction of an intercalating agent between base pairs. Figure adapted from Goftar *et al.*, 2014.

The insertion of the intercalating agent into the DNA helix results in a substantial change in the structure of the DNA (Berman & Young, 1981; Wheate *et al.*, 2007) leading to DNA lengthening, stiffening or unwinding (Berman & Young, 1981). It is thought these changes prevent DNA replication and thereby inhibit further growth of cancers. (Brana *et al.*, 2001; Goftar *et al.*, 2014; Wheate *et al.*, 2007).

Alternatively, this causes cell death due to interference with the recognition and function of DNA excise and repair proteins, such as polymerases, topoisomerases I and II, and transcription factors (Goftar *et al.*, 2014; Wheate *et al.*, 2007). As a result of this interference, cells can no longer divide and ultimately die due to the induced DNA damage (Rescifina, Zagni, Varrica, Pistarà, & Corsaro, 2014). For any cells that manage to survive the direct damage induced by intercalating chemotherapeutics, the elongation of the DNA required for the introduction of the intercalator can cause DNA slippage (Wheate *et al.*, 2007). This leads to insertion/deletion mutations occurring within the DNA during replication and ultimately results in cell death or inhibition of division during re-entry into the cell cycle in the following cell division cycle (Leung & Shilton, 2015).

Commonly used clinical examples of intercalating chemotherapeutic agents, shown in figure 1-17, include compounds of the families of naphthylamides, anthracyclines, actinomycin's and echinomycin's (Goftar *et al.*, 2014).

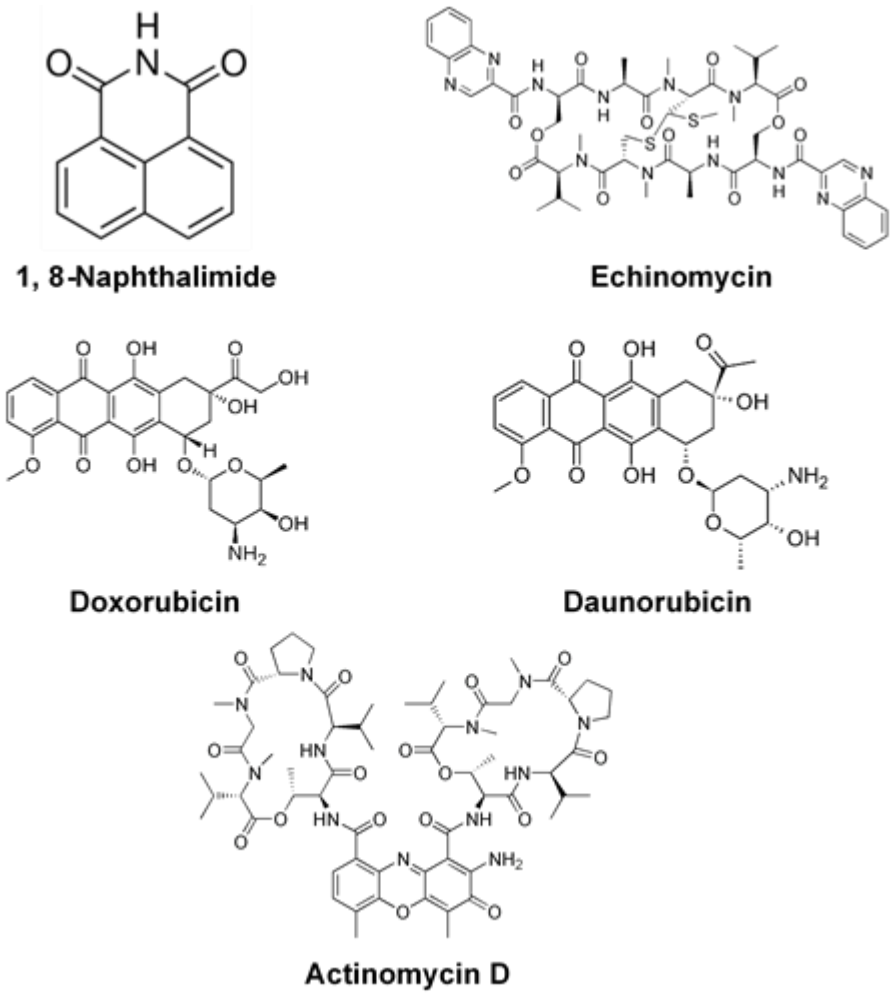

Figure 1-17. The chemical structures of intercalating agents commonly used as chemotherapeutic agents.

1.2.6.3 Topoisomerase inhibitors

Topoisomerase inhibitors, (also known as topoisomerase toxins) are a class of chemotherapeutic agents that target the nuclear enzymes topoisomerase I and topoisomerase II (Sordet, Khan, Kohn, & Pommier, 2003). Topoisomerase I and II are normal cellular enzymes that are found in the nucleus of mammalian cells and are required for normal DNA replication and cellular division (Liu, Qu, Meng, & Shou, 2019; Sinha, 1995).

These enzymes create and then repair single and double stranded nicks in cellular DNA. The nicks allow for the untangling and relaxation of supercoiled double stranded DNA, so that replication can proceed (Liu, Qu, *et al.*, 2019). They also pass double-stranded DNA through the nick to allow relaxation of over-coiled DNA (Hande, 2008; Kellner, Sehested, Jensen, Gieseler, & Rudolph, 2002). The activity of the topoisomerases are highly amplified in rapidly dividing cells and in cancerous cells (Sinha, 1995).

Numerous compounds, shown in figure 1-18, such as camptothecin, irinotecan, topotecan, etoposide, doxorubicin, idarubicin and mitoxantrone have been approved by the USFDA as topoisomerase inhibitors. This class of compounds have been for the treatment of numerous cancers including; ovarian, lung, colorectal, lymphoma, testicular, neuroblastoma, acute lymphocytic leukaemia (Bardal, Waechter, & Martin, 2011).

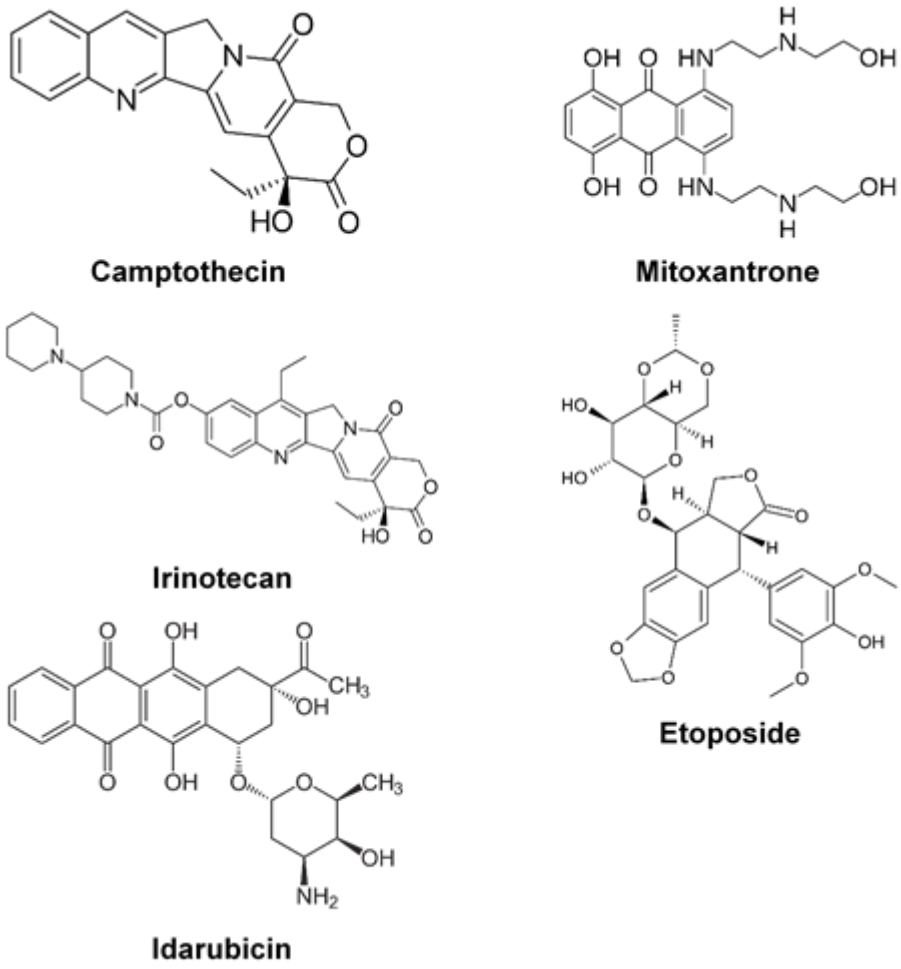

Figure 1-18. The chemical structures of topoisomerase inhibitors commonly used as chemotherapeutic agents.

These agents bind to the DNA topoisomerase complex formed during DNA replication and prevent the sealing of DNA following the formation of single and double stand breaks during the normal DNA repair mechanism (Kuroda, Kagawa, & Fujiwara, 2014). Topoisomerase inhibitors also block the ligation step within the cell cycle, resulting in a cell cycle arrest at the G_2/M stage of the cell cycle (Clifford, Beljin, Stark, & Taylor, 2003; Guo, Liu, Nishikawa, & Plunkett, 2007; Lee & Berger, 2019; Walsby, Coles, Knapper, & Burnett, 2011; Wu *et al.*, 2010). The accumulation of these breaks in the DNA and the inducement of a G_2/M cell cycle arrest results in the inability of DNA to replicate and ultimately results in cell death (Hande, 2008; Lee & Berger, 2019; Liu, Qu, *et al.*, 2019).

1.2.6.4 Anti-metabolites

Anti-metabolites are a class of chemotherapeutics that act as analogues of naturally occurring compounds, which interfere with key metabolic processes (Backus *et al.*, 2001). As a result, these drugs inhibit essential metabolic processes (Galmarini, Mackey, & Dumontet, 2002) via their interaction with key enzymes, leading to the synthesis of aberrant molecules or inhibit the activity of the enzyme (Chen *et al.*, 2014; Xing *et al.*, 2017). However, the enzymes inhibited by anti-metabolites are present in normal cells, though selectivity towards cancer cells is apparent due to their faster division rates (Avendaño & Menendez, 2015).

Amongst the compounds classified as anti-metabolites there are two key types that can be distinguished (Lancellotti, Zamorano, & Galderisi, 2016). These include the antifolates and the pyrimidine analogues, shown in figure 1-19. Approved antifolates for clinical use include methotrexate and pemetrexed (Lancellotti *et al.*, 2016). The pyrimidine analogues approved for clinical use as chemotherapeutics include cytarabine, hydroxyurea, 5-fluorouracil, capecitabine, and gemcitabine (Lancellotti *et al.*, 2016).

Pyrimidine analogues interfere with the synthesis of nucleic acids (Galmarini *et al.*, 2002) by incorporating abnormal DNA bases into synthesising DNA. This interferes with the function of key nucleic enzymes including DNA polymerases, endonucleases and ligases (Galmarini *et al.*, 2002; Lancellotti *et al.*, 2016).

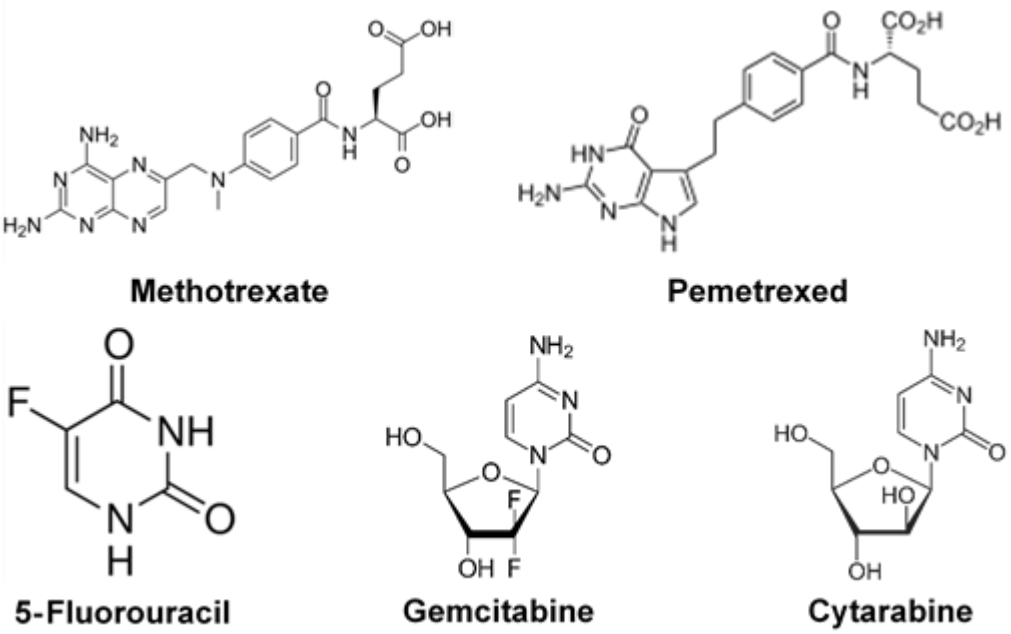

Figure 1-19. The chemical structures of anti-metabolites commonly used as chemotherapeutic agents.

Antimetabolites also have an impact on the cell cycle of cancer cells (O'Connor & Fan, 1996) can induce a cell cycle arrest at the G_1/S phase border (Backus *et al.*, 2001; Chen *et al.*, 2014; Z. Shi *et al.*, 2001; Xing *et al.*, 2017). Specifically, methotrexate and 5-fluorouracil arrest cell cycle progression at the G_1/S phase border as well as in S phase of the cell cycle (Shin *et al.*, 2001; Xing *et al.*, 2017). The result of cell cycle arrest is the inducement of cell death (Chen *et al.*, 2014).

1.2.6.5 Anti-mitotic agents

Anti-mitotic agents are a group of compounds that are designed to interrupt the mitotic stage of the cell cycle, which ultimately resulting in a cell cycle arrest and the inducement of apoptotic cell death (Chi *et al.*, 2019; Tischer & Gergely, 2019). Currently, all anti-mitotic drugs approved for clinical use target the microtubules, with the Taxane and Vinca alkaloid classes of compounds, shown in figure 1-20, showing success against a variety of cancer types (Chi *et al.*, 2019; Gascoigne & Taylor, 2009; Qi *et al.*, 2018; Tischer & Gergely, 2019).

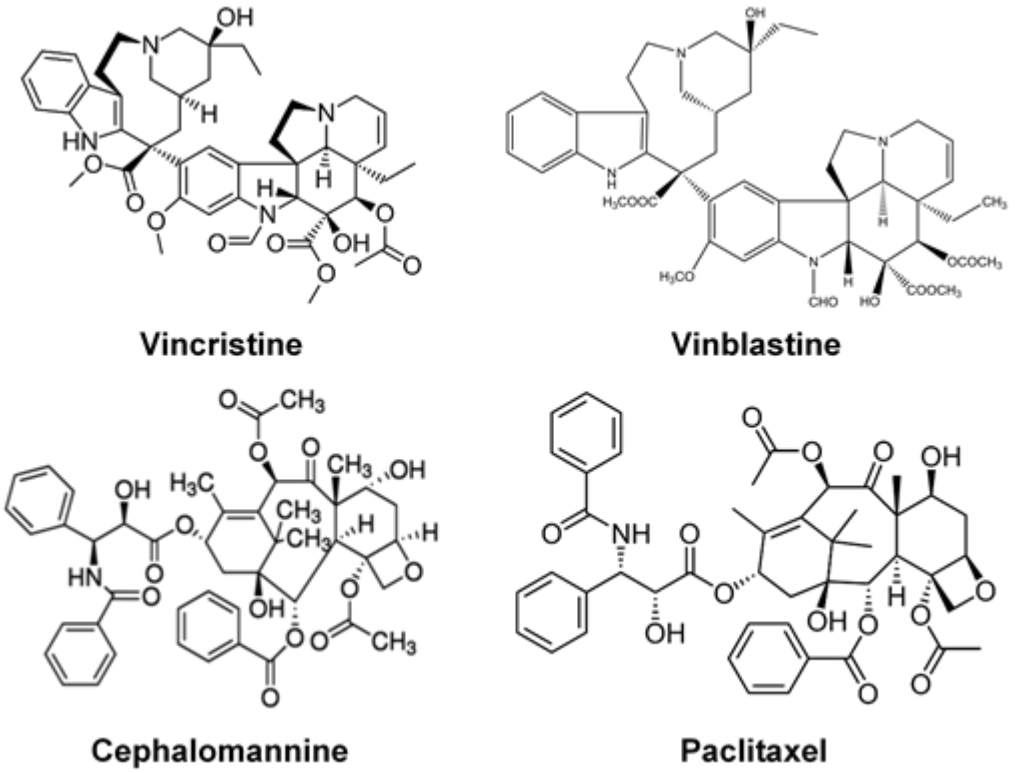

Figure 1-20. The chemical structures of anti-mitotic agents commonly used as chemotherapeutic agents.

Both classes of approved anti-mitotic drugs disrupt the formation of the mitotic spindle and cause cells to become unable to complete mitosis in the conventional manner (Chi *et al.*, 2019; Gascoigne & Taylor, 2009). Microtubule-active compounds generally bind to one of three main classes of sites on tubulin, the paclitaxel site, the *Vinca* domain and the colchicine domain (Jordan & Wilson, 2004). Drugs bound to these sites disrupt essential mitotic spindle dynamics to stop or delay cells from exiting the mitotic stage of the cell cycle (Tischer & Gergely, 2019).

This disruption occurs either by inhibition of microtubule polymerisation, causing microtubule destabilisation (Penna, Henriques, & Bonatto, 2017), or by enhancing polymerisation of the microtubules, resulting in microtubule hyper stabilisation (Jordan & Wilson, 2004; Penna *et al.*, 2017). Stabilisation of the microtubules by compounds such as Taxol, prevents the normal function of the mitotic spindles through the prevention of correct orientation of the chromosomes during mitosis (Gascoigne & Taylor, 2009). The inability to correctly orientate the chromosomes causes a chronic activation of the spindle activation checkpoint, which leads to mitotic arrest (Gascoigne & Taylor, 2009; Shi & Mitchison, 2017). This mitotic arrest can either cause cells to

undergo cell death in the mitosis stage of the cell cycle or undergo a process known as cell cycle slippage (Shi & Mitchison, 2017). Slippage causes cells under mitotic arrest to abnormally re-enter the cell cycle at the G_1 stage of the cell cycle. The entry of abnormal cells into the G_1 stage of the cell cycle can result in one of three outcomes: (1) a return of the abnormal cell to the normal cell cycle, (2) arrest at the G_1 checkpoint or (3) cell death in the G_1 stage (Penna *et al.*, 2017; Qi *et al.*, 2018; Shi & Mitchison, 2017).

Other studies have shown that even at low concentrations, microtubule targeting agents can supress microtubule dynamics without changing the microtubule mass, causing a slowing of cell division or even inducing mitotic block and ultimately resulting in apoptosis (Jordan & Wilson, 2004).

1.2.6.7 Targeted chemotherapeutic agents

The examples given previously are all classical chemotherapies and target all cells in body. Targeted therapies are a new generation of chemotherapeutic treatment designed to interfere with specific molecular targets within a cancer cell (Huang, Shen, Ding, & Geng, 2014; Sawyers, 2004). Targeted chemotherapeutic agents are composed of small molecule compounds and monoclonal antibodies, either individually or conjugates of the both. Monoclonal antibodies have been used to deliver chemotherapeutic drugs and radioactive substances and prodrugs enzyme activators, directly to cancer cells (Padma, 2015). These therapies typically target proteins expressed by cancer cells that are believed to play a critical role in tumour growth or progression (Baudino, 2015; Huang *et al.*, 2014; Padma, 2015; Sawyers, 2004).

These protein targets have been identified through comparative studies of human cancer tissues and normal tissues, to identify cancer cell specific antigens or proteins that are exclusively expressed in cancer cells (Chari, 2008). Further to this, more recent advancements in the field of personalised medicine have allowed it to become possible to specifically target treatments towards an individual patients' cancers (Baudino, 2015).

The first use of targeted chemotherapeutic agents was seen during the treatment of chronic myeloid leukaemia in which the malignancy is driven by the development of a BCR-ABL translocation with the ABL small molecule inhibitor called Imatinib (Druker *et al.*, 2006; O'Brien *et al.*, 2003). Because this translocation occurs in essentially all

patients with chronic myeloid leukaemia, Imatinib therapy results in a complete hematologic response in 98 percent of patients (Gerber, 2008).

Since then numerous monoclonal antibody therapies have been introduced including; rituximab for B-cell lymphomas, trastuzumab for breast cancer, alemtuzumab for certain leukaemia's, and cetuximab, panitumumab, and bevacizumab for colorectal cancers (Baudino, 2015; Chari, 2008; Gerber, 2008). The advantages of using antibodies as a treatment for cancer is that they maintain within circulation for several days or weeks in Humans (Gerber, 2008). In addition to this, monoclonal antibodies are commonly non-toxic when within circulation and only become toxic once they have bound to their target antigen on cancerous cells (Chari, 2008).

As a result of their high specificity for their molecular target, highly specific pathways within cells or on cancer cell membranes can be targeted (Baudino, 2015). These can be targeted through numerous mechanisms including; molecules that bind to specific receptor sites on cells, those that prevent ligand binding, those that inhibit molecular signalling and those that interfere with signalling molecules downstream from the receptor (Gerber, 2008).

Ultimately, the effectiveness of targeted chemotherapeutic agents lies in targeted release of chemotherapeutics at the disease site, whilst minimising the off-target side effects caused to normal tissues, seen in classical chemotherapeutic options (Baudino, 2015; Druker *et al.*, 2006; Gerber, 2008; Padma, 2015).

1.2.7 Cancer treatment side effects

Despite chemotherapeutic agents being highly effective against a wide variety of cancers, they are associated with severe and often life altering side effects (Nurgali, Jagoe, & Abalo, 2018). These side effects commonly defined as acute and chronic effects. The acute side effects occur within the first 0 - 6 months following the start of treatment, and include anaphylaxis, nausea and vomiting, diarrhoea, pain, alopecia and asthenia. However, it is the chronic effects of chemotherapy which are particular severe and can last for the remainder of the patients life (Islam, Anggondowati, *et al.*, 2019; Partridge, Burstein, & Winer, 2001).

1.2.7.1 Chronic side effects associated with chemotherapeutic agents

Commonly occurring chronic side effects include cytopenia's (including leukopenia and neutropenia, thrombocytopenia, and anaemia), hepatotoxicity, ototoxicity, cardiotoxicity, nephrotoxicity, mucositis, stomatitis, anorexia and the psychological effects (Coates *et al.*, 1983; Kayl & Meyers, 2006; Lemieux, Maunsell, & Provencher, 2008; Oun, Moussa, & Wheate, 2018; Tao, Visvanathan, & Wolff, 2015). However, of these the most severe are cardiotoxicity, neurotoxicity, nephrotoxicity and gastrointestinal toxicity.

Nearly all chemotherapeutic agents result in some form of cardiotoxic effect, summarised in table 1-3. These effects can include reversible heart failure and in life-threatening arrhythmias following treatment with alkylating agents and microtubule inhibitors (Monsuez, Charniot, Vignat, & Artigou, 2010). Myocardial ischemia has also been observed following treatment with the antimetabolite class of chemotherapeutic agents (Monsuez *et al.*, 2010). The cardiac side effects are believed to result from induction of oxidative stress and cardiac myocyte apoptosis. The induction of apoptosis has been described to be a direct result of off target cytotoxicity of chemotherapeutic agents (Florescu, Cinteza, & Vinereanu, 2013). This results in cytotoxicity towards the cardiac myocardium in addition to the cancer cells.

Table 1-3. **A summary of the cardiovascular related complications arising following treatment with a variety of different chemotherapeutic agents.**
Table modified from Florescu *et al.* (2013).

Chemotherapeutic agent	Cardiovascular effects
Anthracyclines	Left ventricular dysfunction, heart failure, myocarditis and arrhythmia
5-fluorourcil	Ischemia, heart failure, pericarditis and cardiogenic shock
Taxanes and vinca alkaloids	Sinus bradycardia, ventricular tachycardia, atrioventricular block and Heart failure, ischemia
Cyclophosphamide	Heart failure (neurohumoral activation) and mitral regurgitation
Trastuzumab	Heart failure, left ventricular dysfunction and arrhythmia
Tamoxifen	Thromboembolism and cholesterol metabolism anomalies
Bevacizumab	Hypertension and thromboembolism

Further to this, chemotherapy drugs have also been described to damage the sub cellular organelles within the cardiac myocardium (Schimmel, Richel, van den Brink, & Guchelaar, 2004). Furthermore, hERG interaction and associated arrythmia is a common issue (Florescu *et al.*, 2013; Mladěnka *et al.*, 2018). Furthermore, chemotherapeutic agents have also been shown to target the electron transport chain of cardiac mitochondria, this leads to significant increases in reactive oxygen species and results in further damage to cardiac myocytes alongside disruption to key mechanisms involved in cardiac contractility and calcium handling (Gille & Nohl, 1997).

Treatment with chemotherapeutic agents can also damage the renal system. This damage arises due to excretion of the chemotherapeutics thus accumulation in the kidneys actively damaging the nephrons and tubular cells (Oun *et al.*, 2018; Pabla & Dong, 2012). Renal toxicity is a particular issue with the platinum based chemotherapeutic agents such as cisplatin and carboplatin (Pabla & Dong, 2008, 2012). The specific sensitivity of tubular cells to cisplatin is partly attributed to the fact

that they accumulate the drug more readily than other cells and tissues (Miller, Tadagavadi, Ramesh, & Reeves, 2010) leading to apoptosis or necrosis (Pabla & Dong, 2008; Pabla, Murphy, Liu, & Dong, 2009). Furthermore, the accumulation of chemotherapeutic drugs also causes a significant inflammatory response, which has been shown to further aggravate any predisposed renal injury (Zhang, Ramesh, Norbury, & Reeves, 2007).

Nearly all chemotherapeutic agents induce some form of gastrointestinal complaint during and indeed after the course of treatment (Escalante, McQuade, Stojanovska, & Nurgali, 2017). The most common of these complaints are diarrhoea and constipation (Escalante *et al.*, 2017). These arise due to the development of oral and gastrointestinal mucositis and ulceration (Cinausero *et al.*, 2017). This damage can lead to anorexia, malabsorption, weight loss, anaemia, fatigue and an increased risk of developing sepsis (Cinausero *et al.*, 2017; McQuade, Stojanovska, Abalo, Bornstein, & Nurgali, 2016; Nurgali *et al.*, 2018).

Many chemotherapeutic drugs, including vinca-alkaloids, cisplatin and the taxanes induce central and peripheral neurotoxicity (Newton, 2012; Nurgali *et al.*, 2018; Sundar *et al.*, 2017; Verstappen, Heimans, Hoekman, & Postma, 2003). This toxicity occurs via direct damage to neurons or glia, or indirectly by altering the surrounding microenvironment, such as localised vascular injury (Myers, 2009). Neurotoxicity results in headaches, seizures, ataxia, movement disorders, encephalopathy syndrome, cerebrovascular complications including strokes and the increased likelihood of the development of secondary malignancies (Haykin, Gorman, Van Hoff, Fulbright, & Baehring, 2006; Kerckhove *et al.*, 2017; Land *et al.*, 2007; Magge & DeAngelis, 2015; Newton, 2012; Rao & Camilleri, 2010).

Oxidative stress underpins many chronic side effects associated with chemotherapeutic agents. The drugs of many classes of chemotherapeutic agents are known to generate a high level of oxidative stress in biological systems. These classes of drugs include the anthracyclines, alkylating agents, platinum-coordination complexes, epipodophyllotoxins, and camptothecins (K. A. Conklin, 2004). The anthracyclines generate by far the highest levels of oxidative stress of all chemotherapy drugs (Conklin, 2004). The anthracycline quinone can affect the redox cycle after reductive activation by various reductase enzymes to its free semiquinone

(Langer, 2014; Monsuez *et al.*, 2010). This semiquinone can then react with oxygen to produce highly reactive oxygen species such as superoxide anion and hydrogen peroxide (Langer, 2014).

The mechanisms underpinning the increase in cellular oxidative stress include disruption of the electron transport chain, interference with mitochondrial function, interference with antioxidant systems and interaction with the drugs molecular structure with oxygen to produce oxygen radicals (Conklin, 2004; Yang, Villani, *et al.*, 2018; Zhang, Lei, Chen, Wang, & Qian, 2018). All these mechanisms combine to significantly increase levels of oxidative stress throughout the body

1.2.7.2 The impacts of chemotherapeutic side effects on patients

Studies on patients undergoing chemotherapy show patients rank the acute side effects as more severe than chronic ones. Several studies show that patients and their family perceive nausea, alopecia, fatigue, and vomiting as the most severe side effects (Carelle *et al.*, 2002; C. C. Sun *et al.*, 2005). These side effects have been shown to detrimentally influence the quality of life affecting willingness complete the course of treatment (Carelle *et al.*, 2002). Alongside these the severe chronic side effects have been shown to significantly decrease the life expectancy of patients following the completion of chemotherapy treatments compared to those without cancer (Cupit-Link *et al.*, 2017). In order to minimise these side-effects lower concentrations of chemotherapeutic agents are used clinically. Aside from reducing anti-cancer effectivity, the use of these lower concentrations has led to the development of chemotherapeutic resistance.

1.2.8 Chemotherapeutic resistance

Many patients of nearly all cancer types develop resistance chemotherapeutic agents, causing them to become unresponsive to treatment (Coley, 2008; Eramo *et al.*, 2006; Kim, 2016; Lehnert, 1998; Madan, Pal, Sartor, & Dahut, 2011; Meegan & O'Boyle, 2019; Rubin, 2013; Sonneveld & List, 2001). Drug resistance may be inherent, existing in a patient before treatment (intrinsic) or may develop as a consequence of the chemotherapeutic stimuli (acquired). Further to reducing primary treatment effectively, these mechanisms of resistance are also responsible for the majority of cancer relapses; one of the major causes of cancer related death (Raguz & Yagüe, 2008; Wang, Zhang, & Chen, 2019). Combined, 90% of chemotherapy failures during the

invasion and metastasis of cancers are related to drug resistance (Mansoori, Mohammadi, Davudian, Shirjang, & Baradaran, 2017; Yardley, 2013).

Chemotherapeutic drug resistance can be caused by multiple different mechanisms as, summarised in figure 1-21 include multi-drug resistance, cell death inhibition, alterations in drug metabolism, epigenetic and drug targets, enhancement of DNA repair, gene amplification and the presence of cancer stem cells (Luo, Solimini, & Elledge, 2009; Mansoori *et al.*, 2017; Meegan & O'Boyle, 2019; Oun *et al.*, 2018).

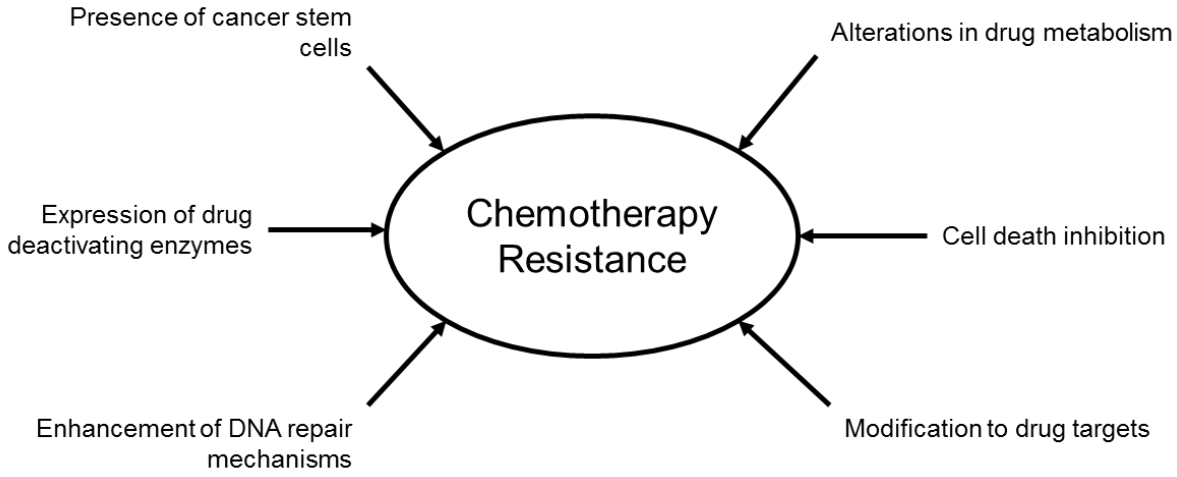

Figure 1-21. Mechanisms of chemotherapy resistance acquired by cancer cells allowing them to evade the cytotoxic activity of chemotherapeutic drugs.

The ability of cancer cells to become resistant to chemotherapeutic agents has posed a challenge in effectively treating patients. Cancer cells develop resistance as a result of mutations arising following treatment with chemotherapeutic agents. These mutations can result in the formation of key alterations in cancer cell function, which aim to minimise the effectiveness of chemotherapies.

A leading cause of resistance emerges because the toxicity associated with chemotherapeutic agents often necessitate a reduction of therapeutic dose and limits the therapeutic window (Pabla & Dong, 2012). This increases the likelihood that certain cells will survive the treatment process, imposing a selection pressure whereby drug-resistant cells survive then go on to multiply (Wang *et al.*, 2019).

Further to this, the uncontrolled cell division associated with cancer leads to high levels of genetic instability (Huang *et al.*, 2014). This instability increases the likelihood of mutations responsible for resistance to chemotherapeutic agents (Huang *et al.*, 2014), resulting in decreased efficacy to further chemotherapeutic treatment (Luo *et al.*, 2009; Pabla & Dong, 2012).

Of all genetic mutations associated with the formation of chemotherapeutic resistance, the most common one is a loss of p53 function, which has been identified in numerous cancer types (Luqmani, 2005). This loss of function results in cells that have damaged DNA but have the ability to continue to replicate (Luqmani, 2005). The damage to the DNA of cancer cells results in further genetic mutations. This leads to the loss of or abnormal function of numerous crucial cellular proteins and transporters associated with the elimination of chemotherapeutic drugs from cells or involved in detoxification of the cell (Coley, 2008; Luqmani, 2005). Key proteins and transporters associated with chemotherapeutic resistance include; ABC transporters, CYP450, MRP's and MDR1/P-glycoprotein (Alfarouk *et al.*, 2015; Lehnert, 1998; Luqmani, 2005; Mickley, Spengler, Knutsen, Biedler, & Fojo, 1997; Yardley, 2013).

Of these proteins, overexpression of MDR1/P-glycoprotein is observed in 30 - 40 % of all cancers and up to 50 % cancers that have metastasised (Lehnert, 1998; Mickley *et al.*, 1997). This makes it one of the key proteins involved in the formation of chemotherapy resistance. MDR1/P-glycoprotein acts as a cell membrane pump extruding a wide variety of structurally unrelated xenobiotics to the extracellular space to reduce their accumulation in cells (Zu, Yang, Tang, Han, & Ma, 2014). Research has shown that MDR1/P-glycoprotein to act in a protective role within non-cancerous cells (Luqmani, 2005). However, further studies have shown MDR1/P-glycoprotein to confer resistance within cancer cells by inhibiting Fas-induced caspase-3 activation and ultimately inhibiting apoptosis (Luqmani, 2005), in addition to participating in the efflux of chemotherapeutic agents out of the cell (Zu *et al.*, 2014).

In addition to MDR1/P-glycoprotein, other proteins have been described to be involved in the development of chemotherapeutic resistance in cancerous cells. Alfarouk *et al.* (2015) described that overexpression of CYP450, an enzyme involved in detoxification and metabolism of foreign chemicals, leads to the increased likelihood of chemotherapy resistance due to elevated detoxification of chemotherapeutic drugs within the cell (Alfarouk *et al.*, 2015; Rochat, 2005; Rodriguez-Antona & Ingelman-Sundberg, 2006). Another family of proteins of interest involved in the development of resistance to chemotherapeutic agents is that of the ABC transporters. ABC transporters are membrane transporter proteins which translocate a variety of molecules out of the intracellular milieu within eukaryotic cells (El-Awady *et al.*, 2017; Hollenstein, Dawson, & Locher, 2007; Wilkens, 2015). In chemotherapy resistant

cancer cells, an overexpression of ABC transporters has been observed. This overexpression results in the rapid efflux of the chemotherapeutic agents out of the cell before they can reach their target. This ultimately results in significantly decreased intracellular drug concentrations and a loss of the efficacy of the chemotherapeutic agent (Perez, 2009; Yardley, 2013).

Alterations of target protein expression and structure in cancer cells also confers resistance (Ji *et al.*, 2019; Mansoori *et al.*, 2017; Wang *et al.*, 2019). One example of this is tubulin, a key microtubule protein involved in cellular mitosis and the regulation of intracellular transport (Franker & Hoogenraad, 2013; Ilan, 2019). Alterations in the structure of tubulin, in addition to changes in tubulin expression is associated with chemotherapy resistance in cancer cells Lehnert (1998).

Resistance to chemotherapeutic drugs has also been observed against modern targeted chemotherapies. A key example of this is the genetic mutation of the BCR-ABL translocation, a hallmark of chronic myeloid leukaemia (CML) cells (Kang *et al.*, 2016; Ren, 2005). This genetic point mutation has been observed in 50 % of all resistant CML cancers (Raguz & Yagüe, 2008). This mutation results in the interference with the ability of targeted therapies, such as Imatinib, to bind to the BCR-ABL target, resulting in the targeted therapy becoming ineffective (Raguz & Yagüe, 2008).

Recent studies have shown that the presence of cancer stem cells (CSC's) play a major role in the development of chemotherapy resistance (Phi *et al.*, 2018; Prieto-Vila, Takahashi, Usuba, Kohama, & Ochiya, 2017). CSC's are derived from the dedifferentiation of cancer cells and normal cells, or mutation or oncogenic activation of normal stem cells (Phi *et al.*, 2018). These CSC's are similar to normal stem cells and possess the ability to self-renew and differentiate into heterogeneous cancer cell types (Phi *et al.*, 2018). Further to this CSC's have been shown to possess many other characteristics that allow them to survive chemotherapy, these include; inducing cellular dormancy, living in a vascular niche, being highly stable at hypoxic conditions, enhanced capability of repair enzymes, overexpression of drug efflux transporters, and expression of anti-apoptotic proteins (Dean, Fojo, & Bates, 2005; López-Lázaro, 2015; Phi *et al.*, 2018; Vinogradov & Wei, 2012).

These characteristics are key in the ability to reinitiate cancer formation and relapse following chemotherapeutic treatment (Dean *et al.*, 2005; Phi *et al.*, 2018; Vinogradov & Wei, 2012). In addition to this, CSC's possess the ability to become quiescent, through self-inducing a G_0 cell cycle arrest (W. Chen, Dong, Haiech, Kilhoffer, & Zeniou, 2016). This is important as many classical and currently used chemotherapeutic agents target actively dividing cells (Najafi, Mortezaee, & Majidpoor, 2019) and as a result cannot target cells that are no longer dividing. These CSC's can also accumulate drug resistance genes derived from previously chemotherapy exposed cancer cells that have dedifferentiated from resistant cancer cells (López-Lázaro, 2015; Prieto-Vila *et al.*, 2017; Vinogradov & Wei, 2012).

All of the complications associated with the use of therapeutic doses of conventional chemotherapeutic agents has resulted in them lowered in clinical practice. This decrease in concentration has not only reduced their immediate effectiveness but has led to the development of resistance (through the mechanism described in section 1.2.8). Combined these complications have resulted in a worsening of patient prognosis. As such, we must develop new chemotherapy drugs that are not only effective against cancer but also produce fewer side-effects. A leading candidate for these is the compounds derived from natural sources.

1.3 *Boswellia* as a potential chemotherapeutic source

1.3.1 Phytochemicals

Plants are an abundant and diverse source of non-nutrient but biologically active compounds known as phytochemicals (Doughari, Human, Benadé, & Ndakidemi, 2009). These phytochemical compounds can be isolated from nearly all parts of the plant including flowers, flower stigmas, pericarp, sprouts, fruits, seeds, roots, rhizomes, stem, leaf, bark and extracted resins (Iqbal *et al.*, 2017). However, studies suggest that only 10 % of the 250,000 known plant species being analysed for their biological activity (Cragg & Pezzuto, 2016; Farombi, 2003; Iqbal *et al.*, 2017), with only between 1 and 5 % of these plant species being robustly analysed for their therapeutic potential (Koparde, Doijad, & Magdum, 2019). This suggests that plants remain an untapped source of potentially biologically active compounds.

Plant derived compounds have been used in medicine for millennia, with a long history of use in the treatment of cancers and tumours (Hartwell, 1982). The first written records of the medicinal uses of plants appeared in about 2600 BC from the Sumerians and Akkaidians (Pezzani *et al.*, 2019; G. Samuelsson & Bohlin, 2017). Further ancient documents including the ancient Egyptian record known as the Ebers Papyrus, which documents over 700 drugs and represents the history of Egyptian medicine dating back from 1500 BC (Cragg & Newman, 2005). These practices are continued in traditional medicine today, mainly through traditional Chinese medicine and Ayurvedic Indian medicine (Fridlender, Kapulnik, & Koltai, 2015; Pezzani *et al.*, 2019). Phytopharmaceuticals used in these traditional practices are commonly prepared in the form of tinctures, teas, powders, poultices and decoctions (Choudhari, Mandave, Deshpande, Ranjekar, & Prakash, 2020). These traditional practices are now being further explored with modern scientific analysis describing many of these phytopharmaceuticals to be biologically active and their mechanisms of action requiring further elucidated (Choudhari *et al.*, 2020).

Today, many developing and developed nations still rely on plant-based compounds for the treatment of diseases and pathologies. According to the WHO, nearly 80% of the world's population uses phytomedicines for the management of various diseases (Khan, 2014). For example, in India approximately 65 % of the country's population regularly used phytomedicines as treatment options against a variety of disease types

(Roy *et al.*, 2019). Whilst on the continent of Africa, 80 % of the population utilise plant-based compounds in the form of traditional therapies for the treatment and management of a wide range of health conditions (Roy *et al.*, 2019).

In developed nations such as the USA the phytomedicine market is worth $14 billion a year and $40 billion worldwide (Pandey, Debnath, Gupta, & Chikara, 2011; Patwardhan, Vaidya, & Chorghade, 2004). This increase can be traced to the increasing cost of prescription drugs, as well as an increased demand in the field of personal health and wellbeing (Doughari *et al.*, 2009). Of all pharmaceutical prescriptions prescribed by clinicians in the USA, approximately 25 % contain a drug consisting of compounds originally derived from plants (Amin, Gali-Muhtasib, Ocker, & Schneider-Stock, 2009; Fridlender *et al.*, 2015; Pandey *et al.*, 2011). These phytomedicinal compounds are utilised today for a wide variety of different medical conditions such as for the treatment of inflammatory conditions, infection and cancer (J. Liu, Willför, & Xu, 2015).

Specifically, in the field of anti-cancer drug development, plants have played a key role in the development of numerous chemotherapeutic agents. There are four main classes of plant derived anti-cancer agents available on the pharmaceutical market today; these are the vinca alkaloids (vinblastine and vincristine), epipodophyllotoxins (etoposide and teniposide) the taxanes (paclitaxel and docetaxel) and the camptothecin derivatives (Desai *et al.*, 2008; Dholwani, Saluja, Gupta, & Shah, 2008; J. Liu *et al.*, 2015; Rowinsky, Onetto, Canetta, & Arbuck, 1992; Swamy, Purushotham, & Sinniah, 2021). However, all are associated with severe side effects and the development of resistance as previously described in sections 1.2.7 and 1.2.8. As a result, the urgent need for new compounds remains.

1.3.2 *Boswellia*

Boswellia is a genus of resin producing, shrub like trees, belonging to the family of *Burseraceae* (Abdel-Tawab, Werz, & Schubert-Zsilavecz, 2011). This genus is distributed throughout the Middle East, the Horn of Africa, India and China, shown in figure 1-22 (Al-Yasiry & Kiczorowska, 2016). There are currently over 30 different species of *Boswellia*, with the most common being *Boswellia serrata*, *Boswellia carterii*, *Boswellia sacra*, *Boswellia papyfera* and *Boswellia frereana* (Al-Yasiry & Kiczorowska, 2016; Assefa *et al.*, 2012; Bekana, Kebede, Assefa, & Kassa, 2014).

Figure 1-22. The geographical distribution of the *Boswellia* genus.

The *Boswellia* genus is distributed throughout the horn of Africa, the Middle East, India and China. Areas highlighted in red indicate regions of natural *Boswellia* growth.

All *Boswellia* species produce a resinous sap termed oleoresin (colloquially known as frankincense), which is extracted from the trees through incisions made into the trunk as shown in figure 1-23A (Hamm, Bleton, Connan, & Tchapla, 2005). This sap extrudes as a transparent, yellow-brown liquid (Abdel-Tawab *et al.*, 2011), which is then air dried to form the olibanum, a translucent white-pale/yellow solid, with an irregular, rounded appearance, shown in figure 1-23B (Abdel-Tawab *et al.*, 2011). The resins produced by each *Boswellia* species differ in their chemical composition according to environmental factors, such as climate, soil quality, elevation and humidity associated with each species' geographical location (Chen *et al.*, 2013).

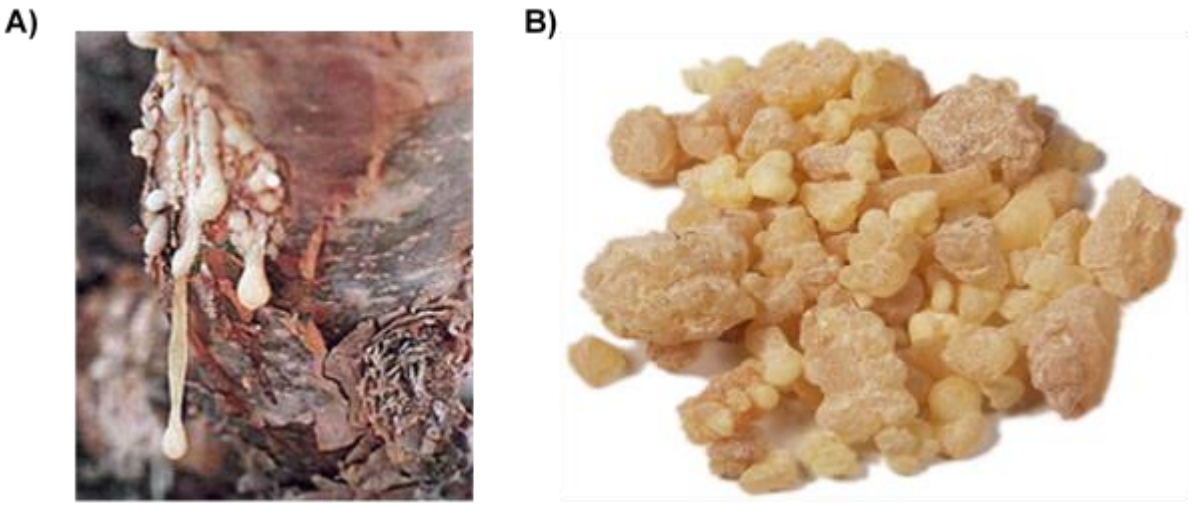

Figure 1-23. The extraction and airdrying of *Boswellia* olibanum.

Boswellia olibanum is extracted from the trunks of trees via excision of the bark. The *Boswellia* olibanum then leaks out to protect the tree from further damage (figure 1-23A). This olibanum is then harvested and airdried to form *Boswellia* oleoresins, shown in figure 1-23B.

Across all species of *Boswellia* the oleoresin typically contains essential oil (between 5 - 9 %), an alcohol insoluble fraction (25 - 30 %), and an alcohol soluble resin fraction of approximately (60 - 70 %) (Buchele, Estrada, Syrovets, & Schneider, 2006; Vuddanda, Singh, & Velaga, 2016). This alcohol soluble resinous fraction has been shown to contain numerous classes of molecules including monoterpenes, diterpenes, triterpenes, tetracyclic triterpenes and pentacyclic triterpenes (Vuddanda *et al.*, 2016). It is these pentacyclic triterpene molecules (further described in section 1.3.4) that are thought to be responsible for the biological activity of the *Boswellia* species. However, the apparent therapeutic effects of *Boswellia* has been recognised for centuries.

1.3.3 The historical use of *Boswellia* oleoresins in traditional medicine

Historically, the oleoresins of *Boswellia* have been used medicinally for millennia. The earliest recorded use of *Boswellia* in medicine was written on the 1550 BC text known as Ebers papyrus (Martinetz, Lohs, & Janzen, 1989), which states that preparations of *Boswellia Carterii* resins were used to treat tumours, carcinomas and oedemas (Aboelsoud, 2010). Further historical mentions of *Boswellia* are found in the journals of Hippocrates, who utilised *Boswellia* oleoresins for the treatment of stomach pains and diseases of the respiratory tract (H. Ammon, 2006; Martinetz *et al.*, 1989). *Boswellia* oleoresin preparations continued to be used by physicians until the early 20th century. However, due to a lack of scientific evidence behind its pharmacological and

clinical applications, the use of *Boswellia* oleoresins began to disappear from conventional medical treatment (H. Ammon, 2006).

To this day, *Boswellia* is utilised in ayurvedic Indian medicine and in traditional Chinese medicine for the treatment of a variety of pathologies (Ahmed, Abd-Rabou, Hassan, & Kotob, 2015; Ni *et al.*, 2012). Its use includes for the treatment of inflammatory conditions such as arthritis, ulcerative colitis, irritable bowel syndrome and asthma, as well as being used in the treatment of bacterial infections (Ernst, 2008; Ismail, Aluru, Sambasivarao, & Matcha, 2014). We now know that boswellic acids within these oleoresins are responsible for the biological activity.

1.3.4 Boswellic acids

First described in 1932, by Winterstein and Stein (1932) with chemical characterisation conducted by Büchele, Zugmaier, and Simmet (2003) identified 12 pentacyclic triterpene molecules within *Boswellia* oleoresin extracts, which were then named boswellic acids (Ammon, 2016). Since their discovery the boswellic acid family of molecules have been described to be the key biologically active molecules found within the oleoresin.

The major boswellic acids are characterised as two main isoforms based on their molecular structure, termed alpha and beta boswellic acids (Roy *et al.*, 2019). Alpha and beta boswellic acids have identical an molecular formula ($C_{30}H_{48}O_3$) with the only difference being the orientation of the triterpene structure as shown in figure 1-24. Key molecular variations in these pentacyclic triterpene structure, such as the addition of a ketone group on Carbon 18 and acetylation of the pentacyclic ring can result in the formation of numerous compounds also described in figure 1-24 (Roy *et al.*, 2019).

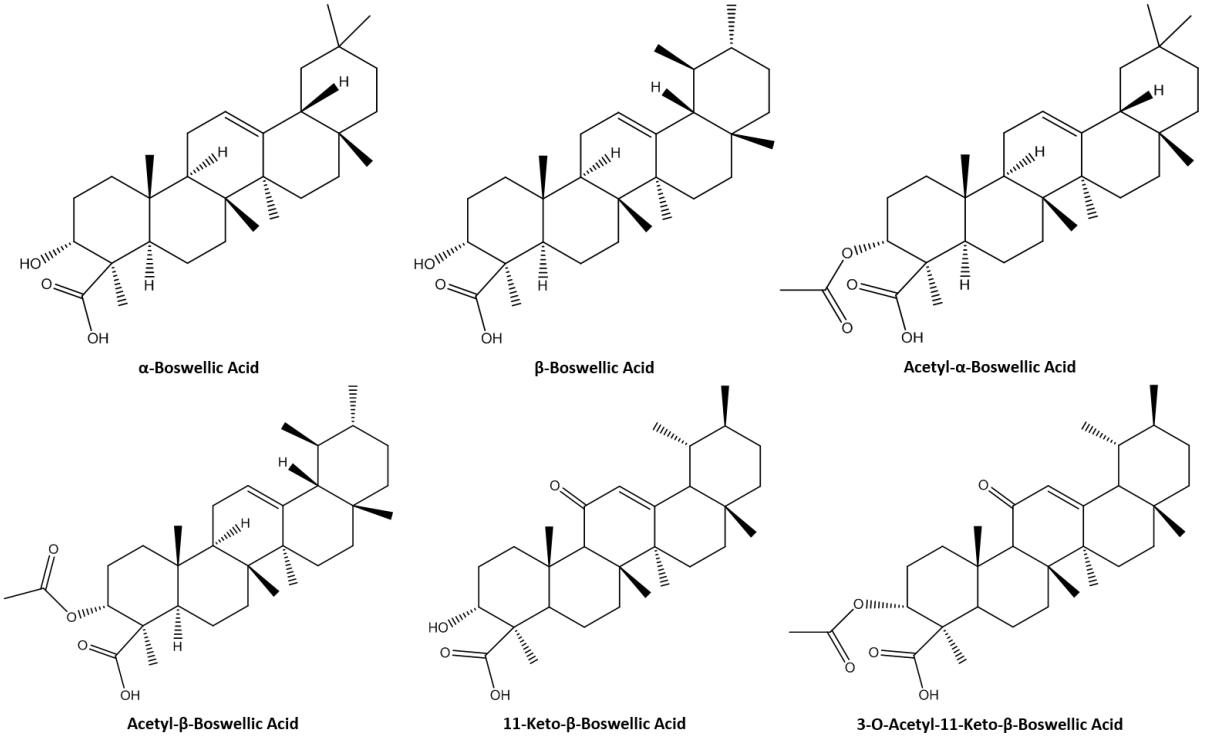

Figure 1-24. The chemical structure of the major boswellic acid family of compounds derived from the oleoresins of the *Boswellia* genus.

Multiple isoforms of boswellic acid have been identified to be present in *Boswellia* oleoresins following chemical characterisation. All of the identified boswellic acids are based on chemical modifications of α-boswellic acid and β-boswellic acid. Key modifications include the addition of ketone group (C=O) (11-keto-β-boswellic acid), the addition of an acetyl group (C_2H_3O) (acetyl-α-boswellic acid and acetyl-β-boswellic acid), or the addition of both (3-O-acetyl-11-keto-β-boswellic acid).

These chemical modifications significantly influence the biological activity of the boswellic acids against numerous disease conditions, with the most potent molecule within this family of compounds being 3-O-acetyl-11-keto-β-boswellic acid (AKBA) (Altmann *et al.*, 2004; Glaser *et al.*, 1999; Henkel *et al.*, 2012; Kunnumakkara, Nair, Sung, Pandey, & Aggarwal, 2009; J.-J. Liu, Nilsson, Oredsson, Badmaev, & Duan, 2002; B. Park, Prasad, Yadav, Sung, & Aggarwal, 2011; Safayhi *et al.*, 1992),

1.3.5 The use of *Boswellia* derivatives in modern medicine

Modern scientific research has led to a better understanding of the biological activity of *Boswellia* oleoresin extracts, *Boswellia* essential oil, and purified boswellic acids. Studies have shown that all of these *Boswellia* derivatives are effective in the treatment of a variety of pathological conditions. However, research has predominantly focused

on three main fields; (1) treatment of cancer, (2) the treatment of inflammatory conditions and (3) the treatment of bacterial and fungal infections.

1.3.5.1 Anti-inflammatory effects of *Boswellia* derivatives

Many studies demonstrate that *Boswellia* derivatives are effective anti-inflammatory agents both *in vivo* (Ammon, Safayhi, Mack, & Sabieraj, 1993; Anthoni *et al.*, 2006; Banno *et al.*, 2006; Su *et al.*, 2015; Umar *et al.*, 2014) and as a part of clinical trials (Gupta *et al.*, 1998; Kimmatkar, Thawani, Hingorani, & Khiyani, 2003; Sengupta *et al.*, 2008).

Banno *et al.* (2006) showed that the methanol extract of *B. carterii* induced an anti-inflammatory response in a rodent model of inflammation. This response was greater than that produced by the potent non-steroidal anti-inflammatory drugs, hydrocortisone and indomethacin. Su *et al.* (2015) and Umar *et al.* (2014) showed *B. serrata* oleoresins extracts to decrease inflammatory cytokines, in addition to decreasing oedema surrounding the inflamed joint in rodent osteoarthritis models (Su *et al.*, 2015).

Studies have also identified that purified boswellic acid isoforms possess anti-inflammatory activity *in vivo*. This is demonstrated by a study by Anthoni *et al.* (2006), who showed AKBA to significantly blunt inflammatory cell recruitment in an experimental mouse model of colonic inflammation. AKBA was also found to protect tissue against disease related injury, in addition to reducing inflammation to levels similar to that observed following treatment with the corticosteroid, dexamethasone (Anthoni *et al.*, 2006).

These anti-inflammatory effects are thought to be associated with interaction with the enzyme 5-lipoxygease (5-LO) and its downstream pathway (Ali & Mansour, 2011; Ammon et al., 1993; Koeberle & Werz, 2018; Sayed, Gomaa, Bader, & El Sayed, 2018; Siddiqui, 2011b; Tausch et al., 2009). The 5-LO pathway is crucial in the production of leukotrienes, key mediators of inflammation, derived from arachidonic acid (Rådmark & Samuelsson, 2009). The 5-LO pathway plays a significant role in inflammation through the catalysation of arachidonic acid to 5(S)-hydroperoxy-6-trans-8,11,14-cis-eicosatetraenoic acid (5-HPETE) and the dehydration of 5-HPETE to leukotriene A_4 (Samuelsson, Dahlen, Lindgren, Rouzer, & Serhan, 1987).

The interaction of boswellic acids with 5-LO was first described by Safayhi *et al.* (1992). In this study, they identified that of all boswellic acid isoforms examined, AKBA was the most potent. Further examination identified that the presence of the 11-keto group on boswellic acids was vital for inducing its ability to inhibit 5-LO (Safayhi, Sailer, & Ammon, 1995). The boswellic acids activity against 5-LO is therefore found to be a specific, non-redox inhibitors of leukotriene synthesis, either interacting directly with 5-LO or by blocking its translocation (Ammon *et al.*, 1993; Safayhi *et al.*, 1995).

The anti-inflammatory activity of *B. serrata* oleoresin extracts have been examined as a part of clinical trials for the treatment of asthma (Gupta *et al.*, 1998), osteoarthritis (Kimmatkar *et al.*, 2003; Sengupta *et al.*, 2008) and chronic colitis (Gupta *et al.*, 1998). In all of these trials, the *B. serrata* extract was been found to be an effective anti-inflammatory agent against all conditions whilst producing no adverse side effects.

1.3.5.2 Anti-microbial effects of *Boswellia* derivatives

Several studies have described *Boswellia* derivatives to possess anti-microbial and anti-fungal activity (Abdoul-latif, Obame, Bassolé, & Dicko, 2012; Al-Dosary, 2018; Bhutada, Muneer Farhan, & Dahikar, 2017; Biggs, Sirdaarta, White, & Cock, 2016; Camarda, Dayton, Di Stefano, Pitonzo, & Schillaci, 2007; Raja *et al.*, 2011).

The extracts of *Boswellia* oleoresins have been described to possess anti-microbial activity. The majority of this activity has been conducted using the oleoresins of *B. serrata* (Al-Dosary, 2018; Bhutada *et al.*, 2017; Biggs *et al.*, 2016). These studies describe the methanolic extract of *B. serrata* to be effective against numerous bacterial strains including *Staphylococcus epidermidis*, *Staphylococcus aureus* and *Salmonella typhi*. Biggs *et al.* (2016) also found that lower concentrations induced bacteriostatic activity, with only significantly higher concentrations inducing a bactericidal effect.

Further to this, the essential oil of *Boswellia* has also been found to possess anti-microbial activity. The essential oil derived from *B. carterii* and *B. serrata* was found to have a high degree of activity against methicillin resistant *Klebsiella pneumoniae*, *E. Coli*, *S. Typhii*, *Streptococcus mutans*, *S. aureus, S. Aureus* 2940 and *P. Aeruginosa* (Abdoul-latif *et al.*, 2012; Camarda *et al.*, 2007).

Minimal research has been conducted using purified boswellic acids, with only a study by Raja *et al.* (2011), analysing the effect of boswellic acids on microorganisms. Their

study identified that AKBA had a strong anti-microbial activity on Gram-positive bacteria. Raja *et al.* (2011) also observed a minimal effect of AKBA on Gram-negative organisms, indicating that AKBA specifically targets components of Gram-positive organisms to induce its anti-bacterial effect.

A limited degree of research has been conducted to determine the anti-fungal activity of *Boswellia* derivatives. *Boswellia* essential oil was discovered to possess anti-fungal activity with effectiveness being shown against *Candida albicans* and *Candida tropicalis* (Camarda *et al.*, 2007). Interestingly, Bhutada *et al.* (2017) found the extracts of *Boswellia* oleoresins to produce no effect on the fungal species *Candida albicans*.

1.3.5.3 Anti-cancer effects of *Boswellia* derivatives

Boswellia derivatives have been shown to possess anti-cancer activity against numerous varieties of cancer types *in vitro* including hepatocellular carcinoma (Ahmed *et al.*, 2015), oral squamous cell carcinoma (Jaafari-Ashkavandi, Hamedi, Assar, & Ebrahimpour, 2017), leukaemia (Kuo, Qian, Morris-Natschke, & Lee, 2009), colon cancer (Ranjbarnejad, Saidijam, Moradkhani, & Najafi, 2017), breast cancer (Schmiech *et al.*, 2019; Yazdanpanahi, Behbahani, & Yektaeian, 2014) and glioma (Winking, Sarikaya, Rahmanian, Jödicke, & Böker, 2000).

The methanolic extract of *B. serrata* was found to be active against hepatocellular carcinoma, colorectal carcinoma and oral squamous cell carcinoma cells (Ahmed *et al.*, 2015; Jaafari-Ashkavandi *et al.*, 2017; Ranjbarnejad *et al.*, 2017). These studies also described that the methanolic extract of *B. serrata* was less cytotoxic against non-cancer cell types, compared to cancerous cell types. Further to this, other species of *Boswellia* have been shown to possess potent cytotoxic activity. The methanolic extracts of *B. thurifera* and *B. sacra* has also been described to possess anti-cancer activity, with this species found to be active against the breast cancer cells (Schmiech *et al.*, 2019; Yazdanpanahi *et al.*, 2014).

Boswellia essential oils has also been shown to cause a decrease in cancer cell viability both *in vitro* (Chen *et al.*, 2013; Frank *et al.*, 2009; Hakkim, Al-Buloshi, & Al-Sabahi, 2015; Ni *et al.*, 2012) and *in vivo* (Suhail *et al.*, 2011). The essential oil of *B. serrata* induced a 50 % decrease in cell viability at dilutions ranging between 1:1250 and 1:3250 (Frank *et al.*, 2009; Hakkim *et al.*, 2015; Ni *et al.*, 2012), dependant on the cancer type used.

Purified boswellic acid isoforms have also been shown to cause a potent decrease in cell viability, with the beta isoforms being found to be more potent than the alpha isoform (Buchele *et al.*, 2006). Of all boswellic acid isoforms described, AKBA was found to be the most potent with IC_{50} values ranging between 10-40 µM, dependant on the cancer type being tested (Jing *et al.*, 1999; Lu, Xia, Hua, & Jing, 2008; Pang *et al.*, 2009; Syrovets *et al.*, 2005; Takahashi *et al.*, 2012; Xia *et al.*, 2005; Yuan *et al.*, 2008).

Further examination across multiple studies (Ahmed *et al.*, 2015; Buchele *et al.*, 2006; Frank *et al.*, 2009; Jaafari-Ashkavandi *et al.*, 2017; Jing *et al.*, 1999; Kuo *et al.*, 2009; Ranjbarnejad *et al.*, 2017; Takahashi *et al.*, 2012; Yazdanpanahi *et al.*, 2014) has described *Boswellia* derivatives to induce apoptotic cell death. Molecular examination into the mechanism underpinning the pro-apoptotic activity of these derivatives on cancer cells has shown an increase caspase-3 expression (Buchele *et al.*, 2006; Frank *et al.*, 2009; Hakkim *et al.*, 2015; Ranjbarnejad *et al.*, 2017), accompanied by an increase in p53 mRNA expression (Yazdanpanahi *et al.*, 2014). Further to this, the anti-apoptotic proteins BCL-2 and BCL-xL have also found to be decreased in several different cancer cell types following treatment with multiple boswellic acid isoforms (Syrovets *et al.*, 2005; Toden *et al.*, 2015; Yuan *et al.*, 2008). Proteomic analysis also identified that treatment with acetylated boswellic acid increased the expression of death receptor 4 (DR4) and death receptor 5 (DR5) pathways to induce apoptotic cell death via the extrinsic pathway of apoptosis (Toden *et al.*, 2015; Xia *et al.*, 2005).

Studies have also shown *Boswellia* derivatives to impact cancer cell proliferation and their progression through the cell cycle. Cell cycle analysis of the effect of all *Boswellia* derivatives showed that they induced an increase in the sub-G_1 and G_1 fractions of cells accompanied by a decrease in cells at the S phase and G_2 stage of the cell cycle (Jing *et al.*, 1999; Ranjbarnejad *et al.*, 2017; Takahashi *et al.*, 2012). These derivatives have been shown to induce this increase in sub-G_1 and G_1 cells by decreasing the expression of CDK4 and cyclin D1 (Ni *et al.*, 2012; Suhail *et al.*, 2011; Takahashi *et al.*, 2012; Yuan *et al.*, 2008).

A limited number of studies have translated the cytotoxic activity of *B. serrata* oleoresin extract and the *B. serrata* essential oil to *in vivo* cancer models. A study by Winking *et al.* (2000), observed that in an *in vivo* glioma mouse model, the *B. serrata* oleoresin

extract decreased tumour volume, alongside inducing a significant increase in apoptotic tumour cells. Further to this, treatment with *B. serrata* oleoresin was found to increase mice life expectancy compared to conventional treatment options. Another *in vivo* study by Suhail *et al.* (2011), showed a significant decrease in cell viability in numerous breast cancer types following treatment with varying concentrations of *B. serrata* essential oil.

1.3.6 *Boswellia carterii*

As described in 1.3.5.3, previous studies show the chemotherapeutic potential of the *Boswellia* genus. However, it also highlights the lack of research regarding the biological activity of the *B. carterii* species, supporting the need for further examination int the activity of this species.

The majority of research conducted on *Boswellia* has focussed on *B. serrata*. However, the biological activity of *B. carterii* is relatively unexplored*. B. carterii* is specifically located in the Dofar mountains of Oman and the Sanaag and Bari regions of Northern Somalia (Abdel-Tawab *et al.*, 2011). These plants take the form of small deciduous trees, which vary in height between 2 and 8 meters (Al-Harrasi & Al-Saidi, 2008). These trees can also tolerate extreme geographical locations, often residing on steep rocky slopes and ravines (Al-Yasiry & Kiczorowska, 2016). For example in Somalia, the oleoresins of *B. carterii* are harvested from the mountainous regions of the Cal Madow, Cal Miskeed and the Karkaar mountains (WSP, 2001). This environmental niche makes it entirely plausible that the chemical composition of the species may differ.

Despite this, limited research has been conducted to ascertain the biological activity and chemical composition of *B. carterii* in comparison to other species of *Boswellia*. This may be because, the political instability in Somalia has limited access to scientists (Isak, 2018; Webersik, Hansen, & Egal, 2018). Combined, there exists a need to better understand the biological activity of the oleoresins of this species.

1.3.7 The method of identifying novel therapeutic agents from plant derived sources

Despite the vast diversity of compounds present in plants, in addition to historical successes in delivering therapeutic agents, many pharmaceutical companies disbanded their natural product drug discovery research groups in favour of automated high throughput screening of synthetic and semisynthetic molecules (Dias, Urban, &

Roessner, 2012; Harvey, 2008). This switch away from natural product research is a result of numerous difficulties associated with working with natural products. These issues include: the complexities of natural product chemistry, the time consuming nature of working with natural products, difficulties in access and supply and concerns about the intellectual property rights associated with natural product isolates (Atanasov, Zotchev, Dirsch, & Supuran, 2021; Harvey, 2008).

Today, the identification of drugs and compounds with biological activity originally derived from natural products has begun to see a resurgence in popularity. This is mainly due to the failure of alternative drug discovery pathways to develop lead compounds for the treatment of various pathological conditions (Butler, 2004).

The use of natural products as leads for drug discovery has numerous advantages and challenges compared to the chemical synthesis of active compounds. One advantage is that the components within natural product extracts could act synergistically within mixture to enhance the biological activity of other components within the natural product extract (Atanasov *et al.*, 2021). However, the chemical complexity of natural product extracts is also a negative. This is due to natural products often containing a vast amount of compounds, which are structurally complex, of high molecular weights, and possess a high number of chiral centres and freely rotatable bonds (Bernardini, Tiezzi, Laghezza Masci, & Ovidi, 2018). This makes them both difficult to separate into individual components and isolate and screen any components deemed to be of interest (Atanasov *et al.*, 2021; Dias *et al.*, 2012).

Further to this, variations in the starting plant material between batches, due to environmental, climatic and genetic variations in individual plants can result in inter-batch variation in the chemical profile associated with the plant, making consistent extracts difficult (Atanasov *et al.*, 2021). All of these factors compound one another to make natural product research more problematic and expensive due to the equipment and techniques required to isolate individual components (Bernardini *et al.*, 2018).

The process of isolating and identifying biologically active compounds from plants is long and complicated requiring the use of multiple analytical chemistry and biological activity screening techniques. The common pattern of natural product drug discovery is shown in figure 1-25. Following initial identification of a plant of interest from literature, historical use, or use in alternative/traditional medicine, a crude extraction of

the plant is required (Atanasov *et al.*, 2021). These crude extracts are commonly isolated using a solvent based extraction protocol, with extraction solvents including water, ethanol, methanol, dichloromethane and hexane. This allows these initial screening of plant extracts to determine if they possess biological activity against the disease of interest, and if no activity is observed the research can be discontinued.

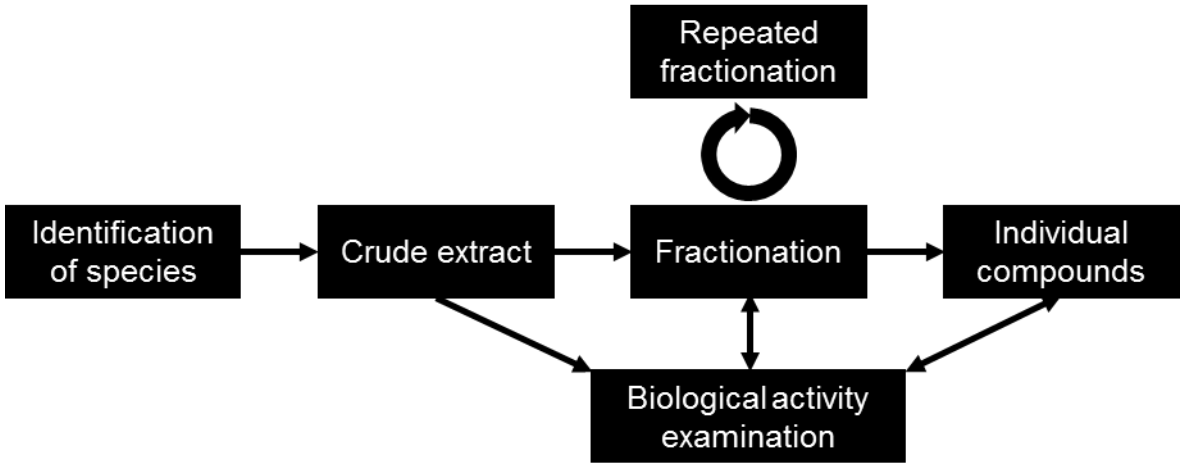

Figure 1-25. The conventional pathway of drug discovery from natural products.

If the crude extract possess' biological activity, multiple analysis pathways can be conducted. One pathway utilises analytical chemistry techniques to isolate individual compounds or fractions containing multiple compounds and determine the identity of these chemical components. The methods used to isolate fractions from these crude extracts often include the use of column chromatography or fractionating high-performance liquid chromatography (HPLC). This isolation process is cyclical and will require multiple rounds of fractionation to isolate and purify individual biologically active compounds. These purified compounds can then be subjected to classical analytical chemistry techniques such as UV absorption spectroscopy, infra-red (IR) spectroscopy, mass spectrometry (MS) and nuclear magnetic resonance spectroscopy (NMR) to allow for the unequivocal structure determination of pure compounds (Dias *et al.*, 2012).

The alternative pathway is to develop a better understanding of the biological activity of the crude extracts before they are subjected to fractionation and isolation of active components. This approach ensures that the crude extract targets a specific pathway or induces a specific effect before they are taken forward and the active component identified.

Following the isolation and chemical characterisation of the biologically active compound, further mechanistic studies can be conducted to ensure that in its purified form the compound maintains the desired mechanism of action. Following this, compounds can be taken forward to an *in vivo* model to determine if the compounds activity is maintained in a living model. In addition, optimal treatment doses and the determination of any off-target effects may also be determined using an *in vivo* animal model. If the results of *in vivo* study are positive, clinical trials would be conducted to establish if the activity observed in the animal model was translatable to humans. These trails would allow the optimal therapeutic concentrations to be identified, as well as determining any side-effects of treatment and ensuring that the compound is safe for clinical use.

However, even as crude extracts, numerous plants have been shown to possess potent biological activity and their crude forms can play a role in the therapy for disease in the form of dietary supplements, drugs or botanical extracts (Bernardini *et al.*, 2018) One potential source which has shown some promise as a novel source of biologically active compounds in recent years is that of the oleoresins derived from the genus *Boswellia*.

1.4 Aims of the study

Existing studies suggest plants within the genus *Boswellia* are a potential source of novel chemotherapeutics. However, previous research is limited, and many questions surrounding extraction methods, chemical profile and mechanisms of action remain unclear or unanswered. It may therefore be the case using alternative extraction methods produce greater yields and biological activity compared to those previously evaluated.

Previous research has shown the *Boswellia* genus to possess cytotoxic activity *in vitro.* However, the species *Boswellia carterii* remains completely unexplored; an important oversight given the cross-species chemical diversity. Based on this, it highlights the need for further examination of this species. Based on the findings of previous studies, it can be hypothesised that *B. carterii* may also possess cytotoxic activity *in vitro.*

Furthermore, based on the difference in geographic, environmental, and climatic conditions in which *B. carterii* grows in comparison to other *Boswellia* species, it could be hypothesised that this difference in conditions results in different abundances of known compounds or the production of novel compounds compared to other members of the *Boswellia* genus.

By elucidating the biological activity and chemical profile of *Boswellia carterii* specifically, this study seeks to ascertain the species' potential as a novel chemotherapeutic source. In doing so, the study ought to advance associated understanding of the genus as a whole. Specifically, the study aimed to:

1) Optimise the extraction of *B. carterii* oleoresin.
2) Determine if extracts of *B. carterii* oleoresin are specifically cytotoxic against a diverse range of cancer cell lines.
3) Establish the modes of cytotoxicity and associated molecular mechanisms.
4) Confirm the presence and profile of boswellic acids in *B. carterii* and provide a detailed chemical profile.

Chapter 2

General Methodology

2.1 Materials, chemicals and reagents used during this study

All materials, chemicals and reagents used during this study were purchased from Fisher Scientific, USA, Sigma Aldrich, USA and Scientific laboratory supplies, UK unless otherwise stated.

2.2 Extraction of compounds from the *B. carterii* oleoresin

B. carterii oleoresin was macerated to a fine powder using a pestle and mortar, before the addition of either: acetonitrile (99.5 %), distilled water (dH_2O), ethanol (99 %), methanol (99.5 %) and propan-2-ol (99.5 %) (all solvents purchased from Fisher Scientific, USA), to a concentration of 0.1 g/ml. The mixture was then agitated continuously for 2 hours. After 2 hours, the supernatant was transferred to a separate container and fresh solvent added to any undissolved material.

This extraction process was repeated three times and the recovered supernatants pooled. The pooled supernatants were filtered through a 0.22 µm polyethersulfone (PES) syringe filter (Fisher Scientific, UK) to eliminate any undissolved material before being dried to a powder, using a rotary evaporator (Eppendorf, USA). The resulting powders were stored at -20 ^{o}C, until required for experimentation.

2.2.1 Preparation of extracts for the assessment of the biological activity

All extracts were dissolved in dimethyl sulphoxide (DMSO) (Fisher Scientific, USA) to a concentration of 50 mg/ml. These stocks were then diluted to the desired concentrations using an appropriate cell culture media for the cancer cell line being examined, as described in section 2.4.

2.3 Cell culture

All cell culture experiments were performed aseptically, within a Class 2 biological safety cabinet (NuAire, USA). Cells were maintained within a CO_2 incubator (NuAire, USA) at 37 ^{o}C with a 5 % CO_2 atmosphere unless otherwise stated.

2.3.1 Disassociation of adherent cancer cell lines

Adherent cancer cell lines, which are predominantly derived from organ-based cancers, possess the ability to anchor to the surface of cell culture vessels allowing them to migrate and form cellular monolayers. This anchorage is caused by the secretion of ECM components, namely collagen, fibronectin and laminin from the cells (Alitalo, Keski-oja, & Vaheri, 1981), allowing them to adhere to the vessel. In order to

remove them from the cell culture vessel for experimentation, trypsinisation is required to break down the ECM and disassociate the cells.

After the cells reached the desired confluency, cells were washed with 1x Phosphate buffered saline (PBS) (Sigma Aldrich, USA) and treated with 5 ml of Tryple trypsin alternative (Gibco, UK) for 2-3 minutes at 37 ^{o}C. The flask was then gently agitated to detach the cells from the flask and 5 ml of complete cell culture media was added to deactivate the Tryple. The mixture was then centrifuged at 200 xG for 10 minutes. After centrifugation, the supernatant was discarded, and the cell pellet resuspended in complete media and a cell count is performed using the method described in section 2.3.2.

2.3.2 Quantification of cancer cell number for the seeding of experiments.

In order to determine the total number of cells and calculate the volume of cells required to seed experiments. To do this, a haemocytometer is used to calculate the cellular density of a disassociated flask.

Following the removal of the cells from their culture flasks and centrifugation, cells were re-suspended in an appropriate volume of an appropriate cell culture media (typically 1-5 ml) dependant on the cancer type being counted. After re-suspension, 10 microlitres (µl) of the cell suspension was removed and mixed with an equal volume of 1x Trypan Blue (Gibco, UK), a dye that is excluded from viable cells, whilst being taken up by non-viable cells. From this mixture, 10 µl was then injected into a haemocytometer and a cell count was performed.

The cell count was performed using a Leica DM500 microscope fitted with a PLAN 10x/0.22 lens (Leica, Germany) and a 4x eyepiece for a total magnification of 40x. Figure 2-1 shows the magnified view of the haemocytometer counting chamber under 40x magnification.

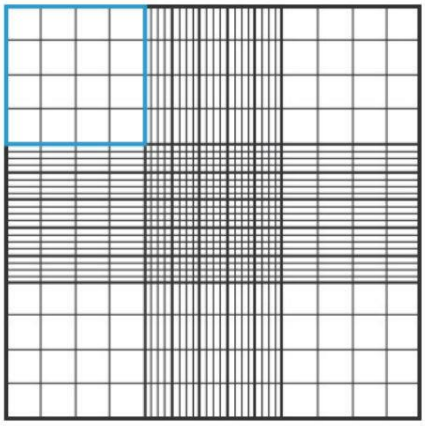

Figure 2-1. Method for determining the number of cultured cells.

A diagram showing the cell counting chamber found within a haemocytometer. The blue square identifies one of the four grids used to perform a cell count. Cells touching the bottom and the right-hand side border of the square were excluded for the cell count.

A cell count was performed using only cells that fell into the large grid, highlighted in blue on figure 2-1. Within this grid, any cells that fell on the bottom and the right edge of the grid were excluded and not counted. Non-viable, blue stained cells were excluded from any cell count, with only clear cells being counted.

An average cell count was taken following the counting of all four of the corner grids in figure 2-1. The equation shown in equation 2-1 was then used to calculate the concentration of cells per ml of solution.

Equation 2-1. Calculation of cell density and viability of isolated cells using a haemocytometer.

Average cell count x 2 **(Trypan blue dilution)**

Above multiplied by the volume of resuspension media **(Dilution factor correction)**

$x10^4$

Convert value to $x10^6$

Once the total cell concentration was known, equation 2-2 was used to calculate the volume of the cell suspension required for further experimentation.

Equation 2-2. Calculation of the volume of cell suspension required to conduct an experiment requiring a set number of cells.

$$\frac{\text{Cell count desired}}{\text{Cell count of suspension per ml}} \times 100 = \text{volume of cell suspension required (ml)}$$

This volume of cell suspension was then centrifuged to pellet the cells and resuspended using an appropriate volume of cell culture media to conduct any desired experiments.

2.3.3 Cryopreservation and recovery of cancer cell lines

2.3.3.1 Recovery of cancer cell lines from cryopreservation

In order to culture cancer cell lines for experimentation, they first need to be recovered from cryostorage in liquid Nitrogen. To do this, cryovials are removed from a liquid Nitrogen dewar and carefully defrosted in a water bath heated to 37 ^{o}C, until a small pellet of ice remains. The cryovial was then aseptically transferred to a cell culture cabinet and the contents of the cryovial removed and added to 9 ml of an appropriate complete cell culture media within a centrifuge tube. The centrifuge tube was then centrifuged at 200 xG for 10 minutes.

Following centrifugation, the supernatant of the tube was discarded, and the cell pellet was resuspended in an appropriate cell culture media for the cancer cell line being recovered. The viability of the cells recovered were assessed using a Trypan blue exclusion test, described in section 2.3.2 and equation 2-3.

Equation 2-3. Calculation of the viability of cells recovered following recovery from cryopreservation.

$$\frac{\text{The number of viable cells}}{\text{Total number of cells counted}} \times 100$$

After the assessment of the viability, cells were incubated at 37 ^{o}C in a 5 % CO_2 atmosphere until they required passage or were required for experimentation.

2.3.3.2 Cryopreservation of cancer cell lines

To preserve cancer cell lines so they were available for later experimentation and to return to earlier passages of the cell line, cells were cryopreserved. To do this, cells were removed from culture, with adherent cells requiring trypsinisation (Section 2.3.1) and counted as described in section 2.3.2. The cell pellet was resuspended in complete

cell culture media containing 10 % v/v DMSO to a cell density of between 1-5 $x10^6$ cells/ml and quickly transferred to cryostorage vials (Fisher Scientific, USA). These were placed into a room temperature “Mr Frosty” freezing container (Nalgene, Thermo Scientific, USA), with the container then being transferred to a -80 ^oC freezer overnight. The following day, the container was removed from the freezer and the cryovials within were transferred into liquid Nitrogen. Cryovials remained in liquid Nitrogen until they were required to be recovered.

2.4 Maintenance and passaging of cancer cell lines.

To maintain cells in culture, cells were required to be given cell culture media and passaged into new flasks. Each cell line used required a different rate of media replenishment and passaging. This is described in sections 2.4.1 - 2.4.9.

2.4.1 Chronic myeloid leukaemia

The chronic myeloid leukaemia cancer cell line, K562 (ATCC® CCL-243), was obtained from the Kidscan children’s cancer research laboratory at the University of Salford, UK. Cells in culture were grown in suspension within a 25 cm^2 cell culture flask (T_{25}) (Fisher Scientific, UK) at 37 ^oC in a 5 % CO_2 atmosphere, until an appropriate cell density was achieved. The media for cell culture of the K562 cell line was Roswell Park Memorial Institute (RPMI) 1640 media (Gibco, UK) with the addition of 10 % v/v Foetal bovine serum (FBS) (Gibco, UK) and 1 % v/v penicillin-streptomycin (Penicillin: 10,000 units/ml, Streptomycin: 10,000 µg/ml) (Gibco, UK). Cell culture media was replenished 2-3 times per week. Cells were passaged into new flasks at a ratio of 1:5, until required for experimentation.

2.4.2 Acute lymphoblastic leukaemia

The acute lymphoblastic leukaemia cancer cell lines, MOLT-4 (ATCC® CRL-1582) and CCRF-CEM (ATCC® CCL-119), were obtained from the Kidscan children’s cancer research laboratory at the University of Salford, UK. Cells in culture were grown in suspension within a T_{25} cell culture flask at 37 ^oC in a 5 % CO_2 atmosphere, until an appropriate cell density was achieved. The media used for the cell culture of both cell lines was RPMI 1640 with the addition of 10 % v/v FBS and 1 % v/v penicillin-streptomycin. Cell culture media was replenished 2-3 times per week. Cells were passaged into new flasks at a ratio of 1:5 until required for experimentation.

2.4.3 Hepatocellular carcinoma

The hepatocellular carcinoma cancer cell line, HEP G2 (ATCC® HB-8065), was obtained from the Kidscan children's cancer research laboratory at the University of Salford, UK. HEP G2 cells were grown in a 75 cm^2 cell culture flask (T_{75}) (Fisher Scientific, UK) at 37 ^oC in a 5 % CO_2 atmosphere, until a confluency of 80 % was achieved. The media for cell culture of the HEP G2 cell line was RPMI 1640 supplemented with 10 % v/v FBS and 1 % v/v penicillin-streptomycin. Cell culture media was replenished 2-3 times per week. Cells were then passaged into new flasks at a ratio of 1:5, until required for experimentation.

2.4.4 Alveolar basal epithelial cell adenocarcinoma

The alveolar basal epithelial cell adenocarcinoma cancer cell line, A549 (ATCC® CCL-185), was obtained from the Kidscan children's cancer research laboratory at the University of Salford, UK. A549 cells were grown in a T_{75} cell culture flask at 37 ^oC in a 5 % CO_2 atmosphere, until a confluency of 80 % was achieved. The media for cell culture of the A549 cell line was Kaighns modification of Ham's F12k media (Gibco, UK) supplemented with 10 % v/v FBS and 1 % v/v penicillin-streptomycin. Cell culture media was replenished 2-3 times per week. Cells were then passaged into new flasks at a ratio of 1:5, until required for experimentation.

2.4.5 Colorectal carcinoma

The colorectal carcinoma cancer cell line, HCT-116 (ATCC® CCL-247), was obtained from the Kidscan children's cancer research laboratory at the University of Salford, UK. HCT-116 cells were grown in a T_{75} cell culture flask at 37 ^oC in a 5 % CO_2 atmosphere, until a confluency of 80 % was achieved. The media for cell culture of the HCT-116 cell line was McCoys 5a media (Gibco, UK) supplemented with 10 % v/v FBS and 1 % v/v penicillin-streptomycin. Cell culture media was replenished 2-3 times per week. Cells were then passaged into new flasks at a ratio of 1:5, until required for experimentation.

2.4.6 Pancreatic cancer

The pancreatic cancer cell line, PANC-1 (ATCC® CRL-1469) was purchased from Public Health England (United Kingdom). PANC-1 cells were cultured in a T_{75} flask at 37 ^oC in a 5 % CO_2 atmosphere, until a confluency of 80 % was achieved. The PANC-1 cells were cultured using Dulbecco's Modified Eagle Medium (DMEM) (Gibco, UK) supplemented with 10 % FBS and 1 % v/v penicillin-streptomycin. Cell culture media

was replenished 2-3 times per week. Cells were then passaged into new flasks at a ratio of 1:2, until required for experimentation.

2.4.7 Breast cancer

The breast cancer cell line, MCF-7 (ATCC® HTB-22) was obtained from the translational medicine research laboratory at the University of Salford. MCF-7 cells were cultured in a T_{75} flask at 37 ^{o}C in a 5 % CO_2 atmosphere, until a confluency of 80 % was achieved. The MCF-7 cells were cultured using DMEM supplemented with 10 % FBS and 1 % v/v penicillin-streptomycin. Cell culture media was replenished 2-3 times per week. Cells were then passaged into new flasks at a ratio of 1:5, until required for experimentation.

2.4.8 Rhabdomyosarcoma

The rhabdomyosarcoma cell line, A-204 (ATCC® HTB-82), was obtained from the Kidscan children's cancer research laboratory at the University of Salford, UK. A-204 cells were grown in a T_{75} cell culture flask at 37 ^{o}C in a 5 % CO_2 atmosphere, until a confluency of 80 % was achieved. The A-204 cell line was cultured using RPMI 1640 media supplemented with 10 % v/v FBS and 1 % v/v penicillin-streptomycin. Cell culture media was replenished 2-3 times per week. Cells were then passaged into new flasks at a ratio of 1:5, until required for experimentation.

2.4.9 Immortalised normal human bronchial epithelium

The Immortalised normal human bronchial epithelium cell line, BEAS-2B (ATCC® CCL-247), was obtained from the Kidscan children's cancer research laboratory at the University of Salford, UK. BEAS-2B cells were grown in a T_{75} cell culture flask at 37 ^{o}C in a 5 % CO_2 atmosphere, until a confluency of 80 % was achieved. The BEAS-2B cell line was cultured using DMEM supplemented with 10 % v/v FBS and 1 % v/v penicillin-streptomycin. Cell culture media was replenished 2-3 times per week. Cells were then passaged into new flasks at a ratio of 1:5, until required for experimentation.

2.5 Identification of the biological activity of *B. carterii* oleoresin solvent extracts

2.5.1 Assessment of biological activity using the 3-(4,5-dimethylthiazol-2-yl)-2–5-diphenyltetrazolium bromide (MTT) assay

Cells were seeded in a 96 well plate (Fisher scientific, USA) to a density of 5-10 x 10^4 cells per well and left for 24 hours in a 37 ^{o}C, 5 % CO_2 incubator. After 24 hours, the

media was removed and replaced with concentrations of the substrate extracts, shown in figure 2-2. Following treatment, the plates were incubated for a further 72 hours at 37 ^{o}C in a 5 % CO_2 atmosphere.

	1	2	3	4	5	6	7	8	9	10	11	12
A	BLANK	Positive Control			Vehicle Control			Negative Control			BLANK	
B		6.25 µg/ml			6.25 µg/ml			6.25 µg/ml				
C		12.5 µg/ml			12.5 µg/ml			12.5 µg/ml				
D		25 µg/ml			25 µg/ml			25 µg/ml				
E		50 µg/ml			50 µg/ml			50 µg/ml				
F		75 µg/ml			75 µg/ml			75 µg/ml				
G		100 µg/ml			100 µg/ml			100 µg/ml				
H		200 µg/ml			200 µg/ml			200 µg/ml				

Figure 2-2. The plate layout for examining the cytotoxic effect of the *B. carterii* oleoresin extracts *in vitro*.

Cells at an appropriate density were seeded into wells A2-H10, with areas designated as blank left empty. After 24 hours, the *B. carterii* oleoresin was added to the wells to the desired concentrations. Positive control indicates wells treated with 50 µM Doxorubicin. Vehicle control indicates wells treated with appropriate media containing 0.5 % DMSO v/v. Negative control indicates wells treated with appropriate cell culture media alone.

Following incubation, the supernatant was removed from each well and replaced with 100 µl of 0.5 mg/ml MTT reagent (Invitrogen, USA). This was incubated for 4 hours at 37 ^{o}C for a colour change to occur. The supernatant was then carefully aspirated and replaced with 100 µl of DMSO and incubated for 10 minutes at 37 ^{o}C. The contents of each well were thoroughly mixed, before the absorbance was analysed at 540 nm using a FLUOstar Omega plate reader (BMG Labtech, Germany) with background absorbance measured at 690 nm. Absorbance of each well was measured in triplicate and exported as a Microsoft Excel file for further evaluation.

For suspension cell lines, modifications to the method were conducted. The first of these modifications was that cells were seeded into U-bottom 96 well plates. The second modification was that the 96 well plates were centrifuged at 200 xG for 5 minutes to pellet the suspension cells in the plate before the removal of supernatants.

All analysis of data was conducted using a custom written Microsoft Excel file to generate the percentage cell viability based on the recorded absorbance's. The effect of each concentration of extract was calculated as percentage viability in comparison to the vehicle control.

2.5.2 Calculation of IC_{50} values as an indicator of cytotoxic activity

The IC_{50} value is the concentration of a drug required to induce a 50 % decrease in the viability of cancer cells. To calculate this, regression analysis and curve fitting was conducted within SigmaPlot 12.3 (Systat Software, Inc, USA). This regression analysis generated an equation from which, the concentration of drug required to cause a 50 % decrease in viability could be accurately calculated.

2.6 Flow cytometry

All flow cytometry experiments were conducted using a Becton Dickinson (BD) FACSverse flow cytometer (Becton Dickinson Bioscience, USA) and analysed using the BD FacSuite software (Becton Dickinson Bioscience, USA). For all experiments a minimum of 10,000 cells per condition were analysed. Cells were identified using the forward scatter and side scatter parameters to determine cell size and granularity. Cells were then gated and subjected to analysis of molecular parameters dependent on the experiment being conducted. All dyes utilised within the study were suitable for flow cytometry, with the individual dye's excitation/emission wavelengths, filters and detection channels described within the specific methodologies used. All data generated by flow cytometry was then exported for offline data analysis.

2.7 Isocratic High-performance liquid chromatography

2.7.1 Equipment

Isocratic high-performance liquid chromatography (HPLC) was carried out using an Agilent 1220 HPLC System fitted with a standard flow cell, variable wavelength detector and a 20 µl injection loop (All Equipment from Agilent Technologies, USA). All analytical HPLC analysis an Agilent 5HC C-18(2) 150 x 4.6mm column (Agilent Technologies, USA).

2.7.2 Sample preparation and injection

Each injected sample was prepared to a concentration of 100 mg/ml and then syringe filtered through a 0.22 µm PES filter (Fisher Scientific, USA) before injection into the

HPLC system. Prior to injection, The HPLC system and column were cleaned using a mobile phase of > 80 % solvent, for 20 minutes at a flow rate of 2 ml/min.

The mobile phase flow rate was then lowered to 1 ml/min, before sample injection. Samples were carefully injected into the HPLC system, using a blunt ended HPLC injection needle (Agilent, USA) and the sample transferred onto the column. HPLC was performed for 120 minutes, with spectra generated at a wavelength of 205 nm. Following analysis all solutions used were sent to the waste.

2.8 Gradient High-performance liquid chromatography

2.8.1 Equipment

Gradient HPLC was performed using an Agilent 1260 infinity HPLC system fitted with a 1260 quaternary pump, a 1260 standard infinity autosampler fitted with a 100 µl sample loop, a 1260 Infinity thermostatted column compartment and a 1260 Infinity diode array and multiwavelength detector (All equipment from Agilent Technologies, USA). The HPLC column used for all analyses was an Agilent 5HC C-18(2) 150 x 4.6mm column.

2.8.2 Sample preparation and injection

Each injected sample was prepared to a concentration of 12.5 mg/ml (12500 parts per million (ppm)) and then syringe filtered through a 0.22 µm PES filter (Fisher Scientific, USA) before injection into the liquid chromatography system.

Prior to injection, the liquid chromatography system and column were cleaned using mobile phase composed of > 80 % solvent, for 20 minutes at a flow rate of 2 ml/min. All gradient HPLC analysis was performed using a mobile phase composed of HPLC grade acetonitrile (Fisher Scientific, USA) and dH_2O.

The mobile phase flow rate was then lowered to 0.8 ml/min, before sample injection. Samples were injected into the liquid chromatography system, using an autosampler system and the sample transferred onto the column. HPLC was performed using a gradient method where the concentration of the mobile phase and flow rate was programmed using the software ChemStation (Agilent Technologies, USA) to automatically adjust over time. The gradient method utilised was modified dependent on the experiment conducted. Specific modifications are described within the respective section.

2.9 Ultra high definition accurate-mass electrospray ionisation quadrupole time-of-flight high-performance liquid chromatography-high resolution mass spectrometry

Chemical characterisation was performed utilising a Ultra high-definition accurate-mass electrospray ionisation (ESI) quadrupole time-of-flight (TOF) HPLC- high resolution MS (HRMS) approach. All HPLC methodologies used were optimised before the conduction of mass spectrometry.

2.9.1 Sample preparation

Each injected sample was prepared to a concentration of 0.2 mg/ml (200 ppm) and then syringe filtered through a 0.22 µm PES filter (Fisher Scientific, USA). Samples were deposited into autosampler vials and placed into a 1260 Infinity High Performance Autosampler (Agilent Technologies, USA) and analysed shortly after sample preparation.

2.9.2 High-performance liquid chromatography separation methodology

High-performance liquid chromatography was performed using an Agilent 1260 infinity HPLC system fitted with a 1260 quaternary pump, a 1260 standard infinity autosampler fitted with a 100 µl sample loop, a 1260 Infinity thermostatted column compartment, set to 25 ^{o}C, and a 1260 Infinity diode array and multiwavelength detector (All equipment from Agilent Technologies, USA). The HPLC column used for all analyses was an Agilent 5HC C-18(2) 150 x 4.6mm column.

Samples were drawn up at a rate of 200 µl/minute to a total injection volume of 20 µl per sample run. Samples were separated using a gradient HPLC method. This method is described in table 2-1.

Table 2-1. The gradient high-performance liquid chromatography method used for all analytical analysis.

A summary of the changes in mobile phase components and flow rate during the gradient high-performance liquid chromatography analysis of the *B. carterii* oleoresin methanolic extract.

Time (min)	Acetonitrile (%)	dH_2O (%)	Flow rate (ml/min)
0	50	50	0.8
3.00	50	50	0.8
6.00	95	5	1
15.00	95	5	1.2
56.00	95	5	1.2
59.30	50	50	0.8

HPLC separation was performed for a run time of 60 minutes, with spectra generated at a wavelength of 205, 230, 250, 270, 290 and 310 nm. Following separation, the samples were further subjected to ultra-high definition mass spectrometry for further analysis.

2.9.3 Ultra-high definition mass spectrometry equipment and methodology

Ultra-high definition (UHD) mass spectrometry was performed using an Agilent QTOF 6540 UHD mass spectrometer. All samples were initially separated using the HPLC method described in section 2.12.2 before flowing into the UHD mass spectrometer. Samples were ionised using a dual Agilent Jet Stream (AJS) technology electrospray ionisation source (ESI) (Agilent Technologies, USA). The UHD mass spectrometry parameters used for analysis were the following; The gas flow rate was 5 ml/minute, a nebuliser value of 15 p.s.i, and a gas temperature of 325 ^{o}C. The mass range was between 60 and 1700 *m/z* with a scan rate of one spectra /minute. Samples were analysed using both positive and negative ionisation modes to allow complete compound detection. A solvent blank was also analysed to eliminate background interference. Following the analysis of each sample data was recorded using MassHunter acquisition software (Agilent Technologies, USA) and stored for further analysis offline.

2.9.4 Mass spectrometry data analysis

Mass spectrometry data was analysed using MassHunter qualitative analysis software, version B.07.00 (Agilent Technologies, USA). Mass spectrometry data was aligned with the associated HPLC spectra and then the mass spectra was extracted for each HPLC peak. At equivalent timepoints as the sample peaks, the mass spectra of the solvent blank were also extracted. This background spectrum was then subtracted from the sample spectra at each HPLC peak identified, resulting in cleaned sample spectra at each identified peak.

At each timepoint the spectra were analysed, and the molecular ion mass to charge ratio (m/z) identified. The molecular formula of each peak was calculated using a formula calculator within the MassHunter qualitative analysis software and all potential formula and molecular weights were recorded for both the positive and negative ionisation modes. All formula generated for each peak was selected within a mass accuracy of less than ± 5 ppm, as calculated using equation 4. This data was then tabulated and evaluated against previously described components of *Boswellia* extracts to elucidate potential compound identifications.

Equation 2-4. Calculation of mass accuracy.

The equation used to calculate the difference between the exact ion m/z compared to the m/z measured using mass spectrometry to determine mass accuracy.

$$\textbf{Mass accuracy (ppm)} = 1 \times 10^{6} \times \frac{(\text{measured } {}^{m}/_{z} - \text{Exact } {}^{m}/_{z})}{\text{Exact } {}^{m}/_{z}}$$

2.10 Statistical analysis

Data was analysed using SigmaPlot 12.3 (Systat Software, Inc, USA). Before comparisons were conducted, normality of the data was determined using a Shapiro-Wilk normality test. A p value of < 0.05 was used to determine if data was normally distributed. Normally distributed data was analysed using parametric statistical tests, whilst data which was found to not to be normally distributed was analysed using non-parametric statistical tests.

Comparisons of the extraction yield was evaluated using one-way analysis of variance (ANOVA) or a Kruskal-Wallis one-way analysis of variance on ranks, followed by a Turkey post hoc test, to allow a pairwise comparison of all extraction methods. All

comparisons between the yield and biological activity of the *B. carterii* oleoresin were conducted using a two-tailed student t-test or Mann-Whitney rank sum test dependent on the distribution of the groups being analysed.

The cytotoxic activity of all extracts, examination of apoptosis detection analysis and cell cycle analysis were analysed using a one-way ANOVA or a Kruskal-Wallis one-way ANOVA on ranks, followed by a Dunnett's post hoc test to allow comparison of treatment against the vehicle control.

Western blotting statistical analysis was also conducted using a one-way ANOVA followed by a Dunnett's post hoc test to allow comparison of treatment against the vehicle control. Analysis was also repeated using a Turkey post hoc test to compare the effect of each concentration on protein expression.

Statistical significance was determined as a p value of less than 0.05 for all analyses.

2.11 Ethical approval

Ethical approval for this study was approved by the University of Salford Research, Innovation and Academic Engagement Ethical Approval Panel. The ethical approval was designated the code STR1718- 35.

Chapter 3

The optimisation of methods used to extract biologically active compounds from *Boswellia carterii* oleoresin

3.1 Introduction

Cancer remains the leading cause of death in the United Kingdom (ONS, 2018), with its incidence rising over the past 40 years (Oke, O'Sullivan, Perera, & Nicholson, 2018). As a result, there exists an ongoing need to develop novel anti-cancer treatments with fewer off target effects (see section 1.2.7).

Natural sources, such as plants provide a considerable pool of pharmacology active compounds that tend to produce fewer harmful side effects than their synthetic equivalents (Cragg & Newman, 2005). As discussed in section 1.3, plants in the genus *Boswellia* show promise as a source of novel chemotherapeutic agents. Despite this, research into the best methods for a complete extraction of those compounds is limited and therefore current assumptions on which these current methods are based may be unjustified.

Many methods are available, and most are solvent-based (Harborne, 1998; Sarker, Latif, & Gray, 2006; Wang & Weller, 2006). However, there is considerable variation in the solvent used. For example, solvents commonly used for plant-based extractions include water, methanol, ethanol, propanol, acetone, chloroform, petroleum ether or azeotropic mixtures (Visht & Chaturvedi, 2012). However it should be noted that no one solvent can extract all compounds of potential interest, and each will specifically allow the extraction of only certain groups of compounds from a given plant material (Sasidharan, Y. Chen, D. Saravanan, K. M. Sundram, & L. Y. Latha, 2011; Solanki & Nagori, 2012; Visht & Chaturvedi, 2012). This variation arises from the fact that the solvents used to extract compounds from plant material differ in polarity (Malavolta, Poletti, Silva, Schreier, & Nakaie, 2008; Visht & Chaturvedi, 2012).

Despite this, it is often the case that, the first solvent used for extraction from unknown plant materials is methanol (Sasidharan *et al.*, 2011). This is due to its semi-polar nature thus ability to extract a relatively wide range of polar and certain non-polar compounds (Truong *et al.*, 2019). Indeed, the methanolic solvent extraction method is commonly used for assessing the biological activity of the *Boswellia* genus (Alipanah & Zareian, 2018; Ranjbarnejad *et al.*, 2017; Zhang, Biggs, Sirdaarta, White, & Cock, 2016).

There have been limited attempts to extract biologically active compounds from *Boswellia* using other solvents (Greve, Kaiser, Brun, & Schmidt, 2017; Yang, Ren, &

Wang, 2018; Zhang *et al.*, 2016). Those that have previously utilised non-polar solvent extraction methods found to produce a lower extraction yield and a lesser biological activity than those utilising polar solvent extractions (Greve *et al.*, 2017). However, other polar solvent extraction methods have yet to be explored so it isn't clear if those can produce higher yields and / or biological activity. As such, important compounds may have been overlooked.

Furthermore, previous research to characterise the biological effects of the *Boswellia* genus has focused on select species, namely *B. serrata* (Ahmed *et al.*, 2015; Hartmann, Fillmann, Morgan Martins, Meurer, & Marroni, 2014; Khan, Ali, Parveen, Najmi, & Ahmad, 2016; Umar *et al.*, 2014). The biological effects of the species *B. carterii* is relatively unexplored. With the *B. carterii* species being located in different region of the world to that of other species of the *Boswellia* genus, it may be the case that geographical and environmental factors influence the chemical composition of this species. Based on this, it is plausible that these conditions generate oleoresins that are very different to others in the genus meaning that species-specific compounds or isoforms are entirely conceivable (see 1.3.3). Furthermore, of the few studies using *B. carterii* oleoresin, only the essential oil has been examined (Frank *et al.*, 2009; Yang, Ren, *et al.*, 2018; Yu *et al.*, 2018).

Indeed, most studies that specifically focus on *B. carterii* have been conducted on distilled essential oils rather than oleoresin *solvent* extracts (Chen *et al.*, 2013; Ni *et al.*, 2012; Suhail *et al.*, 2011). This is likely due to essential oil being readily commercially available as it frequently used within aromatherapy and cosmetic industries (Ernst, 2008; Khan, 2012). These studies show the essential oil to induce apoptotic cell death both *in vitro* and *in vivo* (Frank *et al.*, 2009; Suhail *et al.*, 2011).

However, it should be noted that to produce similar biological effects to solvent extracts of oleoresin, considerably higher concentrations of essential oil were required. (Ranjbarnejad *et al.*, 2017; Yazdanpanahi *et al.*, 2014; Zhang *et al.*, 2016). It is plausible that the attenuated biological effect of the essential oil is a result of incomplete extraction of the compounds responsible, further supporting that the oleoresin may be an untapped source of biologically active compounds.

When all evidence is taken together, it becomes clear that the therapeutic potential *B. carterii* oleoresin remains under explored and necessitates further investigation. In

addition, for the *Boswellia* species that have been investigated to a greater extent, only certain extraction protocols have been utilised. Therefore, it may be the case that certain compounds may have been missed.

3.1.1 Aims of the chapter

To ascertain the optimal extraction method for isolating potentially biologically active compounds from the *B. carterii* oleoresin, numerous solvent based extraction methods were evaluated. Following this, this study used two typical cancer cell lines as biological reporters these being; the chronic myeloid leukaemia cell line K562 and the hepatocellular carcinoma cell line HEP G2.

The main aims of this chapter are as follows:

1) Ascertain if *B. carterii* extracts exhibit fundamental anti-cancer activity.

2) To systematically develop an efficient and effective extraction method that
   - **a.** Generates a practical extraction yield.
   - **b.** Gives confidence that all biologically active compounds are extracted from *B. carterii*.
   - **c.** Allows retrospective assessment of robustness of previous studies that only utilise methanolic extracts.

3.2 Methods

3.2.1 Preparation of extracts

The preparation of all solvent extracts utilised within this chapter is described in section 2.2. Extraction solvents of acetonitrile, dH_2O, ethanol, methanol and propan-2-ol were all examined within this chapter.

3.2.2 Cell culture

The chronic myeloid leukaemia and hepatocellular carcinoma cells used in this chapter were maintained as described in sections 2.3.1 and 2.3.3.

3.2.3 Determination of the effect of *B. carterii* oleoresin solvent extracts on cancer cell viability.

Determination of the cytotoxic effect of the *B. carterii* oleoresin solvent extracts were evaluated using MTT assays as described in section 2.5.1. Cytotoxicity was determined based on the IC_{50} values, which were calculated as described in section 2.5.2.

3.3 Results

3.3.1 The effect of solvent extraction method on *B. carterii* yield

Oleoresin was subjected to different solvent extraction procedures to ascertain which would provide the greatest yield of compounds from the starting material. This was conducted using the method described in section 3.2.1. The yields produced by each of these solvent extraction methods are summarised in table 3-1 and figure 3-1.

Table 3-1. Extraction of *B. carterii* oleoresin using different solvent extractions results in differences in extraction yield.

Five grams of the *B. carterii* oleoresin was subjected to acetonitrile, distilled water, ethanol, methanol and propan-2-ol based solvent extractions. The resultant extract was dried to a powder using rotary evaporation and the yield recorded. Percentage yield calculated based on recovered mass compared to the mass of the starting material. All data expressed as mean ± SEM, n = 3 independent extractions.

Extraction solvent	Yield (g)	Percentage yield
Acetonitrile	0.70 ± 0.24	14.01 ± 4.83
dH_2O	0.40 ± 0.09	8.08± 1.74
Ethanol	2.52 ± 0.36	50.49 ± 7.21
Methanol	2.74 ± 0.14	54.85 ± 2.72
Propan-2-ol	2.48 ± 0.41	49.57 ± 8.26

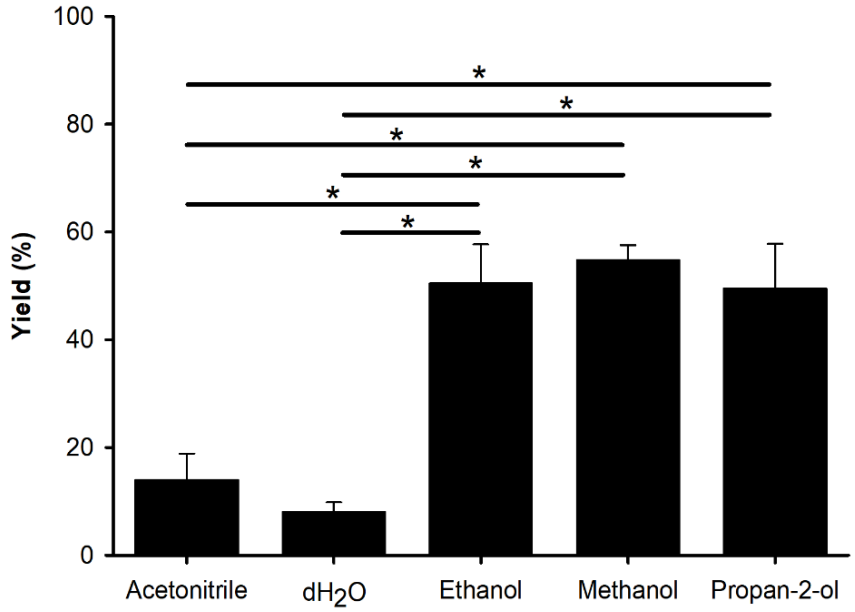

Figure 3-1. The effect of extraction solvent on yield

The percentage yields recovered following the solvent extractions of the *B. carterii* oleoresin using acetonitrile, distilled water, ethanol, methanol and propan-2-ol solvent extractions were compared to identify differences in yield. Comparisons were conducted using a one-way ANOVA followed by a Turkey post-hoc test for pairwise comparisons. Data expressed as mean ± SEM, n = 3 independent extractions. Black lines indicate the two groups being compared, with * indicating statistical significance to a p value of <0.05.

As per table 3-1 and figure 3-1, the non-alcoholic solvents acetonitrile and dH_2O produced relatively low yields of 14.01 ± 4.83 % and 8.081± 1.741 %, respectively. All three alcoholic solvents produced significantly greater absolute and percentage yields to either non-alcoholic solvent. Of the alcoholic solvents, methanol produced a yield (54.850 ± 2.721 %) greater than ethanol (50.487 ± 7.214 %) and propanol (49.568 ± 8.255 %) respectively, though this was not significant.

3.3.2 The effects of *B. carterii* solvent extracts on cancer cell viability

Whilst extraction yield is important practically, it is a different phenomenon to biological activity. It may be that a given solvent produces a discrete quantity of biologically active compounds, whilst another may produce large quantities of biologically inert compounds. As such, the cytotoxic activity of the five solvent extracts of the *B. carterii* oleoresin was evaluated against two cancer cell lines, namely the chronic myeloid leukaemia cell line, K562 (3.3.2.1), and the hepatocellular carcinoma cell line, HEP G2 (3.3.2.2).

3.3.2.1 - The effects of *B. carterii* solvent extracts on chronic myeloid leukaemia cell viability

The cytotoxicity of each oleoresin solvent extract against the K562 cell line is shown in figure 3-2.

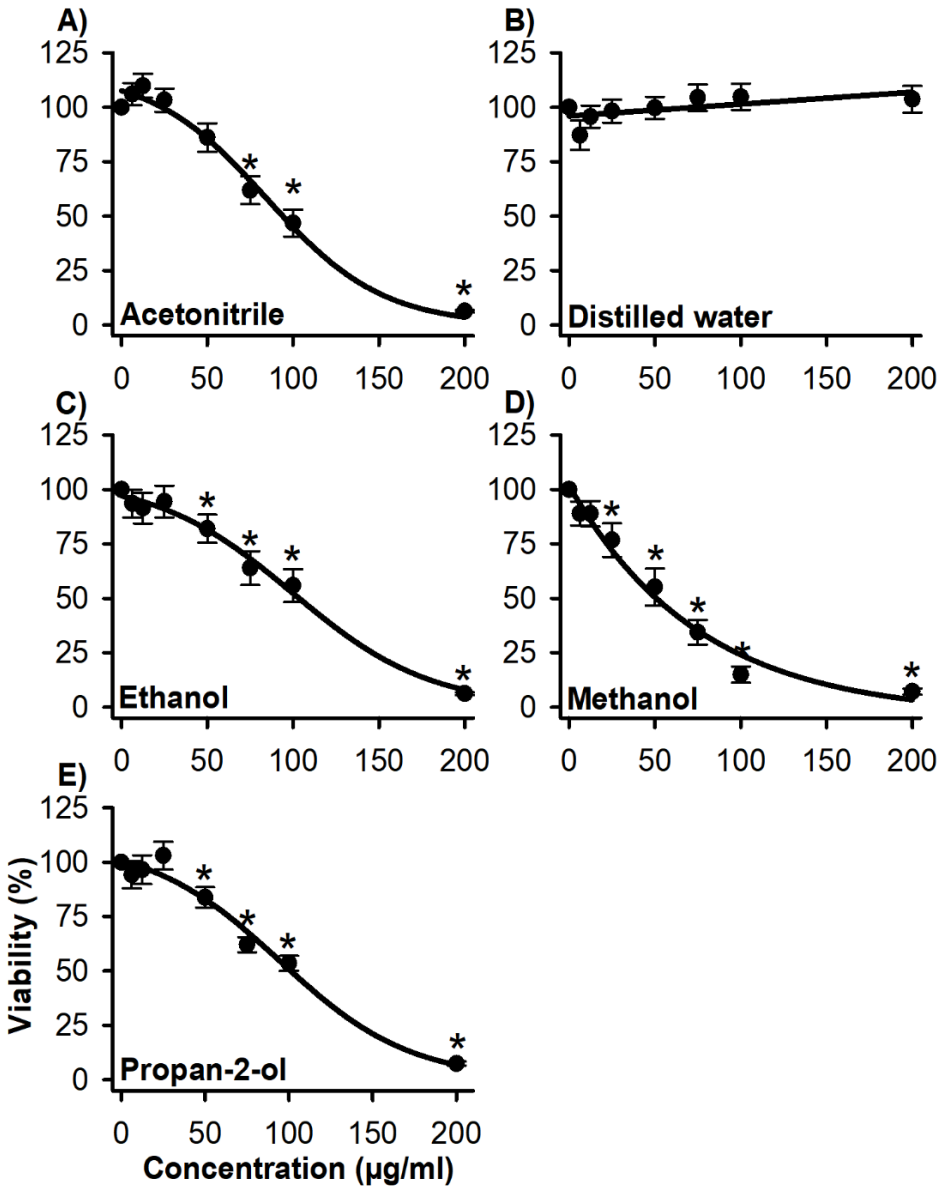

Figure 3-2. The cytotoxic effects of *B. carterii* solvent extractions on chronic myeloid leukaemia.

The cytotoxic activity of solvent extractions of *B. carterii* were assessed using the chronic myeloid leukaemia cell line, K562. Solvents used were **A)** acetonitrile, **B)** distilled water, **C)** ethanol, **D)** methanol and **E)** propan-2-ol. All data were normalised to vehicle alone (0.5 % DMSO v/v) and are given as mean ± SEM. n = 15 biological replicates for all experiments. * indicates a statistically significant difference ($p < 0.05$) compared to vehicle alone as assessed by a one-way ANOVA and Dunnett's post-hoc test.

Only the distilled water extract (figure 3-2B) was found to produce no significant decrease in K562 viability at any of the concentrations examined. All other extracts produced a concentration-depended decrease of cell viability.

The acetonitrile extract of *B. carterii* oleoresin produced a concentration dependent decrease in K562 viability reaching significance at 75 µg/ml (figure 3-2A) At the maximal concentration examined (200 µg/ml) a 93.7 ± 0.6 % ($p < 0.001$, $n = 15$) decreases in viability was observed.

The ethanolic extract (figure 3-2C) was found to produce a concentration dependent decrease in K562 viability reaching significance at a concentration of 50 µg/ml. A maximal concentration of 200 µg/ml produced a 93.7 ± 0.6 % ($p < 0.001$, $n = 15$) decrease in K562 viability.

The methanolic extract of the *B. carterii* oleoresin caused a concentration dependant decrease in K562 viability (figure 3-2D). It was shown to produce significant decreases in viability at a concentration of 25 µg/ml. Treatment with the maximal concentration examined (200 µg/ml) produced a 93.1 ± 1.5 % ($p < 0.001$, $n = 15$) decrease in viability.

The propan-2-ol extract was found to produce a concentration dependent decrease in viability, as shown in figure 3-2E. It was shown to produce significant decreases in viability at a concentration of 50 µg/ml. Treatment with 200 µg/ml induced a 92.5 ± 0.9 % ($p < 0.001$, $n = 15$) decrease in K562 viability compared to vehicle alone.

3.3.2.2 - The effects of *B. carterii* solvent extracts on hepatocellular carcinoma cell viability

To ascertain if the cytotoxic activity of the *B. carterii* oleoresin extracts was reproducible across cancer types, the cytotoxic activity of the extracts was further examined against the hepatocellular carcinoma cell line HEP G2. As per fig 3-3, four of the five extraction methods were found to possess cytotoxic activity against the HEP G2 cell line.

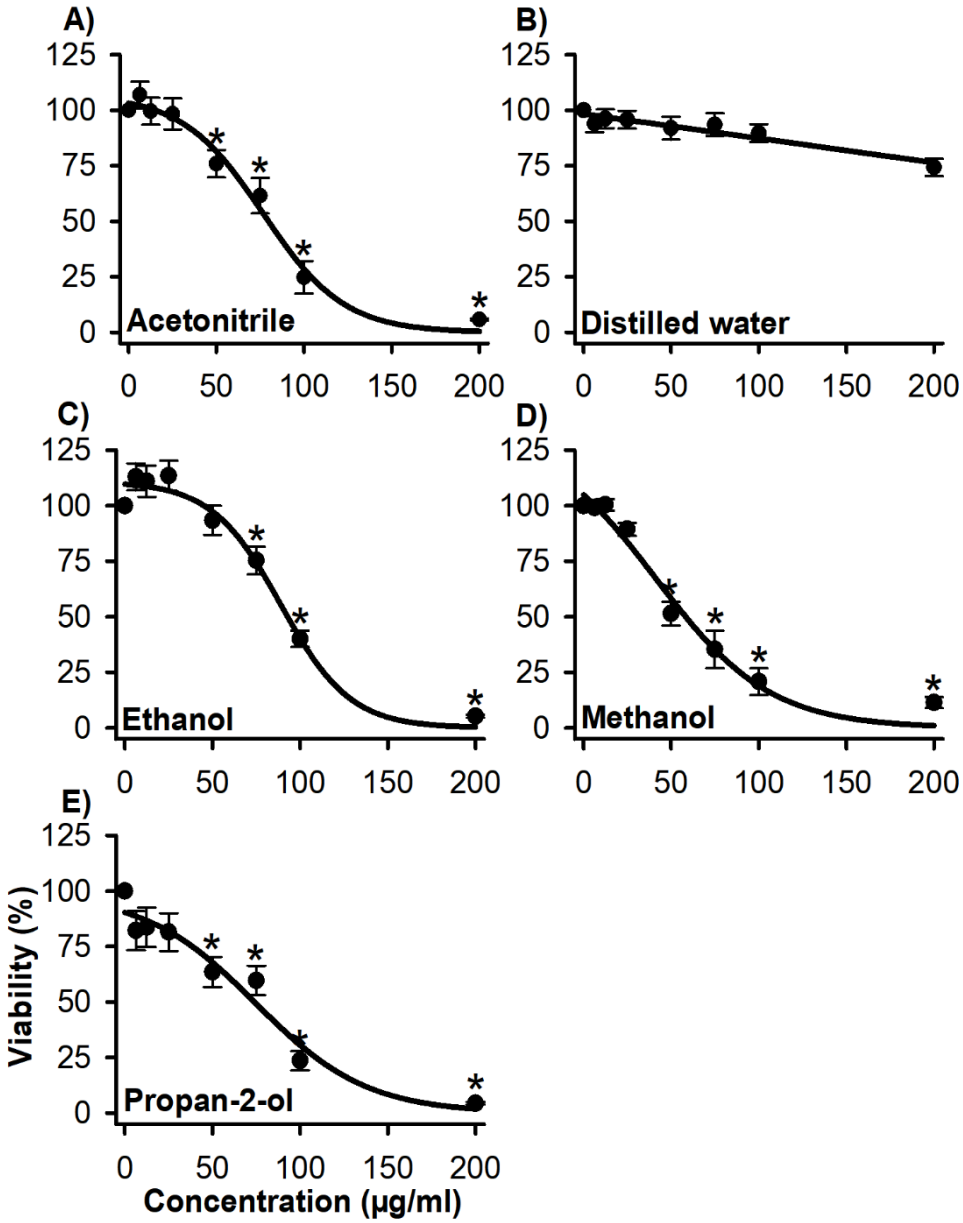

Figure 3-3. Multiple *B. carterii* oleoresin solvent extracts induce cytotoxic effects against hepatocellular carcinoma cells *in vitro*.

The cytotoxic effect of the compounds derived from various solvent **A)** acetonitrile, **B)** distilled water, **C)** ethanol, **D)** methanol and **E)** propan-2-ol extraction methods of *B. carterii* oleoresin against the hepatocellular carcinoma cell line, HEP G2. All data normalised to vehicle alone (0.5 % DMSO v/v). All data expressed as mean ± SEM. n = 15 biological replicates for all experiments. * indicates a statistically significant difference compared to vehicle alone to a p value of <0.05 following a one-way ANOVA followed by a Dunnett's post-hoc test.

The acetonitrile extract of *B. carterii* oleoresin was found to induce a concentration dependent decrease in HEP G2 viability, as shown in figure 3-3A. All concentrations ≥ 50 µg/ml resulted in significant ($p < 0.001$, $n = 15$) decreases in viability. The maximal

concentration examined was found to cause a 94.2 ± 0.5 % ($p < 0.001$, $n = 15$) decrease compared to treatment with the vehicle alone.

The distilled water extraction method was found to generate an extract which produced no significant change to HEP G2 viability (figure 3-3B). The maximal concentration examined (200 µg/ml) was found to induce a non-significant decrease of 25.64 ± 3.91 % ($p = 0.869$, $n = 15$).

The ethanolic extract of the *B. carterii* oleoresin was found to produce a concentration dependent decrease in HEP G2 viability (figure 3-3C). All concentrations ≥ 75 µg/ml produced a significant ($p < 0.001$, $n = 15$) decrease in viability. Treatment with the maximal concentration studied produced a 94.8 ± 0.6 % ($p < 0.001$, $n = 15$) decrease in viability compared to the vehicle alone.

The methanolic extract produced a concentration dependent decrease in HEP G2 viability (figure 3-3D). Concentrations of 50 µg/ml or greater all produced significant ($p < 0.001$, $n = 15$) decreases in HEP G2 viability. The maximal concentration examined caused a 87.85 ± 2.64 % ($p < 0.001$, $n = 15$) decrease in HEP G2 viability compared to treatment with the vehicle alone.

The propan-2-ol extract of *B. carterii* oleoresin was also found to produce a significant decrease in HEP G2 viability at concentrations of 50 µg/ml or greater (figure 3-3E). A concentration of 50 µg/ml was shown to cause a 32.07 ± 5.15 % ($p < 0.001$, $n = 15$) decrease in HEP G2 viability compared to the vehicle alone. Concentrations of greater than 50 µg/ml were found to result in superior decreases in viability. Concentrations of 75, 100 and 200 µg/ml were found to induce 37.59 ± 5.32 % ($p < 0.001$, $n = 15$), 74.38 ± 4.03 % ($p < 0.001$, $n = 15$) and 95.44 ± 0.48 % ($p < 0.001$, $n = 15$) decrease in viability respectively compared to vehicle alone.

3.3.3 Identification of the most potent *B. carterii* solvent extraction method as a source of chemotherapeutic agents

To determine which extraction method would be taken forward for further analysis, the cytotoxicity of each *B. carterii* oleoresin solvent extract was compared using IC_{50} analysis as shown in figure 3-4. Given that in section 3.3.2 dH_2O produced no effect on cell viability, it was excluded from this analysis.

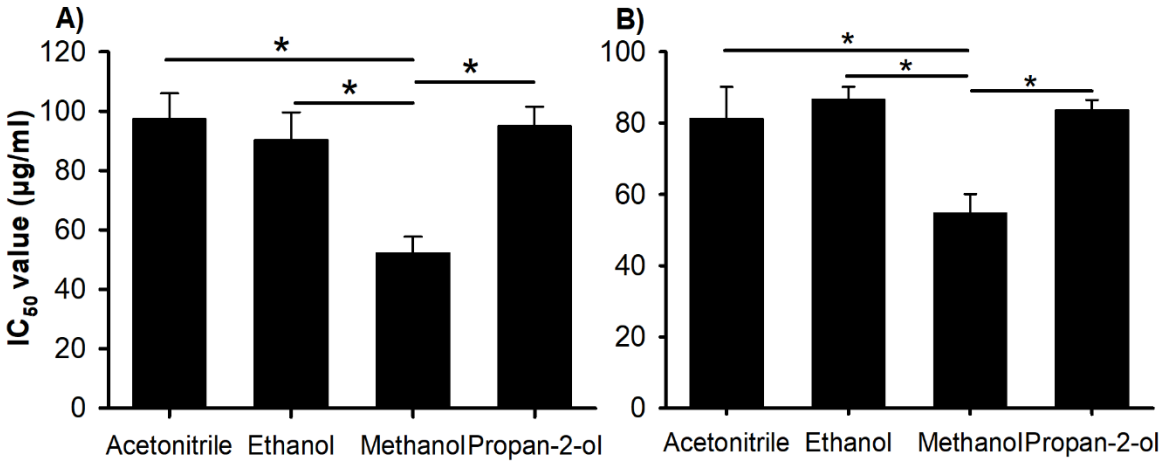

Figure 3-4. The relative cytotoxic effect of each solvent extract.

A comparison of the cytotoxic activity of the *B. carterii* oleoresin acetonitrile, ethanol, methanol and propan-2-ol extracts against **A)** K562 and **B)** HEP G2 cell lines. Cells were treated for 72 hours before analysis. Data expressed as mean IC_{50} ± SEM. n = 15 biological replicates for both K562 and HEP G2. * indicates a statistically significant difference ($p < 0.05$) as determined by a one-way ANOVA followed by a Turkey post-hoc test.

As can be seen in figure 3-4A, the IC_{50} values of acetonitrile, ethanol and propan-2-ol against K562 cells was both relatively high very and similar (acetonitrile; 97.5 ± 8.6 µg/ml, ethanol; 90.3 ± 9.3 µg/ml , propan-2-ol; 95.0 ± 6.5 µg/ml, n = 15 for each, $p > 0.05$). The methanolic extract was significantly more cytotoxic with an IC_{50} 34.5 ± 10.2 % ($p < 0.001$, n = 15), 31.7 ± 13.6 ($p = 0.005$, n = 15) and 39.0 ± 13.4 % ($p = 0.001$, n = 15) lower than acetonitrile, ethanol and propan-2-ol respectively.

As can be seen in figure 3-4B, a similar pattern was observed in HEP G2 cells with the IC_{50} of acetonitrile, ethanol and propan-2-ol being both relatively high very and similar (acetonitrile; 81.4 ± 8.8 µg/ml, ethanol; 86.7 ± 3.5 µg/ml , propan-2-ol; 83.8 ± 2.7 µg/ml, n = 15 for each, $p > 0.05$). The methanolic extract was once again significantly more cytotoxic with an IC_{50} value 30.5 ± 5.5 % ($p < 0.001$, n = 15), 29.4 ± 4.4 ($p = 0.005$, n = 15) and 26.3 ± 4.6 % ($p < 0.001$, n = 15) lower than acetonitrile, ethanol and propan-2-ol respectively.

Comparisons between the cytotoxicity of the *B. carterii* extracts against both cancer types showed that the HEP G2 cells were more sensitive to the acetonitrile, ethanol and propan-2-ol extracts than K562 cells. However, this difference was found non-significant for all three extracts ($p > 0.05$, n = 15). The IC_{50} value of the methanolic extract was found to be similar in both cancer types examined.

3.4 Discussion

This study aimed to determine the best method for extracting potentially biological active compounds from the *B. carterii* oleoresin. Numerous solvents including acetonitrile, dH_2O, ethanol, methanol and propan-2-ol were examined for their ability to extract compounds and to determine if these extracts possessed biological activity against multiple cancer cell lines *in vitro*.

3.4.1 Are the solvent extracts of *B.* carterii fundamentally cancer cytotoxic?

Before determining the most effective method of extracting compounds from the *B. carterii* oleoresin it was first imperative to ascertain if the oleoresin itself was inherently cytotoxic to cancer cells. As if the oleoresins of this species were found to be inert, it would make further analysis redundant.

The findings of this study show that the oleoresins of *B. carterii* are cytotoxic towards both cancer cell types initially examined. Whilst the oleoresins of *Boswellia*, namely that of *B. serrata* has been shown to possess cytotoxic activity (Alipanah & Zareian, 2018; Ranjbarnejad *et al.*, 2017), these studies have been conducted to identify if the alcoholic extracts of different species of *Boswellia* oleoresin possess biological activity. Previous research has shown the methanolic extract of *B. serrata* showed a similar concentration dependant decrease in viability when analysed against the colorectal carcinoma cell line (HT-29) cell viability (Ranjbarnejad *et al.*, 2017) to what this study observed against the K562 cell line. A similar effect was observed when the *B. serrata* hydro-alcoholic extract was also found to produce a concentration dependant cytotoxic activity against the 4T1 breast cancer cell line (Alipanah & Zareian, 2018). A study by Yazdanpanahi *et al.* (2014) showed the *B. Thurifera* methanolic extract to induce a concentration dependant decrease in cancer cell viability with an IC_{50} value 80 µg/ml against the MDA-MB-231 breast cancer cell line. Despite this previous research on the *Boswellia* genus, this study is the first to examine the cytotoxic effect of alcohol- based extraction methods derived from the oleoresins of *B. carterii*.

Despite these studies, the *Boswellia* genus as a whole remains relatively unexplored. This is especially the case for that of *B. carterii* with no previous study examining the cytotoxic effects of the oleoresin of this species. The findings of this study therefore highlight that the potential of *B. carterii* oleoresins as a novel source of chemotherapeutic agents and necessitates the need for further examination.

3.4.2 Which solvent produces highest extraction yield?

Of the extraction methods analysed, it was found that the alcoholic extraction solvents produced a significantly greater extraction yield than those of the non-alcohol-based solvents. Of these the methanolic extract was found to produce the greatest yield, however it's yield was comparable to that of the ethanol and propan-2-ol extractions.

The alcoholic extraction methods may extract a greater yield of compounds due to *Boswellia* oleoresins being reported to contain between 65 - 85% alcohol soluble resinous material (Abdel-Tawab *et al.*, 2011; Al-Harrasi & Al-Saidi, 2008) with a significantly lower amount of water-soluble gum (approximately 6 - 30 %). This lower amount of water-soluble material corroborates our results, as the oleoresin dH_2O extract was found to contain 9.18 % water soluble material, which is comparable to that commonly found within various previously described oleoresin producing species (Asad & Alhomoud, 2016; Zhang *et al.*, 2016).

Previous studies have also described alcohol based extraction methods to recover yields of between 65.0 - 86.9 % from *Boswellia* oleoresins (Yang, Ren, *et al.*, 2018; Zhang *et al.*, 2016). This study found that alcohol-based extractions of *B. carterii* oleoresins ranged between 49.6 and 54.9 %, which is substantially less than that previously described. This difference in yield may arise from variations in the chemical composition of individual *Boswellia* species. These differences may arise due to the variations in specific the characteristics of the substrates based on the environmental and ecological conditions in which the species grow (DeCarlo *et al.*, 2018).

The decreased yield of the acetonitrile extract in comparison to the alcoholic extracts may be due to a lower polarity than that of the alcoholic extraction solvents selected in addition to the composition of the oleoresin (Malavolta *et al.*, 2008; Reichardt & Welton, 2011). The difference in polarities of the solvents have been found to selectively extract targetable flavonoid compounds from the materials of other plant species (Dailey & Vuong, 2015; Wakeel, Jan, Ullah, Shinwari, & Xu, 2019). The solvents utilised as a part of this study were all high on the polarity scale with propan-2-ol possessing the lowest polarity of all of extraction solvents examined (Snyder, 1978).

The results of this study also show that alcoholic extraction methods possess a significant ability to extract compounds from the *B. carterii* oleoresin. This has been shown to be irrespective of the polarity of the alcohol used, with no significant

difference being observed in the extraction yield between the highest polarity and lowest polarity alcohol used as a part of this study.

3.4.3 Which solvent extraction produces the greatest biological activity?

Whilst extraction yield is significant practical aspect, it is a different phenomenon to that of biological activity. It may be that a specific solvent extraction produces a small quantity of biologically active compounds, whilst another may produce large quantities of biologically inert compounds. Therefore, as long as the yield is feasible for further analysis, the biological activity is the crucial aspect. As an result, a understanding into the biological activity of each solvent extract irrespective of their extraction yield is imperative.

3.4.3.1 The biological activity of water extracts of *B. carterii*

Up to 30 % of *Boswellia* biomass is water soluble gum. (Abdel-Tawab *et al.*, 2011; Al-Harrasi & Al-Saidi, 2008). It cannot be assumed that associated compounds are alcohol soluble, yet despite this no previous study has evaluated water as a potential extraction solvent. This study is therefore the first to evaluate the cytotoxic activity of this fraction.

Of all extraction solvents examined, only the dH_2O extract produced no cytotoxic effect at any concentration evaluated. This was the case in both K562 and HEP G2 cells. This suggests that while dH_2O may extract the compounds contained within the water-soluble gum component of the oleoresin, it shows that against the two reporter cancer cell types utilised in this study this material is not biologically active. The findings of this study further validate those of previous research regarding the biological activity of *Boswellia* oleoresin extracts (Alipanah & Zareian, 2018; Ranjbarnejad *et al.*, 2017; Yazdanpanahi *et al.*, 2014) which have exclusively utilised alcohol based extractions by showing that the material not extracted by alcoholic solvents is inert as a cytotoxic agent.

3.4.3.2 The biological activity of acetonitrile extracts of *B. carterii*

This study is the first to test an acetonitrile extract of *B. carterii* against cancer cell lines *in vitro*. The acetonitrile extract of *B. carterii* oleoresin was found to possess cytotoxic activity against both K562 and HEP G2 cancer cell lines with IC_{50} values of 97.5 ± 8.6 µg/ml and 81.3 ± 8.8 µg/ml respectively.

Acetonitrile is a medium-polarity solvent, known to dissolve a wide range of ionic and non-polar compounds (Chemat *et al.*, 2019). Therefore, it may be the case that the source of the biological activity of the acetonitrile extract is these non-polar compounds. Further to this, despite the low yield of the acetonitrile extract (14.0 ± 4.8 %), its biological activity was found to be comparable to that of the ethanol and propan-2-ol. This difference in yield may therefore be a result of selective extraction of the biological activity responsible for the activity of ethanol and propan-2-ol extracts. However, further research is required to confirm this hypothesis.

These findings highlight the potential of utilising acetonitrile for the extraction of biologically active materials. However, despite this biological activity limitations of the extraction yield generated may restrict its use as there may not be enough material generated to further analyse the biological activity of this extract.

3.4.3.3 The biological activity of the alcoholic extracts of *B. carterii*

Previous research has shown that methanolic extractions are most commonly used to extract biologically active compounds from the *Boswellia* oleoresins (Alipanah & Zareian, 2018; Ranjbarnejad *et al.*, 2017; Yazdanpanahi *et al.*, 2014). These previous studies on the oleoresins *B. serrata* (Alipanah & Zareian, 2018; Ranjbarnejad *et al.*, 2017) and *B. thurifera* (Yazdanpanahi *et al.*, 2014) have primarily focused on alcoholic based extractions to isolate biologically active compounds from *Boswellia* oleoresins. However, these studies have exclusively focused on a methanolic extraction method. Based on this, this study aimed to ascertain if this approach was also appropriate for the oleoresins of *B. carterii*. Our findings confirm that a methanolic extraction of the *B. carterii* oleoresin possess' significant cytotoxic activity.

Further to this, this study describes for the first time that the ethanol and propan-2-ol extracts possess biological activity against both epithelial and suspension cancers. However, compared to the methanolic extract both methods were found to be significantly less cytotoxic. This difference in cytotoxicity may be a result of the specific differences in the mechanism of action behind the cytotoxic effect of the oleoresin extracts or differences in the biologically active compounds within the oleoresins.

The data shown in figures 3-2C-E and 3-3C-E shows that the three alcohol-based extraction solvents examined were found to induce a concentration dependent decrease in viability in both cell types examined. Of these, the methanolic extract

produced the greatest cytotoxic effect with an IC_{50} value of 52.20 ± 5.53 µg/ml against the K562 cell line and an IC_{50} value of 54.83 ± 5.27 µg/ml against the HEP G2 cell line.

As described in section 3.3.1, it was found that all three alcohol-based extraction solvents generated a comparable yield, it is therefore interesting that the methanolic extract was found to be significantly more biologically active compared to that of the ethanol and propan-2-ol extract. It may be the case that the methanolic extraction method isolates exclusive compounds which are responsible for this significantly increased biological activity. However, this cannot be confirmed without further characterisation of the chemical composition of each extract.

3.4.4. Selection and justification of extraction solvent for *B. carterii* oleoresin

Based on the findings of this chapter, despite all solvents used being capable of extracting compounds from the oleoresin of *B. carterii* and the majority possessing cytotoxic activity, it can be determined that the selection of a methanolic based extraction is the most appropriate for extracting biologically active compounds from *B. carterii* oleoresin.

The dH_2O extract of *B. carterii* oleoresin was found to generate the lowest extraction yield of all extraction solvents examined (figure 3-1) with a yield of 8.081± 1.741 %. This low quantity of material generated makes it a poor choice as numerous extractions would have to be conducted to generate enough material to conduct further analysis. In addition, the dH_2O extract's lack of cytotoxic activity at the maximal concentration examined (200 µg/ml) indicates the water-soluble gum fraction of the oleoresin contains no compounds which possess cytotoxic activity against the two cancer cell lines used as biological reporters. This therefore indicates that; (1) alternative solvent extracts have not missed any biologically active compounds and justifies the use of alternative extraction solvents and (2) that the dH_2O extraction method is not suitable for use to extract biologically active components from the *B. carterii* oleoresin.

The findings shown in figures 3-2A and 3-3A describe for the first time that the acetonitrile extract of *B. carterii* oleoresin possesses biological activity against both of the cancer cell types examined. Whist it cannot be ruled out that the use of acetonitrile produces compounds exclusive to this method, the low extraction yield generated makes this method impractical for further examination of the cytotoxic activity of *B. carterii* oleoresin.

This study also showed that all alcohol-based extraction methods were capable of extracting biological active compounds from the *B. carterii* oleoresin. Of the alcohol-based extraction methods examined all were found to extract an equivalent yield of compounds, as shown in figure 3-1. Whilst these finding cannot rule out that differing alcoholic extractions isolate a comparable composition of compounds, previous studies and our data suggests that this is not an issue.

Further to this, based on the biological activity of each extraction method shown in figure 3-4, it can be seen that whilst all alcoholic based extractions possess biological activity, the methanolic extraction method produced a significantly greater biological activity in both cancer cell lines examined. This increased biological activity may be a result of the bipolar nature of methanol, allowing it to isolate compounds from other fractions of the oleoresin, in addition to the alcohol soluble fraction. It therefore may be the case that a methanolic extraction method isolates compounds not extracted using other methods which are responsible for this increased biological activity.

This significantly increased cytotoxic activity of the methanolic extract and relatively high extraction yield, highlights that the methanolic extraction method may preferentially isolate key biologically active compounds, which may be missed by other extraction solvents. In addition, it also offers a practical extraction yield allowing it to be further examined for its chemical composition and to further evaluate its potential as an anti-cancer agent. Therefore, due to these factors, the methanolic extract of the *B. carterii* oleoresin offers the optimal extraction method for further examination.

3.4.5 Conclusions

In conclusion, this study has described that the oleoresins of *B. carterii* do possess anti-cancer activity *in vitro*. These findings also suggest that the methanolic extraction method is appropriate due it yielding practical yields while having lowest IC_{50} value. This study also identified that the water-soluble compounds within the *B. carterii* oleoresin possessed no cytotoxic activity against both cancer cell types examined, further supporting the selection of an alcohol-based extraction method. As a result, the methanolic extract of the *B. carterii* oleoresin was taken forward and its cytotoxic effects evaluated further.

Chapter 4

A detailed evaluation of the anti-cancer potential of the methanolic extract of the *B. carterii* oleoresin

4.1 Introduction

In chapter 3, the study identified that the methanolic extract of the *B. carterii* oleoresin possessed the greatest cytotoxic activity against both the K562 and HEP G2 cancer cell lines. This chapter also indicated that the methanolic extraction method was the most efficient at extracting biologically active compounds from the *B. carterii* oleoresin. In doing this, it was shown that the *B. carterii* oleoresin possesses fundamental anti-cancer activity against K562 and HEP G2 cell lines was demonstrated.

Previous work has described that methanolic extracts of *Boswellia* oleoresins induce a cytotoxic effect against certain cancer cell lines both *in vitro* and *in vivo* (Alipanah & Zareian, 2018; Jaafari-Ashkavandi *et al.*, 2017; Ranjbarnejad *et al.*, 2017; Xia *et al.*, 2017; Yazdanpanahi *et al.*, 2014)., However, the range of cancer cell types tested against is far from exhaustive thus the pluripotency of *Boswellia* oleoresin is not clear. This is especially the case for *B. carterii*, where the understanding of its cytotoxic activity is extremely limited.

Whilst previous studies have shown the solvent extracts of *Boswellia serrata* oleoresin to induce a cytotoxic effect against breast, liver and colon cancer *in vitro* (Ahmed *et al.*, 2015; Alipanah & Zareian, 2018; Ranjbarnejad *et al.*, 2017). Limited research has specifically evaluated the cytotoxic activity of the extracts of *B. carterii*. The preliminary studies on the cytotoxic effects of solvent extracts of *B. carterii*, described in section 3.3.3, indicates that the methanolic extract may induce cytotoxic effects against multiple cancer cell types, however further investigation is required to confirm this. It is therefore of particular interest to determine if the extracts of *B. carterii* oleoresins induce cytotoxic effects against cancer cell lines other than those which have been previously described to develop an understanding of the pluripotency of the *B. carterii* oleoresin.

The ability of an anti-cancer agent to target multiple cancer cell types would increase its widespread use in the treatment of cancer due to its ability to target all cancerous cells within the body irrespective of cancer type, similar to that of classical chemotherapeutics. However, these classical chemotherapies are commonly highly toxic to healthy cells in addition to cancerous ones and as a result they are utilised at sub optimal concentrations to minimise the risk of side effects (as previously described in section 1.2.7).

Furthermore, limited research has also been conducted into time-dependence of *Boswellia* oleoresin cytotoxicity. Whilst 72 hours is a common treatment period in studies that seek to ascertain the cytotoxicity of plant-based compounds (Eastman, 2017), anti-cancer drugs commonly show a strong time-dependence of effect or hormetic responses (Riva *et al.*, 2014).

The need to do this for *Boswellia* oleoresins is particularly apparent, given the aforementioned limited previous studies have primarily focused on one specific largely arbitrary exposure period. Therefore, to develop an understanding into how potential anti-cancer drugs interact with cancer cells over time is of vital importance as it facilitates development of an understanding of potential mechanisms of action underpinning the cytotoxicity and a concentration range at which the cytotoxic effect is maximised for a specific treatment regimen. To establish the time-dependence of *Boswellia* cytotoxicity is critical if the pharmacological potential is to be established. This information is also likely to be of wider interest to others in the field.

Further to this, if the methanolic extract of the *B. carterii* oleoresin was found to be active against numerous cancer cell types, it would be imperative that they were examined against healthy cells as damage to these cells is associated with the development of side-effects. Commonly used anti-cancer drugs have been described to have severe long- and short-term side effects (Islam, Lustberg, *et al.*, 2019; Oun *et al.*, 2018; Tao *et al.*, 2015), as described further in 1.2.7. These severe side effects have been described to be as a result of the low selectivity of these drugs towards cancer cells compared to that of normal cells (Al-Qubaisi *et al.*, 2011; Pritchett, Naesens, & Montoya, 2014).

This selectivity of a drug is calculated based on the effectiveness of a potential anti-cancer compound towards cancer cells compared to that of normal cells to generate a value, known as the selectivity index. A selectivity index value of 1 indicating an identical cytotoxic effect observed against cancer and healthy cells, whilst < 1 indicates preferential activity towards healthy cells and > 1 indicating greater activity towards cancer cells (Rusdi, Alam, & Manggau, 2013). This effect of selectivity of anti-cancer drugs is exemplified by the anthracycline, doxorubicin, which has been shown to result in severe patient side effects including cardiomyopathies. Doxorubicin has been described to have a selectivity index ranging between 0.27 and 1.31 dependant on the

cancer type examined *in vitro* (Badmus, Ekpo, Hussein, Meyer, & Hiss, 2019; de Oliveira *et al.*, 2015; Pugachev *et al.*, 2017).

This pattern of selectivity is also observed for other classical and more modern chemotherapeutic agents that are still in use today (Adhikari, Hussain, Phillips, Kaminsky, & Kollipara, 2018; Ibrahim, Gao, & Sinko, 2014). These factors highlight the need to continue developing novel chemotherapeutic agents, with greater selectivity.

A potential source of these agents is plants which have been used for centuries in traditional medicine. These plant sources have been used for millennia for the treatment of a variety of diseases and are not associated with any severe side effects in humans (Desai *et al.*, 2008; Iqbal *et al.*, 2017). As a result, it can be hypothesised that the oleoresins of *B. carterii* may offer a potential source of high selectivity anti-cancer compounds.

4.1.1 Aims of the chapter

This chapter aimed to further evaluate the cytotoxic activity profile of the methanolic extract of *B. carterii* oleoresin. Specifically, this study aimed to establish the wider cytotoxic activity against further cancer cell types. Additionally, this chapter also sought to determine if the methanolic extract of the *B. carterii* oleoresin selectively targets cancer cells *in vitro*.

The main aims of this chapter are as follows:

1) To determine the time dependence of *B. carterii* oleoresin cytotoxicity.
2) To establish the wider anti-cancer potential of *B. carterii* oleoresins.
3) To determine the cancer selectivity and specificity of the cytotoxic activity of *B. carterii* oleoresin.

4.2 Methods

4.2.1 Extraction and preparation of the methanolic extract

Extraction and preparation of the methanolic extract was conducted as described in section 2.5. The methanolic extract was dissolved in DMSO to a stock concentration of 50 mg/ml. This stock was then diluted to the desired concentrations using an appropriate cell culture media for the cancer cell line being examined as described in section 2.3.

4.2.2 Cell culture

Culture of all cancer cell and non-cancer cell lines utilised within this chapter was conducted as described in sections 2.3 and 2.4.

4.2.3 Isolation and culture of PBMC's

4.2.3.1 Isolation of peripheral blood mononuclear cells from whole blood

Whole Human blood was purchased from the National Health Service Blood and Transplant service, UK. Whole blood was diluted to a 1:1 ratio with 1x PBS, before being carefully layered over lymphocyte separation media (Corning, USA) to a ratio of two parts diluted whole blood to one-part lymphocyte separation media, as shown in figure 4-1. This mixture was centrifuged at 400 xG for 30 minutes with no brake.

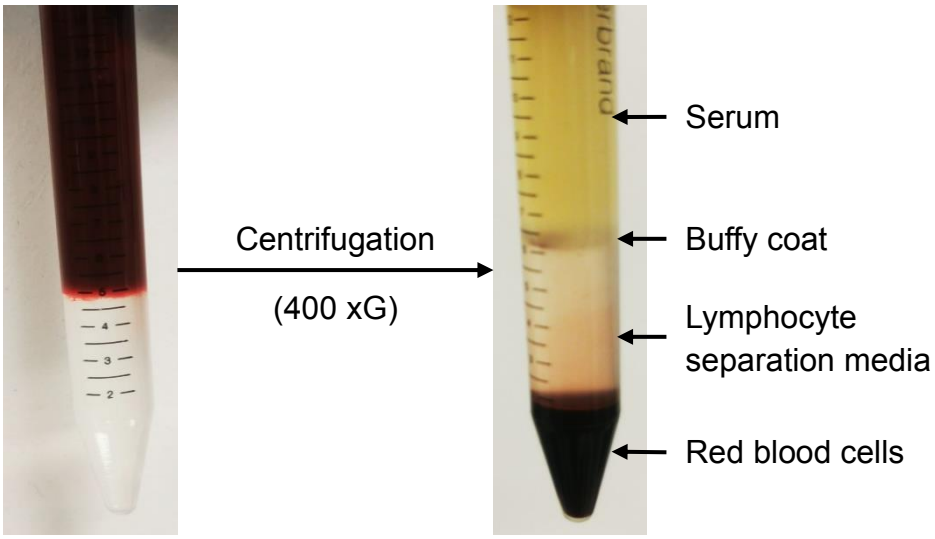

Figure 4-1. The isolation of peripheral blood mononuclear cells from whole blood.

A schematic diagram showing the isolation of peripheral blood mononuclear cells. Whole blood was layered over lymphocyte separation media, before being centrifuged at 400 xG for 30 minutes. Following centrifugation, the buffy coat containing the PBMC's was carefully retrieved.

Following centrifugation, the buffy coat, shown in figure 4-1 was carefully aspirated and pooled into fresh centrifuge tubes. The buffy coats were then washed using 1x PBS and centrifuged at 200 xG for 10 minutes.

4.2.3.2 Maintenance of peripheral blood mononuclear cells in cell culture

Following isolation, the PBMC's were maintained in culture until required for experimentation. PBMC's were seeded to a density of 20 x 10^6 /ml in complete RPMI-1640 (10 % FBS and 1 % penicillin-streptomycin) and incubated at 37 ^oC in a 5 % CO_2 atmosphere. Isolated PBMC's were also placed into long-term liquid Nitrogen storage through the process described in section 2.3.3.2.

4.2.4 Determining the time dependent effects of the *B. carterii* oleoresin methanolic extract

The time dependent cytotoxicity was determined using MTT assays as described in section 2.5.1. The only modification to this method was the time in which the drug was applied. The application time was modified to be either 24, 72 or 120 hours, dependent on the experiment being conducted. Cytotoxicity was determined based on the IC_{50} values, which were calculated as described in section 2.5.2.

4.2.5 Determining the concentration dependent effects of the *B. carterii* oleoresin methanolic extract

Concentration dependent cytotoxicity for all cancer cell types was determined as described in section 2.5.1. Cytotoxicity was determined based on the IC_{50} values, which were calculated as described in section 2.5.2.

4.2.6 Determining the effect of the *B. carterii* oleoresin methanolic extract on non-cancerous cell types

Concentration dependent cytotoxicity for the non-cancer cell types (BEAS-2B and PBMC's) was determined as described in section 2.5.1. The only modification for PBMC's was the seeding density, which was increased from 5,000 cells per well to 50,000 cells per well. Cytotoxicity was determined based on the IC_{50} values, which were calculated as described in section 2.5.2.

4.2.7 Calculating the selectivity of the *B. carterii* oleoresin methanolic extract towards cancer cells

To calculate the selectivity of the cytotoxic activity of *B. carterii* oleoresin towards cancer in comparison to non-cancer cells. The equation shown in equation 4-1 was used to calculate this:

Equation 4-1. The equation used to calculate the selectivity index of the *Boswellia carterii* oleoresin methanolic extract.

$$\text{Selectivity} = IC_{50}^{\text{non-cancer cells}} / IC_{50}^{\text{cancer cells}}$$

4.3 Results

4.3.1 The effect of treatment time on the cytotoxic activity of the *B. carterii* oleoresin methanolic extract

To evaluate if the cytotoxic activity of the methanolic extract of the *B. carterii* oleoresin was time dependant, the cytotoxic effect was evaluated at 24, 72 and 120 hours. This was performed in K562 and HEP G2 cell lines given the data acquired in chapter 3.

The *B. carterii* oleoresin methanolic extract was found to act in a time dependent manner against both the K562 and HEP G2 cancer cell lines, as shown in figures 4-2 and 4-3.

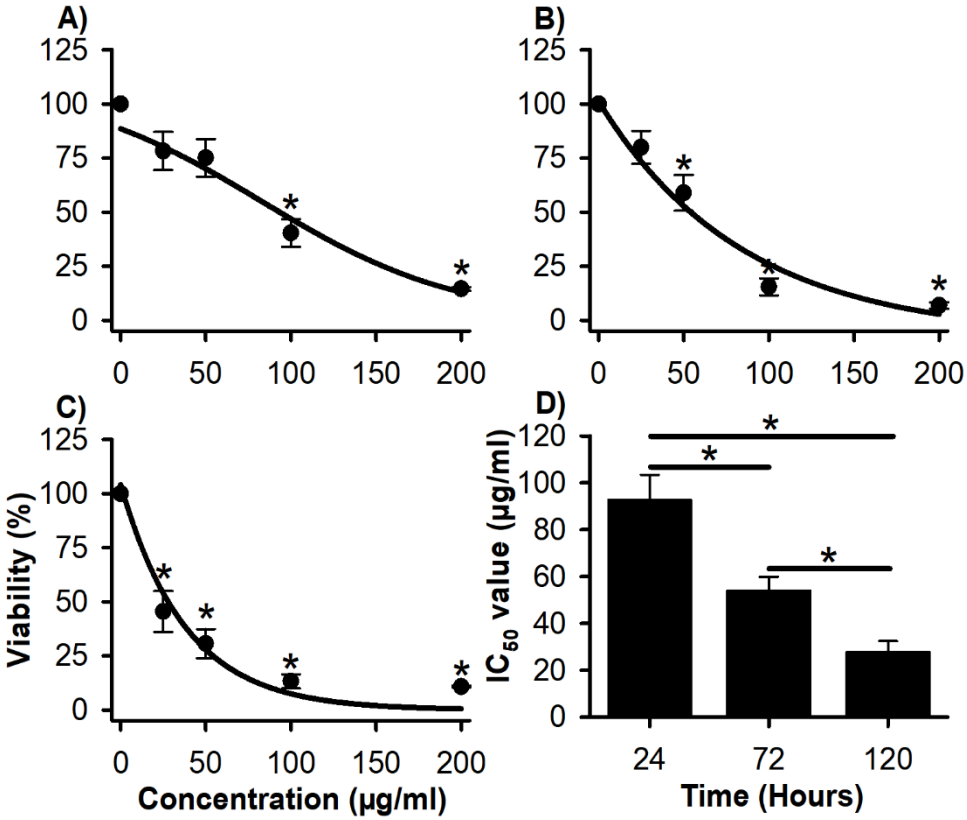

Figure 4-2. The *B. carterii* oleoresin methanolic extract induces time dependent cytotoxicity towards chronic myeloid leukaemia cells.

Chronic myeloid leukaemia cells (K562) were treated with varying concentrations of the *B. carterii* oleoresin methanolic extract for **A)** 24 hours, **B)** 72 hours, and **C)** 120 hours to evaluate the effect of time on the cytotoxicity induced by the oleoresin methanolic extract. Panel **D)** shows a comparison of the IC_{50} values for treatment at each timepoint examined. All data normalised to vehicle alone (0.5 % DMSO v/v). Data expressed as mean ± SEM, n = 12. Lines indicates the groups being compared. * indicates a statistically significant difference compared to vehicle alone to a p value of <0.05.

At all timepoints examined, a concentration dependent decrease in K562 viability was observed, as shown in figures 4-2A-C. When the IC_{50} values at each treatment timepoint were compared, shown in figure 4-2D, a time-dependent increase in cytotoxicity was observed. Treatment for 120 hours was found to result in a 73.9 ± 2.7 % (24 hours; 92.8 ± 10.6 µg/ml, 120 hours; 27.9 ± 4.6 µg/ml, $n = 12$, $p < 0.001$) increase in cytotoxicity compared to treatment for 24 hours. Treatment for 120 hours was also found to be 22.8 ± 25.3 % (72 hours; 54.2 ± 5.8 µg/ml, 120 hours; 27.9 ± 4.6 µg/ml, $n = 12$, $p = 0.046$) more cytotoxic than treatment for 72 hours. It was also identified that treatment for 72 hours induced a 41.1 ± 8.0 % (24 hours; 92.8 ± 10.6 µg/ml, 72 hours; 54.2 ± 5.8 µg/ml, $n = 12$, $p = 0.003$) increase in cytotoxicity compared to treatment for 24 hours.

Further examination of the time-dependent effect of *B. carterii* oleoresin extract was also conducted against HEP G2 cell line. As shown in figure 4-3, the *B. carterii* oleoresin extract was found to induce time-dependent cytotoxic activity.

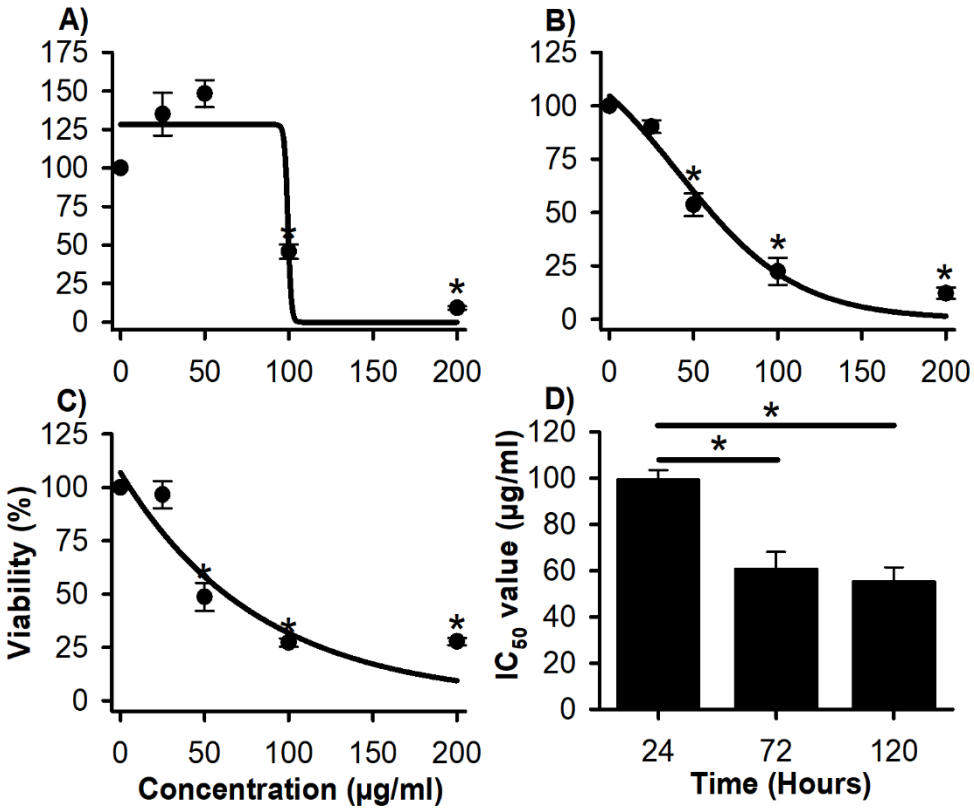

Figure 4-3. The *B. carterii* oleoresin methanolic extract induces time dependent cytotoxicity towards hepatocellular carcinoma cells.

Hepatocellular carcinoma cells (HEP G2) were treated with varying concentrations of the *B. carterii* oleoresin methanolic extract for **A)** 24 hours, **B)** 72 hours, and **C)** 120 hours to evaluate the effect of time on the cytotoxicity induced by the oleoresin methanolic extract. Panel **D)** shows a comparison of the IC_{50} values for treatment at each timepoint examined. All data normalised to vehicle alone (0.5 % DMSO v/v). Data expressed as mean ± SEM, n = 12 biological replicates. Lines indicates the groups being compared. * indicates a statistically significant difference compared to vehicle alone to a p value of < 0.05.

Against the HEP G2 cell line a similar pattern of effect was observed to that previous described in K562 cells, as shown in figures 4-3A-C. When the cytotoxicity at each timepoint was compared, as shown in figure 4-3D, significant differences were observed. Treatment for 120 hours was found to result in an 45.9 ± 6.9 % (24 hours; 99.6 ± 4.0 µg/ml, 120 hours; 55.5 ± 6.9 µg/ml, n = 12, p < 0.001) increase in cytotoxicity compared to treatment for 24 hours. Treatment for 72 hours was also found to significantly increase the cytotoxicity by 35.7 ± 4.8 % (24 hours; 99.6 ± 4.0 µg/ml, 72 hours; 60.9 ± 7.3 µg/ml, n = 12, p < 0.001) compared to treatment for 24 hours. No significant difference was observed between treatment lengths of 72 and 120 hours.

4.3.2 The cytotoxic effects of methanolic extracts of the *B. carterii* oleoresin in other cancer cell types

To further evaluate the cytotoxic potential of the *B. carterii* oleoresin methanolic extract as a potential anti-cancer agent, the extracts of were examined against numerous other cancer cell types. Based on the findings of section 4.3.1 and previous research (Riva *et al.*, 2014), this further analysis was conducted for a exposure time of 72 hours as it offered the most efficient method for determining the anti-cancer activity of the *B. carterii* oleoresin. The results of this analysis are described in sections 4.3.2.1 - 4.3.2.3.

4.3.2.1 The cytotoxic effect of methanolic extracts of the *B. carterii* oleoresin against leukaemia subtypes

The methanolic extract of the *B. carterii* oleoresin was found to be cytotoxic towards chronic myeloid leukaemia cells in a concentration and time dependent manner as previously described in sections 3.3.2 and 4.3.1 respectively. Based on this we aimed to further explore the cytotoxic activity of the methanolic extract of the *B. carterii* oleoresin against other leukaemia cell lines. The cytotoxicity of the oleoresin against the K562 cell line was repeated, whilst being further screened against the acute lymphoblastic leukaemia cell lines CCRF-CEM and MOLT-4. The results of this analysis are shown in figure 4-4.

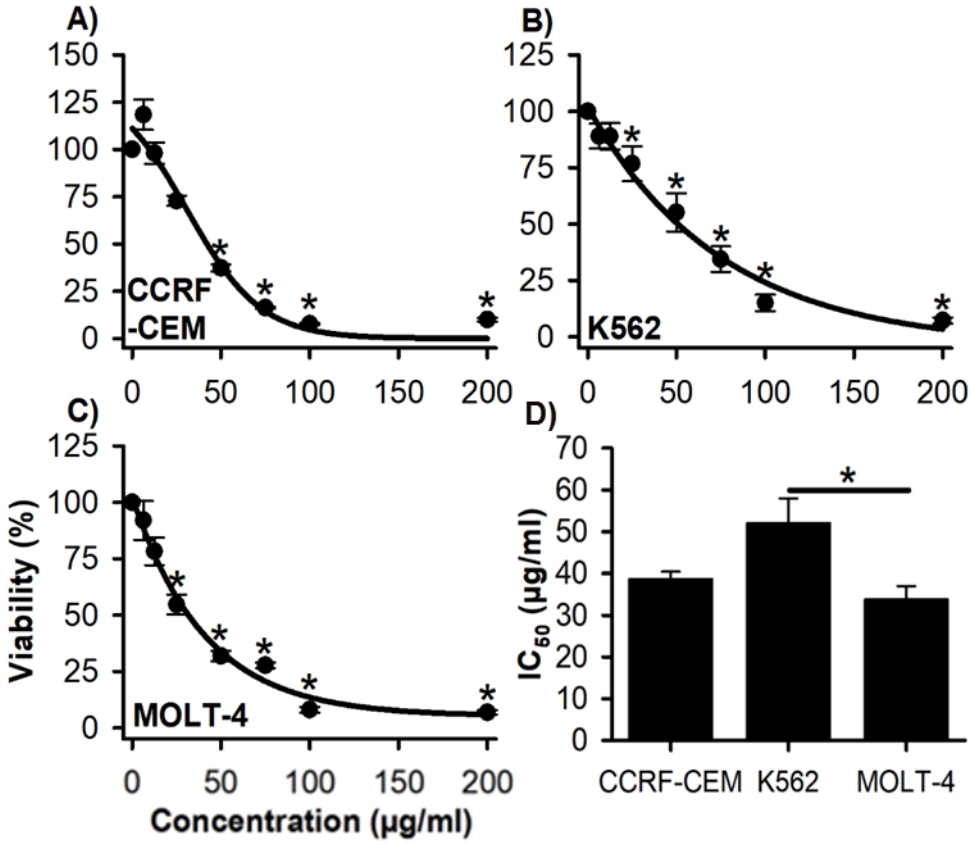

Figure 4-4. The *B. carterii* oleoresin methanolic extract induces significant concentration dependent cytotoxicity against multiple leukaemia types.

The *B. carterii* oleoresin methanolic extract was examined for its cytotoxic activity, across a range of concentrations, against the leukaemia cell lines **A)** CCRF-CEM, **B)** K562, and **C)** MOLT-4. Cells were treated for 72 hours before analysis using MTT assays. All data normalised to vehicle alone (0.5 % DMSO v/v). Data expressed as mean ± SEM. n = 12 biological replicates for CCRF-CEM, n = 18 biological replicates for K562 and MOLT-4. * indicates a statistically significant difference to a p value of < 0.05.

As per figure 4-4A-C, the methanolic extract *B. carterii* oleoresin produced a significant ($p < 0.001$) concentration-dependent decrease in cell viability against all leukaemia cell types examined. Comparisons between the cytotoxic effects of the *B. carterii* oleoresin methanolic extract (figure 4-4D) identified significant differences between the three leukaemia cell types. The IC_{50} for CCRF-CEM and MOLT-4 cells were similar (MOLT-4; 33.8 ± 3.2 and CCRF-CEM; 38.7 ± 1.7 µg/ml respectively). When compared to MOLT-4, K562 cells were found to be significantly less sensitive to the extract (K562; 52.1 ± 5.9 µg/ml, MOLT-4; 33.8 ± 3.2 µg/ml, , n = 18 for both cell types, $p = 0.010$).

4.3.2.2 The cytotoxic effect of methanolic extracts of the *B. carterii* oleoresin against multiple epithelial cancer cell types

As previously described in section 3.3.2, it was identified that the *B. carterii* oleoresin was an effective cytotoxic agent against the epithelial cancer cell line HEP G2. Therefore, we aimed to ascertain if the *B. carterii* oleoresin was also effective against other epithelial cancer cell types *in vitro*. The cytotoxic effect of the *B. carterii* oleoresin was examined against the alveolar basal epithelial cell adenocarcinoma cell line A549, the rhabdomyosarcoma cell line, A-204, the colorectal carcinoma cell line, HCT-116, the hepatocellular carcinoma cell line, HEP G2, the breast cancer cell line, MCF-7, and the pancreatic cancer cell line, PANC-1. The cytotoxic effect of the *B. carterii* oleoresin methanolic extract against these cell types was found to be concentration dependent in nature as shown in figure 4-5. Comparisons between the cytotoxic activity identified that the *B. carterii* oleoresin methanolic extract was most potent against the A-204 cell line, and least effective against the PANC-1 cell line, as shown in figure 4-6.

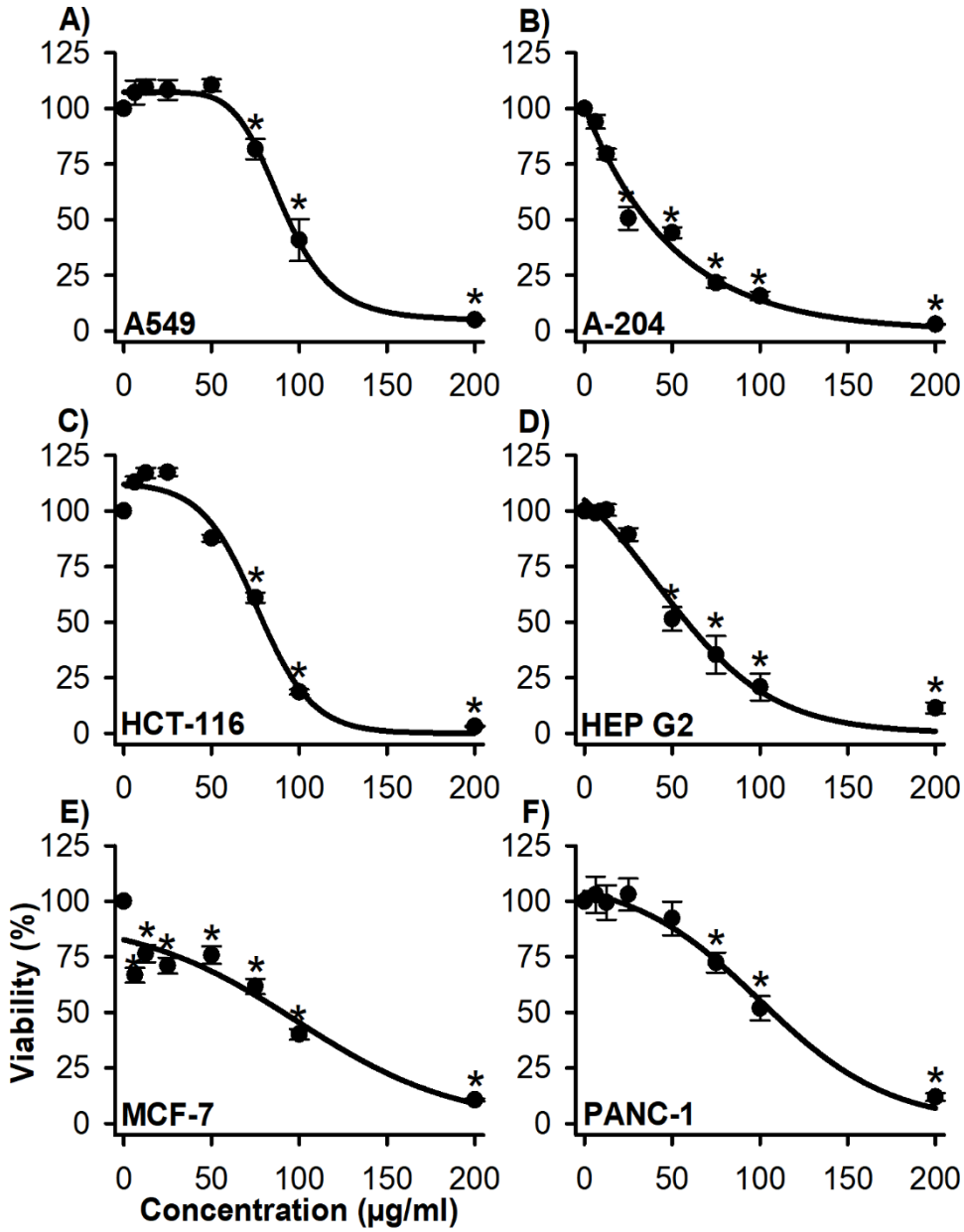

Figure 4-5. The *B. carterii* oleoresin methanolic extract induces concentration dependent decreases in viability against multiple epithelial cancer types.

The *B. carterii* oleoresin methanolic extract was examined for its cytotoxic activity, across a range of concentrations, against the epithelial cancer cell lines **A)** A549, **B)** A-204, **C)** HCT-116, **D)** HEP G2, **E)** MCF-7 and **F)** PANC-1. Cells were treated for 72 hours before analysis of cytotoxicity using MTT assays. All data normalised to vehicle alone (0.5 % DMSO v/v). Data expressed as mean ± SEM. n = 12 biological replicates for all cancer types. * indicates a statistically significant difference to a p value of < 0.05.

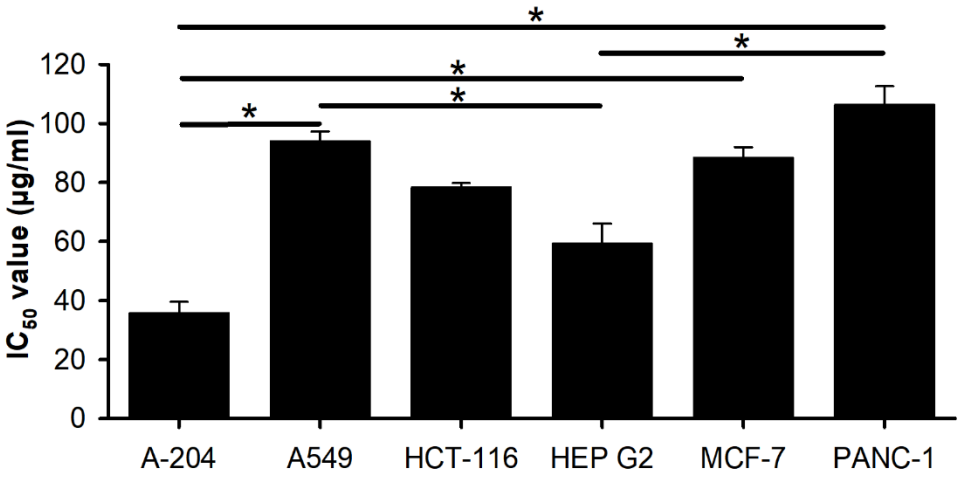

Figure 4-6. A comparison of the cytotoxic effect of each *B. carterii* oleoresin methanolic extract against multiple epithelial cancer cell lines.

A comparison of the cytotoxic activity of the *B. carterii* oleoresin against the A-204, A549, HCT-116, HEP G2, MCF-7 and PANC-1 epithelial cancer cell lines examined. Cells were treated for 72 hours before analysis. Data expressed as mean IC_{50} ± SEM. n = 12 biological replicates for all cancer cell lines. Lines indicate cell lines being compared. * indicates a statistically significant difference to a p value of < 0.05.

The cytotoxic activity against the A-204 cell line was found to be 232.5 ± 40.2 % (A-204; 35.7 ± 3.9 µg/ml, A549; 93.9 ± 3.4 µg/ml, n = 12, $p < 0.05$) greater than that observed against the A549 cell line, 223.6 ± 45.1 % (A-204; 35.7 ± 3.9 µg/ml, MCF-7; 88.3 ± 3.6 µg/ml, n = 12, $p < 0.05$) against the MCF-7 cell line and 253.3 ± 47.3 % (A-204; 35.7 ± 3.9 µg/ml, PANC-1; 106.3 ± 6.3 µg/ml, n = 12, $p < 0.05$) against the PANC-1 cell line.

Significant differences in the cytotoxic activity between the HEP G2, A549 and PANC-1 cell lines were also observed. The cytotoxic activity against the HEP G2 cell line was found to be 68.0 ± 18.9 % (HEP G2; 59.3 ± 6.8 µg/ml, A549; 93.9 ± 3.4 µg/ml, n = 12, $p < 0.05$) greater than against the A549 cell line and 95.5 ± 36.7 % (HEP G2; 59.3 ± 6.8 µg/ml, PANC-1; 106.3 ± 6.3 µg/ml, n = 12, $p < 0.05$) greater than against the PANC-1 cell line.

4.3.3 The cytotoxic activity of the *B. carterii* oleoresin methanolic against non-cancerous cell types

To ascertain if the *B. carterii* oleoresin possessed cytotoxic activity against non-cancer cells, the cytotoxic activity of the oleoresin methanolic extracts was examined against normal cell lines. This was conducted using peripheral blood mononuclear cells (PBMC's) and immortalised epithelial lung cells (BEAS-2B), as shown in figure 4-7.

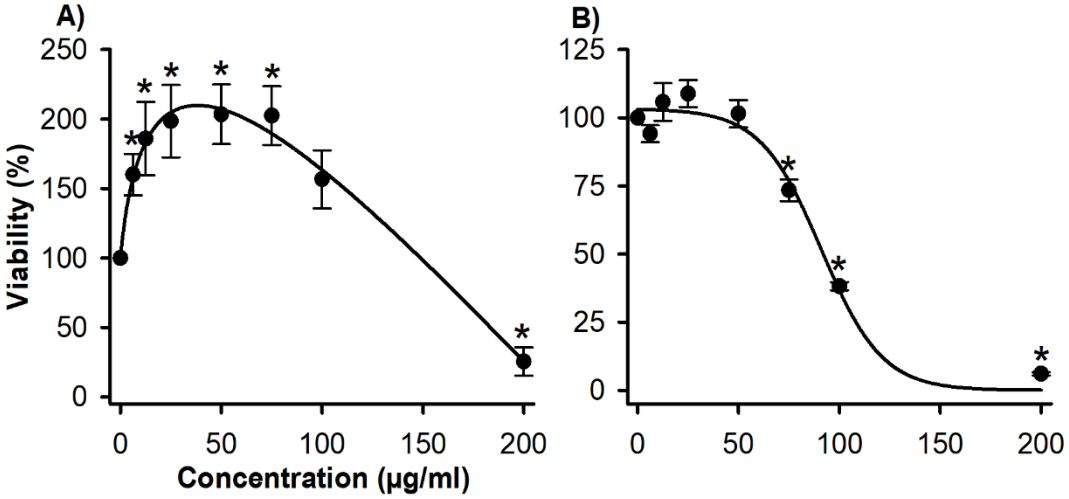

Figure 4-7. The effect of the *B. carterii* oleoresin methanolic extract against immortalised epithelial lung cells and peripheral blood mononuclear cells.

The cytotoxic activity of the *B. carterii* oleoresin methanolic extract against **A)** immortalised epithelial lung cells (BEAS-2B) and **B)** peripheral blood mononuclear cells (PBMC's). Cells were treated for 72 hours before analysis using MTT assays. All data normalised to vehicle alone (0.5 % DMSO v/v). Data expressed as mean ± SEM, n = 12 biological replicates. * indicates a statistically significant difference compared to vehicle alone to a p value of < 0.05.

The methanolic extract of the oleoresin extract (figure 4-7A) was found to induce no significant decreases in BEAS-2B viability at concentrations of less than 200 µg/ml. This maximal concentration examined was found to result in a 94.1 ± 0.5 % (n = 12, p < 0.001) decrease in BEAS-2B viability. Interestingly concentrations of between 6.25 and 100 µg/ml caused a significant in increases BEAS-2B viability, indicative of promoting proliferation compared to control. A 50 % decrease in BEAS-2B viability was observed at a concentration of 173.9 ± 12.9 µg/ml.

The methanolic extract of the oleoresin was found to induce significant decreases in PBMC viability at concentrations of greater than 75 µg/ml, shown in figure 4-7B. A concentration of 75 µg/ml caused a 26.6 ± 4.0 % (n = 12, p < 0.001) decrease in

viability. Concentrations of 100 and 200 µg/ml were found to result in 61.8 ± 1.5 % (n = 12, $p < 0.001$) and 93.9 ± 0.6 % (n = 12, $p < 0.001$) decreases in viability respectively. All concentrations below 75 µg/ml were found to cause no decrease to PBMC viability compared to the vehicle alone. Treatment with the *B. carterii* oleoresin methanolic extract was found to result in an IC_{50} value of 90.8 ± 1.3 µg/ml against PBMC's.

4.3.4 The selectivity of the *B. carterii* methanolic extract towards cancer cells.

To determine the selectivity of the *B. carterii* oleoresin towards cancer cells, the IC_{50} values of cancer cells was compared to that of the non-cancer cell lines, using the equation described in section 4.2.7. The selectivity of the *B. carterii* oleoresin towards multiple cancer cell types is summarised in table 4-1.

Table 4-1. The selectivity of the cytotoxic activity of the *B. carterii* oleoresin methanolic extract towards multiple cancer cell types.

The selectivity of the *B. carterii* oleoresin methanolic extract towards cancer cells was determined based on the IC_{50} values of each towards the cancer and equivalent non-cancer cell lines. Selectivity calculated using the equation described in section 4.2.7. Data expressed as average IC_{50} value. n = 12 biological replicates.

Cell line	Cancer IC_{50} value (µg/ml)	Non-cancer IC_{50} value (µg/ml)	Selectivity index
A549	93.92	173.92	1.85
CEM-CCRF	38.71	92.34	2.39
K562	52.08	91.34	1.75
MOLT-4	33.83	90.75	2.68

Comparisons of the IC_{50} values show differences between the cancer and non-cancer cells following treatment with the *B. carterii* oleoresin. The concentration of the oleoresin extract required to decrease viability by 50 % in lung cancer was found to be 70 µg/ml greater against the equivalent non-cancer cell line. This difference in the IC_{50} values resulted in a selectivity index of the oleoresin against lung cancer cells of 1.85.

The concentration of the *B. carterii* oleoresin methanolic extract required to induce a 50 % decrease in viability was found to be 53.6 µg/ml greater against the non-cancer cell line compared to that of the CCRF-CEM cell line. This difference in the IC_{50} values resulted in a selectivity index of the oleoresin against CCRF-CEM cancer cells of 2.39.

The concentration of the *B. carterii* oleoresin extract required to cause a 50 % decrease in viability was found to be 39.3 µg/ml greater against the PBMC's than that of the K562 cell line. This difference equated to a selectivity index of 1.75. The concentration of the oleoresin extract was found to be 56.9 µg/ml greater against the non-cancer cell line compared to that of the MOLT-4 cell line. This difference in the IC_{50} values resulted in a selectivity index of the oleoresin against MOLT-4 cancer cells of 2.68.

4.4 Discussion

4.4.1 Does exposure time affect the cytotoxic activity of the *B. carterii* oleoresin methanolic extract?

The results of this study show that the cytotoxicity of *B. carterii* oleoresin is time-dependent in both K562 and HEP G2 cell lines. The oleoresin was found to be most cytotoxic after treatment for 120 hours.

However, the pattern of effect differed between the cell types examined. The cytotoxic effect of the oleoresin extract was found to increase overtime against the chronic myeloid leukaemia cell line, K562. However, when identical parameters were examined against the liver carcinoma cell line HEP G2 the cytotoxic activity was found to increase by 38.8 % between the 24- and 72-hour time-points from 99.6 µg/ml to 60.9 µg/ml, however the effect was found to then plateau when treatment time was increased to 120 hours with the activity only increasing by a further 8.89 % to an IC_{50} value of 55.5 µg/ml.

No previous studies have examined the cytotoxic activity of any of the *Boswellia* oleoresins across varied exposure times. However, cell death has been described to range from being evoked rapidly (< 1 hours) to more chronically (> 24 hours) depending on the molecular mechanisms behind cell death and the cell type treated (Elmore, 2007; Panzarini, Inguscio, & Dini, 2011). A study by Zhang, Aguilera, *et al.* (2007) showed that DAOY medulloblastoma cells were killed by the cytotoxic agent MS275 in a time dependent manner with peak cytotoxicity and growth inhibition occurring at the maximal examined timepoint of 144 hours. The oleoresin used during this study exhibit a similar pattern of effect described by Zhang, Aguilera, *et al.* (2007) when using the antiproliferative and apoptosis inducing compound MS275, indicating a similar mechanism of action of the *B. carterii* oleoresin methanolic extract.

The effect of the *B. carterii* oleoresin methanolic extract over time is important to know as it identifies at what point the extracts begin to induce cytotoxic activity and at what concentrations it begins to act on the cell types. In addition, it allows a pattern of effect to be ascertained regarding the cytotoxicity of the extracts. By understanding the pattern of activity of the extracts it could potentially be used to plan a treatment regimen for if the treatment was to be translated to an *in vivo* model to further to examine the cytotoxic effect of the two extracts. However, translation to an *in vivo* model would

require additional considerations, as *in vitro* studies do not directly relate to *in vivo* activity. This is due to various pharmacokinetic, pharmacodynamic and mechanistic differences, which would need to be considered when translating to an *in vivo* model (Checkley *et al.*, 2015; Smith, Xu, Ropella, & Hunt, 2018).

Overall, this study describes for the first time that the oleoresins of *Boswellia* and specifically *B. carterii* induce time dependent cytotoxicity against leukemic and epithelial cancers *in vitro*.

4.4.2 What is the wider anti-cancer potential of the *B. carterii* oleoresin?

This study also aimed to examine the cytotoxic activity of the methanolic extract of *B. carterii* oleoresin against multiple cancer cell types. This was conducted to ascertain if the previously described cytotoxic activity of the *B. carterii* oleoresin methanolic extract (described in section 3.3.2) is heterogeneous across different cancer cell types. This further examination found that the *B. carterii* oleoresin methanolic extract caused a concentration dependent decrease in cancer cell viability, following treatment for 72 hours, irrespective of the cell line examined.

Of all cancer types examined the *B. carterii* oleoresin was found to be most cytotoxic against the acute lymphoblastic leukaemia cell line, MOLT-4, with an IC_{50} value of 33.8 ± 3.2 µg/ml. The cancer cell type that was found to be least affected by the methanolic extract of the *B. carterii* oleoresin was found to be the pancreatic cancer cell line PANC-1, requiring a concentration of 106.3 ± 6.3 µg/ml to induce a 50 % decrease in PANC-1 viability.

Our findings also indicate that the leukaemia cancer cell lines of CCRF-CEM, K562 and MOLT-4 may be more susceptible to treatment with the methanolic extract of the *B. carterii* oleoresin, due to these cell lines requiring lower concentrations than the majority of the other cell lines examined to induce a 50 % decrease in viability. These findings indicate that the *B. carterii* oleoresin may be an effective anti-leukemic agent. Despite being more potent against the leukaemia cells examined, the methanolic extract of *B. carterii* oleoresin was found to also possess anti-cancer activity against epithelial cancers *in vitro*. The cytotoxic activity against epithelial cancers was found to range between 36.1 ± 3.6 and 106.3 ± 6.3 µg/ml dependent on the specific cancer cell type. On average, the concentration required to induce an IC_{50} value was 1.85 times greater in epithelial cancers compared to that of leukaemia's.

This difference in cytotoxicity between the two cancer types may be a result of the increased surface area available to be targeted by compounds due to their ability to grow in suspension. This is particularly important if the *B. carterii* oleoresin extract was found to act on extracellular receptors and induce apoptosis via the extrinsic pathway (as described in section 1.1.5.2). This is plausible, as proteomic analysis has identified acetylated boswellic acid isoforms, which have been described to be present in multiple species of *Boswellia*, to upregulate the expression of DR4 and DR5, key members of the extrinsic pathway of apoptosis (Toden *et al.*, 2015; Xia *et al.*, 2005). Further to this, it may be the case that due to each cancer type having a different genetic makeup, it may be that each cancer cell type has developed various mechanisms of detoxification, such as those seen in resistant cancer cells (as described in section 1.2.8) or possess modified molecular pathways associated with the induction of cell death. Both of these factors highlight the need for further examination of the effect of *B. carterii* oleoresin extracts on cancer cell molecular pathways.

The oleoresin extracts of numerous *Boswellia* species have been shown to induce a cytotoxic effect against multiple different cancer cell lines (Alipanah & Zareian, 2018; Jaafari-Ashkavandi *et al.*, 2017; Ranjbarnejad *et al.*, 2017; Xia *et al.*, 2017). These *Boswellia* extracts induced cytotoxic effects against cancer cell types including colon, breast, liver, squamous cell carcinoma, cervical and colorectal cancers. However, this research has predominantly focused on *B. serrata* and purified boswellic acids with limited research conducted using *B. carterii* oleoresins. Additionally, a limited number of studies are available allowing direct comparisons with this study parameters, highlighting the need for further research on the whole *Boswellia* genus.

A study by Ranjbarnejad *et al.* (2017) identified that the methanolic extract of *B. serrata* oleoresin was found to induce a concentration dependent decrease against the colon cancer cell line HT-29. A 50 % decreasing in cell viability was found to occur at a concentration of 64 µg/ml following treatment for 48 hours. Whilst not an identical comparison to the colon cancer cell line used in this study the concentration required to induce IC_{50} was found to be 19.3 % lower than what observed following treatment for an additional 24 hours compared to the study by Ranjbarnejad *et al.* (2017). This difference in cytotoxic activity could be accounted for by the difference in chemical composition between the *B. serrata* and *B. carterii* oleoresins. As the *B. serrata*

oleoresin has been described to possess additional boswellic acids compared to that of the *B. carterii* oleoresin, likely due to environmental and climatic conditions in which the two species are grown (Büchele *et al.*, 2003).

This study also showed that the methanolic extract of *B. carterii* oleoresin was highly effective at inducing a cytotoxic effect against the three leukaemia cell lines (CCRF-CEM, K562 and MOLT-4) examined. Whilst no other studies have examined the effect of *Boswellia* oleoresins against leukaemia's, one study by Hoernlein *et al.* (1999) examined the effect of AKBA on the acute promyelocytic leukaemia cell line, HL-60. Their study showed that concentrations of 20 µM (equivalent to 10.3 µg/ml) or more induced significant decreases in HL-60 viability, with an IC_{50} value of 35 µM (equivalent to 17.9 µg/ml) following treatment for 48 hours. Whilst the cytotoxic effect of the methanolic extract of the *B. carterii* oleoresin was found to be less than pure boswellic acids. However, this difference is not to the same extent as that observed against colon cancer cells.

Whilst this difference in effect between the cytotoxic activity of the pure boswellic acid and our oleoresin extract is understandable, it is interesting that the cytotoxic effect of AKBA observed against the HL-60 cells is 65.7 % lower than that observed following treatment with the oleoresin against the MOLT-4 cells. This difference in cytotoxicity is likely due to the complex and diverse mixture of compounds present in our extract. Purification of the cytotoxic compound/compounds within our extract may result in a greater cytotoxic effect than that observed following treatment of a leukaemia cell line with the most potent boswellic acid, indicating a potential different active compound or a difference in susceptibility between the cancer cell types.

Studies of the cytotoxic effect of alternative species of *Boswellia* have also shown a concentration dependent effect. A study by Yazdanpanahi *et al.* (2014) examined the cytotoxic activity of the methanolic extract of *B. thurifera* oleoresin against the breast cancer cell line, MDA-MB-231. They showed that following treatment for 48 hours a concentration dependent decrease in viability was observed, resulting in an IC_{50} value of 80 µg/ml. This concentration is similar to the maximal IC_{50} values observed across all of the epithelial cancers examined and comparable to that of the breast cancer cell line examined in this study.

Our findings corroborate those previously described following treatment with the extracts of other *Boswellia* species. Further to this, this study describes for the first time that the methanolic extract of the *B. carterii* oleoresin was capable of inducing anti-cancer activity against multiple cancer cell types in a concentration dependent manner.

4.4.3 Are the cytotoxic effects of the *B. carterii* oleoresin cancer specific?

To evaluate the effect of the *B. carterii* oleoresin methanolic extract against non-cancer cell lines two non-cancer cell lines were used; BEAS-2B and PBMC's. This previously overlooked phenomenon is important to investigate, as a lack of cancer selectivity at this stage would suggest that *B. carterii* oleoresins are likely to develop off-target effects and therefore would not be suitable for further clinical study.

This study found that against the BEAS-2B cells only the maximal concentration examined (200 µg/ml) induced a significant decrease in viability. The oleoresin was found to induce a 50 % decrease in viability at concentrations of 173.9 ± 12.9 µg/ml. When identical analysis was conducted against PBMC's, the oleoresin was found to induce a significant decrease in viability of concentrations of 75 µg/ml or greater. The oleoresin methanolic extract was found to cause a 50 % decrease in viability at concentrations of 90.8 ± 1.3 µg/ml. The oleoresin methanolic extract was found to be less cytotoxic towards the normal cell types compared to that of all cancer cell types examined. Comparisons of the IC_{50} values for the cancer and non-cancer cell lines, conducted using equation 4-1, showed that the *B. carterii* oleoresin was found to selectively target cancer cells compared to non-cancer cells. The selectivity of the *B. carterii* oleoresin methanolic extract was found to range between 1.75 and 2.68.

Drugs/compounds with selectivity indexes of greater than 10 have been described to possess a highly selective activity towards their target diseases compared to healthy cells or tissues (Antwi, Amisigo, Adjimani, & Gwira, 2019), whereas compounds with selectivity indexes between 1 and lower than 10 could be considered to be mildly selective (Peña-Morán, Villarreal, Álvarez-Berber, Meneses-Acosta, & Rodríguez-López, 2016). Based on these criteria, the *B. carterii* oleoresin methanolic extracts would be classified as being non-selective to the cancer types examined, despite them being significantly more cytotoxic to cancer cells compared to non-cancer cells.

This mild selectivity could be a result of the extracts being composed of a crude mixture of compounds. Further isolation of individual compounds may potentially increase the cytotoxic activity of the extract and potentially increase the selectivity value as numerus other compounds within the mixture could be causing the effect on the normal cells rather than the cytotoxic component alone.

Further to this, the *B. carterii* oleoresin used as a part of this study have been previously described to contain a vast array of compounds (Abdel-Tawab *et al.*, 2011; Al-Harrasi & Al-Saidi, 2008). The multitude of compounds within the oleoresin may dampen the cytotoxic activity of the active compound within both *B. carterii* oleoresin. Through the isolation of the active compounds within the oleoresin the concentration required to induce a cytotoxic effect will be decreased, and potentially further enhancing the selectivity towards cancer cells. However, the inverse may occur as the compounds within the oleoresin may be acting synergistically to increase the selectivity of the active compound towards cancer cells. To ascertain which of these is the case further experiments are required, to isolate the active cytotoxic compound and further examine its selectivity towards cancer cells alone as well as in combination with other isolated compounds.

Despite the mild selectivity observed, compared to commonly used chemotherapeutic agents such as doxorubicin, which has been described to have a selectivity index between 0.27 and 1.31 (Badmus *et al.*, 2019; de Oliveira *et al.*, 2015; Pugachev *et al.*, 2017), the selectivity observed following treatment with the *B. carterii* oleoresin extract used in this study are greater than that of doxorubicin. Whilst the difference in selectivity may be a result of the significant cytotoxic activity of doxorubicin compared to the *B. carterii* oleoresin examined. However, our extract was more selective against multiple different cancer cell types than that seen in selectivity studies on doxorubicin.

Previous studies have shown that *Boswellia* extracts have a lesser effect against non-cancer cells than against cancer cells *in vitro*, however, this research is limited in scope. A study by Schmiech *et al.* (2019), showed that the methanolic extract of *B. sacra* oleoresin had a significantly lesser effect on PBMC's compared to the triple negative breast cancer cell line MDA-MB-231. Treatment for 72 hours found that a concentration of 80 µg/ml induced a 50 % decrease in PBMC viability. In comparison to what was observed during this study, the study by Schmiech *et al.* (2019) was found

to be 10.1 % more cytotoxic to PBMC's than the *B. carterii* oleoresin extract used in this study. This difference in cytotoxicity may be a result of the different species used. However, further comparative analysis is required to confirm this hypothesis.

Analysis of the literature showed that no previous research has been conducted on the effect of *Boswellia* extracts on the BEAS-2B, however, a study by Lv, Shao, Zhang, Zhuang, and Qiao (2020) examined the cytotoxic effects of AKBA on the BEAS-2B cell line. They described that AKBA induced a lesser effect on BEAS-2B cell than that of the A549 cancer cell line. A concentration of 20 µg/ml (39 µM) of AKBA did not induce a 50 % decrease in BEAS-2B viability after treatment for 72 hours. The pattern of effect of AKBA is highly similar to that of the *B. carterii* methanolic extracts used as a part of this study, with only the maximal concentrations inducing a significant effect on BEAS-2B viability.

The oleoresins and compounds derived from the *Boswellia* genus have also been shown to possess anti-inflammatory and antioxidant activity both *in vitro* and *in vivo* (as described in section 1.3.5.1) (Beghelli et al., 2017; Bertocchi et al., 2018; Hartmann et al., 2014; Sengupta et al., 2008; Siddiqui, 2011a). Many of the off-target effects associated with anti-cancer therapies are a result of increased levels of oxidative stress and inflammation, both locally and systematically. This has been described to lead to treatment failure through further developing a premetastatic tumour microenvironment (Gartung *et al.*, 2019; Loman, Jordan, Haynes, Bailey, & Pyter, 2019; Vyas, Laput, & Vyas, 2014). Based on this previously described anti-inflammatory and antioxidant activity of *Boswellia* substrates, it can be hypothesised that this activity could self-mitigate any increases in inflammation and oxidative stress induced by its cytotoxic activity, resulting in its increased selectivity towards cancer cells.

Overall, the findings of this study corroborate that of previous studies, showing that the oleoresins of the *Boswellia* genus and for the first time that those of *B. carterii* may result in minimal side effects if translated to an *in vivo* model. This decreased cytotoxicity against non-cancer cells accompanied by the increased cytotoxic activity against cancer cells indicates the compounds within the *B. carterii* oleoresin extract are of particular interest as potential sources of novel chemotherapeutic agents.

4.4.4 Conclusion

In conclusion, these findings show that the methanolic extract of the *B. carterii* oleoresin acts in a time and concentration manner. This effect was observed against numerous cancer cell types *in vitro* indicating they could be effective treatment of multiple cancer cell types. Additionally, we also determined that the extract acted in a selective manner towards cancer cells compared to the non-cancer cell types examined. However, further isolation of the specific compound responsible for the cytotoxic activity may enhance both the cytotoxic activity and selectivity of *B. carterii* oleoresin.

Chapter 5

The mechanisms of *B. carterii* oleoresin cytotoxicity

5.1 Introduction

Chapter 4 demonstrates that methanolic extract of the *B. carterii* oleoresin induces a concentration and time dependent decrease in cancer cell viability. This effect is relatively selective and present in several cancer cell types. This chapter seeks to elucidate the mechanisms of this cytotoxicity.

Ideal chemotherapeutics induce apoptotic, rather than necrotic cell death given the considerable immunological response associated with necrosis (see section 1.1.3) (Festjens, Berghe, & Vandenabeele, 2006). The mechanisms of apoptosis (described in detail in section 1.1.4), do not produce a major immunological response as dead cells are cleared by immune cells before they can evoke an inflammatory response (Poon, Lucas, Rossi, & Ravichandran, 2014; Suber & Rosen, 2009). By comparison, necrotic cell death (described in detail within section 1.1.3) results in the leakage of intracellular components into the extracellular space, triggering a more severe immune response (Martin, 2016; Rock & Kono, 2008).

This necrotic immune response significantly increases levels of pro-inflammatory compounds and oxidative stress (Martin, 2016; Reuter, Gupta, Chaturvedi, & Aggarwal, 2010). Given that, cancer cells have developed mechanisms to thrive under high levels of inflammation and oxidative stress, necrosis may actually promote cancer progression and tumour expansion (Coussens & Werb, 2002). Furthermore, elevated levels of inflammation and oxidative stress are associated with the pathogenesis of multiple pathological conditions such as inflammatory bowel disease, neuroinflammation, arthritis and mucositis (Almoallim *et al.*, 2017; Lian *et al.*, 2017; Naidu, Ramana, Rani, Suman, & Roy, 2004). It is therefore imperative to mitigate further increases in inflammation and oxidative stress. This is why the induction of tightly regulated and relatively clean cell death via apoptosis is ideal for chemotherapeutic agents.

Oleoresins of certain *Boswellia* species and purified boswellic acids have been previously shown to induce apoptosis in multiple cancer cell types (Liu, Huang, & Hooi, 2006; Ranjbarnejad *et al.*, 2017; Syrovets *et al.*, 2005). However, the specific mechanisms associated with *B. carterii* oleoresins cytotoxicity remain unexplored.

It is also important to ascertain if *B. carterii* oleoresins impact the cancer cell cycle. The transition through the cell cycle is normally tightly regulated via the modification of expression of cell cycle regulating proteins, such as cyclins and cyclin dependent kinases, as described in section 1.1.2 (Ding *et al.*, 2020; Lim & Kaldis, 2013). In cancer, dysregulation of the cell cycle allows cancer cells to ignore cell division checkpoints and divide indefinitely (see section 1.2.4.1 for further details). Therefore, modulation of the cancer cell cycle presents a therapeutic target. Indeed, certain, chemotherapeutic agents can modify the expression of cell cycle regulatory proteins, resulting in cell cycle arrests and prevention of cancer cell division (Bonelli, La Monica, Fumarola, & Alfieri, 2019; Murray, 1994).

Treatment of cancer cells with *Boswellia* oleoresin extracts and purified boswellic acids have been previously shown to induce cell cycle arrests. For example, extracts of *B. serrata* oleoresin and purified boswellic acids have both been shown to induce a sub G_1/G_1 cell cycle arrest, whilst decreasing the number of cells within the S and G_2/M phases of the cell cycle (Takahashi *et al.*, 2012). This has been shown to be a result of increased expression of the cell cycle regulator, p21, in addition to the downregulation of cyclin D1 and C-Myc expression (Toden *et al.*, 2015; Yuan *et al.*, 2008). Furthermore, a study by Pang *et al.* (2009) showed that boswellic acids significantly suppressed key genes associated with cellular proliferation, including the AKT, ERK and mTOR pathways. Again, research into the specific effects of *B. carterii* on the cancer cell cycle is limited.

A better understanding of how *B. carterii* oleoresin produces cell death and alters the cell cycle is of vital importance when assessing their suitability as potential chemotherapeutic agents.

5.1.1 Chapter aims

This chapter seeks to determine the detailed cytotoxic mechanisms of action of *B. carterii* oleoresin by elucidating its mechanism on cell death and cell cycle regulation, in several cancer cell types:

1) Determine the mode of cell death induced by *B. carterii* oleoresin and its associated molecular mechanisms.

2) Determine the effects of *B. carterii* oleoresin on the cell cycle, it's regulation and associated molecular targets.

5.2 Methods

5.2.1 Extraction and preparation of extracts used

Extraction and preparation of the methanolic extract used within the chapter was conducted as described in section 2.2. The methanolic extract was dissolved in DMSO (Fisher Scientific, USA) to a stock concentration of 50 mg/ml. This stock was then diluted to the desired concentrations using an appropriate cell culture media for the cancer cell line being examined.

5.2.2 Cell culture

The culture of all cancer cell lines utilised within this chapter was conducted as describe in sections 2.3 and 2.4.

5.2.3 Determination of the method of cell death using flow cytometry.

The flow cytometry-based approach for detecting apoptosis is based on the flipping of phosphatidylserine from the cytosolic leaflet of the cell membrane to the extracellular side of the membrane (Segawa & Nagata, 2015). This mechanism is induced by cellular mechanisms associated with apoptotic cell death (Mariño & Kroemer, 2013). This relocation of phosphatidylserine allows the protein Annexin V (AV) to bind, allowing visualisation of phosphatidylserine translocation. To analyse this, a flow cytometry method was conducted as described within section 2.6. To evaluate the mechanism of cell death induced by the *B. carterii* oleoresin, flow cytometry analysis was conducted.

Cells were removed from culture and seeded into a 24 well plate at a concentration of 0.5×10^6 cells per well. The seeded wells were then treated with select concentrations of the *B. carterii* oleoresin methanolic extract determined by the results of the MTT assay, for 48 hours.

After 48 hours, the cells were transferred to Eppendorf tubes and centrifuged at 200 xG for 5 minutes. The supernatant was then removed, and the cells re-suspended in 1 ml of 1x PBS and washed through centrifugation at 200 xG for 5 minutes. This process was repeated using 1x AV binding buffer (Invitrogen, Thermo Scientific). The cells were then re-suspended in 1 ml of 1x AV binding buffer to a concentration of 1×10^6 cells per ml. A volume of 100 µl of each cell suspension was transferred to fresh Eppendorf tubes and 5 µl of Fluorescein (FITC) (Ex:490 nm/Em:525 nm) conjugated AV

(Invitrogen, Thermo Scientific) was added to each tube. The cells were then incubated for 15 minutes at room temperature in the dark.

Following incubation, the cells were centrifuged at 200 xG for 5 minutes, the supernatant was removed, and the cell pellet was washed with 500 µl of 1x AV binding buffer through centrifugation. The supernatant was discarded, and the cell pellet was re-suspended in 200 µl of 1x AV binding buffer, before the addition of 5 µl of 20 µg/ml Propidium Iodide (PI) (Ex:535 nm/Em:617 nm) staining solution (Invitrogen, Fisher Scientific) to each tube. Cells were then incubated for 10 minutes at room temperature in the dark. The cells were then analysed by flow cytometry using the method described in section 2.6. AV fluorescence was detected via the FITC channel, with PI fluorescence detected in the PE channel using a 610/10 bandpass filter.

Viable cells, cells in the stages of apoptosis (early and late) and necrotic cells were determined based on the fluorescence of AV and PI. Each of these populations of cells was determined based on the parameters described in table 5-1.

Table 5-1. The annexin V and propidium iodide staining status for determining the cell death mechanism using flow cytometry.

Cell death status	AV staining	PI staining
Viable	Negative	Negative
Early apoptotic	Positive	Negative
Primary necrotic	Negative	Positive
Late apoptotic/ secondary necrotic	Positive	Positive

5.2.4 Flow cytometry analysis of the cell cycle regulation using propidium iodide staining

The premise of this assay is that as cells progress through the cell cycle, they synthesise more DNA to replicate their genetic material and divide into a new cell (Pozarowski & Darzynkiewicz, 2004). Dyes such as PI bind to nuclear material stoichiometrically, allowing differentiation and visualisation of the stages of the cell cycle based on the differences in fluorescence of the bound dye (Darzynkiewicz, Juan, & Bedner, 1999). To determine how the *B. carterii* oleoresin methanolic extract effects the cancer cell division cycle, DNA staining and flow cytometry analysis was conducted.

Cells were removed from culture and seeded into a 6-well plate at a density of 1 x 10^6 cells per well. Cells were left to grow into the well for 24 hours before the addition of treatment to the wells. Cells were treated with vehicle (media + 0.5 % v/v DMSO) or varying concentrations of the methanolic extract of the *B. carterii* substrates. Plates were then incubated for 48 hours at 37 ^oC in a 5 % CO_2 atmosphere.

Following incubation, the cells were removed from the plate, transferred to centrifuge tubes and washed using 1x PBS. Cells were then fixed using 70 % ethanol at -20 ^oC for 20 minutes. Once fixed, cells were washed using 1x PBS before the addition of 100 µl RNase A (100 µg/ml) (ThermoFisher Scientific, USA). The mixture was then incubated for 10 minutes. After incubation, 200 µl of PI (50 µg/ml) (Acros Organics, USA) was added to each tube and incubated for 10 minutes at room temperature in the dark. The cell cycle was then analysed by flow cytometry as described in section 2.6 with PI fluorescence quantified using the PE flow cytometry channel.

5.2.5 Western blotting analysis of protein expression

5.2.5.1 Antibodies

For all Western blotting experiments both the primary and secondary antibodies were purchased from Cell Signalling Technologies, USA. All primary antibodies were monoclonal antibodies (mAb) for their target protein.

The antibodies used to evaluate apoptosis were the following: Cleaved Caspase-7 (Asp198) (D6H1) Rabbit mAb, Caspase-7 (D2Q3L) Rabbit mAb, Cleaved Caspase-9 (Asp330) (E5Z7N) Rabbit mAb, Caspase-9 (C9) Mouse mAb, Cleaved PARP (Asp214) (D64E10) XP® Rabbit mAb, PARP Antibody, Caspase-3 (D3R6Y) Rabbit mAb, and Cleaved Caspase-3 (Asp175) (5A1E) Rabbit mAb.

The antibodies used to evaluate cell cycle regulation were the following: p53 (7F5) Rabbit mAb, p27 Kip1 (D69C12) XP® Rabbit mAb, CDK2 (78B2) Rabbit mAb, CDK6 (DCS83) Mouse mAb, Cyclin D3 (DCS22) Mouse mAb, and CDK4 (D9G3E) Rabbit mAb.

The expression of the housekeeper protein Glyceraldehyde-3-phosphate dehydrogenase (GAPDH) was examined using the antibody GAPDH (D16H11) XP® Rabbit mAb.

The secondary antibodies used were the following: anti-mouse IgG, Horseradish peroxidase (HRP)-linked antibody and anti-rabbit IgG, HRP-linked polyclonal antibodies.

5.2.5.2 Protein extraction

To evaluate changes in protein expression following treatment with the *B. carterii* oleoresin, proteins were required to be extracted from cancer cells following treatment.

To extract proteins from cancer cells, 10 x 10^6 cells per extraction were incubated with varying concentrations of *B. carterii* oleoresin and vehicle alone for 48 hours in 12 well plates. Following incubation, all cells and their supernatant was collected and centrifuged at 200 xG for 5 minutes at 4 ^oC. The supernatant was then discarded, and the cells washed with ice cold PBS, before being centrifuged at 200 xG for 5 minutes at 4 ^oC. The supernatant was then discarded, and the pellet was resuspended in 200 µl of ice cold Radioimmunoprecipitation (RIPA) lysis buffer (Thermo Fisher Scientific, USA). The suspension was incubated for 30 minutes on ice, with frequent agitation. Following incubation, the cells were centrifuged at 16,000 xG for 20 minutes at 4 ^oC. The supernatant was then collected in fresh tubes and kept on ice and quantified for their protein concentration using a Bradford assay as described in section 5.2.5.3.

5.2.5.3 Protein quantification

To quantify the protein concentrations within the extracted samples, a Bradford assay was performed. Initially, standard protein concentrations were prepared, this was done by preparing a 2 mg/ml stock solution of bovine serum albumin (BSA) (Fisher Scientific, USA). The stock was then diluted to concentrations of 2, 1, 0.8, 0.6, 0.5, 0.4, 0.3, 0.2, 0.1 and 0.05 mg/ml, alongside these standard concentrations a negative control of dH_2O was also prepared.

Before quantification of the unknown samples, a portion of the sample was removed from the stock and diluted to a ratio of either 1:10 or 1:20 to allow for an accurate calculation of their protein concentration.

Following sample and standard preparation, a Bradford assay was performed to quantify the protein. This was done by adding 200 µl of Bradford reagent (Thermo Fisher Scientific, USA) to the wells of a 96 well plate. Following this, 10 µl of each standard and unknown sample were added to their corresponding well. All samples and standards were quantified in triplicate. The contents of the wells were mixed

thoroughly and incubated at room temperature for 10 minutes. The absorbance at 480 nm was then measured using an FLUOstar Omega plate reader. These measurements were also taken in triplicate and averaged for each well.

All data was then exported, and the quantification was conducted using a custom written Microsoft Excel spreadsheet, which generated a standard curve and quantified all unknowns in relation to the standards. Post quantification, the extracted samples were stored at - 80 ^{o}C until required for experimentation.

5.2.5.4 Sample preparation

To prepare extracted protein samples, described in section 5.2.5.2, for electrophoresis samples were initially re-quantified following defrosting them to 4 ^{o}C using the method described in 5.2.5.3. Using this quantification, the volume of sample which contained 20 µg of protein could be ascertained for each sample to be analysed. Following this the protein was mixed with 4x lithium dodecyl sulphate (LDS) sample loading buffer (Sigma Aldrich, USA), 10x Dithiothreitol (DTT) sample reducer (Sigma Aldrich, USA) and dH_2O in the values described in table 5-2, to a total volume of 20 µl.

Table 5-2. Preparation of protein samples for gel electrophoresis.

The reagents and volumes required to prepare protein samples for electrophoresis. X indicates the volume of protein required for 20 µg of total protein, determined through the quantification method described in section 5.2.5.3.

Reagent	Volume required (µl)
4x LDS Sample buffer	5
10x DTT Sample reducer	2
Protein sample	X
dH_2O	13 - X
Total volume	**20**

Following preparation, the samples were heated to 70 ^{o}C for 10 minutes in a heat block. The samples were then transferred to ice until undergoing separation using electrophoresis.

5.2.5.5 One dimensional sodium dodecyl sulphate – polyacrylamide gel electrophoresis

To separate proteins based on their molecular weight, sodium dodecyl sulphate – polyacrylamide gel electrophoresis (SDS - PAGE). Proteins were separated on a 17 well TruPAGE precast gradient gel (Sigma Aldrich, USA), with polyacrylamide concentrations ranging between 4 % to 20 %. Gels were removed from their storage solution and washed thoroughly with dH_2O before being placed into the gel tank. The gel tank was then filled with 1x TruPAGE Triethanolamine (TEA) - Trycine SDS running buffer (Sigma Aldrich, USA) (composition detailed in table 5-3), until both gels were fully covered. The wells of the gels were then rinsed with running buffer to remove any trace amounts storage buffer within the wells.

Table 5-3. The composition of TruPAGE Triethanolamine - Trycine SDS gel electrophoresis running buffer.

Before use, the 20x solution was diluted to 1x using dH_2O.

Reagent	Concentration in 20x solution	Concentration in 1x solution
Triethanolamine	1.2 M	0.06 M
Tricine	0.8 M	0.04 M
Sodium Dodecyl Sulphate	2.0 % w/v	0.1 % w/v

Into the first and last wells 5 µl of PageRuler™ Plus Prestained Protein Ladder (Thermo scientific, USA) was loaded with 20 µl of sample (prepared as described in 5.2.5.4) loaded in triplicate into each of the wells of the gel, in the pattern shown in figure 5-1. Two gels were run concurrently to ensure even voltage across the gel tank.

Gels were then run for 45 minutes at a voltage of 180 volts, until the dye font of the loading buffer reached three quarters of the way down the gel. Once electrophoresis was complete, the gels were removed from the tank and carefully removed from their cassettes. The gels were then placed into InstantBlue Ultrafast protein stain (Expedion, UK) and in incubated at room temperature with continual agitation for 15 minutes. The gels were then removed from the stain and electrophoresis confirmed with bands of protein present in each sample containing lane. The gels were destained through repeated washes with dH_2O until all stain was removed. The gels were kept in dH_2O until the protein transfer was conducted.

	1	2	3	4	5	6	7	8	9	10	11	12	13	14	15	16	17	
	Protein ladder	Vehicle	25 µg/ml	50 µg/ml	100 µg/ml	Blank	Vehicle	25 µg/ml	50 µg/ml	100 µg/ml	Blank	Vehicle	25 µg/ml	50 µg/ml	100 µg/ml	Blank	Protein ladder	

Figure 5-1. The method of loading polyacrylamide gels for the separation of protein extracts.

The pattern used to load gels for SDS-PAGE gel electrophoresis for analysis of changes in protein expression, following treatment with varying concentrations of the *B. carterii* oleoresin methanolic extract.

5.2.5.6 Protein transfer

To allow the proteins of interest to be stained with antibody, all proteins within the gel were transferred onto a membrane. To do this, a protein transfer method was conducted. Prior to conducting the transfer, the gel, filter papers (Thermo Fisher Scientific, USA), Immobilon-E transfer membranes (Millipore, USA) and transfer sponges were all equilibrated in ice cold 1x transfer buffer (composition detailed in table 5-4) for 10 minutes. Following equilibration, the transfer stack was assembled as shown in figure 5-2, ensuring that all air was removed from between each layer.

Table 5-4. The composition of the transfer buffer used for protein transfer.

Table describes the chemical composition used to prepare a 20x transfer buffer and the process of diluting the buffer to the working concentration.

Reagent	Concentration
Tris base	0.25 M
Glycine	1.92 M
To prepare 1x transfer buffer	
20 x Transfer buffer	5 % v/v
Methanol	20 % v/v
dH_2O	75 % v/v

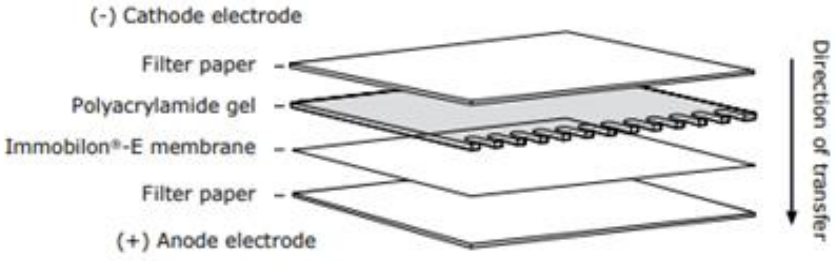

Figure 5-2. The preparation of the protein transfer stack.

A schematic diagram showing the preparation of the transfer stack used for protein transfer was prepared. Stacks were prepared in a bath of ice-cold transfer buffer, to ensure components of the stack did not dry out during preparation.

Following preparation of the transfer stack, it was placed into a transfer tank filled with ice cold 1x transfer buffer. The transfer was then conducted on ice for 75 minutes at a current of 250 mA.

After the transfer was complete, the transfer membrane was removed from the stack and washed with dH_2O. Validation of protein transfer was evaluated using Ponceau S staining. Ponceau S stain (0.1 % w/v Ponceau S, 5 % v/v acetic acid and 95 % v/v dH_2O) was poured over them membrane and continually agitated for one hour. The excess stain was removed using dH_2O, and protein bands on the membrane were stained red. The membranes were destained by repeated washes in tris buffered saline (TBS) containing 0.1 % v/v Tween-20 (Fisher Scientific, USA) (TBST) (the composition of TBST described in table 5-5). The membranes were then ready to undergo antibody staining.

Table 5-5. The composition of TBS and TBST.

The chemical composition used to prepare a 10x TBS solution and the process of preparing TBS-T. 10x TBS was adjusted to pH 7.6 before volumizing to desired volume.

Reagent	Concentration
Tris Base	0.2 M
NaCl	1.5 M
To prepare 1x TBST	
10x TBS	10 % v/v
dH_2O	89.90 % v/v
Tween-20	0.10 % v/v

5.2.5.7 Blotting with primary and secondary antibodies

Before antibody staining, the membranes were blocked with membrane blocking buffer (5 % w/v non-fat dried milk in 1x TBST) for 1 hour under constant agitation to prevent non-specific binding. Following blocking, the membranes were washed with ice cold TBS-T three times, before staining with primary antibody.

All primary antibodies (described in section 5.2.5.1) used were diluted 1:1000 in 5 % w/v bovine serum albumin in 1x TBST. Membranes were incubated with primary antibody overnight at 4 ^{o}C under constant agitation.

After incubation with primary antibody, the membranes were washed with ice cold TBS-T three times before incubation with secondary antibody. All secondary antibodies (described in section 2.10.1) were diluted 1:2000 in membrane blocking buffer and incubated at 4 ^{o}C for three hours. Following incubation, the membranes were washed using 1x TBST three times and imaged.

5.2.5.8 Protein imaging

To image the protein of interest on the membrane, the blots were removed from 1x TBST and incubated with Immobilon Crescendo Western HRP Substrate (Millipore, USA) for 3 - 5 minutes. The blots were then imaged using a G:Box Chemi-XX6 imager (Syngene, USA) and the GeneSys V1.5.2.0 software (Syngene, USA). All imaged blots were saved for offline processing and futher analysis.

5.2.5.9 Western blotting data analysis

Images of the bolts were analysed using the software package Image J (National Institutes of Health, USA) to quantify the abundance of protein in each band blotted. Proteins were quantified based on the darkness of the bands within the gel quantification tool within Image J. The values from image J were exported to Microsoft Excel for further analysis.

Within Microsoft Excel, the values of the housekeeper protein GAPDH was used as a control for even protein loading. All proteins of interest were ratioed against the GAPDH for a specific blot. The control value was then normalised to a value of one and all concentrations were compared to this value.

5.3 Results

5.3.1 The mechanism of cell death induced by the methanolic extract of *B. carterii* oleoresin

To determine the mechanism of cell death which occurred following the treatment with the *B. carterii* oleoresin methanolic extract, a flow cytometry approach was conducted to evaluate the translocation of phosphatidylserine, as described in section 5.2.3, which is a hallmark of apoptosis. To do this, fluorescent probe conjugated protein, known as AV, which specifically binds to, was utilised in combination with the DNA intercalating dye propidium iodide, to distinguish between early apoptotic, late apoptotic/secondary necrotic and primary necrotic cell death, as described in table 5-1. This analysis was conducted against susceptible leukaemia and epithelial cancer cell types (described in chapter 4) to characterise the mechanism of cell death induced by the *B. carterii* oleoresin. The results of this analysis for each cancer cell type are described within sections 5.3.1.1 - 5.3.1.5.

5.3.1.1 Chronic myeloid leukaemia

As per figure 5-3, concentrations of 50 µg/ml or greater produced a significant increase in late apoptotic/secondary necrotic K652 cells, accompanied by a significant decrease in viable cells.

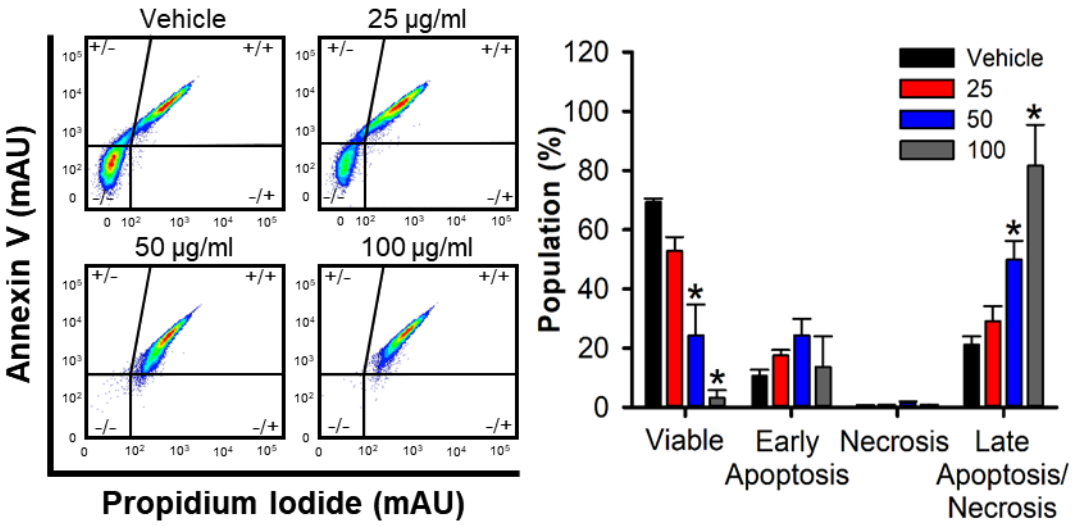

Figure 5-3. The *B. carterii* oleoresin induces apoptosis in the K562 cell line.

Apoptosis was evaluated using AV-FITC/PI co-staining and analysed via flow cytometry. K562 cells were treated with vehicle alone (media + 0.5 % v/v DMSO) (Black) or 25 (Red), 50 (Blue) or 100 µg/ml (Grey) of the *B. carterii* oleoresin methanolic extract for 48 hours before analysis. Data expressed as mean ± SEM. * indicates a statistically significant difference from vehicle alone to a p value of < 0.05. n = 4 independent biological replicates.

Treatment with 25 µg/ml of the *B. carterii* oleoresin methanolic extract was found to cause no significant increase in apoptosis or necrosis compared to the vehicle alone. However, 50 µg/ml induced a 64.29 ± 15.89 % (Vehicle: 69.4 ± 1.2 %, 50 µg/ml; 24.3 ± 10.5 %, n = 4, $p < 0.05$) decrease in viable cells accompanied by a 139.4 ± 26.7 % (Vehicle: 21.1 ± 2.8 %, 50 µg/ml; 49.9 ± 6.3 %, n = 4, $p < 0.05$) increase in late apoptotic/secondary necrotic cells.

Treatment with 100 µg/ml decreased the number of viable cells further, by 95.1 ± 3.8 % (Vehicle: 69.4 ± 1.2 %, 100 µg/ml; 3.3 ± 2.5 %, n = 4, $p < 0.05$) compared to vehicle alone. This decrease in viable cells was the result of further increases in late apoptotic/secondary necrotic cells, which were found to 285.2 ± 51.9 % (Vehicle: 21.1 ± 2.8 %, 100 µg/ml; 81.7 ± 13.8 %, n = 4, $p < 0.05$) greater than the vehicle alone. All concentrations examined of the *B. carterii* oleoresin methanolic extract were found to result in no significant changes to the number of cells with positive markers for early apoptosis or necrosis.

5.3.1.2 Acute lymphoblastic leukaemia

As per figure 5-4, concentrations of 50 µg/ml or greater produced a significant increase in early and late apoptotic/secondary necrotic MOLT-4 cells, accompanied by a significant decrease in viable cells.

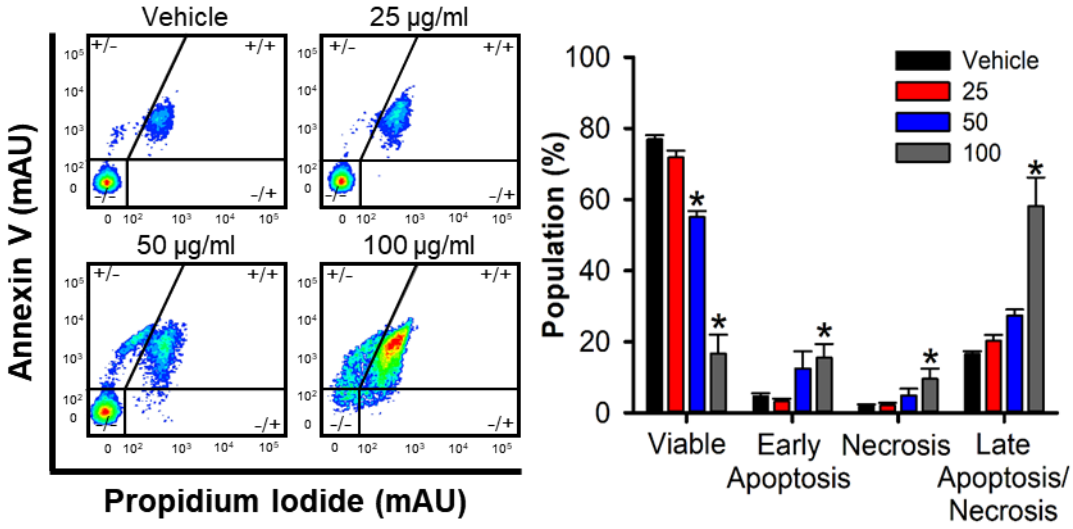

Figure 5-4. The *B. carterii* oleoresin induces apoptosis in the MOLT-4 cell line.

Apoptosis was evaluated using AV-FITC/PI co-staining and analysed via flow cytometry. MOLT-4 cells were treated with vehicle alone (media + 0.5 % v/v DMSO) (Black) or 25 (Red), 50 (Blue) or 100 µg/ml (Grey) of the *B. carterii* oleoresin methanolic extract for 48 hours before analysis. Data expressed as mean ± SEM. * indicates a statistically significant difference from vehicle alone to a p value of < 0.05. n = 4 independent biological replicates.

A concentration of 25 µg/ml of the *B. carterii* oleoresin methanolic extract was found to cause no significant change in cell death when analysed by flow cytometry. When the concentration was increased to 50 µg/ml, a significant decrease of 28.3 ± 2.5 % (Vehicle: 76.9 ± 1.9 %, 50 µg/ml; 55.1 ± 1.6 %, n = 4, $p < 0.05$) in viable cells was observed. This decrease in viability was accompanied by non-significant increases in early and late apoptotic/secondary necrotic cells, which were found to be increased by 235.6 ± 142.2 % (Vehicle: 4.7 ± 0.9 %, 50 µg/ml; 12.6 ± 4.8 %, n = 4, $p = 0.228$) and 66.9 ± 13.4 % (Vehicle: 16.6 ± 0.8 %, 50 µg/ml; 27.4 ± 1.7 %, n = 4, $p = 0.211$) respectively.

This was seen to a greater extent when the concentration was further increased to 100 µg/ml, with viable cells decreasing by 78.1 ± 7.1 % (Vehicle: 76.9 ± 1.2 %, 100 µg/ml; 16.7 ± 5.3 %, n = 4, $p < 0.05$) compared to treatment with the vehicle alone. At this concentration, significant decreases in early and late apoptotic/secondary necrotic

cells were identified. Treatment with 100 µg/ml was found to induce a 230.1 ± 46.3 % (Vehicle: 4.7 ± 0.9 %, 100 µg/ml; 15.5 ± 3.9 %, n = 4, $p < 0.05$) increase in early apoptotic cells, whilst also increasing late apoptotic/secondary necrotic cells by 249.1 ± 39.1 % (Vehicle: 16.6 ± 0.8 %, 100 µg/ml; 58.2 ± 8.0 %, n = 4, $p < 0.05$) compared to the vehicle alone. Treatment with 100 µg/ml of the *B. carterii* oleoresin methanolic extract was found to cause a significant increase in necrosis compared to the vehicle alone. This concentration was found to increase the number of necrotic cells by 539.9 ± 224.7 % (Vehicle: 1.8 ± 0.6 %, 100 µg/ml; 9.6 ± 2.8 %, n = 4, $p < 0.05$) compared to the vehicle alone.

5.3.1.3 Hepatocellular carcinoma

As shown in figure 5-5, concentrations of 50 µg/ml or greater produced significant increases in early and late apoptotic/secondary necrotic HEP G2 cells, accompanied by significant decreases in viable cells.

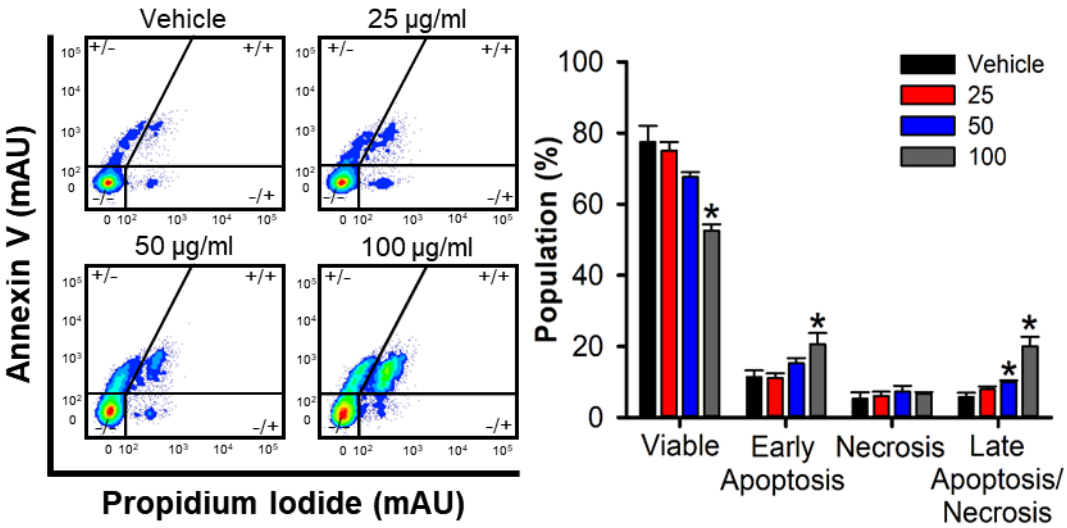

Figure 5-5. The *B. carterii* oleoresin induces apoptosis in the HEP G2 cell line.

Apoptosis was evaluated using AV-FITC/PI co-staining and analysed via flow cytometry. HEP G2 cells were treated with vehicle alone (media + 0.5 % v/v DMSO) (Black) or 25 (Red), 50 (Blue) or 100 µg/ml (Grey) of the *B. carterii* oleoresin methanolic extract for 48 hours before analysis. Data expressed as mean ± SEM. * indicates a statistically significant difference from vehicle alone to a p value of < 0.05. n = 4 independent biological replicates.

Treatment of HEP G2 cells with a concentration of 25 µg/ml was found to result in no significant change in the number of viable, early apoptotic, necrotic or late apoptotic/secondary necrotic cells compared to treatment with the vehicle alone. An increase in concentration to 50 µg/ml produced a non-significant decrease of 11.9 ±

5.2 % (Vehicle: 77.5 ± 4.5 %, 50 µg/ml; 67.6 ± 1.4 %, n = 4, p = 0.066) in viable cells compared to the vehicle alone. This was accompanied by a significant increase in late apoptotic/ secondary necrotic cells of 90.8 ± 36.9 % (Vehicle: 5.9 ± 1.1 %, 50 µg/ml; 9.9 ± 0.5 %, n = 4, p < 0.05) compared to treatment with the vehicle alone.

Further increasing the concentration to 100 µg/ml was found to cause a significant decrease in viability of 31.6 ± 4.1 % (Vehicle: 77.5 ± 4.5 %, 100 µg/ml; 52.6 ± 1.7 %, n = 4, p < 0.05) compared to the vehicle alone. This was associated with significant increases in early apoptotic cells and late apoptotic/ secondary necrotic cells. Treatment with 100 µg/ml was found to increase the number of early apoptotic cells by 86.4 ± 20.2 % (Vehicle: 11.4 ± 1.8 %, 100 µg/ml; 20.6 ± 3.1 %, n = 4, p < 0.05) and late apoptotic/ secondary necrotic cells by 299.0 ± 107.8 % (Vehicle: 5.9 ± 1.1 %, 100 µg/ml; 20.1 ± 2.7 %, n = 4, p < 0.05) compared to the vehicle alone. All concentrations were found to cause no significant increase in the number of necrotic cells.

5.3.1.4 Alveolar basal epithelial cell adenocarcinoma

As shown in figure 5-6, concentrations of 50 µg/ml or greater produced significant increases in early and late apoptotic/ secondary necrotic A549 cells, accompanied by significant decreases in viable cells.

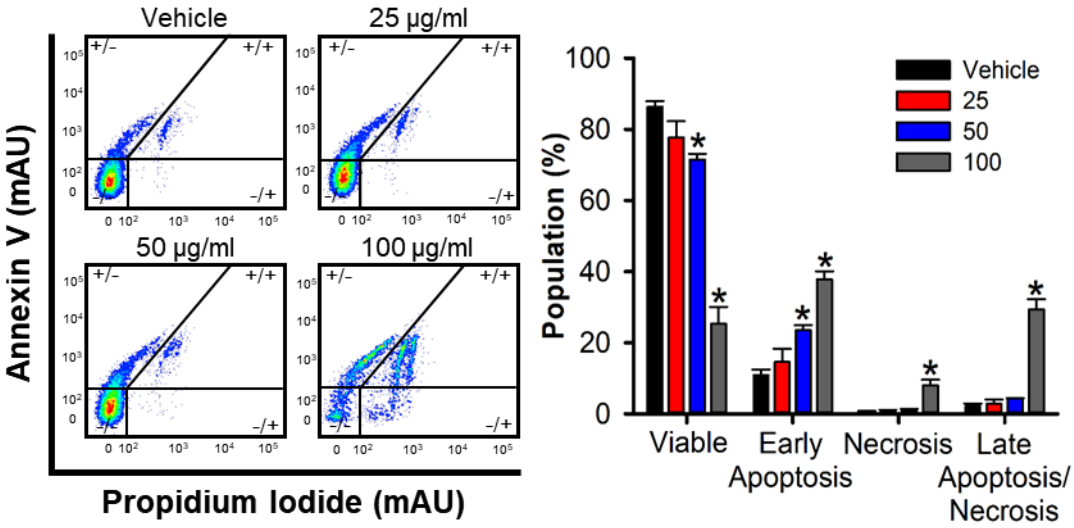

Figure 5-6. The *B. carterii* oleoresin induces apoptosis in the A549 cell line.

Apoptosis was evaluated using AV-FITC/PI co-staining and analysed via flow cytometry. A549 cells were treated with vehicle alone (media + 0.5 % v/v DMSO) (Black) or 25 (Red), 50 (Blue) or 100 µg/ml (Grey) of the *B. carterii* oleoresin methanolic extract for 48 hours before analysis. Data expressed as mean ± SEM. * indicates a statistically significant difference from vehicle alone to a p value of < 0.05. n = 4 independent biological replicates.

Treatment with a concentration of 25 µg/ml of the *B. carterii* oleoresin methanolic extract caused no change in the number of viable, early apoptotic, necrotic or late apoptotic/ secondary necrotic cells. When the concentration was increased to 50 µg/ml, a significant decrease in the number of viable cells was observed. Treatment at this concentration was found to cause an 17.8 ± 2.4 % (Control: 86.4 ± 1.6 %, 50 µg/ml; 71.0 ± 1.6 %, n = 4, p = 0.023) decrease in viability compared to the vehicle alone. This decrease in viable cells was associated with a significant increase in early apoptotic cells, of 129.1 ± 36.1 % (Vehicle: 10.9 ± 1.6 %, 50 µg/ml; 23.6 ± 1.4 %, n = 4, p = 0.008) compared to the vehicle alone. Treatment with 50 µg/ml was found to cause no change to the number of late apoptotic/ secondary necrotic or necrotic cells following treatment.

Further increases in concentration to 100 µg/ml was found to substantially decrease A549 viability, treatment with this concentration was found to significantly decrease viability by 71.3 ± 5.9 % (Vehicle: 86.4 ± 1.6 %, 100 µg/ml; 24.6 ± 4.8 %, n = 4, p < 0.001) compared to the vehicle alone. The decrease in viability was found to be a result of significant increases in the number of early and late apoptotic/ secondary necrotic cells following treatment at this concentration. These increases were found to be 277.1 ± 71.8 % (Vehicle: 10.9 ± 1.6 %, 100 µg/ml; 37.8 ± 2.3 %, n = 4, p < 0.001) and 2188.3 ± 846.2 % (Vehicle: 2.1 ± 0.8 %, 100 µg/ml; 29.4 ± 2.9 %, n = 4, p < 0.001) respectively compared to the vehicle alone. Treatment with 100 µg/ml of the *B. carterii* oleoresin methanolic extract also significantly increased the number of necrotic cells. It was found to increase the number of necrotic cells by 1542.2 ± 565.8 % (Vehicle: 0.7 ± 0.2 %, 100 µg/ml; 8.1 ± 1.5 %, n = 4, p < 0.05) compared to the vehicle alone.

5.3.1.5 Colorectal carcinoma

As shown in figure 5-7, concentrations of 50 µg/ml or greater were found to induce significant increases in early and late apoptotic/ secondary necrotic HCT-116 cells, accompanied by significant decreases in viable cells.

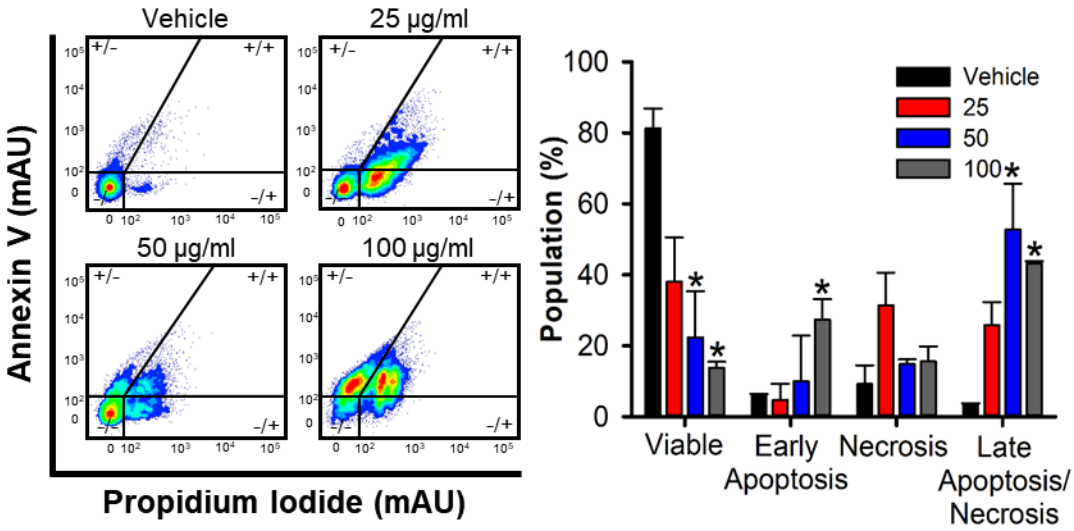

Figure 5-7. The *B. carterii* oleoresin induces apoptosis in the HCT-116 cell line.

Apoptosis was evaluated using AV-FITC/PI co-staining and analysed via flow cytometry. A549 cells were treated with vehicle alone (media + 0.5 % v/v DMSO) (Black) or 25 (Red), 50 (Blue) or 100 µg/ml (Grey) of the *B. carterii* oleoresin methanolic extract for 48 hours before analysis. Data expressed as mean ± SEM. * indicates a statistically significant difference from vehicle alone to a p value of < 0.05. n = 4 independent biological replicates.

Treatment with 25 µg/ml of the *B. carterii* oleoresin methanolic extract was found to cause a non-significant decrease in viable cells of 34.9 ± 21.3 % (Vehicle: 81.7 ± 5.7 %, 25 µg/ml; 50.4 ± 13.9 %, n = 4, p = 0.143) compared to treatment with the vehicle alone. This decrease in viability was associated with a 505.5 ± 282.5 % (Vehicle: 8.7 ± 5.5 %, 25 µg/ml; 23.1 ± 10.9 %, n = 4, p = 0.496) increase in the number of necrotic cells and an 726.0 ± 218.2 % (Vehicle: 3.4 ± 25.8 %, 25 µg/ml; 25.8 ± 6.6 %, n = 4, p = 0.120) increase in late apoptotic/ secondary necrotic cells compared to the vehicle alone. No change was observed in the number of early apoptotic cells following treatment with a concentration of 25 µg/ml.

Treatment with an increased concentration of 50 µg/ml was found to result in significant decreases in HCT-116 viability and significant increases in the number of late apoptotic/ secondary necrotic cells. This decrease in viable cells was found to be a 53.4 ± 21.3 % (Vehicle: 81.7 ± 5.7 %, 50 µg/ml; 35.4 ± 15.0 %, n = 4, p = 0.025) decrease compared to treatment with the vehicle alone. The increase in late apoptotic/ secondary necrotic cells was found to be a 1645.1 ± 511.9 % (Vehicle: 3.4 ± 25.8 %, 50 µg/ml; 52.8 ± 12.9 %, n = 4, p = 0.001) increase compared to the vehicle alone. At a concentration of 50 µg/ml, the number of necrotic cells was increased compared to

the vehicle alone, however the number of necrotic cells was substantially lower than following treatment with 25 µg/ml.

When the concentration of the *B. carterii* oleoresin methanolic extract was increased to a concentration of 100 µg/ml, further decreases in the number of viable cells was observed. Treatment with 100 µg/ml was found to decrease the number of viable cells by 80.3 ± 3.5 % (Vehicle: 81.7 ± 5.7 %, 100 µg/ml; 15.6 ± 1.8 %, n = 4, p = 0.002) compared to the vehicle alone. This was accompanied by significant increases in the number of early and late apoptotic/ secondary necrotic cells. These early and late apoptotic/ secondary necrotic cells were found to be significantly increase by 347.6 ± 105.3 % (Vehicle: 6.1 ± 0.4 %, 100 µg/ml; 27.4 ± 6.4 %, n = 4, p = 0.003) and 1225.4 ± 151.0 % (Vehicle: 3.4 ± 25.8 %, 100 µg/ml; 43.2 ± 0.7 %, n = 4, p = 0.006) respectively. No significant change in necrotic cells was observed following treatment of 100 µg/ml of the *B. carterii* oleoresin methanolic extract.

5.3.2 The effect of *B. carterii* oleoresin on apoptotic regulatory proteins

Within section 5.3.1, it was identified that the *B. carterii* oleoresin methanolic extract was found to likely induce apoptotic cell death against multiple cancer cell types *in vitro*. The study then aimed to confirm the method of cell death induced and ascertain the molecular mechanisms underpinning the apoptosis induced. To determine the molecular mechanism, modification of protein expression following treatment was determined using Western blotting analysis, using the method described in section 5.2.5. The chronic myeloid leukaemia cell line was selected for further examination due to the significant pro-apoptotic activity observed in section 5.3.1.1. The changes in key apoptotic protein expression induced by the methanolic extract of the *B. carterii* oleoresin are shown in figure 5-8.

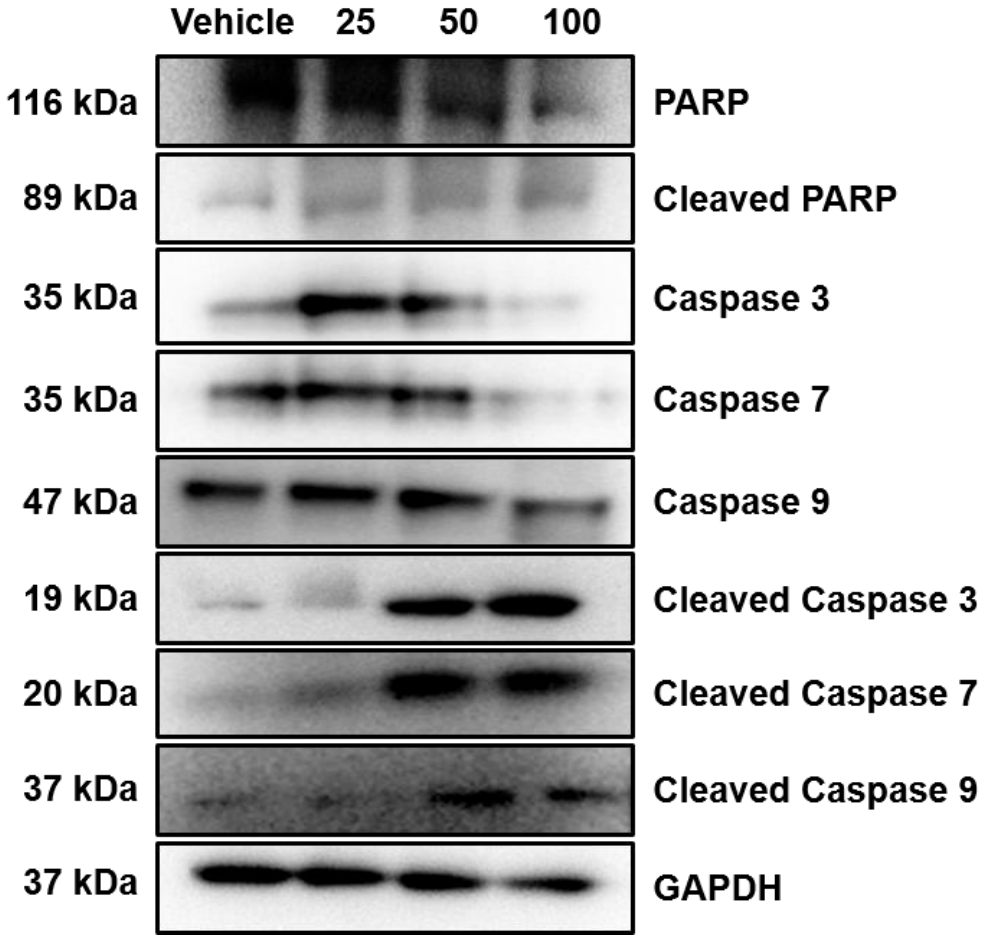

Figure 5-8. The *B. carterii* oleoresin methanolic extract modifies key apoptosis protein expression in the K562 cell line.

Protein lysates were prepared from K562 cells were treated with various concentrations of the *B. carterii* oleoresin methanolic extract for 48 hours. Lysates were then separated using 4-20 % SDS PAGE gel electrophoresis as described in section 5.2.5.5. Proteins were then transferred to 0.45 PVDF membrane and probed for the protein of interest as described in section 5.2.5.6 and imaged as described in section 5.2.5.8. Figure representative of three independent repeats for each protein of interest.

The expression of full-length PARP and its cleavage fragment were found to significantly modified following the treatment with the *B. carterii* oleoresin methanolic extract, as shown in figure 5-9.

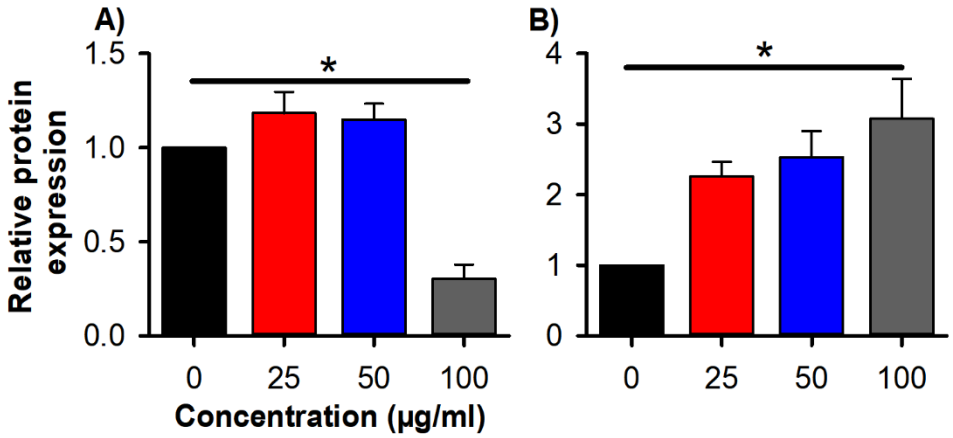

Figure 5-9. The *B. carterii* oleoresin methanolic extract induces a significant decrease in PARP whilst increasing PARP cleavage in the K562 cell line.

Quantification of relative protein expression of **A)** Full-length PARP, **B)** Cleaved PARP relative to GAPDH expression. Data expressed as mean ± SEM. Lines indicate groups being compared. * indicates a statistically significant difference to a p value of < 0.05. n = 3 independent experiments.

Treatment with a concentration of less than 100 µg/ml was found to induce no significant decrease in full-length PARP expression. When the concentration was increased to 100 µg/ml a significant decrease in full-length PARP expression was observed. This concentration was found to decrease expression by 69.7 ± 9.3 % (n = 3, p = 0.003) compared to treatment with the vehicle alone.

This decrease in full-length PARP was found to be a result of PARP cleavage. Cleaved PARP was found to be significantly increased following treatment of K562 cells with the *B. carterii* oleoresin methanolic extract, as shown in figure 5-9B. Treatment with concentrations of less than 100 µg/ml was found to increase PARP cleavage to non-significant levels. Treatment with 100 µg/ml induced a 207.7 ± 69.0 % (n = 3, p = 0.023) increase in PARP cleavage compared to treatment with the vehicle alone.

Next, the effect of the *B. carterii* methanolic extract on caspases-3, -7 and -9, and their cleavage fragments were assessed as shown in figure 5-10.

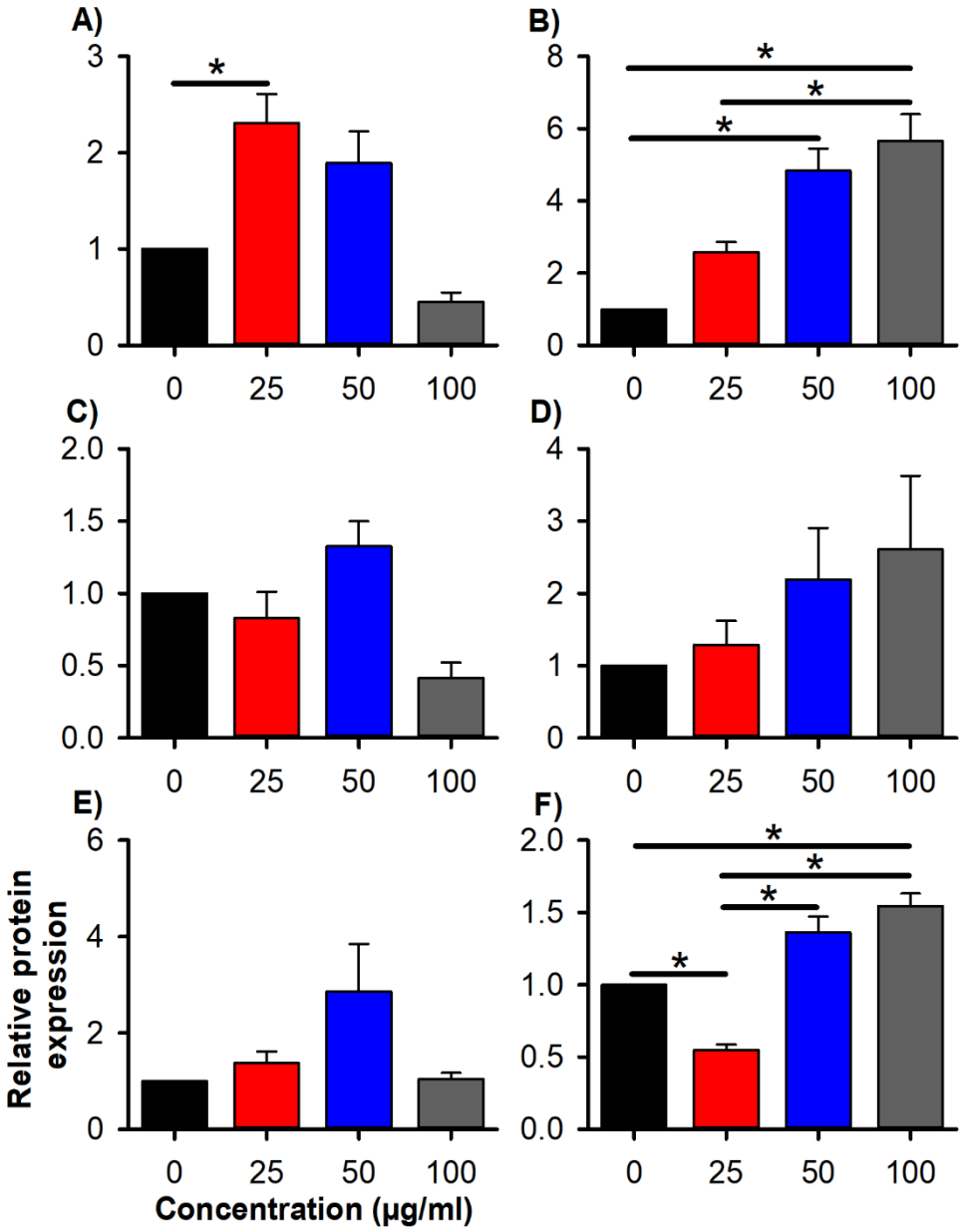

Figure 5-10. The *B. carterii* oleoresin methanolic extract induces significant increases in cleaved caspase expression in K562 cells.

The relative protein expression of **A)** Caspase-3, **B)** Cleaved caspase-3, **C)** Caspase-7, **D)** Cleaved Caspase-7, **E)** Caspase-9, and **F)** Cleaved Caspase-9 relative to GAPDH expression. Data expressed as mean ± SEM. * indicates a statistically significant difference from vehicle alone to a p value of < 0.05. n = 3 independent experiments for each protein.

Caspase-3 expression was found to be increased at concentrations of less than 100 µg/ml compared to treatment with the vehicle alone, as shown in figure 5-10A. Treatment with 25 µg/ml was found to significantly increase caspase-3 expression by 130.8 ± 36.9 % (n = 3, p = 0.027) compared to treatment with the vehicle alone. An increase in concentration to 50 µg/ml was found to increase caspase 3 cleavage by

89.3 ± 40.2 % (n = 3, p = 0.125) compared to the vehicle alone. However, it was found to decrease caspase-3 expression compared to treatment with 25 µg/ml by 19.3 ± 4.1 % (n = 3, p = 0.490). At a concentration of 100 µg/ml, caspase-3 expression was found to be decreased by 54.8 ± 12.0 % (n = 3, p = 0.419) compared to treatment with the vehicle alone.

The expression of the cleavage fragment of caspase-3 was found to increase in a concentration dependent manner following treatment with the *B. carterii* oleoresin methanolic extract as shown in figure 5-10B. Treatment with a concentration of 25 µg/ml was found to cause a 157.8 ± 34.9 % (n = 3, p = 0.335) increase in caspase-3 cleavage compared to treatment with the vehicle alone. Further increases in concentration to 50 and 100 µg/ml were found to increase caspase-3 cleavage by 383.3 ± 75.1 % (n = 3, p = 0.010) and 465.2 ± 91.3 % (n = 3, p = 0.003) respectively, compared to treatment with the vehicle alone.

Caspase-7 expression was found to not significantly change following with the treatment with concentration of the methanolic extract of the *B. carterii* oleoresin, as shown in figure 5-10C. Treatment with the maximal concentration examined was however found to decrease caspase-7 expression by 58.4 ± 12.9 % (n = 3, p = 0.091) compared to treatment with the vehicle alone.

The *B. carterii* oleoresin methanolic extract was found to increase the expression of the cleavage fragment of caspase-7 in a concentration dependent manner, as shown in figure 5-10D. No concentration examined was found to significantly increase the expression of cleaved caspase-7. Treatment with the maximal concentration of examined of 100 µg/ml was found to increase cleaved caspase-7 expression by 160.9 ± 124.7 % (n = 3, p = 0.475) compared to treatment with the vehicle alone.

Caspase-9 expression was found to not significantly change as a result of treatment with the *B. carterii* oleoresin methanolic extract, as shown in figure 5-10E. Concentrations of 25 and 50 µg/ml were found to increase caspase-9 expression by 37.0 ± 29.8 % (n = 3, p = 0.700) and 185.3 ± 121.6 % (n = 3, p = 0.202) respectively compared to treatment with the vehicle alone. When the concentration was increased to 100 µg/ml, a 3.8 ± 16.1 % (n = 3, p = 0.824) increase in caspase-9 expression was observed compared to treatment with the vehicle alone.

Treatment with the *B. carterii* oleoresin methanolic extract was found to significantly increase caspase-9 cleavage in a concentration dependent manner (figure 5-10F). Treatment with 25 µg/ml was found to decrease caspase-9 cleavage by 45.3 ± 4.8 % (n = 3, p = 0.029) compared to treatment with the vehicle alone. Further increases to 50 and 100 µg/ml was found to increase caspase-9 cleavage by 36.0 ± 13.6 % (n = 3, p = 0.081) and 54.4 ± 10.6 % (n = 3, p = 0.011) respectively.

5.3.3 The effect of the methanolic extracts of *B. carterii* oleoresin on cell cycle regulation

To determine the effect of the *B. carterii* oleoresin methanolic extract on the cell cycle regulation, the DNA content of multiple cancer cell types was analysed using flow cytometry following treatment with *B. carterii* oleoresin methanolic extract. Any change in DNA content was representative of a shift in the cell cycle progression following treatment, with significant changes in DNA content to be representative of cell cycle arrests at a specific stage. Additionally, decreases in the number of S phase cells is indicative of a loss of actively dividing cells as a result of treatment. The effect of both *B. carterii* oleoresin on the cell cycle of multiple cancer cell lines is described in sections 5.3.3.1 - 5.3.3.5.

5.3.3.1 Chronic myeloid leukaemia

As shown in figure 5-11, concentrations of the *B. carterii* oleoresin of 50 µg/ml or greater were found to cause significant increases in the number of cells in the sub G_1 and G_1 phases, whilst significantly decreasing the number of cells in the S and G_2/M phases.

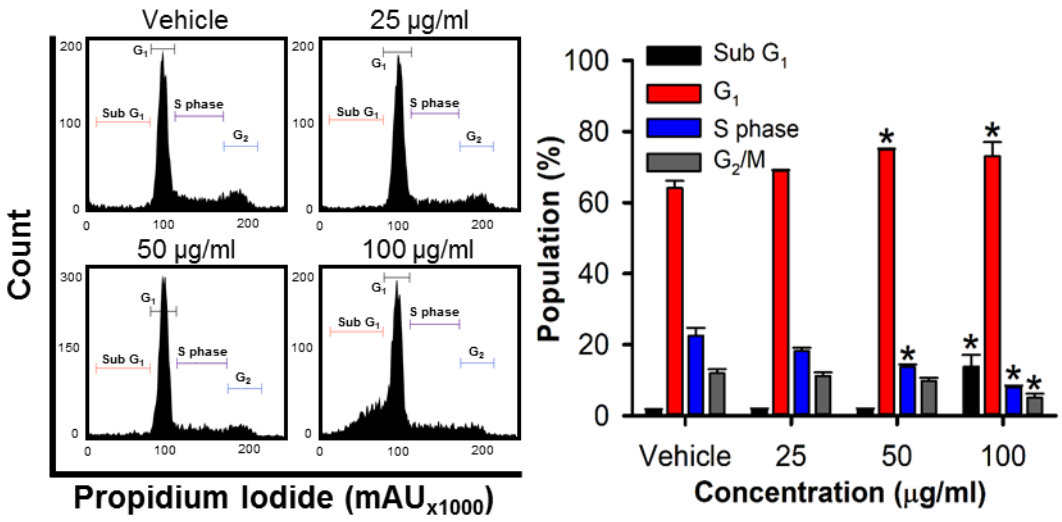

Figure 5-11. The *B. carterii* oleoresin methanolic extract induces a sub G_1/G_1 cell cycle arrest in the K562 cell line.

Cell cycle analysis was conducted by flow cytometry following cellular fixation and incubation with 100 µg/ml RNase A and 50 µg/ml PI. K562 cells were treated with vehicle alone (media + 0.5 % v/v DMSO) or 25, 50 or 100 µg/ml of the *B. carterii* oleoresin methanolic extract for 48 hours before analysis. Cells were gated into populations based on their DNA content in either sub G_1 (black), G_1 (red), S phase (blue) and G_2/M (grey). Data expressed as mean ± SEM. * indicates a statistically significant difference from vehicle alone to a p value of < 0.05. n = 8 independent biological replicates.

A concentration of 25 µg/ml was found to induce no significant change to the K562 cell cycle compared to treatment with the vehicle alone. When the concentration was increased to 50 µg/ml, a significant 17.2 ± 3.8 % (Vehicle: 64.1 ± 2.0 %, 50 µg/ml; 74.9 ± 0.3 %, n = 8, p = 0.013) increase was observed in the number of G_1 cells. This increase was found to be the result of a significant decrease of 31.0 ± 4.4 % (Vehicle: 19.8 ± 1.5 %, 50 µg/ml; 13.2 ± 0.3 %, n = 8, p < 0.001) in actively dividing S phase cells. At a concentration of 50 µg/ml, no significant change in the number of G_2/M cells was observed.

A further increase in concentration to 100 µg/ml was found to significantly increase the number of sub G_1 cells by 865.1 ± 122.6 % (Vehicle: 1.5 ± 0.4 %, 100 µg/ml; 13.8 ± 3.3 %, n = 8, p < 0.001) compared to the vehicle alone. Treatment with 100 µg/ml also significantly increased the number of G_1 cells by 14.4 ± 7.8 % (Vehicle: 64.1 ± 2.0 %, 100 µg/ml; 73.0 ± 4.0 %, n = 8, p = 0.039) This increased concentration also resulted in a further decrease in S phase cells of 52.0 ± 6.8 % (Vehicle: 19.8 ± 1.5 %, 100 µg/ml;

8.9 ± 0.7 %, n = 8, p < 0.001) compared to treatment with the vehicle alone. Treatment with 100 µg/ml was also found to significantly decrease the number of G_2/M cells by 52.2 ± 5.8 % (Vehicle: 11.4 ± 0.6 %, 100 µg/ml; 5.5 ± 0.7 %, n = 8, p < 0.001) compared to the vehicle alone.

5.3.3.2 Acute lymphoblastic leukaemia

As shown in figure 5-12, concentrations of 50 µg/ml or greater were found to produce significant increases in sub G_1 and G_1 cells accompanied by significant decreases in S phase cells.

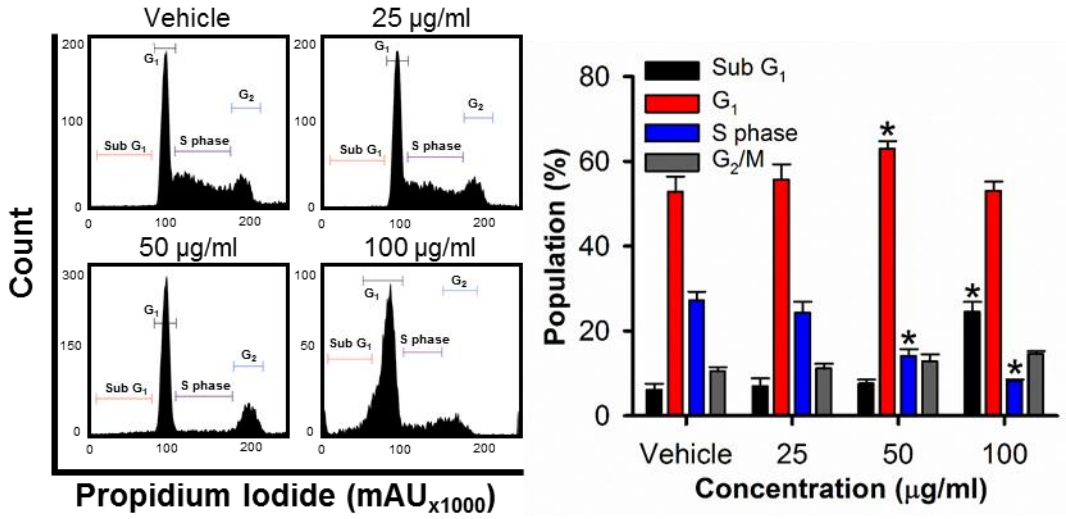

Figure 5-12. The *B. carterii* oleoresin induces a sub G_1/G_1 cell cycle arrest in the MOLT-4 cell line.

Cell cycle analysis was conducted by flow cytometry following cellular fixation and incubation with 100 µg/ml RNase A and 50 µg/ml PI. MOLT-4 cells were treated with vehicle alone (media + 0.5 % v/v DMSO) or 25, 50 or 100 µg/ml of the *B. carterii* oleoresin methanolic extract for 48 hours before analysis. Cells were gated into populations based on their DNA content in either sub G_1 (black), G_1 (red), S phase (blue) and G_2/M (grey). Data expressed as mean ± SEM. * indicates a statistically significant difference from vehicle alone to a p value of < 0.05. n = 9 independent biological replicates.

When MOLT-4 cells were treated with a concentration of 25 µg/ml no significant change in the number of cells at any stage of the cell cycle was observed. When the concentration was increased to 50 µg/ml, a significant increase in G_1 cells of 24.1 ± 9.2 % (Vehicle: 52.7 ± 3.7 %, 50 µg/ml; 62.9 ± 1.9 %, n = 9, p = 0.016) was observed. This concentration was also found to induce an 45.1 ± 7.6 % (Vehicle: 27.1 ± 2.2 %, 50

µg/ml; 14.0 ± 1.7 %, n = 9, p < 0.001) decrease in actively dividing S phase cells compared to treatment with the vehicle alone.

When the concentration was further increased to 100 µg/ml, this increase in G_1 cells was lost and a significant increase in sub G_1 cells was observed, with an increase of 1745.1 ± 818.5 % (Vehicle: 6.0 ± 1.5 %, 100 µg/ml; 24.4 ± 2.4 %, n = 9, p < 0.001). At this concentration, a further significant decrease in S phase cells of 68.8 ± 3.0 % (Vehicle: 27.1 ± 2.2 %, 100 µg/ml; 8.0 ± 0.5 %, n = 9, p < 0.001) was observed. At all concentrations examined, no significant change in the number of G_2/M cells was observed.

5.3.3.3 Hepatocellular carcinoma

The effect of the *B. carterii* oleoresin methanolic extract on the HEP G2 cell cycle, shown in figure 5-13, displayed a significant increase in the number of sub G_1 cells, whilst inducing decreases in the number of S and G_2/M phase cells.

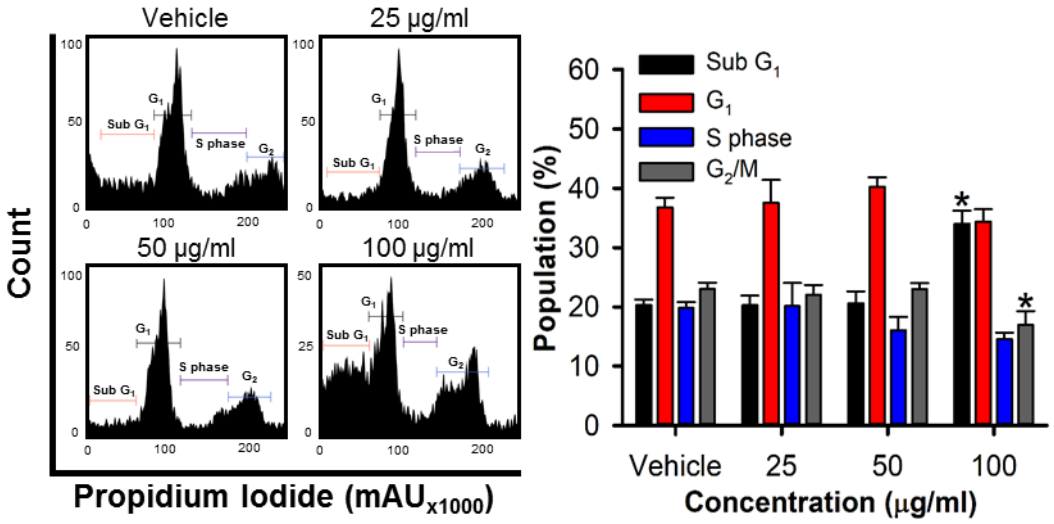

Figure 5-13. The *B. carterii* oleoresin methanolic extract induces a significant increase in the number of sub G_1 HEP G2 cells.

Cell cycle analysis was conducted by flow cytometry following cellular fixation and incubation with 100 µg/ml RNase A and 50 µg/ml PI. HEP G2 cells were treated with vehicle alone (media + 0.5 % v/v DMSO) or 25, 50 or 100 µg/ml of the *B. carterii* oleoresin methanolic extract for 48 hours before analysis. Cells were gated into populations based on their DNA content in either sub G_1 (black), G_1 (red), S phase (blue) and G_2/M (grey). Data expressed as mean ± SEM. * indicates a statistically significant difference from vehicle alone to a p value of < 0.05. n = 7 independent biological replicates.

Treatment with concentrations of the *B. carterii* oleoresin methanolic extract of ≤ 50 µg/ml showed no significant change in sub G_1, G_1, S and G_2/M cells compared to the vehicle alone. When the concentration was increased to 100 µg/ml a significant increase in the number of sub G_1 cells. This was found to be a 72.7 ± 16.5 % (Vehicle: 20.3 ± 1.4 %, 100 µg/ml; 34.0 ± 1.7 %, n = 7, p = 0.001) increase compared to treatment with the vehicle alone. At this concentration, a significant decrease in the number of G_2/M of 22.5 ± 12.6 % (Vehicle: 23.1 ± 1.7 %, 100 µg/ml; 17.0 ± 1.8 %, n = 7, p = 0.028) was also observed. Whilst the number of actively dividing S phase cells decreased following treatment with *B. carterii* oleoresin methanolic extract, the decrease was found to not be significantly difference from treatment with the vehicle alone.

5.3.3.4 Alveolar basal epithelial cell adenocarcinoma

As shown in figure 5-14, The *B. carterii* oleoresin methanolic extract was found to was found to result in a significant increase in the number of cells in the sub G_1 population of cells.

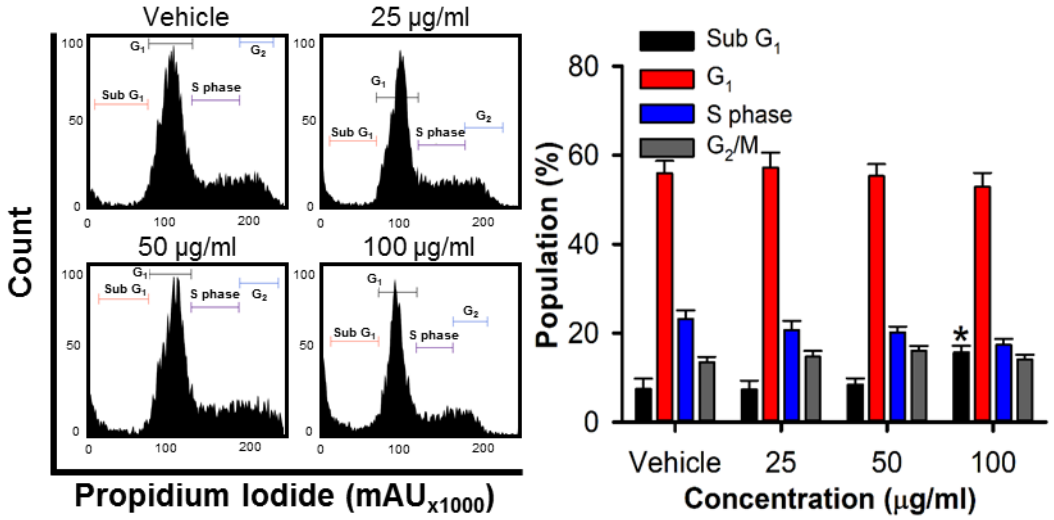

Figure 5-14. The *B. carterii* oleoresin induces a significant increase in the number of sub G_1 A549 cells.

Cell cycle analysis was conducted by flow cytometry following cellular fixation and incubation with 100 µg/ml RNase A and 50 µg/ml PI. A549 cells were treated with vehicle alone (media + 0.5 % v/v DMSO) or 25, 50 or 100 µg/ml of the *B. carterii* oleoresin methanolic extract for 48 hours before analysis. Cells were gated into populations based on their DNA content in either sub G_1 (black), G_1 (red), S phase (blue) and G_2/M (grey). Data expressed as mean ± SEM. * indicates a statistically significant difference from vehicle alone to a p value of < 0.05. n = 8 independent biological replicates.

The *B. carterii* oleoresin methanolic extract significantly increased in the sub G_1 population at a concentration of 100 µg/ml. This was found to be an 203.5 ± 67.1 % (Vehicle; 7.4 ± 2.3 %, 100 µg/ml; 15.7 ± 1.5 %, n = 8, p = 0.010) increase compared to treatment with the vehicle alone. At this concentration, a 25.7 ± 5.9 % (Vehicle: 23.8 ± 1.8 %, 100 µg/ml; 17.2 ± 1.1 %, n = 8, p = 0.059) decrease in the number of actively dividing S phase cells compared to vehicle alone. No change in the abundance of G_2/M cells was observed at any concentration examined.

5.3.3.5 Colorectal carcinoma

As per figure 5-15, concentrations of *B. carterii* oleoresin extract of 50 µg/ml or greater induced a significant increase in sub G_1 cells accompanied by significant decreases in S and G_2/M cells.

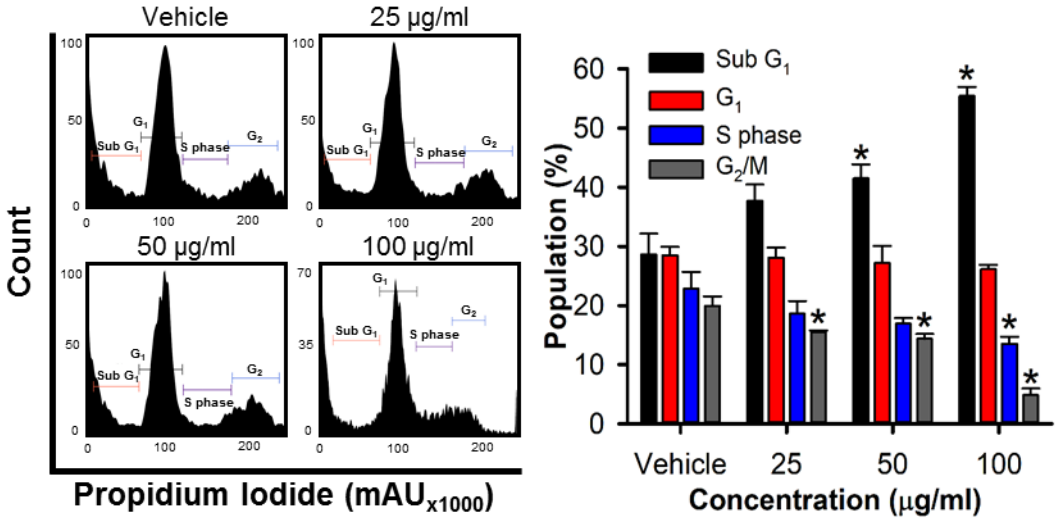

Figure 5-15. The *B. carterii* oleoresin induces a significant increase in the number of sub G_1 HCT-116 cells.

Cell cycle analysis was conducted by flow cytometry following cellular fixation and incubation with 100 µg/ml RNase A and 50 µg/ml PI. HCT-116 cells were treated with vehicle alone (media + 0.5 % v/v DMSO) or 25, 50 or 100 µg/ml of the *B. carterii* oleoresin methanolic extract for 48 hours before analysis. Cells were gated into populations based on their DNA content in either sub G_1 (black), G_1 (red), S phase (blue) and G_2/M (grey). Data expressed as mean ± SEM. * indicates a statistically significant difference from vehicle alone to a p value of < 0.05. n = 4 independent biological replicates.

At a concentration of 25 µg/ml no significant change was observed in the number of cells in the sub G_1, G_1 and S phases of the cell cycle, compared to treatment with the vehicle alone. However, the number of cells in the G_2/M stage of the cell cycle was

found to be significantly decreased by 20.7 ± 7.4 % (Vehicle: 20.0 ± 1.6 %, 25 µg/ml; 15.5 ± 0.3 %, n = 4, p = 0.028) compared to the vehicle alone.

When the concentration was increased to 50 µg/ml, a significant increase in the number of cells in the sub G_1 stage of the cell cycle was observed. This was found to be an increase of 53.9 ± 25.0 % (Vehicle: 28.7 ± 3.5 %, 50 µg/ml; 41.5 ± 2.4 %, n = 4, p = 0.013) compared to the vehicle alone. This increase was found to be due to a 23.1 ± 9.0 % (Vehicle: 22.9 ± 2.9 %, 50 µg/ml; 16.9 ± 1.0 %, n = 4, p = 0.123) non-significant decrease in the number of S phase cells and an 26.6 ± 7.8 % (Vehicle: 20.0 ± 1.6 %, 50 µg/ml; 14.3 ± 0.8 %, n = 4, p = 0.007) decrease in the number of cells in the G_2/M stage compared to treatment with the vehicle alone.

When the concentration of the *B. carterii* oleoresin methanolic extract was further increased to 100 µg/ml, a further increase in the number of cells within the sub G_1 stage of the cell cycle was observed. This concentration was found to increase the number of sub G_1 cells by 101.2 ± 21.6 % (Vehicle: 28.7 ± 3.5 %, 100 µg/ml; 55.4 ± 1.5 %, n = 4, p < 0.001) compared to treatment with the vehicle alone. Treatment with 100 µg/ml was also found to induce an 39.6 ± 3.8 % (Vehicle: 22.9 ± 2.9 %, 100 µg/ml; 13.6 ± 1.2 %, n = 4, p = 0.014) decrease in the number of actively dividing S phase cells, whilst further decreasing the number of cells in the G_2/M by 74.9 ± 5.9 % (Vehicle: 20.0 ± 1.6 %, 100 µg/ml; 4.9 ± 1.1 %, n = 4, p < 0.001) compared to treatment with the vehicle alone.

5.3.4 The molecular changes associated with a G_1 cell cycle arrest

Within section 5.3.3, it was identified that the *B. carterii* oleoresin methanolic extract induced a G_1 cell cycle arrest against chronic myeloid leukaemia cells. Based on these findings, we then wanted to ascertain the molecular mechanisms underpinning this effect. This was conducted through the analysis of protein expression associated with cell cycle regulation using Western blotting techniques. To determine the molecular mechanism underpinning the cell cycle arrest in the K562 cell line following treatment with the *B. carterii* oleoresin methanolic extract, described in section 5.3.3.1, the change in expression of key cell cycle regulatory proteins was evaluated using Western blotting.

The change in protein expression of key cell cycle regulatory proteins following the treatment of K562 cells with varying concentrations of the *B. carterii* oleoresin methanolic extract is shown in figure 5-16. The relative change in protein expression compared to the housekeeper protein GAPDH across a range of concentrations is shown in figure 5-17.

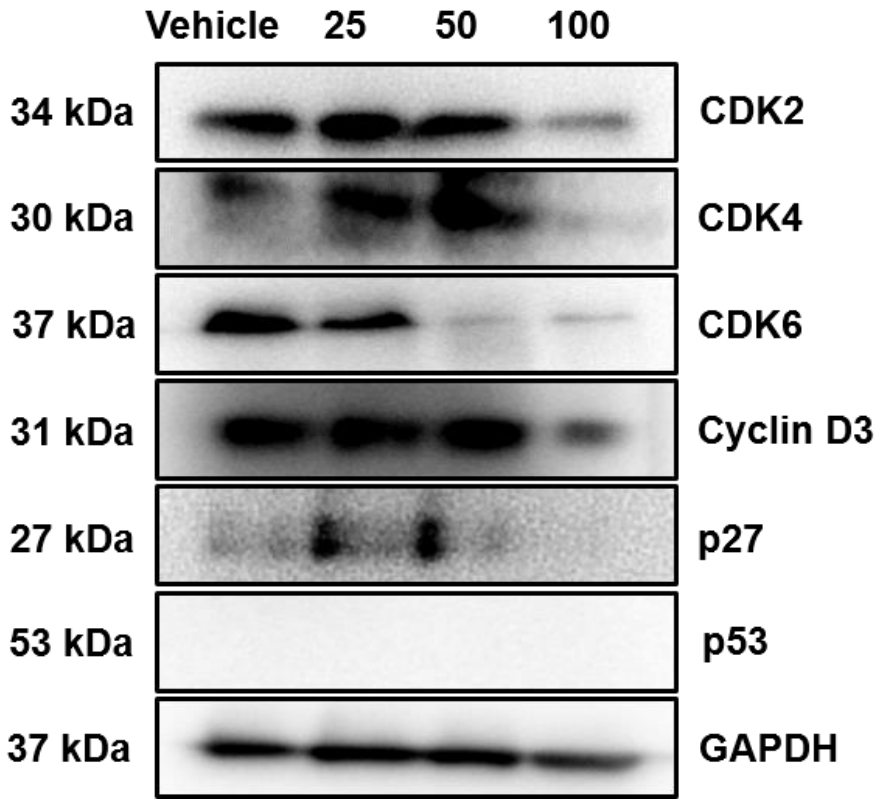

Figure 5-16. The *B. carterii* oleoresin methanolic extract modifies key cell cycle protein expression in the K562 cell line.

Protein lysates were prepared from K562 cells were treated with various concentrations of the *B. carterii* oleoresin methanolic extract for 48 hours. Lysates were then separated using 4-20 % SDS PAGE gel electrophoresis as described in section 5.2.5.5. Proteins were then transferred to 0.45 PVDF membrane and probed for the protein of interest as described in section 5.2.5.6 and imaged as described in section 5.2.5.8. Figure representative of three independent repeats for each protein of interest.

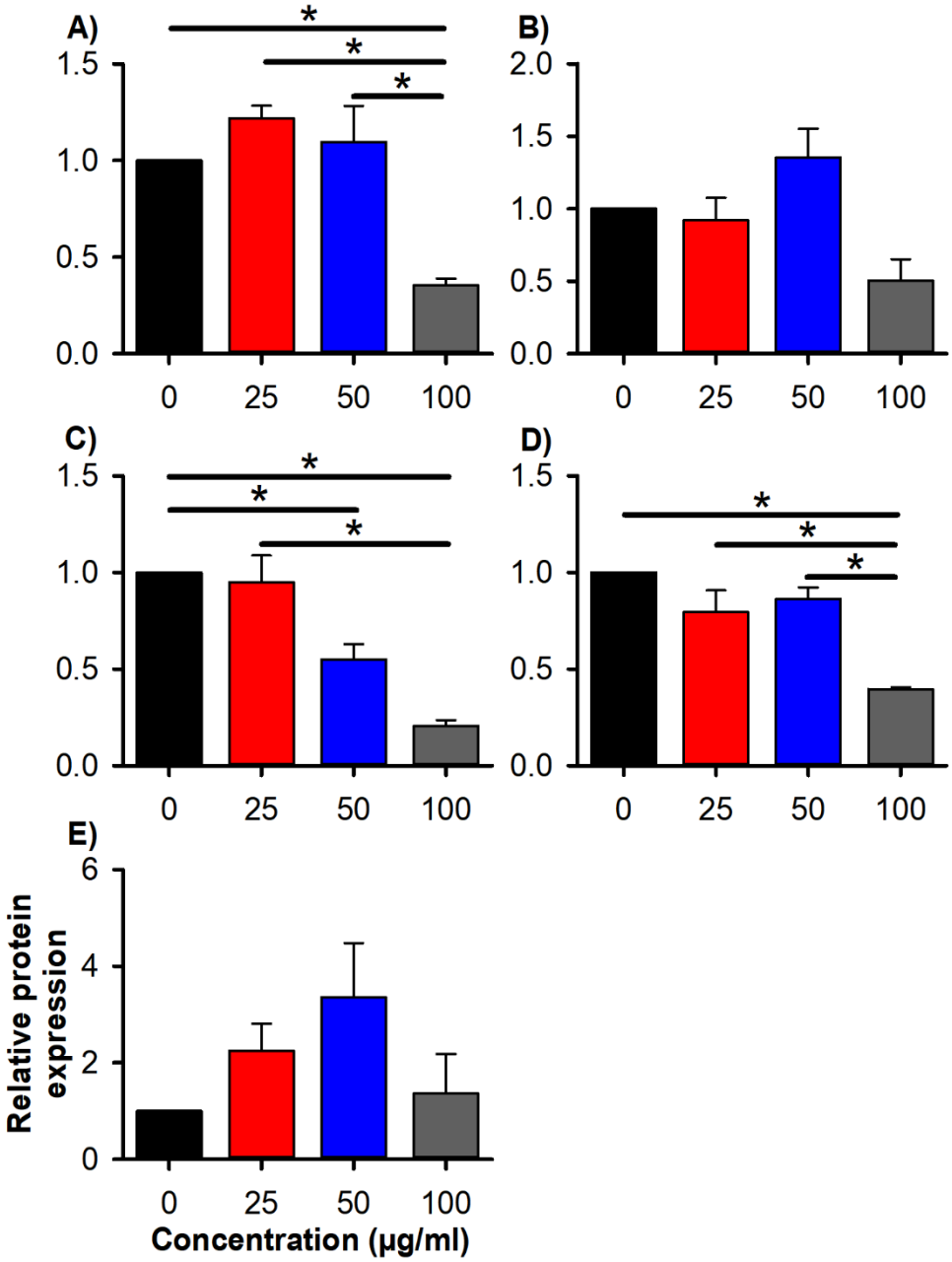

Figure 5-17. The effects of the *B. carterii* oleoresin methanolic extract on cell cycle protein expression.

The protein expression of **A)** CDK2, **B)** CDK4, **C)** CDK6, **D)** Cyclin D3 and **F)** p27 was examined relative to GAPDH expression following treatment with the *B. carterii* oleoresin for 48 hours. Protein expression for each blot was quantified using ImageJ. and analysed offline to compare expression relative to GAPDH expression. Data expressed as mean ± SEM. * indicates a statistically significant difference from vehicle alone to a p value of < 0.05. n = 3 independent experiments for all proteins.

The expression of CDK2, shown in figure 5-17A, was found to be significantly decreased following treatment with a concentration of 100 µg/ml. Treatment with 100

µg/ml was found to decrease CDK2 expression by 64.6 ± 4.2 % (n = 3, p = 0.025) compared to treatment with the vehicle alone. Treatment with 100 µg/ml was also found to be significantly decreased compared to treatment with concentrations of 25 and 50 µg/ml. A concentration of 100 µg/ml was found to decrease CDK2 expression by 71.1 ± 1.5 % (n = 3, p = 0.005) and 64.4 ± 8.3 % (n = 3, p = 0.012) compared to treatment with concentrations of 25 and 50 µg/ml respectively. Treatment with concentrations of 25 and 50 µg/ml were found to cause no significant change in CDK2 expression compared to treatment with the vehicle alone.

The *B. carterii* oleoresin methanolic extract was found to be induce no significant change in CDK4 expression at all concentrations examined, as shown in figure 5-17B. Treatment with 25 µg/ml was found to not significantly alter CDK4 expression. An increase in concentration to 50 µg/ml was found to increase CDK4 expression by 35.5 ± 20.0 % (n = 3, p = NS). However, when the concentration was increased to 100 µg/ml, a 49.4 ± 14.9 % (n = 3, p = 0.059) decrease compared to treatment with the vehicle alone.

The expression of CDK6 was found to be significantly decreased following treatment with the *B. carterii* oleoresin methanolic extract, as shown in figure 5-17C. Treatment with a concentration of 25 µg/ml was found to induce no significant difference in CDK6 expression. When the concentration was increased to 50 µg/ml, a significant decrease in CDK6 expression was observed. A concentration of 50 µg/ml induced a 45.0 ± 9.7 % (n = 3, p = 0.050) decrease in CDK6 expression. A further increase in concentration to 100 µg/ml, was found to induce a 79.4 ± 3.7 % (n = 3, p = 0.002) decrease in CDK6 expression compared to treatment with the vehicle alone.

Treatment with the *B. carterii* oleoresin methanolic extract was found to significantly decrease cyclin D3 expression, shown in figure 5-17D, compared to treatment with the vehicle alone. Treatment with concentrations of 25 and 50 µg/ml were found to result in no significant change in cyclin D3 expression compared to treatment with the vehicle alone. When the concentration was further increased to 100 µg/ml, a significant decrease in cyclin D3 expression was observed. This concentration was found to decrease cyclin D3 expression by 60.3 ± 1.1 % (n = 3, p = 0.003) compared to treatment with the vehicle alone.

The relative expression of p27, shown in figure 5-17E, was found to be increased following treatment with concentrations of 25 and 50 µg/ml of the *B. carterii* oleoresin methanolic extract. Treatment with these concentrations were found to induce increases in p27 expression of 124.5 ± 68.7 % (n = 3, p = NS) and 235.9 ± 137.7 % (n = 3, p = 0.336) respectively. When the concentration was increased to 100 µg/ml, this increase in p27 expression was lost, however compared to treatment with the vehicle alone, p27 expression was found to be increased by 36.1 ± 100.2 % (n = 3, p = NS) following treatment with 100 µg/ml.

5.4 Discussion

5.4.1 What mechanism of *B. carterii* oleoresin methanolic extract mediated cell death?

The mechanism of cell death induced by anti-cancer drugs is vitally important, as the different mechanisms of cell death, specifically necrosis, can result in off target effects and downstream toxicity. The ideal mechanism of cell death induced by anti-cancer drugs is apoptosis, due to dying cells self-encapsulating their intracellular contents, preventing their release into the extracellular environment (Wickman, Julian, & Olson, 2012). The inverse is observed in necrotic cell death, in which damage to the cell membrane leads to the release of cellular contents into the extracellular space (Rock & Kono, 2008). This release can induce downstream immune reactions in response to the molecules released into the extracellular environment (Davidovich, Kearney, & Martin, 2014). Therefore, an understanding of the mechanism of cell death induced by the *B. carterii* oleoresin is required if they are to be taken further down the drug development pathway.

Cell death analysis by flow cytometry, shown in figures 5-3 - 5-7, found that the *B. carterii* oleoresin methanolic extract to induce predominately late apoptosis/secondary necrosis, with a minimal increase in necrosis in the majority of the cancer cell types examined. However, the technique utilised to evaluate apoptotic cell death was unable to discriminate between late apoptotic and secondary necrotic cells as both cell types would both test positive for both annexin V and propidium iodide. This study also identified that the *B. carterii* oleoresin methanolic extract was found to induce early apoptosis in the majority of cancer cell types at lower concentrations, indicative that *B. carterii* oleoresin induces apoptotic cell death, however further molecular examination was required to confirm this. Further to this, this study showed that the *B. carterii* oleoresin methanolic extract was found to more effective at inducing apoptotic cell death in leukaemia cells compared to that of epithelial based cancer cell types.

Analysis of the molecular mechanisms underpinning the potential pro-apoptotic activity, observed in section 5.3.1, was conducted using the chronic myeloid leukaemia cell line, K562, based on the increased effectiveness towards this cell type. The oleoresin methanolic extracts were seen to increase the activation, via cleavage, of caspases-3, -7 and -9. This increase in the cleavage of the caspases by the

apoptosome converts them to their active forms resulting in the degradation of cellular proteins and ultimately cell death (Shi, 2004). The activation of caspases mediated by the initiator caspase-9, indicates that the *B. carterii* oleoresin methanolic extract induces apoptotic cell death by activating the intrinsic pathway of apoptosis (Li *et al.*, 2017; Shi, 2002).

Further analysis evaluated the upstream signalling mechanisms associated with the activation of the intrinsic pathway. Multiple causative factors have been described to activate the intrinsic pathway of apoptosis, namely growth factor deprivation, intracellular oxidative stress, DNA damage and ischemia (Loreto *et al.*, 2014; Pfeffer & Singh, 2018). Therefore, the development of an understanding regarding how the *B. carterii* oleoresin activates the intrinsic pathway of apoptosis is of vital importance.

Treatment with the *B. carterii* oleoresin methanolic extract was found to decrease whole PARP expression at the maximal concentration examined, whilst increasing PARP cleavage in a concentration dependent manner. Whole PARP is a nuclear protein with a wide range of physiological processes (Chaitanya, Alexander, & Babu, 2010). However, a central role of PARP is its ability to repair damaged DNA (Chaitanya *et al.*, 2010).

In apoptosis, the activation of caspases -3 and -7 leads to the cleavage of whole PARP and the formation of 89 or 85 kDa cleavage fragments dependent on the caspase inducing the cleavage (Kaufmann, Desnoyers, Ottaviano, Davidson, & Poirier, 1993). The cleavage of PARP to these fragments, deactivates the protein and prevents it from performing its normal DNA repair function (Kaufmann *et al.*, 1993). Therefore, the cleavage of PARP is considered a hallmark of apoptotic cell death. The molecular changes that occurred as a result of the *B. carterii* oleoresin methanolic extract corroborates these findings, with both cleaved caspases -3 and -7 were found to be elevated alongside an increase in PARP cleavage. This further supports our findings that the apoptotic cell death induced by the *B. carterii* oleoresin methanolic extract.

Whilst the complete molecular mechanism underpinning the anti-cancer activity of the *B. carterii* oleoresin has yet to be fully examined, our findings corroborate those conducted using the oleoresins of other *Boswellia* species. Multiple studies by Jaafari-Ashkavandi *et al.* (2017), Ranjbarnejad *et al.* (2017) and Ahmed *et al.* (2015) have shown the extracts of *B. serrata* oleoresin to induce apoptotic cell death in multiple

cancer cell types *in vitro*. Further molecular examination by Ranjbarnejad *et al.* (2017) showed the apoptosis to be result of increased caspase-3 activation, which corroborates the findings of this study. The findings of this study further expand on the findings of previous studies by for the first time identifying that the *B. carterii* oleoresins also increase the activation of caspase-9 and PARP.

Purified boswellic acid isoforms derived from the oleoresin of the *B. serrata* have also been shown to induce apoptosis in multiple cancer cell lines *in vitro* (Buchele *et al.*, 2006; Jing *et al.*, 1999; Takahashi *et al.*, 2012). Examination into the molecular effects of boswellic acids by Buchele *et al.* (2006) identified that boswellic acids induce apoptosis by increased activation of caspase-3, matching that identified within this study. These findings indicate that the *B. carterii* oleoresin methanolic extract induces apoptosis in a similar manner to that of the isolated boswellic acids via the activation of the intrinsic pathway of apoptosis.

However, studies by Xia *et al.* (2005) and Lu *et al.* (2008) showed the boswellic acid isoforms boswellic acid acetate and AKBA to increase the expression of DR4 and DR5 in myelogenous leukaemia and prostate cancer cells. These findings indicate that in addition to activation the intrinsic pathway of apoptosis, boswellic acid isoforms can also activate the extrinsic pathway of apoptosis, which has yet to be explored using oleoresin extracts from any species of *Boswellia*. This therefore offers a potentially novel mechanism to further explore in future study of the cytotoxic activity of *B. carterii* oleoresin.

Despite developing an understanding into the mechanisms underpinning the apoptotic activity of the *B. carterii* oleoresin, further pathways could be explored to better understand if these substrates have an impact on other signalling pathways associated with apoptosis. Our findings identified that both *B. carterii* oleoresin activated the intrinsic pathway of apoptosis, via the activation of caspase-9, however the upstream signalling pathways could be explored to determine the mechanism through which this pathway is activated.

Examination of the release of cytochrome C from the mitochondria and modification to the mitochondrial membrane potential could be explored, as these changes are key to the formation of the apoptosome and therefore the activation of caspase-9. Further to this, the mechanisms which cause the release of cytochrome C from the mitochondria

should also be explored. This would be conducted via the analysis of the expression of the proteins BID, BAK and BAX, in addition to their associated inhibitors BCL-2 and BCL-xL (Hardwick & Soane, 2013), which have all been shown to play a key role in the upstream signalling cascade in the intrinsic pathway of pathway.

In addition to further exploration of the intrinsic pathway of apoptosis, *Boswellia* oleoresins and isolated boswellic acids have been described to also effect other pathways involved in the inducement of apoptotic cell death. These pathways involve the upregulation of the death receptor pathway via increased expression of DR4 and DR5 (Lu *et al.*, 2008; Xia *et al.*, 2005), as well as the inhibition of Topoisomerases I and II (Hoernlein *et al.*, 1999; Syrovets, Büchele, Gedig, Slupsky, & Simmet, 2000; Zhao *et al.*, 2003). The effect of the *B. carterii* oleoresin on these pathways has yet to be explored and therefore it is not currently known if the *B. carterii* oleoresin affects these pathways and offers potentially novel pathways to further explore.

5.4.2 Does the *B. carterii* oleoresin induce cell cycle arrest?

Cancer cells possess the ability to divide indefinitely and ignore the mechanisms through which normal cells are prevented from doing so (Hanahan & Weinberg, 2011). This commonly arises due to mutations within cancer cells, resulting in the over expression of cell division promoting genes/proteins or though downregulation of cell division inhibitors (Bertram, 2000; Nenclares & Harrington, 2020). These changes lead to the further progression and development of the cancer. Therefore, the potential to modify the expression of the proteins involved with the enhancement of cell division is important in both the management of the disease and increase the likelihood of treatments being effective.

The relative DNA content within the cell following treatment with the *B. carterii* oleoresin was measured using flow cytometry. Based on the amount of DNA within the cell, its position within the cell cycle was determined. As per figures 5-11 - 5-15 the *B. carterii* oleoresin methanolic extract was found to arrest multiple cancer cell types in the G_1 stage of the cell cycle or significantly increase the number of sub G1 cells. This arrest was also found to result in significant decreases in the number of actively dividing cells, within the S phase of the cell cycle in multiple cancer types. Whilst significant decreases in actively dividing cells were observed in the majority of cancer types examined, no significant change was observed against the alveolar basal epithelial cell

adenocarcinoma cells examined. This indicates that the *B. carterii* oleoresin only induces apoptosis, with a minimal effect on the cell cycle of this cancer type at the concentrations examined in this study.

When further analysis of the change in key cell cycle regulation protein expression was conducted using the K562 cell line, significant modifications to protein expression were identified The *B. carterii* oleoresin was found to cause decreases in the CDK 2 CDK 6 cyclin D3 expression. Both substrates were also found to increase the expression of CDK inhibitor p27. Interestingly, the *B. carterii* oleoresin methanolic extract did not significantly decrease expression of CDK4 at any concentration used compared to treatment with the vehicle alone. No previous research has been conducted to examine the effects of *B. carterii* oleoresin extracts on the cancer cell cycle, therefore this study provides novel insights into their effects against multiple cancer cell types.

The downregulation of CDK's 2, 4 and 6 have been associated with a G_1 cell cycle arrest in multiple studies (Ding *et al.*, 2020; Huang *et al.*, 2012; Neganova *et al.*, 2011). This is further supported by the decrease in expression of cyclin D3, which has been shown to arrest cancer growth in the G_1 stage of the cell cycle in multiple cancer cell types following treatment with chemotherapeutic agents (García-Morales *et al.*, 2006; Goda, Erikson, Ahn, & Kim, 2015; Miyatake *et al.*, 1995; Yang, Yin, Zhong, Liao, & Li, 2015).

The activation of D cyclins and their subsequent complexing with CDK's 4 and 6, results in the transition out of the G_1 into the S phase of the cell cycle (Wiman & Zhivotovsky, 2017). Therefore, the downregulation of cyclin D3, CDK4, and CDK6 following treatment with the *B. carterii* oleoresin methanolic extract further corroborates the inducement of a G_1 cell cycle arrest due to the inability to transition into the S phase of the cell cycle.

Additionally, the upregulation of p27 has been associated with decrease in CDK expression and therefore inhibition of cell cycle progression (Abbastabar *et al.*, 2018). These molecular changes in combination following treatment with the *B. carterii* oleoresin confirms the findings of the cell cycle analysis using flow cytometry which identified both substrates to induce a G_1 cell cycle arrest.

These findings corroborate those of multiple studies which identified that the oleoresin of *B. serrata* to increase the number of cells in the sub G_1 phase and induce G_1 cell cycle arrests in multiple cancer cell lines (Ranjbarnejad *et al.*, 2017; Yazdanpanahi *et al.*, 2014).

The findings of this study are also supported by the effects on the cell cycle induced by purified boswellic acids. Boswellic acids have been described to induce an increase in the number of sub G_1 cells (Takahashi *et al.*, 2012), whilst also being described to induce a G_1 cell cycle arrest (Jing *et al.*, 1999; Yuan *et al.*, 2008). The findings of this study is further supported by analysis of the effect of the essential oils of *B. serrata* and *B. sacra* on the cancer cell cycle. Studies by Ni *et al.* (2012) and Suhail *et al.* (2011) described the essential oil isolated from these species to induce cell cycle arrests at the G_1 stage of the cell cycle.

Limited research has been conducted regarding the molecular effects of extracts of *Boswellia* oleoresin, with this study offering novel insights into their molecular effects on the cancer cell cycle. However, the molecular effect on the cancer cell cycle induced by the *B. carterii* oleoresin methanolic extract was also found act in a similar fashion to that of purified boswellic acids and the essential oil derived from *Boswellia* species.

Numerous studies have sown both the *Boswellia* essential oil and purified boswellic acids to significantly decrease the expression of D cyclins and CDK4 (Suhail *et al.*, 2011; Syrovets *et al.*, 2005; Takahashi *et al.*, 2012). These findings corroborate those from this study and further support the suggestion that a G_1 cell cycle arrest is induced by the *B. carterii* oleoresin. The methanolic extract of *B. thurifera* oleoresin has been described to p53 mRNA expression following treatment for 12 hours (Yazdanpanahi *et al.*, 2014). The K562 cell line used in this study to examine the molecular mechanisms underpinning the activity of the *B. carterii* oleoresin is p53 deficient and therefore does not express this protein (as confirmed in figure 5-16), as a result this study was unable to examine the change in p53 expression following treatment. Future work will utilise a cancer type which expresses p53 to examine the effects of the *B. carterii* oleoresin on p53 expression.

Analysis of the change in mRNA expression following treatment with AKBA, conducted by Toden *et al.* (2015), also identified a downregulation of the D cyclins. In addition, they also identified that AKBA causes a decrease in the proto-oncogene C-Myc

expression, which has been described as a master cell cycle regulator. C-Myc has been shown to have multiple downstream effects including the upregulation of E and D cyclins, as well as increasing the expression of CDK's 4 and 6, whist downregulating cell cycle inhibitors p21 and p27 (Bretones, Delgado, & León, 2015).

This gene has also been shown to play a key role in numerous factors in cellular functions by acting as a transcription factor for numerous pathways including cell differentiation, apoptosis and cellular transformation leading to tumour pathogenesis (Melnik *et al.*, 2019). This oncogene has been observed to be overexpressed in up to 40 % of cancers (Miller, Thomas, Islam, Muench, & Sedoris, 2012). Therefore, the potential to decrease its expression using *Boswellia* derivatives may offer a novel mechanism of action which could be further explored.

Further experiments on the effects of the *B. carterii* oleoresin on the cancer cell cycle could be conducted to ascertain a better understanding regarding the up and downstream effects associated with the induction of a G_1 cell cycle arrest. The MAPK signalling pathway has been described to activate CDK's 4 and 6 via the upregulation of D cyclin expression, resulting in a subsequent increase in the expression of CDK's 4 and 6. Additionally, ERK, a signal transduction protein, has been shown to phosphorylate CDK's 4 and 6 allowing them to complex with cyclin D1, and induce their downstream effects (Villanueva, Yung, Walker, & Assoian, 2007). Therefore, a greater understanding of the effect the *B. carterii* oleoresin have on the MAPK signalling pathway is important for better understanding the causative mechanism behind the decreased expression of D cyclins and CDKs.

Additionally, the downstream effects of the cyclin D/CDK4,6 complexing can be examined to determine if the downregulation of D cyclins and CDK's has an impact of the inhibition of Rb and the liberation of E2F. This liberation of E2F allows cells to exit G_1 and enter the S phase of the cell cycle (Henley & Dick, 2012), and therefore modification to the expression of Rb and E2F would confirm the arrest of cells at the G_1 checkpoint.

This study also highlighted the increase in expression of CDK inhibitor proteins by the upregulation of p27 at concentrations of 25 and 50 µg/ml, before being lost at a concentration 100 µg/ml. This loss of p27 expression at the maximal concentration may be examined may be due to the chronic timepoint examined. A study by Larrea *et*

al. (2008) showed that p27 expression was found to be substantially increase within 12 hours before declining to less than untreated control after 24 hours post treatment with epidermal growth factor (EGF). Based on this, it can be hypothesised that the examination of a more acute protein expression timepoint may allow us to better understand the expression of cell cycle inhibitory proteins.

In addition to this, further examination of other CDK inhibitor proteins could be examined. The expression of p57, in addition to p21, p18 and p27 have all been shown to be upregulated during cell cycle arrests, due to their ability to inhibit CDK's (Guo, Tian, Nan, & Wang, 2010). Therefore, analysing the expression of these proteins will allow us to better ascertain the mechanism by which CDK's are downregulated as a result of treatment with the *B. carterii* oleoresin methanolic extract.

5.4.3 Conclusions

Overall, this study has confirmed that the *B. carterii* oleoresin induces apoptosis by the activation of the intrinsic apoptosis pathway. Further to this, it was identified that the *B. carterii* oleoresin induced a G_1 cell cycle arrest in K562 cells as a result of inhibition of the cell cycle regulatory proteins cyclin D3, CDK's 2, 4 and 6.

Chapter 6

Chemical characterisation of the *B. carterii* oleoresin methanolic extract.

6.1 Introduction

The previous chapters demonstrate the potential of *B. carterii* oleoresin as a novel chemotherapeutic. However, it is important to remember that the extracts used contain all methanol soluble constituents. It is highly likely that only certain compounds within this milieu are responsible for the aforementioned biological effects.

The oleoresins of the *Boswellia* genus are generally composed of 60 - 70 % alcohol soluble resin, 5 - 10 % essential oil, and 25 - 30 % water soluble gum (Al-Yasiry & Kiczorowska, 2016; Buchele *et al.*, 2006; A. Frank & Unger, 2006; Vuddanda *et al.*, 2016). The alcohol soluble resin fraction of certain *Boswellia* oleoresins is known to contain numerous compounds including monoterpenes, diterpenes, triterpenes, tetracyclic triterpenes, and pentacyclic triterpenes (Al-Yasiry & Kiczorowska, 2016; Vuddanda *et al.*, 2016). Of these groups of compounds, the key molecules associated with previously described biological activity are the pentacyclic triterpenes, known as boswellic acids (previously described in section 1.3.4). However, the chemical composition of the *Boswellia* genus differs between individual species and is dependent upon the specific climate, harvest conditions, soil composition and geographical source of individual *Boswellia* trees (Frank *et al.*, 2009; Mikhaeil, Maatooq, Badria, & Amer, 2003; Van Vuuren, Kamatou, & Viljoen, 2010).

Despite these variations between individual *Boswellia* species, the chemical composition of *B. carterii* has yet to be fully characterised, with the majority of previous research focused on *B. serrata*. As such, the chemical profile of *B. carterii* oleoresin and whether there are any key differences to that of other *Boswellia* species remains unknown. This means that while for other species of *Boswellia*, the compounds responsible for biological effects are identified, this is not the case for *B. carterii.*

The process of chemical characterisation involves identifying the individual compounds within complex mixtures, such as natural product extractions (Rasul, 2018; S. Sasidharan, Y. Chen, D. Saravanan, K. Sundram, & L. Y. Latha, 2011). The complete characterisation of natural product extracts commonly requires many different analytical chemistry methods as described in section 1.3.7 (Brusotti, Cesari, Dentamaro, Caccialanza, & Massolini, 2014; Rasul, 2018; Van Elswijk & Irth, 2002) but usually begins with an initial separation of all compounds within the extract using chromatography. Chromatography methods such as liquid chromatography and gas

chromatography separate compounds within a mixture based on their solubility, more specifically their affinity for a mobile phase or a stationary phase which is packed into a column that forms part of a series of equipment shown in figure 6-1A (Kupiec, 2004). A compound's affinity for the stationary phase determines how quickly it is eluted from the column. Each compound within the mixture has a different affinity for the stationary phase and therefore each compound remains within the column for a different amount of time, termed retention time. This results in the separation of complex mixtures into their individual chemical constituents, shown in figure 6-1B.

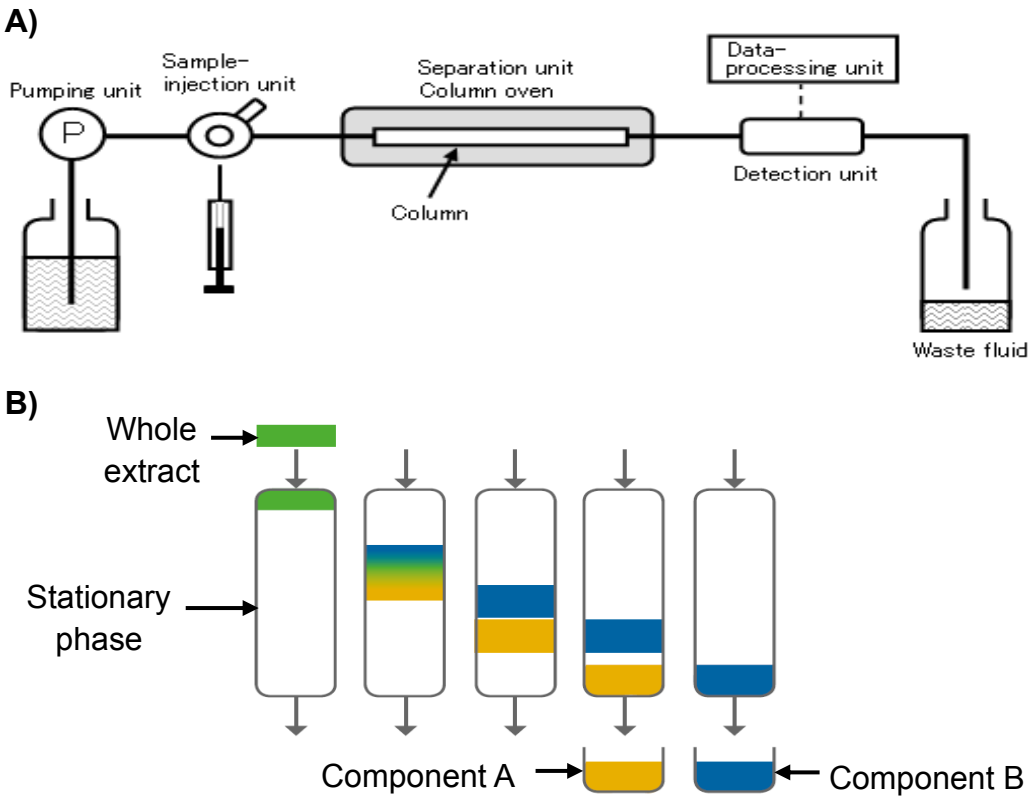

Figure 6-1. The method of compound separation by high-performance liquid chromatography.

A) A schematic diagram showing the sequence and equipment required to conduct high performance liquid chromatography. **B)** A schematic summarising the mechanism of compound separation within a HPLC column.

After separation of the compounds within a mixture, they can be identified. Following HPLC-based separation, mass spectrometry, which identifies compounds based on their mass to charge ratio (m/z), is commonly used. This can be done directly, as compounds elute off the HPLC column (Paré & Yaylayan, 1997). However, for

detection by MS, all compounds must carry a charge, therefore before entering the analyser, compounds are converted to a gaseous phase then ionised by the removal of an electron from their molecular structure (Baghel, Singh, Singh, & Sinha, 2017; Han, Aslanian, & Yates III, 2008). The process of ionisation can also break the molecule into positively ionised fragments. This occurs in a specific pattern for every molecule, known as fragmentation patterns (Olshina & Sharon, 2016). These patterns are associated with various molecular and structural aspects of the original ion, allowing the elucidation of the molecular structure of the original ion (Nicolescu, 2017). An example of fragmentation is shown in figure 6-2.

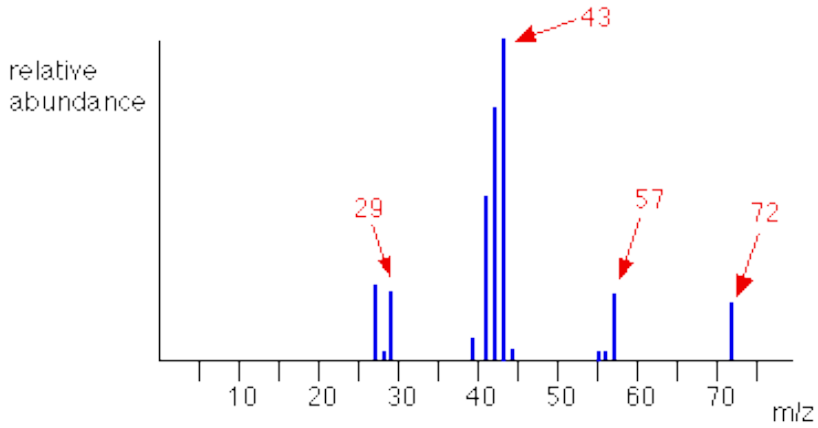

Figure 6-2. An example mass spectra and determination of mass spectral fragmentation patterns.

An example fragmentation pattern derived from the mass spectrometry analysis of pentane ($CH_3CH_2CH_2CH_2CH_3$). Red arrows indicate the ionisation fragments associated with pentane and their respective m/z ratios.

Following ionisation, all ions are accelerated to the same kinetic state then sorted within a mass analyser which sorts compounds based on the degree of deflection by electromagnetic fields (Murayama, Kimura, & Setou, 2009). Subsequently, ions hit a detector, which measures the abundance and mass / charge (m/z) ratio of each (Loos, Van Schepdael, & Cabooter, 2016). A computer then uses the data generated by the mass spectrometer to produce mass spectrums, which provide a graphical representation of a specific molecular ion and its associated fragment (Murayama *et al.*, 2009). These fragmentation patterns can then be utilised to determine the identity of compounds.

6.1.1 Aims of the chapter

There has been limited research on the chemical composition of the oleoresins derived from *B. carterii*. This chapter therefore aims to generate a chemical fingerprint of the oleoresins of *B. carterii* as well as ascertaining the boswellic acid isoforms present within the *B. carterii* species.

The main aims of this chapter as the following:

1) To generate a chemical fingerprint of the *B. carterii* oleoresin.

2) To determine which boswellic acid isoforms *the B. carterii* oleoresin contains.

6.2 Methods

6.2.1 Optimisation of mobile phase constituents and loading concentration using isocratic HPLC

Isocratic HPLC was performed using the equipment described in section 2.7.1. Sample preparation and sample injection was conducted using the method described in section 2.7.2.

Preliminary optimisation experiments to determine the optimal mobile phase constituents, mobile phase concentration and sample loading concentration were all performed using this isocratic HPLC approach. The findings of this optimisation identified acetonitrile to be the optimal mobile phase constituent for HPLC analysis. The results of this optimisation are shown in figure 6-3.

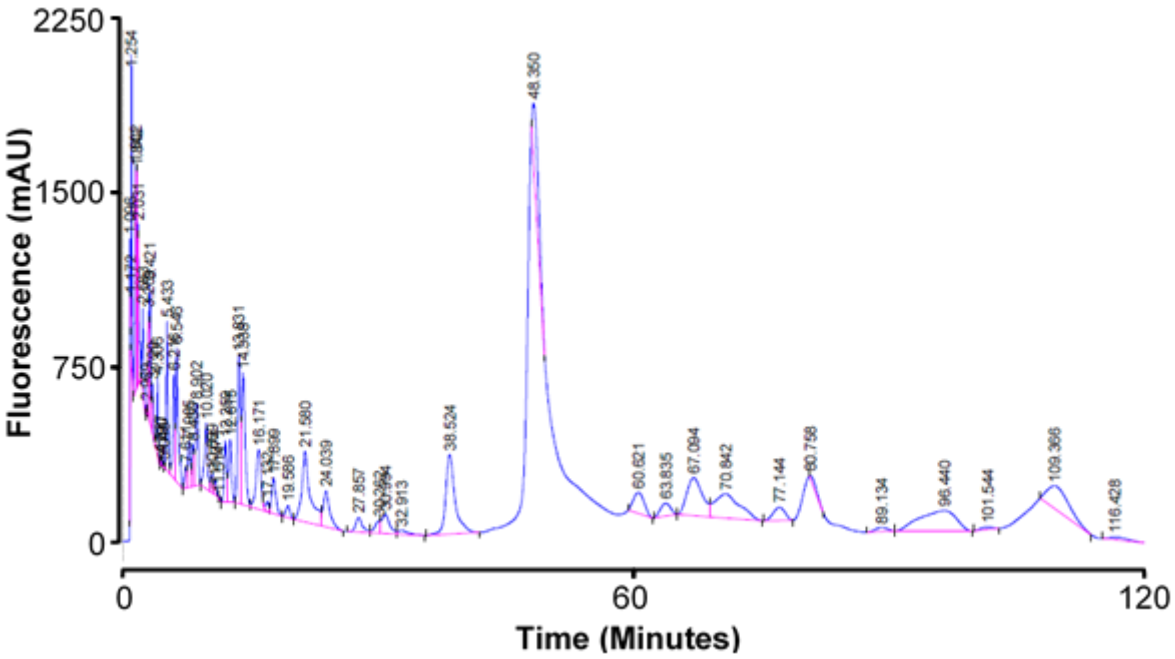

Figure 6-3. Isocratic high-performance liquid chromatography analysis of the *B. carterii* oleoresin methanolic extract.

An isocratic HPLC spectra generated following the triplicate injection of the methanolic extract of *B. carterii* oleoresin. The mobile phase used was composed of 70 % acetonitrile, 30 % dH_2O. A constant flow rate of 1 ml/min was used throughout the analysis. Sample injection volume of 50 µl of 25 mg/ml (25000 ppm) of *B. carterii* oleoresin methanolic extract.

However, a more powerful gradient HPLC approach was utilised for the remainder of the analysis.

6.2.2 Gradient HPLC

All equipment and sample preparation were conducted as described in section 2.8.

The gradient methodology was modified as described within the result section through the optimisation of the gradient method.

The method used for the gradient HPLC separations described in sections 6.3.2 and 6.3.3 were conducted as described in described in table 6-1.

Table 6-1. The gradient high-performance liquid chromatography method used for all analytical analysis.

A summary of the changes in mobile phase components and flow rate during the gradient high-performance liquid chromatography analysis of the *B. carterii* oleoresin.

Time (min)	Acetonitrile (%)	dH_2O (%)	Flow rate (ml/min)
0	50	50	0.8
3.00	50	50	0.8
6.00	95	5	1
15.00	95	5	1.2
56.00	95	5	1.2
59.30	50	50	0.8

For all gradient HPLC analyses performed the total run time of 60 minutes, with spectra generated at wavelengths of 205, 230, 250, 270, 290 and 310 nm. All spectra shown as figures are a wavelength of 205 nm. Following analysis, the sample analysed, and all solutions used were sent to the waste.

6.2.3 Ultra high-definition accurate-mass ESI quadrupole TOF HPLC-MS analysis of the *B. carterii* oleoresin methanolic extract.

All sample preparations, separations and Ultra high-definition accurate-mass ESI quadrupole TOF mass spectrometry analysis was conducted as described in section 2.9.

6.3 Results

Before the *B. carterii* oleoresin methanolic extract could be chemically characterised using mass spectrometry, the prerequisite separation by HPLC required optimisation.

6.3.1 Gradient high-performance liquid chromatography optimisation

Following the optimisation of mobile phase components and sample loading concentration using isocratic HPLC, the method was transitioned to a more powerful gradient HPLC method. The gradient HPLC approach allows a dynamic change of the mobile phase concentration and flow rate whilst the sample is being analysed. This potentially allows improved peak resolution and reduced total sample analysis times but requires optimisation to determine the ideal gradient for separating the compounds within both *B. carterii* oleoresin methanolic extract.

Initial optimisation of the method development procedure was conducted using the *B. carterii* oleoresin methanolic extract at a concentration of 12.5 mg/ml (12500 ppm). The initial injection of the *B. carterii* oleoresin methanolic extract was conducted under the following conditions; for the first 25 minutes the mobile phase increased in acetonitrile concentration from an initial 50 % to 95 %. During this period the flow rate was also increased over the course of 25 minutes from 0.8 ml/min to 1.2 ml/min. These conditions were maintained for a further 25 minutes. After a total analysis time of 50 minutes the concentration of the mobile phase was lowered to 50 % over the course of 7 minutes. These conditions were maintained for the final 3 minutes of the sample analysis. The results of this analysis are shown in figure 6-4.

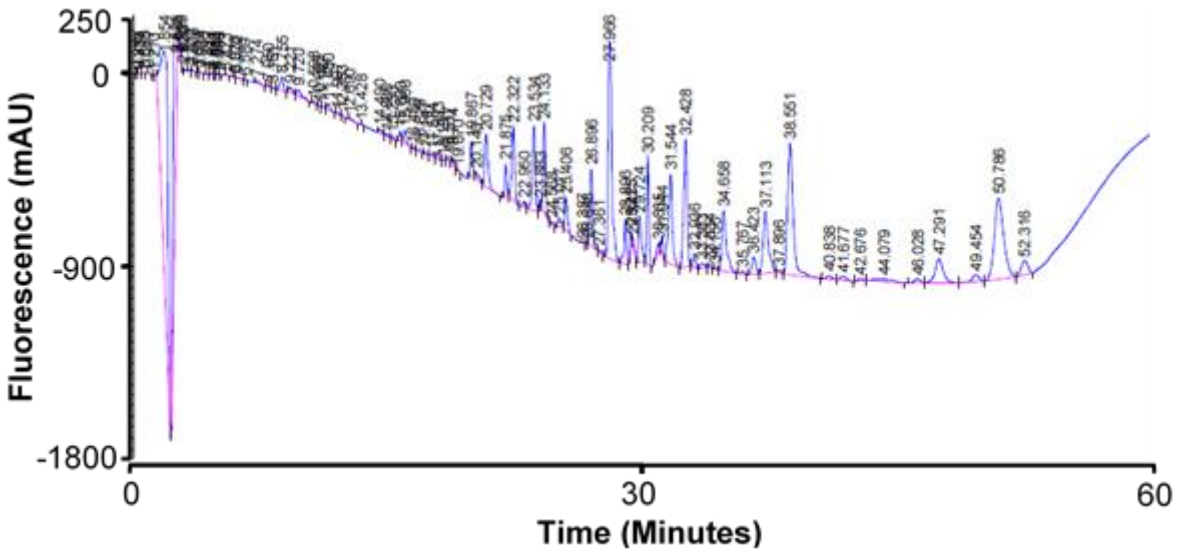

Figure 6-4. Initial injection of *B. carterii* oleoresin methanolic extract using a gradient HPLC method.

Gradient HPLC was performed using the method described in section 6.2.2. Sample injection volume of 20 µl of 12.5 mg/ml (12500 ppm) of *B. carterii* oleoresin methanolic extract was analysed at a UV detector wavelength of 205 nm for a total analysis time of 60 minutes.

The initial injection of the methanolic extract of the *B. carterii* oleoresin using a gradient HPLC method identified 97 peaks within the methanolic extract, substantially more than when using the isocratic HPLC method (shown in figure 6-3). Within the initial gradient HPLC spectrum, shown in figure 6-4, a key peak was found to elute at 27.966 minutes having the greatest abundance within the sample, accounting for 9.1439 % of the total sample area. Other peaks such as those at 32.428, 38.551 and 50.786 were found to abundant within the sample, with abundances of 4.8579 %, 8.3947 % and 8.4851 % respectively.

Based on the complete elution time of the sample using the initial gradient HPLC method taking 52.316 minutes, further modifications to the gradient method and mobile phase composition were performed to further reduce analysis time and improve peak resolution.

The subsequent injection of the methanolic extract of the *B. carterii* oleoresin was conducted under modified conditions; 50 % acetonitrile for 5 minutes at 0.8 ml/min, after 5 minutes the concentration was increased to 95 % over 20 minutes at a constant flow rate of 0.8 ml/min. This mobile phase concentration and flow rate was then held for a further 25 minutes before being lowered over 7 minutes to 50 % at a flow rate of

1.2 ml/min. This was then held for the final three minutes of the analysis. The HPLC spectra generated following modification to the gradient method is shown in figure 6-5.

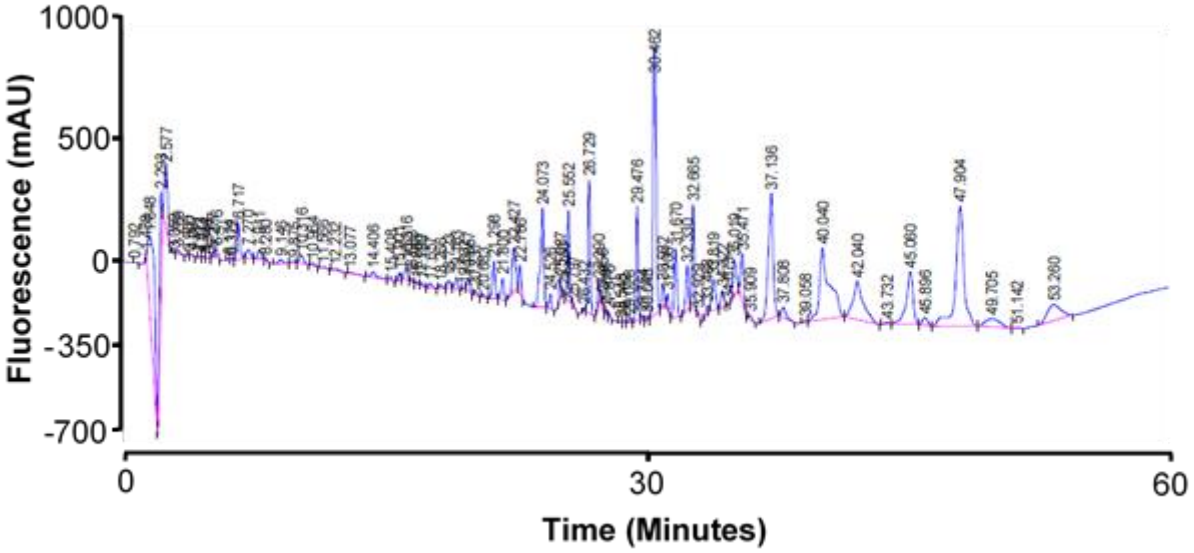

Figure 6-5. The second method development injection of *B. carterii* oleoresin methanolic extract using a modified gradient HPLC method.

Gradient HPLC was performed using the method described in section 6.2.2. Sample injection volume of 20 µl of 12.5 mg/ml (12500 ppm) of *B. carterii* oleoresin methanolic extract was analysed at a UV detector wavelength of 205 nm for a total analysis time of 60 minutes.

This change in methodology increase the speed at which all compounds eluted off the column by 2 minutes compared to that of the previous method used. However, further modification to the method could decrease the time for compounds to elute off the column and increase peak resolution.

Further development of the method was conducted under the following conditions; 50 % acetonitrile at a flow rate of 0.8 ml/min for the initial 3 minutes. This was then increased to 95 % over the course of 7 minutes, this was then held at this concentration for 40 minutes. After 40 minutes, the concentration was decreased to 50 % over 5 minutes at a flow rate of 1.2 ml/min and was held for the final 5 minutes of the analysis. The spectra generated as a result of this change to the gradient method are shown in figure 6-6.

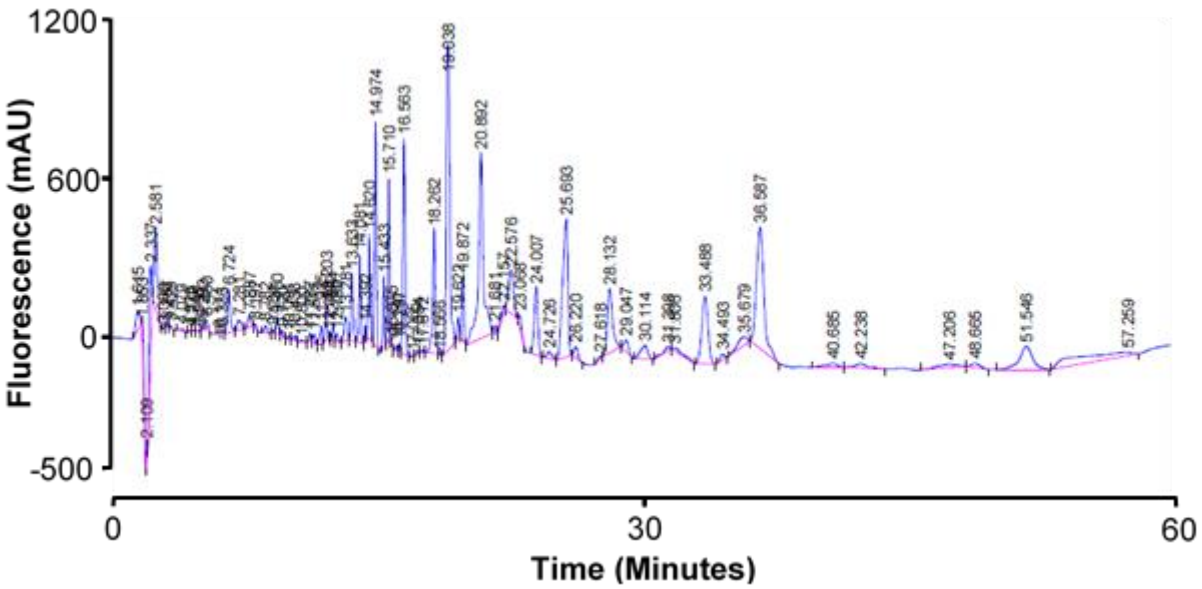

Figure 6-6. The third method development injection of *B. carterii* oleoresin methanolic extract using a modified gradient HPLC method.

Gradient HPLC was performed using the method described in section 6.2.2. Sample injection volume of 20 µl of 12.5 mg/ml (12500 ppm) of *B. carterii* oleoresin methanolic extract was analysed at a UV detector wavelength of 205 nm for a total analysis time of 60 minutes.

These modifications to the gradient HPLC method resulted in a 11-minute decrease in peak retention of compounds eluting off the HPLC column after 10 minutes. All peaks found after 36.587 minutes were found in the blank and therefore excluded. This resulted in a complete elution time of less than 40 minutes.

Additional method development was conducted using the following method; 50 % acetonitrile at a flow rate of 0.8 ml/min for 3 minutes. This was then increased to 95 % over the course of 3 minutes. This concentration was used at an increased flow rate of 1.0 ml/min for 9 minutes before being further increased to 1.2 ml/min for the next 41 minutes. The mobile phase concentration was then lowered to 50 % over the course of 40 seconds and held at this concentration and flow rate for the remainder of the analysis. The results of this method are shown in figure 6-7.

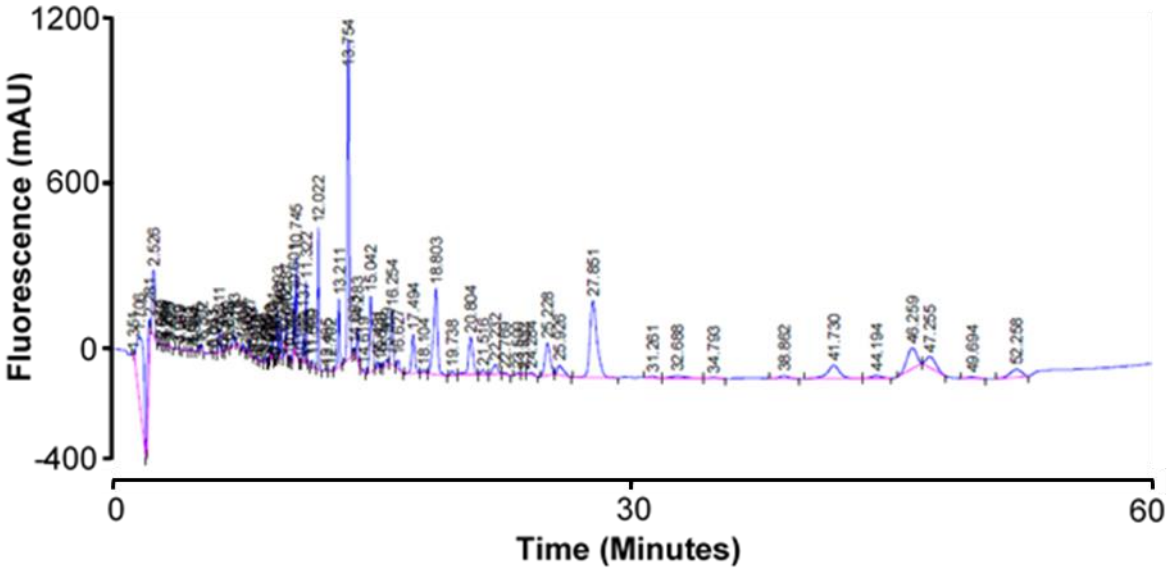

Figure 6-7. The fourth method development injection of *B. carterii* oleoresin methanolic extract using a further modified gradient HPLC method.

Gradient HPLC was performed using the method described in section 6.2.2. Sample injection volume of 20 µl of 12.5 mg/ml (12500 ppm) of *B. carterii* oleoresin methanolic extract was analysed at a UV detector wavelength of 205 nm for a total analysis time of 60 minutes.

This change in HPLC methodology resulted in a further decrease in retention time, whilst maintaining the resolution between individual peaks. This methodological change resulted in an 8-minute decrease in retention time compared to the previous method with the final peak eluting off the column at 27.851 minutes. With peaks identified after 27.851 minutes being found in the blank and therefore excluded. Following these optimisation experiments, this method will be used for future analysis and separation of compounds within both the *B. carterii* oleoresin methanolic extract.

Following the completion of gradient HPLC method optimisation the following method, summarised in table 6-2, was utilised for all further gradient HPLC analysis.

Table 6-2. The gradient HPLC method developed to separate the chemical constituents of the *B. carterii* oleoresin methanolic extract.

Time (min)	AcN (%)	Water (%)	Flow rate (ml/min)
0	50	50	0.8
3.00	50	50	0.8
6.00	95	5	1
15.00	95	5	1.2
56.00	95	5	1.2
59.30	50	50	0.8

6.3.2 Gradient HPLC separation for mass spectrometry analysis

Method development identified the gradient HPLC method described in table 6-2, as the ideal method for separating the *B. carterii* oleoresin into its chemical components Using this method, separations of the methanolic extracts of *B. carterii* oleoresin are shown in figure 6-8.

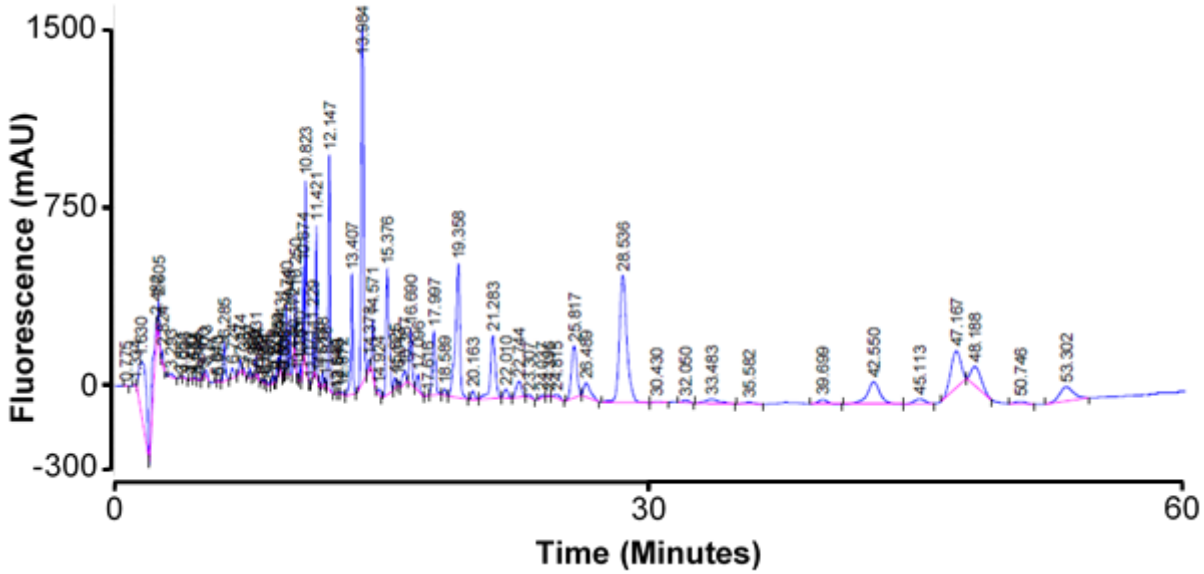

Figure 6-8. A gradient HPLC spectra of the *B. carterii* oleoresin methanolic extract.

A gradient HPLC spectra of the *B. carterii* oleoresin methanolic extract following the removal of the solvent blank. Gradient HPLC was performed using the method described in section 6.2.2. The sample was analysed using the optimised gradient HPLC method, described in table 6-2. Sample injection volume of 20 µl of 12.5 mg/ml (12500 ppm) of *B. carterii* oleoresin methanolic extract at a UV detector wavelength of 205 nm for a total analysis time of 60 minutes.

Separation of the *B. carterii* oleoresin methanolic extract, shown in figure 6-8, was found to contain a total of 86 peaks after the exclusion of the blank. Based on the percentage area of each peak, numerous peaks were identified as being highly abundant within the *B. carterii* oleoresin methanolic extract. These peaks included those found to elute after 10.823, 11.421 and 12.147 minutes, which were found to have areas of 3.7075 %, 2.2232 % and 4.5195 % respectively. Additionally, further peaks found at timepoints of 13.407, 13.984, 15.376 and 19.358 minutes were also found to account for a significant proportion of the sample. With these peaks accounting for 2.9917 %, 11.89661 %, 4.7561 % and 7.4114 % respectively.

Further peaks were also identified which accounted for substantial abundance within the oleoresin methanolic extract. Peaks identified included those at 21.283, 28.536 and 48.167 minutes. These peaks were found to account for 3.7675 %, 11.5607 % and 4.5097 % of the total sample, based on the area of the peak.

6.3.2 The effect of formic acid on HPLC separation

To analyse the separated *B. carterii* oleoresin methanolic extract (fig 6-8) using mass spec required the addition of ionisation additives which enhance ionisation thus mass spectral (not HPLC) signal intensity. The additive selected was formic acid, which was added to the optimised acetonitrile and water mobile phases (see table 6-2) to achieve a final concentration of 0.1 % in both.

To control for the addition of 0.1 % formic acid to the mobile phases, the *B. carterii* oleoresin methanol extract was re-analysed with the inclusion of 0.1 % formic acid as shown in figure 6-9.

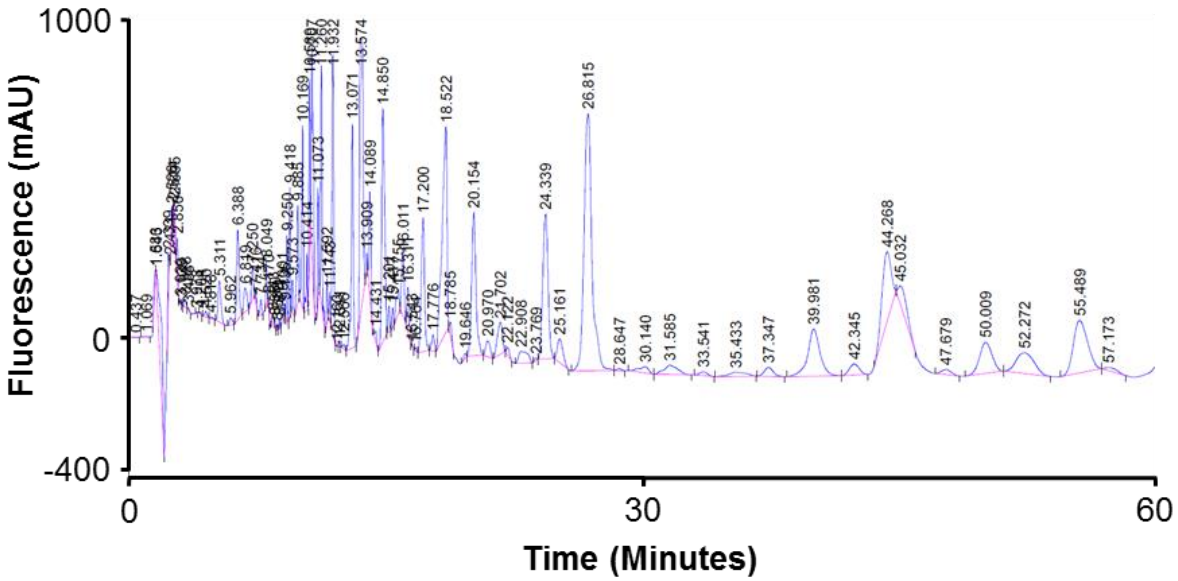

Figure 6-9. The effect of the addition of 0.1 % v/v formic acid on the HPLC separation of compounds in the *B. carterii* oleoresin methanolic extract.

The effect of the addition of formic acid was evaluated for analysis of the *B. carterii* oleoresin methanolic extract. Gradient HPLC was performed using the method described in section 6.2.2. Both extracts were analysed using the method described in table 6-2 with a mobile phase of acetonitrile + 0.1 % v/v formic acid and distilled water + 0.1 % v/v formic acid. Sample injection volume of 20 µl of 12.5 mg/ml (12500 ppm) of *B. carterii* oleoresin methanolic extract at a UV detector wavelength of 205 nm for a total analysis time of 60 minutes.

By comparing fig 6-8 with 6-9, it is clear that addition of 0.1 % formic did not alter the position of peaks (i.e. retention times) within the spectra following the addition of 0.1 % formic acid to the mobile phase. However, the amplitude of certain peaks was altered. For example, the amplitude of the peak at 27.089 minutes, was increased from 230 mAU to 610 mAU. However, the amplitude of peaks at 12.017 and 13.747 minutes were decreased. While the amplitude of peaks within HPLC spectra can be used to estimate abundance, here this is achieved more definitively by subsequent mass spec analysis. Analysis by mass spec is only influenced by peak position which was unaltered. As such, the effect on amplitude is of no concern.

6.3.3 Chemical characterisation of the *B. carterii* oleoresin extract using HPLC-MS.

Chemical characterisation of the *B. carterii* oleoresin methanolic extract was conducted using the method described in section 2.9. Separation of the *B. carterii* oleoresin methanolic extract was conducted using the method optimised within sections 6.3.1.

Following separation by HPLC (shown in figure 6-9), the components were transferred to a mass spectrometer for ionisation and determination of each components molecular weight. The number of ions generated at each timepoint in both positive and negative ionisation modes following the injection of the methanolic extract of the *B. carterii* oleoresin was visualised through the form of total ion chromatograms in both positive and negative ionisation modes shown in figure 6-10A and 6-10B respectively.

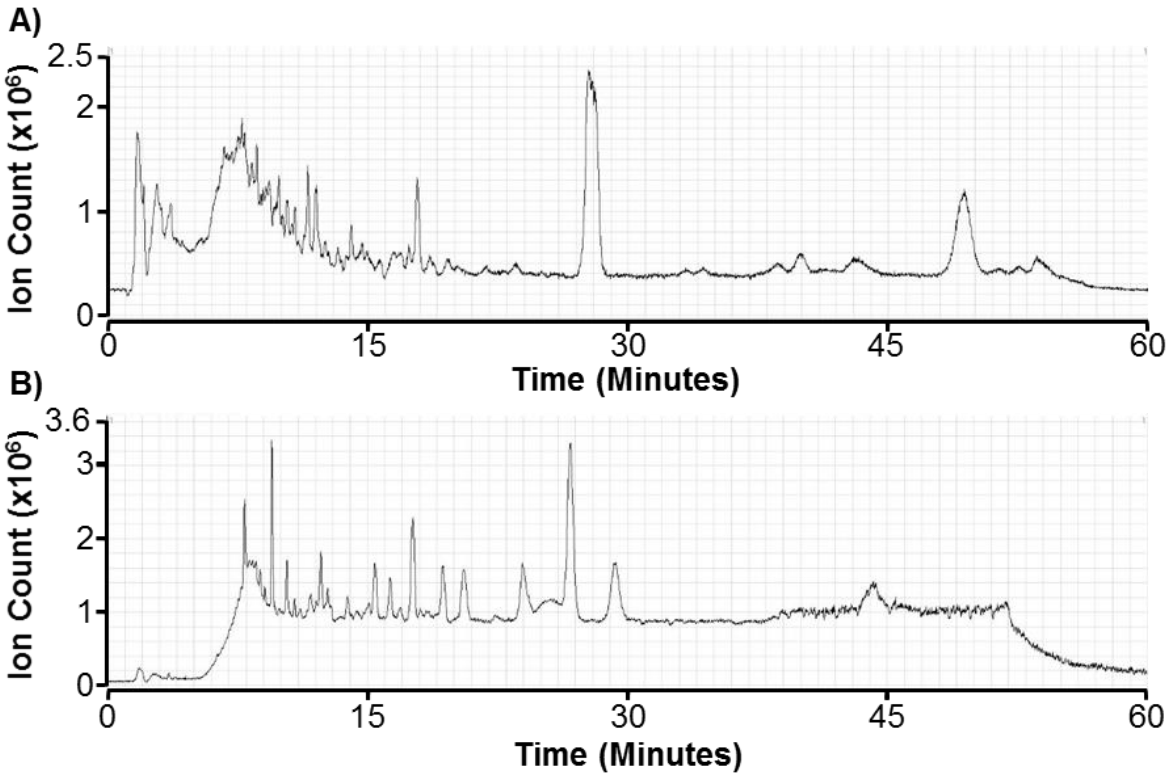

Figure 6-10. Total ion chromatograms of the methanolic extract of *B. carterii* oleoresin.

High-resolution mass spectrometry was conducted using the method described in section 2.9, following separation by HPLC, as described in section 2.8 and 6.2.2. Total ion chromatograms for the methanolic extract of the *B. carterii* oleoresin were generated in both **A)** positive ionisation and **B)** negative ionisation modes. Both spectra have been corrected using mass spectrometry analysis of the dissolution solvent alone. Sample was injected at a concentration of 0.2 mg/ml (200 ppm) at a volume of 20 µl per injection. Mass spectrometry was conducted for a total run time of 60 minutes for both ionisation modes.

Following the generation of total ion chromatograms, each was aligned to the associated HPLC spectra, and the spectra probed at identified timepoints to determine the molecular formulae associated with those HPLC peaks.

Within the *B. carterii* oleoresin methanolic extract, a total of 570 potential compounds were identified. Of these, 281 potential compound formulae were identified following positive ionisation mass spectrometry, shown in appendix 1, whilst 289 potential compound formulae were identified following negative ionisation mass spectrometry, shown in appendix 2.

Of these 570 compounds identified within the *B. carterii* oleoresin methanolic extract, several key compounds were identified; those previously described to be present in the oleoresins of the *Boswellia* genus. These compounds include multiple isoforms of boswellic acid, which have been described to be the biologically active compound within *Boswellia* oleoresins.

Within the *B. carterii* oleoresin, four isoforms of the boswellic acids were identified based on the molecule mass and the difference between the theoretical and actual molecular weights observed. The boswellic acid isoforms identified within the *B. carterii* oleoresin methanolic extract were 3-acetyl-11-keto-β-boswellic acid, 3-*O*-acetyl-α-boswellic acid, 11-keto-β-boswellic acid and α or β-boswellic acid.

3-acetyl-11-keto-β-boswellic acid was identified to have a retention time of 11.074 minutes with an identified m/z of 513.3566 $[M+H]^+$. This was found to be a difference of 1.66 ppm compared to the theoretical ion mass of 513.3575. Following the removal of the H+ ion, the compound molecular weight of 512.3502 and a molecule formula of C32 H48 O5 was identified.

3-*O*-acetyl-β-boswellic acid was identified to have a retention time of 1.074 and 15.749 minutes with an identified m/z of 499.3779 and 499.3795 $[M+H]^+$. This was found to be a difference of 0.57 and -2.64 ppm compared to the theoretical ion mass of 499.3782. Following the removal of the H^+ ion, the compound molecular weight of 498.3709 and a molecular formula of C32 H50 O4 was identified.

11-keto-β-boswellic acid was identified to have a retention time of 7.730 minutes with an identified m/z of 471.3492 $[M+H]^+$. This was found to be a difference of -4.92 ppm compared to the theoretical ion mass of 471.3469. Following the removal of the H+ ion, the compound molecular weight of 470.3396 and a molecular formula of C30 H46 O4 was identified.

α or β-boswellic acid was identified to have a retention time of 16.015 minutes with an identified m/z of 457.3669 $[M+H]^+$. This was found to be a difference of 1.58 ppm compared to the theoretical ion mass of 457.3676. Following the removal of the H+ ion, the compound molecular weight of 456.3603 and a molecular formula of C30 H48 O3 was identified.

Of all other compounds identified as within the *B. carterii* oleoresin, comparisons with mass spectrometry databases and further chemical characterisation techniques are required to determine the specific compounds and molecular formulae associated with each molecule.

6.4 Discussion

6.4.1 Method development for chemical separation of the *B. carterii* oleoresin methanolic extract.

Before the chemical composition of *B. carterii* oleoresin methanolic extract could be analysed the chemical constituents required separation. This required optimisation of a high-performance liquid chromatography methodology; namely the type of HPLC conducted, the mobile phase constituents and optimisation of the running conditions used.

Optimisation of the HPLC mobile phase was initially conducted using an isocratic HPLC approach (data not shown). The main constituents of the mobile phase selected were acetonitrile and methanol, due to their common use in separating plant extracts (Celeghini, Vilegas, & Lanças, 2001; Seo *et al.*, 2016). The findings of this study show that a mobile phase composed of acetonitrile was found to provide the best resolution and separation of compounds in the *B. carterii* oleoresin methanolic extract compared to that of a methanol based mobile phase. Additionally, it was identified that the use of an acetonitrile based mobile phase over methanol significantly decreased the column backpressure when conducting HPLC analysis.

Similar effects on backpressure were reported in Snyder, Kirkland, and Glajch (2012) and result from the decreased viscosity of acetonitrile (0.00036 Pa*s) compared to methanol (0.00055 Pa*s) (Agrahari, Bajpai, & Nanda, 2013; Snyder *et al.*, 2012). Decreased pressure offers multiple advantages including; the ability to utilise higher flow rates, to decrease the elution time of compounds off the column, to allow higher concentrations of sample to be injected without increasing the pressure to dangerous levels, and to produce narrower and sharper chromatographic peaks (Agrahari *et al.*, 2013; Technologies, 2016). These findings further support the decision to use a acetonitrile-based mobile phase for further analysis of the *B. carterii* oleoresin methanolic extract.

Though convenient for fundamental optimisation of mobile phase composition, isocratic HPLC has limitations. As such, the next experiment aimed to determine if a gradient HPLC approach would decrease elution time and peak resolution compares to an isocratic method. The findings of section 6.3.1 show that a transition to the use of gradient HPLC (without any additional modification of parameters) was found to

significantly decrease the time required for all compounds to elute off the column (figure 6-4). Overall run time was cut by 50 % when transferred to a gradient method compared to the isocratic method shown in figure 6-3.

Further to increased speed, another advantage of using gradient HPLC is that software can be used to dynamically fine tune the composition of the mobile phase in increments as low as 0.1 %. This allows for optimisation without the need to prepare set mobile phase concentrations, making the process more efficient and economical. Additionally, the flow rate of the mobile phase through the column can be modified during analysis, allowing dynamic control of retention time. For example, compounds with longer retention times to potentially be sped up, via the increase of the flow rate or mobile phase concentrations. The modification of these factors has been shown by Cabo-Calvet, Ortiz-Bolsico, Baeza-Baeza, and García-Alvarez-Coque (2014), to have a significant impact on the retention times of standard compounds. The showed that an increase in mobile phase solvent composition and an increase in flow rate significantly decreased the retention time.

Crucially, the decreased column retention time permitted by gradient HPLC method allows for sharper, higher resolution peaks on output spectra, facilitating accurate compound identification. This is validated by Schellinger and Carr (2006), who compared equivalent spectra produced using isocratic and gradient HPLC. They found that the use of a gradient HPLC method not only decreased retention time of the majority of compounds in the mixture but also significantly decreased peak width, thus increasing resolution. This increased resolution is critical for the discrimination of individual compounds in complex mixtures. These findings are further supported by the increase in the number of peaks observed when changing from an isocratic to a gradient HPLC approach, in addition to further optimisation of the gradient method.

This is especially important when analysing unknown complex mixtures, such as those extracted from plant extracts. Here, low abundancy peaks may be important active chemical constituents, however at low resolution, they may be masked by high abundancy inactive constituents. Therefore, increasing the peak resolution not only facilitates compound discrimination, but also allows a more complete representation of the chemical composition of the whole extract.

The findings of this study and those of previous work have shown that gradient HPLC offers numerous benefits over isocratic HPLC, specifically increased peak resolution and quicker compound elution. Further to this, optimisation of gradient HPLC resulted in an efficient and reproducible method of producing a chemical fingerprinting of the *B. carterii* oleoresin methanolic extract which could be utilised for further chemical characterisation.

6.4.2 Chemical characterisation of the *B. carterii* oleoresin methanolic extract.

Following optimisation of the gradient HPLC method, certain separated compounds within methanolic extracts of *B. carterii* oleoresin, were identified using mass spectrometry.

Mass spectrometry identified 570 potential compounds within the 86 peaks produced by HPLC. Of these, 281 required use of positive ionisation, and 289 required use of negative ionisation mode for identification. This gave an average of 6.63 potential compound identifications per HPLC peak across both ionisation modes. The compound identifications were then screened for the presence of previously described biologically active boswellic acids known to be present in *Boswellia* oleoresins. This was achieved by cross reference to a standard database based on matching molecular formulae within the mass spectral data generated to known molecular masses of each boswellic acid isoform.

B. carterii oleoresin methanolic extract was found to contain; 3-acetyl-11-keto-β-boswellic acid, 3-*O*-acetyl-β-boswellic acid, 11-keto-β-boswellic acid and α or β-boswellic acid. However, at this stage not possible to discriminate between α and β isoforms. These findings describe for the first time that the oleoresins of *B. carterii* contain boswellic acids, as well as identifying the isoforms present within this species.

These findings have implications regarding the anti-cancer activity of the *B. carterii* oleoresin, as boswellic acids have been previously described to be potent anti-cancer agents both *in vitro* and *in vivo* (Al-Harrasi, Hussain, Csuk, & Khan, 2018; Lv *et al.*, 2020; Roy *et al.*, 2019; Wang *et al.*, 2020). Despite identifying multiple boswellic acid isoforms within the *B. carterii* oleoresin, it cannot be ruled out that other compounds within the complex milieu of the oleoresin extract also possess biological activity. Therefore, further characterisation of the *B. carterii* oleoresin is required to determine if it is solely their boswellic acid content, which possesses anti-cancer activity or if other

currently uncharacterised compounds are also biologically active and therefore novel chemotherapeutic agents.

These findings may also have wider scope as research on other species has focussed on characterisation of essential oil rather than whole oleoresin. This is likely due to these being the most commercially important components of *Boswellia* oleoresins. Studies have shown nearly all *Boswellia* derived essential oils share similar chemical components; namely the presence of α-pinene, α-thujene, limonene, myrcene, α-terpineol, β-pinene and β-thujene (DeCarlo *et al.*, 2019; Gupta *et al.*, 2017; Johnson *et al.*, 2019; Van Vuuren *et al.*, 2010; Woolley *et al.*, 2012). However, the relative abundances of each of these compounds differs between species, giving the essential oils unique chemical profiles, allowing them to be differentiated from one another. These variations in the essential oil of the *Boswellia* genus has been shown to vary significantly dependent on the region, climate and growth conditions from which the oleoresins they are derived from were extracted (DeCarlo *et al.*, 2018). This variation in the chemical profile of the essential oil further supports the idea that the composition and boswellic acid content of the *B. carterii* oleoresin may be different to that previously described in literature.

Further to this, the chemical profile generated during this study identified substantially more compounds than those previously described to be present in the oleoresins of the *Boswellia* genus. A review by Roy *et al.* (2019), which aimed to summarise many of the key compounds present in *Boswellia* oleoresins reported the presence of multiple boswellic acid isoforms, namely; α and β-boswellic acids, acetylated α and β-boswellic acids, 11-keto-β-boswellic acid, and 3-O-acetyl-11-keto-β-boswellic acid. In addition to 3α,24-dihydroxyurs-12-ene, 3α,24-dihydroxyolean-12-ene, α-thujene, serratol, tirucall-8,24-dien-21-oic acids, oilbanumols D-G, α-pinene, and octyl acetate (Buchele et al., 2006; Roy et al., 2019; Siddiqui, 2011a).

However, these previously reported compounds do not account for the total number of compounds identified within the oleoresin methanolic extract used in this study. This therefore shows that a significant proportion of the oleoresin of all *Boswellia* species has yet to be chemically characterised. Additionally, the process of drying the extract to a powder, using rotary evaporation, subjects the extract to both increased temperatures and vacuum, which may result in the loss of volatile compounds such as

those commonly extracted within the essential oil. This would potentially result in a further decrease in the number of compounds present within the oleoresin extract used in this study, however further analysis is required to confirm this. The findings of this study and the limited characterisation of the *Boswellia* genus as a whole further supports the need for additional characterisation, to identify the components within the oleoresin and provide a complete chemical profile of the *B. carterii* oleoresin.

Despite identifying the presence of multiple boswellic acid isoforms within the *B. carterii* oleoresin methanolic extract, a lack of known analytical standards for other boswellic acid isoforms prevent the complete characterisation of the boswellic acid content of *B. carterii* oleoresins. This lack of analytical standards prevents; (1) the generation of conformational mass spectra for each isoform, (2) the identification of the retention time of each boswellic acid isoform using the optimised gradient method and (3) the quantification of the amount of each boswellic acid isoform within the methanolic extract. This was not conducted due to the significant financial implications of purchasing the high purity analytical standards for each boswellic acid isoform, however, if the study was to be continued, the use of analytical standards would substantially enhance the understanding of the boswellic acid content within the *B. carterii* oleoresin.

6.4.3 Conclusions

Overall, this analysis identified that the *B. carterii* oleoresin was found to contain multiple boswellic acid isoforms including: 3-acetyl-11-keto-β-boswellic acid, 3-*O*-acetyl-β-boswellic acid, 11-keto-β-boswellic acid and α or β-boswellic acid. However, confirmatory studies and further chemical analysis are now required to determine the identity of the remainder of compounds within the *B. carterii* oleoresin and to ascertain if these compounds are biologically active.

Chapter 7

General Discussion

7.1 Considerations for the extraction of *Boswellia* oleoresins

An effective extraction method must (1) provide confidence that all biologically active compounds are solubilised and (2) produce a yield that is practically useful. Many factors, such as starting material, time and solvent used will influence the extraction so must be optimised.

Initially, this study examined five different solvent-based extraction methods to ascertain their effectiveness at extracting compounds from the *B. carterii* oleoresin. This study found that the alcoholic solvents ethanol, methanol and propan-2-ol extraction solvents extracted significantly more compounds than the acetonitrile and dH_2O-based methods (figure 3-1).

Individual studies have previously examined the yield of compounds isolated from *Boswellia* oleoresins (Greve *et al.*, 2017; Zhang *et al.*, 2016). However, no study to date has directly compared the extraction efficiency of multiple methods under equivalent conditions. This is an important oversight as studies cannot be sure which extraction method is best and whether extraction methods have missed key biologically active compounds. Therefore, this study is the first to directly compare the effects of different solvents on extract yield using *B. carterii* as a case study. This would also optimise the extraction of *B. carterii* for subsequent experiments designed to probe the biological effects of this species specifically.

The extraction yield of the *B. carterii* oleoresin using all methods was found to range between 8.1 - 54.9 %, with the maximal yield recovered using a methanolic extraction method. These findings disagree with those of Zhang *et al.* (2016) and Yang, Ren, *et al.* (2018) whom both utilised polar solvent extractions and recovered yields of 71.5 and 72.0 % respectively. Despite finding a lower yield from all extraction methods examined, it is hypothesised that the oleoresins of the same species from different geographical and environmental conditions may have a significant impact on the overall chemical composition. This indicates the extraction yield could vary wildly between batches, dependent of the conditions the oleoresins were derived from. This also highlights, the need for further evaluation of the extraction yield from different environments to better understand how environmental factors impact the chemistry of *Boswellia* oleoresins.

While an acceptable total yield is important for practical applications, its importance is perhaps secondary to ensuring all biologically active compounds are solubilised by a given extraction. A lower yield (that remains practically suitable) that contains all biologically active compounds is favourable to a higher yield that may not. As such, the fundamental cytotoxicity of *B. carterii* oleoresin extracts were compared using two typical cancer types to provide a proxy indication of active compound content.

Four out of the five of the *B. carterii* oleoresin solvent extraction methods were found to induce cytotoxic effects against both CML and hepatocellular carcinoma, as shown in figures 3-2 and 3-3. The methanolic extract was found to be the most potent of all methods examined with IC_{50} values of 52.2 ± 5.5 and 54.8 ± 5.3 µg/ml against the CML and hepatocellular carcinoma cell lines respectively. The cytotoxicity of the other solvent extracts of *B. carterii* oleoresin, which showed cytotoxic activity *in vitro* to range between 81.4 and 97.5 µg/ml dependent on the extraction method and the cancer type examined. Of all extraction methods examined only the dH_2O extract was found to possess no cytotoxic effect against CML and hepatocellular carcinoma cells at the maximal concentration examined.

Despite previous research highlighting the methanolic extract of *Boswellia* oleoresins to possess cytotoxic activity (Ranjbarnejad *et al.*, 2017; Yazdanpanahi *et al.*, 2014), limited research has examined the cytotoxic activity of the alternative extraction methods (Alipanah & Zareian, 2018).

Comparisons within this study confirmed that the methanolic extract of the *B. carterii* oleoresin possessed the most potent cytotoxic activity of all extraction methods examined. This corroborates the findings of previous studies who utilised a methanolic extraction to evaluate the effects of the *Boswellia* oleoresins (Alipanah & Zareian, 2018; Ranjbarnejad *et al.*, 2017; Yazdanpanahi *et al.*, 2014). Whilst it cannot be ruled out that there may be some heterogeneity in the exact chemical composition across all the *B. carterii* extracts examined. Based on the findings of section 3.3, it can be determined that the methanolic extraction of *B. carterii* oleoresin exclusively extracts a compound or compounds with potent anti-cancer activity, based on the significantly enhanced cytotoxic activity compared to other extraction methods utilised.

Whilst previous studies have shown that a methanolic extraction of *Boswellia* oleoresins extracts cytotoxic compounds, this study provides evidence that this is also

true for the oleoresins of *B. carterii*. However, this study expands on those previously conducted, as it is the first of its kind to examine the effects of multiple solvent extracts on the cytotoxic activity of *Boswellia* oleoresins. In addition, this study is the first to confirm that the methanolic extract of the *B. carterii* oleoresin is the most potent extraction method when a comparative analysis of multiple extraction solvents was conducted.

7.2 The anti-cancer activity of *B. carterii* oleoresin, and its mechanisms of action

7.2.1 The wider anti-cancer activity of the *B. carterii* oleoresin

This study found that the *B. carterii* oleoresin methanolic extract induced time (figures 4-2 and 4-3) and concentration (figures 4-4 and 4-5) dependent cytotoxicity against multiple cancer types *in vitro*. The relative degree of cytotoxicity was found to vary considerably according to the cancer type. Indeed, IC_{50} values ranged between 33.34 and 106.34 µg/ml, as summarised in table 7-1.

Table 7-1. The cytotoxicity of the *B. carterii* oleoresin against multiple cancer and non-cancer cell types.

Cell line	Cancer type	Cancer nature	IC_{50} value (µg/ml)
A549	Lung carcinoma	Epithelial	93.92
A-204	Rhabdomyosarcoma	Epithelial	35.67
BEAS-2B	Non-cancer	Epithelial	173.92
CCRF-CEM	ALL	Suspension	38.71
HCT-116	Colorectal carcinoma	Epithelial	78.33
HEP G2	Hepatocellular carcinoma	Epithelial	59.25
K562	CML	Suspension	52.08
MCF-7	Breast cancer	Epithelial	88.33
MOLT-4	ALL	Suspension	33.83
PANC-1	Pancreatic cancer	Epithelial	106.34
PBMC's	Non-cancer	Suspension	90.75

Of all cancer types examined as a part of this study, the *B. carterii* oleoresin extract was found on average to be more potent towards leukaemia cells compared to the epithelial cancer types examined.

The findings of this study corroborate and further expand on the previous literature (Alipanah & Zareian, 2018; Jaafari-Ashkavandi *et al.*, 2017; Ranjbarnejad *et al.*, 2017; Xia *et al.*, 2017), by showing that the oleoresins of the *Boswellia* genus possess cytotoxicity against a wide range of cancer cell types. In addition, this study expands on this previous literature by describing for the first time the cytotoxic activity of the *Boswellia* genus against previously uncharacterised cancer cell types. This study also describes for the first time the heterogenicity of the cytotoxic activity induced by the *B. carterii* oleoresin methanolic extract.

These findings indicate that the *B. carterii* oleoresin methanolic extract does not target a specific cellular pathway which is exclusive to a specific cancer type, such as that of tyrosine kinase inhibitors which specifically target the BCR-ABL tyrosine kinase produced within CML (Druker *et al.*, 2006). Rather the *B. carterii* oleoresin methanolic extract acts via a mechanism which is conserved throughout the majority of cancer cell types. This board spectrum effect may simply arise from some fundamental, indiscriminate and non-cancer specific cytotoxic mechanism which would limit the therapeutic potential considerably. However, the heterogeneity of potency observed across the cell lines studied suggest this is not the case and a conserved, but cancer specific mechanism remains the target.

In further support of this, this study identified that the cytotoxicity was significantly greater against cancer cells than equivalent non-cancer cell types (figure 4-7). These findings are supported by those of Schmiech *et al.* (2019), who also found a significant difference between cancer and non-cancer cells following treatment with the *B. sacra* oleoresin. Interestingly, the IC_{50} observed against PBMC's in this study was 10 µg/ml higher than the concentration of extract found to produce the same effect in Schmiech *et al.* (2019). These findings indicate that the *B. carterii* oleoresin extract used for this study is less cytotoxic towards non-cancer cells than other *Boswellia* species and therefore suggests that fewer side effects may be observed if translated to an *in vivo* study.

This study's findings also corroborate the findings of Lv *et al.* (2020), who found purified AKBA to not induce a 50 % decrease in BEAS-2B viability at a concentration of 20 µg/ml. These findings support those of this study as AKBA has been described to be the most potent of the family of compounds, which have been described to be

responsible for the cytotoxic effects of the *Boswellia* genus (Roy *et al.*, 2019). Therefore, the similar pattern of effect observed following treatment with AKBA offers promise that the purification of any previously described chemotherapeutic agents within the oleoresin may result in minimal effects to non-cancerous tissues and cells.

To quantify the effect difference between cancer and equivalent normal cells, the selectivity of the *B. carterii* oleoresin methanolic extract was calculated (described in table 4-1). This study shows for the first time that *B. carterii* oleoresin methanolic extract is selective, with a selectivity index ranging between 1.75 - 2.68. Whilst this contradicts the findings of Peña-Morán *et al.* (2016) who demonstrated poor selectively. This disparity is likely due to the high diversity of compounds within the *B. carterii* oleoresin as described in section 6.3.4. This diversity of compounds may decrease the biological activity the active components within the oleoresin, through the presence of inert compounds within the extract masking those with biological activity. Therefore, the isolation of active compounds within the oleoresin may result both increased cytotoxicity and selectivity of the components derived from the *B. carterii* oleoresin methanolic extract.

7.2.2 The mechanism of cell death induced by the *B. carterii* oleoresin

B. carterii oleoresin methanolic extracts induced significant late apoptotic/secondary necrotic, but not necrotic cell death in all cancer cell types (shown in figures 5-3 - 5-7). These findings corroborate those of Jaafari-Ashkavandi *et al.* (2017), Ahmed *et al.* (2015), and Ranjbarnejad *et al.* (2017), which all found that the oleoresins of the *Boswellia* genus induced apoptotic cell death when examined by flow cytometry.

This study found confirmed that *B. carterii* oleoresin possesses apoptotic activity as a result of increased cleavage of caspases -3, -7 and -9 (as shown in figure 5-10), accompanied by increased PARP cleavage (figures 5-9). Based on these findings it can be hypothesised that the *B. carterii* oleoresin methanolic extract acts on the intrinsic pathway of apoptosis via the mechanism proposed in figure 7-1.

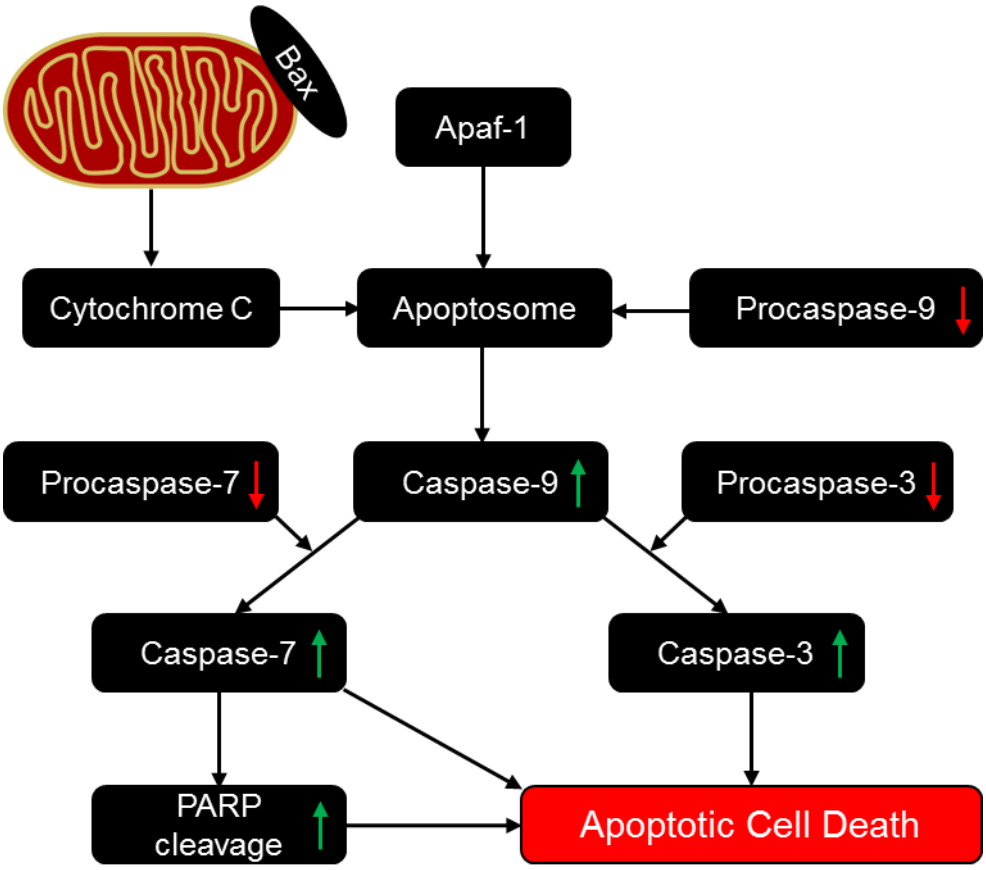

Figure 7-1. The proposed mechanism underpinning the pro-apoptotic activity of the *B. carterii* oleoresin methanolic extract.

The findings of this study corroborates and expand on the work of Ranjbarnejad *et al.* (2017) who observed an increase in caspase-3 cleavage in colorectal cancer cells following treatment with a methanolic extract of *B. serrata*; this study expands on this by observing increased caspase -7 and -9 cleavage, which further supports that the *B. carterii* oleoresin induces apoptosis via the intrinsic pathway of apoptosis (fully described in section 1.1.5.1).

Interestingly, the findings of Xia *et al.* (2005) and Lu *et al.* (2008), observed upregulation of DR4 and DR5 following treatment with purified boswellic acids, which indicates apoptosis via the extrinsic pathway (described in section 1.1.5.2). These boswellic acids have been shown to be the compounds responsible for the biological activity of the *Boswellia* oleoresins (Ammon, 2016; Roy *et al.*, 2019). However, this study showed the *B. carterii* oleoresin to induce apoptosis by the intrinsic pathway. It can be hypothesised that due to the diversity of compounds present within the oleoresin, multiple chemical components can act on the cell simultaneously via different mechanisms resulting in activation of apoptosis by both the intrinsic and

extrinsic pathway. Further examination is therefore required to ascertain if the chemical composition of the oleoresin underpins these observed differences in mechanism or if the *B. carterii* oleoresin methanolic extract used in this study acts on both the intrinsic and extrinsic pathways of apoptosis.

7.2.3 The effect of *B. carterii* oleoresin on the cancer cell cycle

The oleoresin of *B. carterii* induces an increase in the number of sub G_1 and G_1 cells in multiple cancer cell types (figures 5-11 - 5-15), when examined by flow cytometry. *B. carterii* oleoresin induced increases in the number of sub G_1 cells by between 67.31 and 829.31 % dependent on the cancer type evaluated, as shown in table 7-2. Further to this a significant increase in G_1 cells was observed in K562 and MOLT-4 cells. This increase in sub G_1 and G_1 cells was accompanied by a decrease in actively dividing S phase cells ranging between 25.7 and 68.8 % dependent on the cancer cell type examined as described in table 7-2. In all cancer cell types, no significant increase in the number of G_2/M cells were observed.

Table 7-2. The effect of the *B. carterii* oleoresin methanolic extract on cell cycle staging following treatment with the maximal concentration examined.

Cancer cell line	Increase in sub G_1 cells (%)	Change in G_1 (%)	Decrease in S phase (%)
K562	829.31	13.93	52.00
MOLT-4	304.95	0.49	68.80
HEP G2	67.31	-6.39	26.41
A549	111.49	-5.47	25.68
HCT-116	93.30	-8.23	39.59

Further to this, it was identified that the *B. carterii* oleoresin methanolic extract was more potent at inducing a G_1 cell cycle arrest at lower concentrations (25 and 50 µg/ml), before an increase in sub G_1 cells at the maximal concentration examined. This is likely due to the previously described cytotoxicity at this concentration. This study corroborates the previous studies by Ranjbarnejad *et al.* (2017) and Yazdanpanahi *et al.* (2014) have described the oleoresins of the *Boswellia* genus to induce sub G_1/G_1 cell cycle arrest against multiple cancer cell lines. Further to this, the findings of this study also corroborate the findings observed following treatment with both the *Boswellia* essential oil (Ni *et al.*, 2012) and purified boswellic acids (Takahashi *et al.*,

2012; Yuan *et al.*, 2008). These studies also found a significant increase the abundance of sub G_1 and G_1 cells, accompanied by a decrease in S phase cells as observed in this study.

Molecular analysis conducted corroborated these findings, with protein expression studies identifying that treatment with the *B. carterii* oleoresin methanolic extract decreased the expression CDK's 2, 4 and 6, accompanied by decreased cyclin D3 expression (figures 5-16 and 5-17). This study also showed that the CDK inhibitor p27 appears to be increased at lower concentrations of the *B. carterii* oleoresin, however, this effect was lost at the maximal concentration examined and therefore cannot be confirmed to be the cause of the observed G_1 cell cycle arrest. These findings indicate that the potential mechanism underpinning the G_1 cell cycle arrest observed is that which is suggested in figure 7-2.

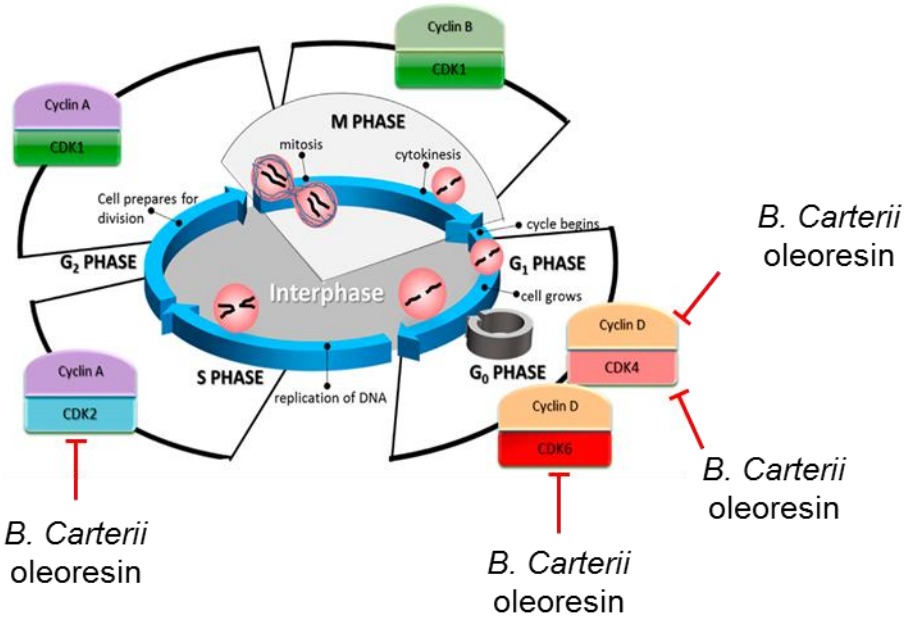

Figure 7-2. The proposed mechanism of action underpinning the cell cycle arrest observed following treatment with the *B. carterii* oleoresin.

The loss of p27 expression at the highest concentration examined may result from the cytotoxic activity of this high concentration and the relatively chronic exposure time used in this study leading to the degradation of the protein. Sheaff, Groudine, Gordon, Roberts, and Clurman (1997) showed that the activation of p27 was found to increase rapidly (less than 30 minutes) following the development of cyclin E/CDK2 complexes. This further supports the need to examine more acute exposure times to determine if p27 is responsible for the induction of any cell cycle arrests. This potential activation

of p27 may be the result of phosphorylation. It may be the case that unphosphorylated p27 becomes phosphorylated and therefore becomes undetectable using the antibody used during this study for unphosphorylated p27. To develop a better understanding of this, the effect of the *B. carterii* oleoresin should be further examined against the phosphorylated form of p27 to ascertain if the *B. carterii* oleoresin methanolic extract increases p27 activation.

These findings corroborate those of Suhail *et al.* (2011), Takahashi *et al.* (2012) and Toden *et al.* (2015) who identified that the *Boswellia* essential oil and purified boswellic acid isoforms were found to decrease the expression of D cyclins and CDK4. However, these findings expand on this on this by showing that *B. carterii* oleoresin induces a decrease in expression of both CDK2 and CDK6 in CML cells. This further supports that *Boswellia,* and its associated family of compounds induce a G_1 cell cycle arrest.

Overall, this study describes the therapeutic potential of the *B. carterii* oleoresin as a novel chemotherapeutic agent, through the induction of apoptosis, via the intrinsic pathway and the arrest of cancer cells in the sub G_1/G_1 stage of the cell cycle. The study then aimed to better understand the chemical profile of the *B. carterii* oleoresin.

7.3 The chemical composition of the *B. carterii* oleoresin

7.3.1 Does the oleoresin of *B. carterii* contain key biologically active compounds?

Chemical characterisation of the *B. carterii* oleoresin was conducted using a HPLC-MS approach. This approach allowed the initial separation of the oleoresin into its individual components using HPLC, before determining each component's molecular weight via MS (as described in section 6.3.3). Mass spectrometry was conducted using both positive and negative ionisation to reduce the possibility of missing any given compound.

Mass spectrometry analysis of the *B. carterii* oleoresin, shown in figure 6-10, identified a total of 570 potential compound identities present in the oleoresin (data shown in appendices 1 and 2). Separation of this data based on the ionisation mode utilised identified 281 potential compounds following analysis in positive ionisation mode, with a further 289 compounds found in negative ionisation mode. Comparisons of the mass spectra generated following analysis of the *B. carterii* oleoresin against previously

described components of the *Boswellia* genus identified multiple compounds of interest. Of these compounds, multiple boswellic acid isoforms were identified. This analysis identified the presence of α or β-boswellic acid, 11-keto-β-boswellic acid, 3-*O*-acetyl-α-boswellic acid, and 3-acetyl-11-keto-β-boswellic acid.

These findings corroborate those of Büchele *et al.* (2003) and Winterstein and Stein (1932) who first described the presence of boswellic acid isoforms within the oleoresins of *Boswellia*. Additional studies by Buchele *et al.* (2006), have also identified the presence of 3α,24-dihydroxyurs-12-ene, α-thujene, serratol and α-pinene. None of these compounds were identified within the *B. carterii* oleoresin. Many of these compounds are also found within the *Boswellia* essential oil and are therefore volatile in nature (DeCarlo *et al.*, 2018; Johnson *et al.*, 2019). These volatiles may have been lost from this extract due to the rotary evaporation process (described in section 2.2). The findings of this study also support those of Sharma *et al.* (2016), who specifically isolated and quantified the abundance of boswellic acid isoforms within the oleoresins of *B. serrata*. However, all of these studies focused on other species of *Boswellia*, with no previous research describing boswellic acid profile of oleoresins of *B. carterii*.

The presence of multiple boswellic acid isoforms within the *B. carterii* oleoresin is important as this study describes for the first time their presence within this species. This may therefore offer an alternative source for the isolation of pure boswellic acids, which are currently only isolated from *B. serrata*. Further to this, the identification of these boswellic acid isoforms within the *B. carterii* oleoresin may also have implications on the anti-cancer activity of the oleoresin extract used during this study.

Previous studies have described that the boswellic acid family of compounds to be responsible for the biological activity of the *Boswellia* genus (Ammon, 2016; Hoernlein *et al.*, 1999; Liu, Wang, *et al.*, 2019; Shah, Qazi, & Taneja, 2009; Syrovets *et al.*, 2000; Dan Wang, Ge, Bai, & Song, 2018; Yuan *et al.*, 2008; Zhao *et al.*, 2003). Whilst many of these studies used purified boswellic acid isoforms, originally isolated from *B. serrata*, the presence in *B. carterii* oleoresins, indicates that this family of compounds may be responsible for the biological activity of this species. However, with this study only identifying the presence of boswellic acids in the *B. carterii* oleoresins, it may be the case that other compounds within the oleoresin may also possess biological activity. However, further characterisation is required to confirm this hypothesis.

7.3.2 The development of a chemical fingerprinting method for *Boswellia* oleoresins

In addition to identifying the presence of multiple boswellic acid isoforms within the *B. carterii* oleoresin extract, the study has also developed a methodology, which could be potentially utilised to fingerprint the chemical composition of *Boswellia* oleoresins. The gradient HPLC methodology described in table 6-2, was capable of efficiently separating the compounds within the *B. carterii* oleoresin methanolic extract to a high resolution. Further to this, the triplicate injection of *B. carterii* oleoresin, shown in figure 6-8, also showed that the method developed was consistent across independent sample injections. These findings could be utilised as a part of a tool to rapidly distinguish between the species of the *Boswellia* genus. This fingerprinting tool may have commercial applications with the ability to identify the species from which unknown *Boswellia* oleoresins arise from.

Further to this, it may also provide a tool to rapidly determine if a species is under stress as a result of overharvesting for commercial oil production. In recent years the demand for *Boswellia* derived essential oil has increased dramatically and as a result the demand for *Boswellia* oleoresins has risen to levels which are greater than the trees can safely sustainably produce (Johnson *et al.*, 2019). As a result, *Boswellia* is at risk of becoming extinct, (Johnson *et al.*, 2019). However, when under stress *Boswellia* trees modify the chemical composition of their oleoresins (DeCarlo *et al.*, 2018; Johnson *et al.*, 2019). A key marker that has been associated with the stress of overharvesting has been identified to be methoxydecane (Johnson *et al.*, 2019). The fingerprinting methodology developed as a part of this study may be capable of identifying those *Boswellia* species which are at risk earlier and potentially prevent the extinction of specific *Boswellia* species.

7.3.3 The wider implications of chemically characterising *B. carterii* oleoresins

One of the key findings of this research is that whilst this study identified the presence of boswellic acid isoforms within the *B. carterii* oleoresin, HPLC fingerprinting (described in section 6.3.2) identified 86 different compounds in total. This number of compounds is significantly greater than other comparable studies which have aimed to characterise the oleoresins of other *Boswellia* species (Roy *et al.*, 2019; Schmiech *et al.*, 2019). This difference in the overall number of compounds identified is likely due

to other studies focusing on the boswellic acid content of other *Boswellia* species due to their previously described biological activity.

Indeed, this study identified that boswellic acid isoforms are present in the oleoresin of *B. carterii* and may be contributing to the biological activity of the oleoresin used in this study. However, it cannot be ruled out that of the 86 compounds identified it is only the boswellic acids within the extract which are producing the observed anti-cancer effect. While many of these compounds identified may be biologically inert, some of these compounds may possess biological activity, which have been previously missed due to the emphasis placed on the boswellic acid content of the *Boswellia* genus. With much of the modern research on *Boswellia* derivatives focused on boswellic acid isoforms, it may be that these previously ignored compounds may have biological importance, necessitating the need for further and more detailed chemical characterisation of the *B. carterii* oleoresin.

7.4 Is *B. carterii* oleoresin the basis of a new chemotherapeutic agent?

The oleoresin of *B. carterii* was shown to possess heterogenous anti-cancer activity via the induction of intrinsic apoptosis and a sub G_1/G_1 cell cycle arrest. This highlights the potential of *B. carterii* oleoresins as a source of anti-cancer compounds.

The identification of this biological activity of the *B. carterii* oleoresin against multiple cancer types is of great therapeutic interest. Specifically, due to the increased risk of resistance to conventional chemotherapeutics and treatment failure observed in recent years (Nurgali *et al.*, 2018). In addition, many currently used chemotherapeutic agents have been shown to possess severe side effects (Gartung *et al.*, 2019). The oleoresins of *Boswellia* have been shown to be well tolerated and induce minimal side effects when used in clinical trials for the treatment of osteoarthritis and bronchial asthma (Gupta *et al.*, 1998; Sengupta *et al.*, 2008). Whilst this may not necessarily be the case for the those derived from *B. carterii*, similarities in the chemical composition to that previously described have been observed, suggesting the levels of off-target effects ought to similar. In addition, *in vivo* studies of purified boswellic acids have also shown minimal side effects in both mouse and rat cancer models (Liu, Wang, *et al.*, 2019; Wang *et al.*, 2020).

Identification of the cytotoxicity of the whole *B. carterii* oleoresin extract may also have an impact on their potential clinical use in developing countries. Within low income and developing countries, plant-based medicine and traditional medicines account for the majority of therapeutics utilised (Khan, 2014). The extracts of the *B. carterii* oleoresins would be ideal for use if the *in vitro* effects observed in this study were proven to translatable to an *in vivo* model. This is supported by previous studies which has shown *in vivo* and clinical trial data for other disease conditions has shown that the extracts other *Boswellia* species are well tolerated and possess minimal side-effects (Al-Harrasi & Al-Saidi, 2008; Gupta *et al.*, 1998). They would be suitable due to the abundance of the raw plant materials in the counties where it would be utilised, in addition the extraction method is both inexpensive and simple to conduct, meaning that the total cost of treatment could be low. This is important as many chemotherapeutic agents used today are too expensive to be available to low income countries. However, further research into the pharmacodynamics and pharmacokinetics associated with the *B. carterii* oleoresin methanolic extract is required before these extracts could be used clinically.

Given similarity to other *Boswellia* species, the presence of boswellic acids was to be expected. However, this study is the first to characterise the specific boswellic acid profile of *B. carterii*. While clinical trials using the oleoresins of *B. serrata* and purified boswellic acids have been conducted for other disease conditions, it is interesting that no similar cancer clinical trials have been conducted to date. This is despite these compounds showing potent anti-cancer potential (Buchele *et al.*, 2006; Liu, Wang, *et al.*, 2019; Syrovets *et al.*, 2005; Wang *et al.*, 2020). This may be due to the limited number of *in vivo* studies conducted to date which may not yet provide enough evidence to support the transition to clinical trials.

Therefore, to better understand the cytotoxic activity of the *B. carterii* oleoresin, *in vivo* studies should be performed. These studies would determine if the cytotoxic effect observed in *in vitro* studies such as this translate to an *in vivo* model. They would also allow a better understanding of the pharmacodynamics and pharmacokinetics of the compound to be ascertained, along with any major side effects, before attempting clinical trials. However, given several further isolations, purification, and characterisation of both the chemical composition and biological activity is required, it may be some time before clinical trials can be fully justified then begin.

Further to this, in the process of identifying the presence of the boswellic acid isoforms within the *B. carterii* oleoresin this study developed a finger printing method that could be applied to chemically profile other *Boswellia* oleoresins more robustly. It may be this could be utilised to retrospectively better analyse the chemical profile of other species of *Boswellia* to ensure they are not underexploited for the treatment of cancer or other disease. In addition, this technique could also be utilised to rapidly distinguish the identity of *Boswellia* oleoresins from unreliable commercial sources. This would not only ensure the integrity of commercial and scientific ventures, but also prevent fraudulent commercial oleoresin transactions, which have become common in the rapidly growing essential oil industry.

7.5 Limitations

This study utilised robust methods to elucidate the biological and chemical characteristics of the *B. carterii* oleoresin. Nonetheless, further methodologies could be employed to develop this understanding further still.

For example, the use of known chemical analytical reference standards for all previously discovered boswellic acid isoforms may enhance the chemical characterisation. These reference standards are single compounds of high purity to allow for equipment calibration, as well as the confirmation and quantification of a specific compound's abundance within a mixture of compounds. The use of these reference standards would allow us to (1) improve the confidence in the presence of key compounds within the *B. carterii* oleoresin methanolic extract, such as that of the boswellic acid family of compounds and (2) to quantify the amount of each of these compounds within the *B. carterii* oleoresin extracts, through the development of known concentration standard curves. However, financial implications of purchasing these analytical reference standards is considerable due to the purity of compounds required and due to the apparent complexity of the extract, many would be required. As such, it was not viable to utilise analytical standards at this stage of the project. However, if the project was to be continued both the employment of a mass spectral database in addition to purchasing analytical reference standards for key compounds within the *B. carterii* oleoresin, such as that of the boswellic acid isoforms.

7.6 Future work

This study identified that the *B. carterii* oleoresin methanolic extract induced apoptotic cell death in multiple cell lines, further to this, this study found this to be induced by activation of the intrinsic pathway of apoptosis. However, this study mainly focused on the downstream end of the intrinsic pathway. Additional research should therefore be conducted to determine the upstream mechanisms which induced the activation of caspases -3, -7 and -9.

The intrinsic pathway of apoptosis is associated with mitochondrial dysfunction due to mitochondrial outer membrane permeabilisation due to the formation of BAX/BAK-mediated pores, and thus the release of cytochrome C from the mitochondria (Riley *et al*., 2018), as described fully in section 1.1.5.1. This dysfunction of the mitochondria and the depolarisation of the mitochondrial outer membrane have been previously described to occur following the treatment of cancer cells with multiple boswellic acid isoforms (Lv *et al*., 2020; Xia *et al*., 2005). However, no further work has been conducted to better understand if *B. carterii* oleoresins act via similar mechanisms. This therefore highlights potential further pathways and proteins to explore to better understand how *B. carterii* oleoresin affects their expression and to confirm that the *B. carterii* oleoresin acts via the intrinsic pathway of apoptosis. Key proteins of interest which could be explored include: cytochrome C and Apaf-1 (key components of the apoptosome), the BCL-2 family of proteins (BID, BAX, BAK, NOXA and PUMA) and the associated inhibitors of the intrinsic pathway (BCL-2, BCL-x_L and MCL-1) to better understand the mechanism of apoptosis induced by the *B. carterii* oleoresin methanolic extract.

Further to this, previous studies using purified boswellic acid isoforms have shown the extrinsic pathway of apoptosis, specifically the activation of DR4 and DR5 to be affected by these compounds (Lu *et al.*, 2008; Xia *et al.*, 2005). No previous studies have been conducted to determine if a similar effect is observed following treatment with the solvent extracts of the *B. carterii* oleoresin. Therefore, further examination on the effect of the *B. carterii* oleoresin methanolic extract on this pathway should be explored to ascertain if this pathway is involved in the apoptotic cell death induced.

Also, it would also be logical to examine alternative pathways which result in the G_1 cell cycle arrest observed in the K562 cells used in this study. Key proteins of interest

include the CDK inhibitor proteins, p57, p21, p18 and p27 which have all been shown to be associated with cell cycle arrests following the treatment of cancer cells *in vitro* (Abbas & Dutta, 2009; Abbastabar *et al.*, 2018; Guo *et al.*, 2010). Further to this, the phosphorylation state of these CDK inhibitory proteins have also been shown to play a role in the inhibitory activity of these proteins (Ciarallo *et al.*, 2002). Therefore, the examination of the change in phosphorylation states of these proteins may allow us to better ascertain the specific molecular mechanism of action of the *B. carterii* oleoresin methanolic extract.

This study examined the change in protein expression following treatment for 48 hours. Addition of more acute timepoints may allow us to better resolve the time course over which these changes occur. This is important as modifications to protein expression has been shown to vary considerably with some modifications occurring rapidly (within hours) with others taking a substantially longer period of time (days). Commonly in cancer research more acute timepoints following treatment of between minutes and days post treatment are examined. Studies by Musgrove, Swarbrick, Lee, Cornish, and Sutherland (1998) and Cha *et al.* (1998) showed that the steroidal hormone progestin and dexamethasone to act on the expression of cell cycle proteins within 6 - 24 hours post application. While the examination of a more chronic timepoint will show the change in effect at the end point of treatment, some proteins may be rapidly generated and then degraded before this chronic timepoint, and as a result the modification to the expression of these proteins may be missed. Examination at more acute timepoints would also allow us to determine if the time dependent cytotoxicity, observed in section 4.3.1, following treatment with the *B. carterii* oleoresin methanolic extract was reflected in the molecular changes within cancer cells.

This study also conducted chemical characterisation of the *B. carterii* oleoresin methanolic extract and identified the presence of multiple boswellic acid isoforms. These compounds are highly sought after due to their previously described biological activity as anti-inflammatory, anti-microbial and anti-cancer agents (Ammon, 2016; Khan *et al.*, 2016; Raja *et al.*, 2011). Therefore, the ability to isolate this family of compounds from the *B. carterii* oleoresin would be important both biologically and economically as this offers an alternative source to the routinely utilised *B. serrata* species. Further to this, Sharma *et al*, (2016) developed a method to isolate boswellic acids from the oleoresins of *B. serrata*, which could potentially be applied to *B. carterii*

oleoresin. This could ultimately allow both the extraction of the essential oil from the *Boswellia* oleoresins, followed by the isolation of the boswellic acids from the remainder of the oleoresin, further increasing efficiency of use.

Additionally, further isolations of the *B. carterii* oleoresin methanolic extract and additional chemical characterisation of any identified biologically active fractions could be conducted. This would support the study by allowing us to ascertain the identities of all compounds present within individual fractions. The use of further isolations via fractionating HPLC or column chromatography would also allow us to confirm which compound is responsible for the biological activity of the *B. carterii* oleoresin methanolic extract. Fractionation would also allow the use of other, more powerful, analytical chemistry techniques, NMR, and FTIR. This approach would also allow us to better characterise the chemical components within the *B. carterii* oleoresin and identify the molecular structures of any unidentified or previously undescribed compounds. This would ultimately allow us to completely characterise the chemical composition of the *B. carterii* oleoresin.

7.7 Summary

This study is the first to show that methanolic extracts of *B. carterii* oleoresin are selectively cytotoxic against multiple cancer types. Cytotoxicity is produced by apoptosis, with evidence for necrosis. Furthermore, a sub G_1/G_1 cell cycle arrest prevents cancer cell division.

B. carterii oleoresin methanolic extract induces apoptosis via the intrinsic pathway; specifically, by activation of caspases -3, -7 and -9, in addition to cleavage of the DNA repair protein, PARP. The sub G_1/G_1 cell cycle arrest results from increased expression of the CDK inhibitory protein p27, accompanied by decreased expression of cell cycle regulating proteins cyclin D3, CDK 2, CDK 4 and CDK 6.

HPLC and mass spectrometry confirmed the presence of several boswellic acid isoforms which are likely responsible for the observed biological effects. However, development of a robust methanolic extraction method revealed several previously uncharacterised compounds which may also poses contributing biological activity.

These findings suggest that *B. carterii oleoresin* is a potential source of novel chemotherapeutics. Furthermore, given the chemical complexity of *B. carterii* it is likely

the entire genus is therapeutically underexploited. Combined, this highlights a need to further characterise the chemical profile and biological activity of the *Boswellia* genus, with the aim of developing novel chemotherapeutic drugs.

Chapter 8

Appendices

Appendix 1 - Mass spectral data following analysis of the *B. carterii* oleoresin in positive mode

Retention time (mins)	Ionisation mode	Identified m/z	Ion m/z	Ion formula $[M+H]^+$	Molecule formula	Molecule Mass	Difference (ppm)
0.426	Positive	411.3609	411.3608	C27 H45 N3	C27 H44 N3	410.3535	-0.24
			411.3621	C29 H47 O	C29 H46 O	410.3549	3.03
1.074	Positive	499.3779	499.3782	C32 H51 O4	C32 H50 O4	498.3709	0.57
			499.3768	C30 H49 N3 O3	C30 H48 N3 O3	498.3696	-2.12
1.590	Positive	284.3314	284.3312	C19 H42 N	C19 H41 N	283.3239	-0.79
1.640	Positive	228.2684	228.2686	C15 H34 N	C15 H33 N	227.2613	0.78
2.339	Positive	216.1594	216.1594	C11 H22 N O3	C11 H21 N O3	215.1521	0.09
2.439	Positive	260.1867	260.1856	C13 H26 N O4	C13 H25 N O4	259.1784	-4.11
2.522	Positive	267.1795	267.1789	C10 H25 N3 O5	C10 H24 N3 O5	266.1716	-2.36
			267.1802	C12 H27 O6	C12 H26 O6	266.1729	2.69
2.622	Positive	230.1749	230.1751	C12 H24 N O3	C12 H23 N O3	229.1678	0.74
2.705	Positive	243.2069	243.2067	C13 H27 N2 O2	C13 H26 N2 O2	242.1994	-0.81
2.855	Positive	231.1750	231.1743	C16 H23 O	C16 H22 O	230.1671	-2.86
3.021	Positive	242.1752	242.1751	C13 H24 N O3	C13 H23 N O3	241.1678	-0.54
3.138	Positive	321.2429	321.2424	C20 H33 O3	C20 H32 O3	320.2351	-1.49
3.321	Positive	272.1854	272.1856	C14 H26 N O4	C14 H25 N O4	271.1784	0.87
3.487	Positive	246.1965	246.1965	C15 H24 N3	C15 H23 N3	245.1892	-0.11

Table continues on pages 219 - 230

3.936	Positive	439.3587	439.3571	C30 H47 O2	C30 H46 O2	438.3498	-3.75
4.202	Positive	337.2382	337.2373	C20 H33 O4	C20 H32 O4	336.2301	-2.57
4.518	Positive	356.2501	356.2499	C27 H32	C27 H31	355.2426	-0.7
			356.2517	C15 H36 N2 O7	C15 H35 N2 O7	355.2444	4.51
4.818	Positive	407.3676	407.3672	C30 H47	C30 H46	406.36	-0.92
5.300	Positive	337.2368	337.2373	C20 H33 O4	C20 H32 O4	336.2301	1.59
			337.236	C18 H31 N3 O3	C18 H30 N3 O3	336.2287	-2.4
5.966	Positive	487.3432	487.3445	C33 H45 N O2	C33 H44 N O2	486.3372	2.63
			487.3418	C30 H47 O5	C30 H46 O5	486.3345	-2.88
6.382	Positive	339.2535	339.253	C20 H35 O4	C20 H34 O4	338.2457	-1.52
6.815	Positive	432.2425	432.2434	C30 H30 N3	C30 H29 N3	431.2361	2.14
			432.2439	C17 H38 N O11	C17 H37 N O11	431.2367	3.33
			432.2407	C27 H32 N2 O3	C27 H31 N2 O3	431.2335	-4.07
7.247	Positive	427.3555	427.3557	C27 H45 N3 O	C27 H44 N3 O	426.3484	0.5
			427.3571	C29 H47 O2	C29 H46 O2	426.3498	3.65
7.413	Positive	386.3261	386.3265	C22 H44 N O4	C22 H43 N O4	385.3192	1
7.730	Positive	471.3492	471.3496	C33 H45 N O	C33 H44 N O	470.3423	0.78
			471.3514	C21 H49 N3 O8	C21 H48 N3 O8	470.3441	4.71
			471.3469	C30 H47 O4	C30 H46 O4	470.3396	-4.92
8.046	Positive	599.4995	599.4994	C34 H67 N2 O6	C34 H66 N2 O6	598.4921	-0.23
			599.502	C37 H65 N3 O3	C37 H64 N3 O3	598.4948	4.25
8.162	Positive	621.4832	621.4837	C36 H65 N2 O6	C36 H64 N2 O6	620.4764	0.83
			621.481	C33 H67 N O9	C33 H66 N O9	620.4738	-3.49

			758.2205	C40 H38 O15	C40 H37 O15	757.2132	-0.63
			758.22	C53 H30 N2 O4	C53 H29 N2 O4	757.2127	-1.31
			758.2197	C25 H44 N O25	C25 H43 N O25	757.2124	-1.73
			758.2224	C28 H42 N2 O22	C28 H41 N2 O22	757.2151	1.81
8.445	Positive	758.221	758.2227	C56 H28 N3 O	C56 H27 N3 O	757.2154	2.23
			758.2192	C38 H36 N3 O14	C38 H35 N3 O14	757.2119	-2.4
			758.2232	C43 H36 N O12	C43 H35 N O12	757.2159	2.91
			758.224	C58 H30 O2	C58 H29 O2	757.2168	4
			758.2173	C50 H32 N O7	C50 H31 N O7	757.2101	-4.85
			747.4156	C50 H55 N2 O4	C50 H54 N2 O4	746.4084	0.18
			747.4161	C37 H63 O15	C37 H62 O15	746.4089	0.87
			747.4148	C35 H61 N3 O14	C35 H60 N3 O14	746.4075	-0.93
8.545	Positive	747.4155	747.413	C47 H57 N O7	C47 H56 N O7	746.4057	-3.41
			747.4183	C53 H53 N3 O	C53 H52 N3 O	746.411	3.77
			747.4188	C40 H61 N O12	C40 H60 N O12	746.4116	4.46
			747.4121	C32 H63 N2 O17	C32 H62 N2 O17	746.4048	-4.52
8.678	Positive	508.5824	508.5816	C35 H74 N	C35 H73 N	507.5743	-1.62
8.811	Positive	392.3151	392.3159	C24 H42 N O3	C24 H41 N O3	391.3086	2.1
			392.3132	C21 H44 O6	C21 H43 O6	391.306	-4.75
9.011	Positive	458.3489	458.3476	C25 H48 N O6	C25 H47 N O6	457.3403	-2.81
			458.3503	C28 H46 N2 O3	C28 H45 N2 O3	457.343	3.05

			458.2842	C34 H36 N	C34 H35 N	457.277	0.06
9.127	Positive	458.2842	458.2834	C19 H42 N2 O10	C19 H41 N2 O10	457.2761	-1.76
			458.2861	C22 H40 N3 O7	C22 H39 N3 O7	457.2788	4.1
9.244	Positive	556.4424	556.4446	C31 H60 N2 O6	C31 H59 N2 O6	555.4373	3.94
9.427	Positive	569.488	569.4888	C33 H65 N2 O5	C33 H64 N2 O5	568.4815	1.41
			627.4817	C34 H65 N3 O7	C34 H64 N3 O7	626.4744	-0.31
9.560	Positive	627.4819	627.483	C36 H67 O8	C36 H66 O8	626.4758	1.83
			627.4799	C46 H61 N	C46 H60 N	626.4726	-3.27
			627.479	C31 H67 N2 O10	C31 H66 N2 O10	626.4717	-4.59
9.876	Positive	374.3030	374.3027	C21 H42 O5	C21 H41 O5	373.2954	-0.87
			374.3013	C19 H40 N3 O4	C19 H39 N3 O4	373.2941	-4.47
10.159	Positive	615.4877	615.4884	C41 H63 N2 O2	C41 H62 N2 O2	614.4811	1.15
			615.4857	C38 H65 N O5	C38 H64 N O5	614.4784	-3.21
			620.5064	C44 H64 N2	C44 H63 N2	619.4991	-0.48
10.408	Positive	620.5067	620.5096	C34 H70 N O8	C34 H69 N O8	619.5023	4.67
			620.5037	C41 H66 N O3	C41 H65 N O3	619.4964	-4.81
10.558	Positive	598.5227	598.5221	C42 H66 N2	C42 H65 N2	597.5148	-1.09
10.708	Positive	356.3527	356.3523	C22 H46 N O2	C22 H45 N O2	355.345	-1.11
11.074	Positive	513.3566	513.3561	C30 H47 N3 O4	C30 H46 N3 O4	512.3488	-0.96
			513.3575	C32 H49 O5	C32 H48 O5	512.3502	1.66
11.257	Positive	370.3097	370.3104	C25 H40 N O	C25 H38 N O	369.3032	2.01

			685.5514	C42 H73 N2 O5	C42 H72 N2 O5	684.5441	0.73
11.590	Positive	685.5509	685.5487	C39 H75 N O8	C39 H74 N O8	684.5414	-3.18
			685.5541	C45 H71 N3 O2	C45 H70 N3 O2	684.5468	4.65
			440.3609	C25 H48 N2 O4	C25 H47 N2 O4	439.3536	-1.23
11.739	Positive	440.3614	440.3635	C28 H46 N3 O	C28 H45 N3 O	439.3563	4.87
			491.3929	C25 H53 N3 O6	C25 H52 N3 O6	490.3856	-1.25
11.939	Positive	491.3935	491.3942	C27 H55 O7	C27 H54 O7	490.387	1.49
			456.3558	C25 H48 N2 O5	C25 H47 N2 O5	455.3485	-2.03
12.155	Positive	456.3567	456.3585	C28 H46 N3 O2	C28 H45 N3 O2	455.3512	3.85
			498.3663	C27 H50 N2 O6	C27 H49 N2 O6	497.3591	0.68
12.305	Positive	498.3660	498.3637	C24 H52 N O9	C24 H51 N O9	497.3564	-4.71
			931.6829	C50 H95 N2 O13	C50 H94 N2 O13	930.6756	0.5
			931.6837	C65 H89 N O3	C65 H88 N O3	930.6764	1.39
			931.681	C62 H91 O6	C62 H90 O6	930.6737	-1.49
			931.6802	C47 H97 N O16	C47 H96 N O16	930.6729	-2.38
12.555	Positive	931.6824	931.6797	C60 H89 N3 O5	C60 H88 N3 O5	930.6724	-2.93
			931.6855	C53 H93 N3 O10	C53 H92 N3 O10	930.6783	3.38
			931.6864	C68 H87 N2	C68 H86 N2	930.6791	4.27
			931.6869	C55 H95 O11	C55 H94 O11	930.6796	4.82
			570.3875	C30 H54 N2 O8	C30 H53 N2 O8	569.3802	0.47
12.721	Positive	570.3872	570.3856	C42 H50 O	C42 H49 O	569.3783	-2.78
			570.3848	C27 H56 N O11	C27 H55 N O11	569.3775	-4.24

13.070	Positive	548.4111	548.4098	C36 H54 N O3	C36 H53 N O3	547.4025	-2.34
			548.4125	C39 H52 N2	C39 H51 N2	547.4052	2.56
13.569	Positive	619.6162	619.6176	C45 H79	C45 H78	618.6104	2.31
			619.6136	C40 H79 N2 O2	C40 H78 N2 O2	618.6063	-4.19
13.902	Positive	567.5833	567.5823	C36 H75 N2 O2	C36 H74 N2 O2	566.575	-1.75
14.085	Positive	593.5990	593.598	C38 H77 N2 O2	C38 H76 N2 O2	592.5907	-1.76
14.435	Positive	687.2022	687.2013	C44 H31 O8	C44 H30 O8	686.1941	-1.25
			687.2032	C32 H35 N2 O15	C32 H34 N2 O15	686.1959	1.45
			687.2005	C29 H37 N O18	C29 H36 N O18	686.1932	-2.46
			687.204	C47 H29 N O5	C47 H28 N O5	686.1967	2.66
			687.2	C42 H29 N3 O7	C42 H28 N3 O7	686.1927	-3.2
14.851	Positive	476.3498	476.3496	C29 H48 O5	C29 H47 O5	475.3423	-0.37
			476.3483	C27 H46 N3 O4	C27 H45 N3 O4	475.341	-3.19
15.200	Positive	688.1955	688.1958	C28 H36 N2 O18	C28 H35 N2 O18	687.1885	0.38
			688.1966	C43 H30 N O8	C43 H29 N O8	687.1893	1.59
			688.1939	C40 H32 O11	C40 H31 O11	687.1866	-2.31
			688.1934	C53 H24 N2	C53 H23 N2	687.1861	-3.06
			688.1931	C25 H38 N O21	C25 H37 N O21	687.1858	-3.52
			688.1926	C38 H30 N3 O10	C38 H29 N3 O10	687.1853	-4.26
			688.1984	C31 H34 N3 O15	C31 H33 N3 O15	687.1912	4.28
15.416	Positive	479.3927	479.3929	C24 H53 N3 O6	C24 H52 N3 O6	478.3856	0.39
			479.3942	C26 H55 O7	C26 H54 O7	478.387	3.2

15.749	Positive	499.3795	499.3782	C32 H51 O4	C32 H50 O4	498.3709	-2.64
			499.3809	C35 H49 N O	C35 H48 N O	498.3736	2.74
16.015	Positive	457.3669	457.3663	C28 H47 N3 O2	C28 H46 N3 O2	456.359	-1.36
			457.3676	C30 H49 O3	C30 H48 O3	456.3603	1.58
16.315	Positive	441.3723	441.3727	C30 H49 O2	C30 H48 O2	440.3654	0.92
			441.3714	C28 H47 N3 O	C28 H46 N3 O	440.3641	-2.12
16.548	Positive	592.3905	592.3911	C41 H52 O3	C41 H51 O3	591.3838	1.01
			592.3898	C39 H50 N3 O2	C39 H49 N3 O2	591.3825	-1.26
			592.3929	C29 H56 N2 O10	C29 H55 N2 O10	591.3857	4.14
16.764	Positive	537.3955	537.3965	C38 H51 N O	C38 H50 N O	536.3892	1.9
			537.3938	C35 H53 O4	C35 H52 O4	536.3866	-3.1
17.197	Positive	613.1640	613.1637	C26 H31 N O16	C26 H30 N O16	612.1565	-0.43
			613.1646	C41 H25 O6	C41 H24 O6	612.1573	0.92
			613.1632	C39 H23 N3 O5	C39 H22 N3 O5	612.1559	-1.27
			613.1664	C29 H29 N2 O13	C29 H28 N2 O13	612.1591	3.95
			613.1611	C23 H33 O19	C23 H32 O19	612.1538	-4.81
17.779	Positive	699.6660	699.665	C47 H87 O3	C47 H86 O3	698.6577	-1.47
			699.6677	C50 H85 N	C50 H84 N	698.6604	2.37
			699.6636	C45 H85 N3 O2	C45 H84 N3 O2	698.6564	-3.39
18.511	Positive	487.4349	487.4344	C27 H57 N3 O4	C27 H56 N3 O4	486.4271	-1.11
			487.4357	C29 H59 O5	C29 H58 O5	486.4284	1.65
18.794	Positive	517.4066	517.4085	C27 H55 N3 O6	C27 H54 N3 O6	516.4013	3.75

19.343	Positive	504.3809	504.3809	C31 H52 O5	C31 H51 O5	503.3736	0.05
			504.3796	C29 H50 N3 O4	C29 H49 N3 O4	503.3723	-2.62
19.642	Positive	526.3646	526.3639	C31 H48 N3 O4	C31 H47 N3 O4	525.3567	-1.27
			526.3653	C33 H50 O5	C33 H49 O5	525.358	1.29
20.141	Positive	584.2065	584.2068	C37 H30 N O6	C37 H29 N O6	583.1995	0.45
			584.2059	C22 H36 N2 O16	C22 H35 N2 O16	583.1987	-0.97
			584.2086	C25 H34 N3 O13	C25 H33 N3 O13	583.2013	3.63
			584.2041	C34 H32 O9	C34 H31 O9	583.1968	-4.14
20.541	Positive	485.4004	485.4016	C35 H51 N	C35 H50 N	484.3943	2.48
			485.3989	C32 H53 O3	C32 H52 O3	484.3916	-3.05
20.973	Positive	441.3730	441.3727	C30 H49 O2	C30 H48 O2	440.3654	-0.66
			441.3714	C28 H47 N3 O	C28 H46 N3 O	440.3641	-3.71
21.705	Positive	447.3467	447.3469	C28 H47 O4	C28 H46 O4	446.3396	0.42
			447.3455	C26 H45 N3 O3	C26 H44 N3 O3	446.3383	-2.59
22.121	Positive	437.3590	437.3585	C22 H49 N2 O6	C22 H48 N2 O6	436.3512	-1.11
22.903	Positive	850.2309	850.231	C55 H34 N2 O8	C55 H33 N2 O8	849.2237	0.08
			850.2307	C27 H48 N O29	C27 H47 N O29	849.2234	-0.29
			850.2315	C42 H42 O19	C42 H41 O19	849.2242	0.68
			850.2301	C40 H40 N3 O18	C40 H39 N3 O18	849.2229	-0.9
			850.2291	C67 H30 O	C67 H29 O	849.2218	-2.1
			850.2333	C30 H46 N2 O26	C30 H45 N2 O26	849.2261	2.86
			850.2283	C52 H36 N O11	C52 H35 N O11	849.221	-3.08
			850.2336	C58 H32 N3 O5	C58 H31 N3 O5	849.2264	3.24

22.903	Positive	850.2309	850.2278	C65 H28 N3	C65 H27 N3	849.2205	-3.68
			850.2342	C45 H40 N O16	C45 H39 N O16	849.2269	3.84
			850.2275	C37 H42 N2 O21	C37 H41 N2 O21	849.2202	-4.05
			850.235	C60 H34 O6	C60 H33 O6	849.2277	4.82
23.769	Positive	781.5695	781.5698	C44 H79 N O10	C44 H78 N O10	780.5626	0.45
			781.5707	C59 H73	C59 H72	780.5634	1.51
			781.5672	C41 H81 O13	C41 H80 O13	780.5599	-2.99
			781.5667	C54 H73 N2 O2	C54 H72 N2 O2	780.5594	-3.64
			781.5725	C47 H77 N2 O7	C47 H76 N2 O7	780.5653	3.88
			781.5658	C39 H79 N3 O12	C39 H78 N3 O12	780.5585	-4.71
24.334	Positive	504.4697	504.469	C37 H60	C37 H59	503.4617	-1.48
25.166	Positive	805.2662	805.2662	C37 H45 N2 O18	C37 H44 N2 O18	804.2589	-0.01
			805.267	C52 H39 N O8	C52 H38 N O8	804.2597	1.02
			805.2643	C49 H41 O11	C49 H40 O11	804.2571	-2.31
			805.2638	C62 H33 N2	C62 H32 N2	804.2565	-2.95
			805.2689	C40 H43 N3 O15	C40 H42 N3 O15	804.2616	3.32
			805.2635	C34 H47 N O21	C34 H46 N O21	804.2562	-3.35
			805.2694	C27 H51 N O26	C27 H50 N O26	804.2621	3.96
			805.263	C47 H39 N3 O10	C47 H38 N3 O10	804.2557	-3.98
			805.2697	C55 H37 N2 O5	C55 H36 N2 O5	804.2624	4.35
			805.2702	C42 H45 O16	C42 H44 O16	804.2629	4.99
26.813	Positive	460.3923	460.3911	C30 H52 O3	C30 H51 O3	459.3838	-2.62
			460.3938	C33 H50 N	C33 H49 N	459.3865	3.22

27.825	Positive	533.4118	533.4102	C35 H53 N2 O2	C35 H52 N2 O2	532.4029	-3.09
			533.4142	C40 H53	C40 H52	532.4069	4.47
28.643	Positive	659.2220	659.2217	C47 H31 O4	C47 H30 O4	658.2144	-0.48
			659.2227	C20 H41 N3 O21	C20 H40 N3 O21	658.2154	1.07
			659.2209	C32 H37 N O14	C32 H36 N O14	658.2136	-1.74
			659.2235	C35 H35 N2 O11	C35 H34 N2 O11	658.2163	2.33
			659.2203	C45 H29 N3 O3	C45 H28 N3 O3	658.2131	-2.52
			659.224	C22 H43 O22	C22 H42 O22	658.2168	3.11
			659.2244	C50 H29 N O	C50 H28 N O	658.2171	3.59
29.326	Positive	627.1791	627.1789	C40 H25 N3 O5	C40 H24 N3 O5	626.1716	-0.36
			627.1794	C27 H33 N O16	C27 H32 N O16	626.1721	0.46
			627.1802	C42 H27 O6	C42 H26 O6	626.1729	1.78
			627.1767	C24 H35 O19	C24 H34 O19	626.1694	-3.82
			627.1762	C37 H27 N2 O8	C37 H26 N2 O8	626.1689	-4.64
			627.1821	C30 H31 N2 O13	C30 H30 N2 O13	626.1748	4.74
30.141	Positive	624.4177	624.4173	C42 H56 O4	C42 H55 O4	623.41	-0.62
			624.4192	C30 H60 N2 O11	C30 H59 N2 O11	623.4119	2.35
			624.416	C40 H54 N3 O3	C40 H53 N3 O3	623.4087	-2.78
			624.42	C45 H54 N O	C45 H53 N O	623.4127	3.68
31.588	Positive	764.2000	764.2001	C44 H32 N2 O11	C44 H31 N2 O11	763.1928	0.08
			764.2006	C31 H40 O22	C31 H39 O22	763.1933	0.75
			764.1992	C29 H38 N3 O21	C29 H37 N3 O21	763.192	-1.01
			764.2009	C59 H26 N O	C59 H25 N O	763.1936	1.17

31.588	Positive	764.2000	764.1982	C56 H28 O4	C56 H27 O4	763.1909	-2.34
			764.1974	C41 H34 N O14	C41 H33 N O14	763.1901	-3.43
			764.2027	C47 H30 N3 O8	C47 H29 N3 O8	763.1955	3.59
			764.1969	C54 H26 N3 O3	C54 H25 N3 O3	763.1896	-4.1
			764.2033	C34 H38 N O19	C34 H37 N O19	763.196	4.26
			764.1966	C26 H40 N2 O24	C26 H39 N2 O24	763.1893	-4.52
33.535	Positive	913.2291	913.229	C30 H47 N3 O29	C30 H46 N3 O29	912.2217	-0.14
			913.2298	C45 H41 N2 O19	C45 H40 N2 O19	912.2225	0.77
			913.228	C57 H37 O12	C57 H36 O12	912.2207	-1.26
			913.2303	C32 H49 O30	C32 H48 O30	912.223	1.33
			913.2306	C60 H35 N O9	C60 H34 N O9	912.2234	1.68
			913.2274	C70 H29 N2 O	C70 H28 N2 O	912.2202	-1.82
			913.2271	C42 H43 N O22	C42 H42 N O22	912.2198	-2.17
			913.2266	C55 H35 N3 O11	C55 H34 N3 O11	912.2193	-2.73
			913.2325	C48 H39 N3 O16	C48 H38 N3 O16	912.2252	3.71
			913.233	C35 H47 N O27	C35 H46 N O27	912.2257	4.27
			913.2333	C63 H33 N2 O6	C63 H32 N2 O6	912.226	4.62
			913.2248	C67 H31 N O4	C67 H30 N O4	912.2175	-4.76
37.378	Positive	597.4048	597.4051	C39 H53 N2 O3	C39 H52 N2 O3	596.3978	0.45
			597.4024	C36 H55 N O6	C36 H54 N O6	596.3951	-4.04
			597.4078	C42 H51 N3	C42 H50 N3	596.4005	4.95

39.974	Positive	613.1826	613.1825	C48 H23 N	C48 H22 N	612.1752	-0.16
			613.1822	C20 H37 O21	C20 H36 O21	612.1749	-0.68
			613.1817	C33 H29 N2 O10	C33 H28 N2 O10	612.1744	-1.52
			613.1844	C36 H27 N3 O7	C36 H26 N3 O7	612.1771	2.86
			613.1808	C18 H35 N3 O20	C18 H34 N3 O20	612.1736	-2.87
			613.1849	C23 H35 N O18	C23 H34 N O18	612.1776	3.7
			613.1798	C45 H25 O3	C45 H24 O3	612.1725	-4.54
42.336	Positive	703.1973	703.1981	C32 H35 N2 O16	C32 H34 N2 O16	702.1908	1.15
			703.1963	C44 H31 O9	C44 H30 O9	702.189	-1.48
			703.1989	C47 H29 N O6	C47 H28 N O6	702.1917	2.33
			703.1954	C29 H37 N O19	C29 H36 N O19	702.1882	-2.66
			703.1949	C42 H29 N3 O8	C42 H28 N3 O8	702.1876	-3.39
			703.2008	C35 H33 N3 O13	C35 H32 N3 O13	702.1935	4.97
44.283	Positive	911.2404	911.2415	C63 H33 N3 O5	C63 H32 N3 O5	910.2342	1.18
			911.2393	C47 H43 O19	C47 H42 O19	910.232	-1.2
			911.242	C50 H41 N O16	C50 H40 N O16	910.2347	1.74
			911.2388	C60 H35 N2 O8	C60 H34 N2 O8	910.2315	-1.77
			911.2428	C65 H35 O6	C65 H34 O6	910.2355	2.65
			911.238	C45 H41 N3 O18	C45 H40 N3 O18	910.2307	-2.68
			911.2438	C38 H45 N3 O23	C38 H44 N3 O23	910.2366	3.78
			911.2369	C72 H31 O	C72 H30 O	910.2297	-3.8
			911.2447	C53 H39 N2 O13	C53 H38 N2 O13	910.2374	4.69
			911.2361	C57 H37 N O11	C57 H36 N O11	910.2288	-4.71

45.032	Positive	439.3752	439.3742	C22 H51 N2 O6	C22 H50 N2 O6	438.3669	-2.36
			439.3768	C25 H49 N3 O3	C25 H48 N3 O3	438.3696	3.75
47.677	Positive	345.1738	345.1742	C11 H27 N3 O9	C11 H26 N3 O9	344.1669	1.11
			345.1723	C23 H23 N O2	C23 H22 N O2	344.1651	-4.27
50.007	Positive	766.5815	766.5828	C44 H80 N O9	C44 H79 N O9	765.5755	1.65
			766.5801	C41 H82 O12	C41 H81 O12	765.5728	-1.86
			766.5796	C54 H74 N2 O	C54 H73 N2 O	765.5723	-2.53
			766.5787	C39 H80 N3 O11	C39 H79 N3 O11	765.5715	-3.61
52.269	Positive	836.2182	836.218	C57 H30 N3 O5	C57 H29 N3 O5	835.2107	-0.24
			836.2185	C44 H38 N O16	C44 H37 N O16	835.2112	0.37
			836.2193	C59 H32 O6	C59 H31 O6	835.2121	1.37
			836.2204	C32 H42 N3 O23	C32 H41 N3 O23	835.2131	2.59
			836.2158	C41 H40 O19	C41 H39 O19	835.2086	-2.84
			836.2153	C54 H32 N2 O8	C54 H31 N2 O8	835.208	-3.45
			836.2212	C47 H36 N2 O13	C47 H35 N2 O13	835.2139	3.58
			836.2217	C34 H44 O24	C34 H43 O24	835.2144	4.2
			836.2145	C39 H38 N3 O18	C39 H37 N3 O18	835.2072	-4.44
			836.222	C62 H30 N O3	C62 H29 N O3	835.2147	4.57
55.480	Positive	228.1956	228.1958	C13 H26 N O2	C13 H25 N O2	227.1885	0.9
57.161	Positive	273.2539	273.2537	C15 H33 N2 O2	C15 H32 N2 O2	272.2464	-0.9

Appendix 2 - Mass spectral data generated following analysis of the *B. carterii* oleoresin in negative mode

Retention time (mins)	Ionisation mode	Identified m/z	Ion m/z	Ion formula $[M-H]^-$	Molecule formula	Molecule Mass	Difference (ppm)
0.426	Negative			Noise			
1.074	Negative			Noise			
1.590	Negative			Noise			
1.640	Negative	387.1234	387.1238	C24 H19 O5	C24 H20 O5	388.1311	1.02
			387.1225	C22 H17 N3 O4	C22 H18 N3 O4	388.1297	-2.44
2.339	Negative	144.9926	144.9931	C8 H O3	C8 H2 O3	146.0004	3.54
2.439	Negative	421.1945	421.1953	C18 H31 N O10	C18 H32 N O10	422.2026	2
			421.1962	C33 H25	C33 H26	422.2035	3.97
2.522	Negative	214.1475	214.1475	C14 H18 N2	C14 H19 N2	215.1548	0.22
2.622	Negative	421.1936	421.1922	C28 H25 N2 O2	C28 H26 N2 O2	422.1994	-3.43
			421.1953	C18 H31 N O10	C18 H32 N O10	422.2026	4.13
2.705	Negative	399.2470	399.2474	C17 H37 N O9	C17 H38 N O9	400.2547	0.95
2.855	Negative	228.1636	228.1632	C15 H20 N2	C15 H21 N2	229.1705	-1.76
3.021	Negative	228.1639	228.1632	C15 H20 N2	C15 H21 N2	229.1705	-3.07
3.138	Negative	495.2041	495.2043	C16 H35 N2 O15	C16 H36 N2 O15	496.2116	0.39
			495.2051	C31 H29 N O5	C31 H30 N O5	496.2124	2.06
			495.2024	C28 H31 O8	C28 H32 O8	496.2097	-3.34
3.321	Negative	195.0531	195.0537	C9 H9 N O4	C9 H10 N O4	196.061	3.09

Table continues on pages 232 - 244

3.487	Negative	356.1772	356.1768	C23 H22 N3 O	C23 H23 N3 O	357.1841	-1.02
			356.1782	C25 H24 O2	C25 H25 O2	357.1855	2.74
3.936	Negative	463.2044	463.2054	C33 H25 N3	C33 H26 N3	464.2127	2.15
			463.2032	C17 H35 O14	C17 H36 O14	464.2105	-2.52
			463.2059	C20 H33 N O11	C20 H34 N O11	464.2132	3.25
			463.2027	C30 H27 N2 O3	C30 H28 N2 O3	464.21	-3.63
4.202	Negative	429.2011	429.2004	C20 H31 N O9	C20 H32 N O9	430.2077	-1.56
			429.2031	C23 H29 N2 O6	C23 H30 N2 O6	430.2104	4.67
4.518	Negative			Noise			
4.818	Negative			Noise			
5.300	Negative	365.2420	365.2419	C17 H35 N O7	C17 H36 N O7	366.2492	-0.27
5.966	Negative	307.0061	307.0064	C23 H N O	C23 H2 N O	308.0136	0.85
			307.0055	C8 H7 N2 O11	C8 H8 N2 O11	308.0128	-1.84
6.382	Negative	341.0112	341.0118	C23 H3 N O3	C23 H4 N O3	342.0191	1.88
6.815	Negative	533.3621	533.3623	C33 H47 N3 O3	C33 H48 N3 O3	534.3696	0.36
			533.3636	C35 H49 O4	C35 H50 O4	534.3709	2.87
			533.3596	C30 H49 N2 O6	C30 H50 N2 O6	534.3669	-4.66
7.247	Negative	507.0183	507.0192	C22 H9 N3 O12	C22 H10 N3 O12	508.0264	1.72
			507.0173	C34 H5 N O5	C34 H6 N O5	508.0246	-1.93
			507.02	C37 H3 N2 O2	C37 H6 N2 O2	508.0273	3.35
			507.0165	C19 H11 N2 O15	C19 H12 N2 O15	508.0238	-3.56
			507.0205	C24 H11 O13	C24 H12 O13	508.0278	4.36

7.413	Negative	430.3272	430.3286	C22 H44 N3 O5	C22 H45 N3 O5	431.3359	3.35
7.730	Negative	471.3600	471.3592	C29 H47 N2 O3	C29 H48 N2 O3	472.3665	-1.66
			471.3619	C32 H45 N3	C32 H46 N3	472.3692	4.02
8.046	Negative	469.3439	469.3436	C29 H45 N2 O3	C29 H46 N2 O3	470.3508	-0.71
			469.3462	C32 H43 N3	C32 H44 N3	470.3535	4.99
8.162	Negative	467.3282	467.3279	C29 H43 N2 O3	C29 H44 N2 O3	468.3352	-0.6
8.445	Negative	513.3706	513.3698	C31 H49 N2 O4	C31 H50 N2 O4	514.3771	-1.59
			513.3725	C34 H47 N3 O	C34 H48 N3 O	514.3797	3.62
8.545	Negative	416.3477	416.3494	C22 H46 N3 O4	C22 H47 N3 O4	417.3567	4.03
8.678	Negative	319.1643	319.1637	C14 H25 N O7	C14 H26 N O7	320.1709	-2.03
8.811	Negative	369.2511	369.2521	C20 H35 N O5	C20 H36 N O5	370.2593	2.62
9.011	Negative	471.3598	471.3592	C29 H47 N2 O3	C29 H48 N2 O3	472.3665	-1.23
			471.3619	C32 H45 N3	C32 H46 N3	472.3692	4.44
9.127	Negative	507.1346	507.1342	C18 H25 N3 O14	C18 H26 N3 O14	508.1415	-0.78
			507.135	C33 H19 N2 O4	C33 H20 N2 O4	508.1423	0.85
			507.1355	C20 H27 O15	C20 H28 O15	508.1428	1.86
			507.1324	C30 H21 N O7	C30 H22 N O7	508.1396	-4.43
9.244	Negative	469.3447	469.3436	C29 H45 N2 O3	C29 H46 N2 O3	470.3508	-2.41
			469.3462	C32 H43 N3	C32 H44 N3	470.3535	3.29
9.427	Negative	513.3722	513.3725	C34 H47 N3 O	C34 H48 N3 O	514.3797	0.51
			513.3738	C36 H49 O2	C36 H50 O2	514.3811	3.12
			513.3698	C31 H49 N2 O4	C31 H50 N2 O4	514.3771	-4.7

9.560	Negative	513.3725	513.3725	C34 H47 N3 O	C34 H48 N3 O	514.3797	-0.07
			513.3738	C36 H49 O2	C36 H50 O2	514.3811	2.54
9.876	Negative	487.3551	487.3541	C29 H47 N2 O4	C29 H48 N2 O4	488.3614	-1.98
			487.3568	C32 H45 N3 O	C32 H46 N3 O	488.3641	3.5
10.159	Negative	627.5124	627.5133	C42 H65 N3 O	C42 H66 N3 O	628.5206	1.45
			627.5106	C39 H67 N2 O4	C39 H68 N2 O4	628.5179	-2.81
			627.5147	C44 H67 O2	C44 H68 O2	628.5219	3.59
10.408	Negative	581.1548	581.1547	C44 H21 O2	C44 H22 O2	582.162	-0.17
			581.1557	C17 H31 N3 O19	C17 H32 N3 O19	582.163	1.59
			581.1539	C29 H27 N O12	C29 H28 N O12	582.1612	-1.59
			581.1534	C42 H19 N3 O	C42 H20 N3 O	582.1606	-2.47
			581.1566	C32 H25 N2 O9	C32 H26 N2 O9	582.1638	3.01
			581.1571	C19 H33 O20	C19 H34 O20	582.1643	3.89
10.558	Negative	487.3550	487.3541	C29 H47 N2 O4	C29 H48 N2 O4	488.3614	-1.78
			487.3568	C32 H45 N3 O	C32 H46 N3 O	488.3641	3.71
10.708	Negative	641.5294	641.529	C43 H67 N3 O	C43 H68 N3 O	642.5362	-0.68
			641.5303	C45 H69 O2	C45 H70 O2	642.5376	1.41
			641.5263	C40 H69 N2 O4	C40 H70 N2 O4	642.5336	-4.85
11.074	Negative	529.3674	529.3674	C34 H47 N3 O2	C34 H48 N3 O2	530.3747	-0.04
			529.3687	C36 H49 O3	C36 H50 O3	530.376	2.49
11.257	Negative	731.1781	731.1789	C29 H35 N2 O20	C29 H36 N2 O20	732.1861	1.05
			731.177	C41 H31 O13	C41 H32 O13	732.1843	-1.48
			731.1797	C44 H29 N O10	C44 H30 N O10	732.187	2.18

			731.1765	C54 H23 N2 O2	C54 H24 N2 O2	732.1838	-2.18
			731.1762	C26 H37 N O23	C26 H38 N O23	732.1835	-2.62
11.257	Negative	731.1781	731.1805	C59 H23	C59 H24	732.1878	3.31
			731.1757	C39 H29 N3 O12	C39 H30 N3 O12	732.1829	-3.32
			731.1815	C32 H33 N3 O17	C32 H34 N3 O17	732.1888	4.71
11.590	Negative	423.3344	423.3354	C25 H45 N O4	C25 H46 N O4	424.3427	2.37
			667.5518	C40 H75 O7	C40 H76 O7	668.5591	0.49
11.739	Negative	667.5515	667.5505	C38 H73 N3 O6	C38 H74 N3 O6	668.5578	-1.52
			667.5545	C43 H73 N O4	C43 H74 N O4	668.5618	4.5
			511.3568	C34 H45 N3 O	C34 H46 N3 O	512.3641	1
11.939	Negative	511.3563	511.3582	C36 H47 O2	C36 H48 O2	512.3654	3.62
			511.3541	C31 H47 N2 O4	C31 H48 N2 O4	512.3614	-4.23
12.155	Negative	501.3485	501.3487	C33 H45 N2 O2	C33 H46 N2 O2	502.3559	0.3
			655.1762	C43 H27 O7	C43 H28 O7	656.1835	0.5
			655.1754	C28 H33 N O17	C28 H34 N O17	656.1827	-0.77
			655.1749	C41 H25 N3 O6	C41 H26 N3 O6	656.1822	-1.55
12.305	Negative	655.1759	655.1781	C31 H31 N2 O14	C31 H32 N2 O14	656.1854	3.32
			655.1789	C46 H25 N O4	C46 H26 N O4	656.1862	4.58
			655.1727	C25 H35 O20	C25 H36 O20	656.18	-4.85
			529.3687	C36 H49 O3	C36 H50 O3	530.376	0.98
12.555	Negative	529.3682	529.3674	C34 H47 N3 O2	C34 H48 N3 O2	530.3747	-1.55
			529.3706	C24 H53 N2 O10	C24 H54 N2 O10	530.3778	4.47

12.721	Negative	499.3553	499.3541	C30 H47 N2 O4	C30 H48 N2 O4	500.3614	-2.34
			499.3568	C33 H45 N3 O	C33 H46 N3 O	500.3641	3.02
13.070	Negative	469.0318	469.0314	C24 H9 N2 O9	C24 H10 N2 O9	470.0386	-0.95
			469.034	C27 H7 N3 O6	C27 H8 N3 O6	470.0413	4.75
			469.0295	C36 H5 O2	C36 H6 O2	470.0368	4.89
13.569	Negative	517.3658	517.3647	C30 H49 N2 O5	C30 H50 N2 O5	518.372	-2.13
			517.3674	C33 H47 N3 O2	C33 H48 N3 O2	518.3747	3.04
13.902	Negative	455.3638	455.3643	C29 H47 N2 O2	C29 H48 N2 O2	456.3716	1.1
			455.3616	C26 H49 N O5	C26 H50 N O5	456.3689	-4.77
14.085	Negative	501.3702	501.3698	C30 H49 N2 O4	C30 H50 N2 O4	502.3771	-0.83
			501.3725	C33 H47 N3 O	C33 H48 N3 O	502.3797	4.5
14.435	Negative	715.1794	715.1789	C51 H25 N O4	C51 H26 N O4	716.1862	-0.69
			715.1786	C23 H39 O25	C23 H40 O25	716.1859	-1.13
			715.1781	C36 H31 N2 O14	C36 H32 N2 O14	716.1854	-1.85
			715.1808	C39 H29 N3 O11	C39 H30 N3 O11	716.188	1.9
			715.1813	C26 H37 N O22	C26 H38 N O22	716.1885	2.61
			715.1772	C21 H37 N3 O24	C21 H38 N3 O24	716.1845	-3.01
			715.1816	C54 H23 N2 O	C54 H24 N2 O	716.1889	3.05
			715.1821	C41 H31 O12	C41 H32 O12	716.1894	3.77
			715.1762	C48 H27 O7	C48 H28 O7	716.1835	-4.43
14.851	Negative	503.3856	503.3854	C30 H51 N2 O4	C30 H52 N2 O4	504.3927	-0.33
			503.3881	C33 H49 N3 O	C33 H50 N3 O	504.3954	4.98

			543.383	C35 H49 N3 O2	C35 H50 N3 O2	544.3903	0.6
15.200	Negative	543.3827	543.3844	C37 H51 O3	C37 H52 O3	544.3916	3.07
			543.3803	C32 H51 N2 O5	C32 H52 N2 O5	544.3876	-4.32
			387.1053	C30 H13 N	C30 H14 N	388.1126	0.12
15.416	Negative	387.1053	387.1045	C15 H19 N2 O10	C15 H20 N2 O10	388.1118	-2.01
			387.1072	C18 H17 N3 O7	C18 H18 N3 O7	388.1145	4.89
			729.1964	C40 H31 N3 O11	C40 H32 N3 O11	730.2037	1.24
			729.1946	C52 H27 N O4	C52 H28 N O4	730.2018	-1.29
			729.1942	C24 H41 O25	C24 H42 O25	730.2015	-1.72
			729.1969	C27 H39 N O22	C27 H40 N O22	730.2042	1.95
15.749	Negative	729.1955	729.1972	C55 H25 N2 O	C55 H26 N2 O	730.2045	2.38
			729.1937	C37 H33 N2 O14	C37 H34 N2 O14	730.201	-2.43
			729.1978	C42 H33 O12	C42 H34 O12	730.205	3.08
			729.1929	C22 H39 N3 O24	C22 H40 N3 O24	730.2002	-3.56
			729.1919	C49 H29 O7	C49 H30 O7	730.1992	-4.96
16.015	Negative	455.3621	455.3616	C26 H49 N O5	C26 H50 N O5	456.3689	-1.05
			455.3643	C29 H47 N2 O2	C29 H48 N2 O2	456.3716	4.83
16.315	Negative	455.3636	455.3643	C29 H47 N2 O2	C29 H48 N2 O2	456.3716	1.54
			455.3616	C26 H49 N O5	C26 H50 N O5	456.3689	-4.33
16.548	Negative	497.3748	497.3749	C31 H49 N2 O3	C31 H50 N2 O3	498.3821	0.13
16.764	Negative	471.3584	471.3592	C29 H47 N2 O3	C29 H48 N2 O3	472.3665	1.73
			471.3565	C26 H49 N O6	C26 H50 N O6	472.3638	-3.94

17.197	Negative	503.3866	503.3854	C30 H51 N2 O4	C30 H52 N2 O4	504.3927	-2.32
			503.3881	C33 H49 N3 O	C33 H50 N3 O	504.3954	3
17.779	Negative	501.3711	501.3698	C30 H49 N2 O4	C30 H50 N2 O4	502.3771	-2.62
			501.3725	C33 H47 N3 O	C33 H48 N3 O	502.3797	2.71
18.511	Negative		Noise				
18.794	Negative	789.2015	789.2023	C38 H35 N3 O16	C38 H36 N3 O16	790.2096	0.99
			789.2004	C50 H31 N O9	C50 H32 N O9	790.2077	-1.35
			789.2028	C25 H43 N O27	C25 H44 N O27	790.2101	1.64
			789.2031	C53 H29 N2 O6	C53 H30 N2 O6	790.2104	2.04
			789.1996	C35 H37 N2 O19	C35 H38 N2 O19	790.2069	-2.4
			789.2036	C40 H37 O17	C40 H38 O17	790.2109	2.69
			789.1978	C47 H33 O12	C47 H34 O12	790.205	-4.75
19.343	Negative	497.3755	497.3749	C31 H49 N2 O3	C31 H50 N2 O3	498.3821	-1.27
			497.3775	C34 H47 N3	C34 H48 N3	498.3848	4.11
19.642	Negative	497.3749	497.3749	C31 H49 N2 O3	C31 H50 N2 O3	498.3821	-0.07
20.141	Negative		Noise				
20.541	Negative	803.2194	803.2193	C41 H39 O17	C41 H40 O17	804.2265	-0.16
			803.2188	C54 H31 N2 O6	C54 H32 N2 O6	804.226	-0.8
			803.2184	C26 H45 N O27	C26 H46 N O27	804.2257	-1.19
			803.2179	C39 H37 N3 O16	C39 H38 N3 O16	804.2252	-1.83
			803.2211	C29 H43 N2 O24	C29 H44 N2 O24	804.2284	2.14
			803.2214	C57 H29 N3 O3	C57 H30 N3 O3	804.2287	2.54
			803.222	C44 H37 N O14	C44 H38 N O14	804.2292	3.18

20.541	Negative	803.2194	803.2161	C51 H33 N O9	C51 H34 N O9	804.2234	-4.13
			803.2228	C59 H31 O4	C59 H32 O4	804.2301	4.21
			803.2193	C41 H39 O17	C41 H40 O17	804.2265	-1.03
			803.2211	C29 H43 N2 O24	C29 H44 N2 O24	804.2284	1.27
			803.2188	C54 H31 N2 O6	C54 H32 N2 O6	804.226	-1.67
			803.2214	C57 H29 N3 O3	C57 H30 N3 O3	804.2287	1.67
20.973	Negative	803.2201	803.2184	C26 H45 N O27	C26 H46 N O27	804.2257	-2.06
			803.222	C44 H37 N O14	C44 H38 N O14	804.2292	2.3
			803.2179	C39 H37 N3 O16	C39 H38 N3 O16	804.2252	-2.7
			803.2228	C59 H31 O4	C59 H32 O4	804.2301	3.34
			803.2238	C32 H41 N3 O21	C32 H42 N3 O21	804.2311	4.61
			803.2161	C51 H33 N O9	C51 H34 N O9	804.2234	-5
			559.0334	C34 H9 N O8	C34 H10 N O8	560.0406	-0.42
21.705	Negative	559.0336	559.0325	C19 H15 N2 O18	C19 H16 N2 O18	560.0398	-1.9
			559.0352	C22 H13 N3 O15	C22 H14 N3 O15	560.0425	2.88
			559.036	C37 H7 N2 O5	C37 H8 N2 O5	560.0433	4.37
			469.0372	C17 H13 N2 O14	C17 H14 N2 O14	470.0445	-0.37
22.121	Negative	469.0374	469.0381	C32 H7 N O4	C32 H8 N O4	470.0453	1.4
			469.0354	C29 H9 O7	C29 H10 O7	470.0427	-4.31
22.903	Negative	497.3739	497.3749	C31 H49 N2 O3	C31 H50 N2 O3	498.3821	1.94
			497.3722	C28 H51 N O6	C28 H52 N O6	498.3795	-3.44
23.769	Negative	497.3760	497.3749	C31 H49 N2 O3	C31 H50 N2 O3	498.3821	-2.27
			497.3775	C34 H47 N3	C34 H48 N3	498.3848	3.1

			540.3443	C31 H46 N3 O5	C31 H47 N3 O5	541.3516	0.55
24.334	Negative	540.3440	540.3456	C33 H48 O6	C33 H49 O6	541.3529	3.03
			540.3416	C28 H48 N2 O8	C28 H49 N2 O8	541.3489	-4.41
			1101.3002	C68 H47 N O14	C68 H48 N O14	1102.3075	-0.54
			1101.3021	C56 H51 N3 O21	C56 H52 N3 O21	1102.3093	1.14
			1101.2994	C53 H53 N2 O24	C53 H54 N2 O24	1102.3067	-1.29
			1101.3029	C71 H45 N2 O11	C71 H46 N2 O11	1102.3102	1.89
			1101.3034	C58 H53 O22	C58 H54 O22	1102.3107	2.36
			1101.2975	C65 H49 O17	C65 H50 O17	1102.3048	-2.97
25.166	Negative	1101.3008	1101.297	C78 H41 N2 O6	C78 H42 N2 O6	1102.3043	-3.44
			1101.2967	C50 H55 N O27	C50 H56 N O27	1102.304	-3.72
			1101.3052	C46 H57 N2 O29	C46 H58 N2 O29	1102.3125	4.03
			1101.2962	C63 H47 N3 O16	C63 H48 N3 O16	1102.3035	-4.19
			1101.3056	C74 H43 N3 O8	C74 H44 N3 O8	1102.3128	4.32
			1101.3061	C61 H51 N O19	C61 H52 N O19	1102.3134	4.79
			497.3775	C34 H47 N3	C34 H48 N3	498.3848	1.1
26.813	Negative	497.3770	497.3789	C36 H49 O	C36 H50 O	498.3862	3.79
			497.3749	C31 H49 N2 O3	C31 H50 N2 O3	498.3821	-4.28
			1249.3406	C63 H61 O27	C63 H62 O27	1250.3478	-0.74
			1249.3427	C79 H51 N3 O13	C79 H52 N3 O13	1250.35	0.99
28.643	Negative	1249.3415	1249.3401	C76 H53 N2 O16	C76 H54 N2 O16	1250.3473	-1.15
			1249.3433	C66 H59 N O24	C66 H60 N O24	1250.3505	1.4
			1249.3392	C61 H59 N3 O26	C61 H60 N3 O26	1250.3465	-1.82

			1249.3374	C73 H55 N O19	C73 H56 N O19	1250.3447	-3.3
28.643	Negative	1249.3415	1249.3459	C69 H57 N2 O21	C69 H58 N2 O21	1250.3532	3.54
			1249.3365	C58 H61 N2 O29	C58 H62 N2 O29	1250.3438	-3.96
			877.2426	C28 H49 N2 O29	C28 H50 N2 O29	878.2499	0.17
			877.243	C56 H35 N3 O8	C56 H36 N3 O8	878.2502	0.53
			877.2435	C43 H43 N O19	C43 H44 N O19	878.2508	1.11
			877.2411	C68 H31 N O	C68 H32 N O	878.2484	-1.58
			877.2408	C40 H45 O22	C40 H46 O22	878.2481	-1.94
29.326	Negative	877.2425	877.2443	C58 H37 O9	C58 H38 O9	878.2516	2.06
			877.2403	C53 H37 N2 O11	C53 H38 N2 O11	878.2476	-2.52
			877.2453	C31 H47 N3 O26	C31 H48 N3 O26	878.2526	3.22
			877.2395	C38 H43 N3 O21	C38 H44 N3 O21	878.2467	-3.47
			877.2462	C46 H41 N2 O16	C46 H42 N2 O16	878.2534	4.16
			877.2384	C65 H33 O4	C65 H34 O4	878.2457	-4.63
			877.2467	C33 H49 O27	C33 H50 O27	878.2539	4.75
			1249.3433	C66 H59 N O24	C66 H60 N O24	1250.3505	-0.76
			1249.3427	C79 H51 N3 O13	C79 H52 N3 O13	1250.35	-1.17
			1249.3459	C69 H57 N2 O21	C69 H58 N2 O21	1250.3532	1.38
30.141	Negative	1249.3442	1249.3406	C63 H61 O27	C63 H62 O27	1250.3478	-2.9
			1249.3401	C76 H53 N2 O16	C76 H54 N2 O16	1250.3473	-3.31
			1249.3486	C72 H55 N3 O18	C72 H56 N3 O18	1250.3559	3.53
			1249.3491	C59 H63 N O29	C59 H64 N O29	1250.3564	3.94
			1249.3392	C61 H59 N3 O26	C61 H60 N3 O26	1250.3465	-3.98

30.141	Negative	1249.3442	1249.35	C74 H57 O19	C74 H58 O19	1250.3572	4.6
			1248.3467	C65 H58 N3 O23	C65 H59 N3 O23	1249.3539	0.29
			1248.3475	C80 H52 N2 O13	C80 H53 N2 O13	1249.3548	0.95
			1248.3448	C77 H54 N O16	C77 H55 N O16	1249.3521	-1.19
			1248.348	C67 H60 O24	C67 H61 O24	1249.3553	1.36
31.588	Negative	1248.3463	1248.344	C62 H60 N2 O26	C62 H61 N2 O26	1249.3513	-1.86
			1248.3421	C74 H56 O19	C74 H57 O19	1249.3494	-3.34
			1248.3507	C70 H58 N O21	C70 H59 N O21	1249.358	3.51
			1248.3413	C59 H62 N O29	C59 H63 N O29	1249.3486	-4
			1248.3408	C72 H54 N3 O18	C72 H55 N3 O18	1249.3481	-4.41
			1248.3525	C58 H62 N3 O28	C58 H63 N3 O28	1249.3598	4.99
			391.0064	C30 H N O	C30 H2 N O	392.0136	-1.37
33.535	Negative	391.0069	391.0082	C18 H5 N3 O8	C18 H6 N3 O8	392.0155	3.35
			391.0055	C15 H7 N2 O11	C15 H8 N2 O11	392.0128	-3.49
37.378	Negative	581.5408	581.5415	C39 H69 N2 O	C39 H70 N2 O	582.5488	1.27
			581.5389	C36 H71 N O4	C36 H72 N O4	582.5461	-3.33
39.974	Negative		Noise				
			1033.9916	C71 H6 O11	C71 H7 O11	1034.9988	0.06
			1033.9907	C56 H12 N O21	C56 H13 N O21	1034.998	-0.74
42.336	Negative	1033.9915	1033.9926	C44 H16 N3 O28	C44 H17 N3 O28	1034.9999	1.04
			1033.9902	C69 H4 N3 O10	C69 H5 N3 O10	1034.9975	-1.24
			1033.9934	C59 H10 N2 O18	C59 H11 N2 O18	1035.0007	1.85
			1033.9939	C46 H18 O29	C46 H19 O29	1035.0012	2.34

42.336	Negative	1033.9915	1033.9942	C74 H4 N O8	C74 H5 N O8	1035.0015	2.65
			1033.988	C53 H14 O24	C53 H15 O24	1034.9953	-3.33
			1033.9875	C66 H6 N2 O13	C66 H7 N2 O13	1034.9948	-3.83
			1033.9961	C62 H8 N3 O15	C62 H9 N3 O15	1035.0034	4.43
			1033.9867	C51 H12 N3 O23	C51 H13 N3 O23	1034.994	-4.63
			1033.9966	C49 H16 N O26	C49 H17 N O26	1035.0039	4.93
44.283	Negative	966.0013	966.0009	C53 H12 N O19	C53 H13 N O19	967.0082	-0.41
			966.0017	C68 H6 O9	C68 H7 O9	967.009	0.45
			966.0004	C66 H4 N3 O8	C66 H5 N3 O8	967.0077	-0.94
			966.0001	C38 H18 N2 O29	C38 H19 N2 O29	967.0073	-1.27
			966.0028	C41 H16 N3 O26	C41 H17 N3 O26	967.01	1.5
			966.0036	C56 H10 N2 O16	C56 H11 N2 O16	967.0109	2.36
			965.9985	C78 N O	C78 H N O	967.0058	-2.86
			966.0041	C43 H18 O27	C43 H19 O27	967.0114	2.89
			965.9982	C50 H14 O22	C50 H15 O22	967.0055	-3.18
			966.0044	C71 H4 N O6	C71 H5 N O6	967.0117	3.22
			965.9977	C63 H6 N2 O11	C63 H7 N2 O11	967.005	-3.71
			965.9969	C48 H12 N3 O21	C48 H13 N3 O21	967.0042	-4.57
45.032	Negative	951.2351	951.2353	C49 H43 O20	C49 H44 O20	952.2426	0.23
			951.2348	C62 H35 N2 O9	C62 H36 N2 O9	952.2421	-0.31
			951.2345	C34 H49 N O30	C34 H50 N O30	952.2418	-0.64
			951.234	C47 H41 N3 O19	C47 H42 N3 O19	952.2413	-1.18
			951.2372	C37 H47 N2 O27	C37 H48 N2 O27	952.2444	2.17

45.032	Negative	951.2351	951.233	C74 H31 O2	C74 H32 O2	952.2402	-2.25
			951.2375	C65 H33 N3 O6	C65 H34 N3 O6	952.2448	2.5
			951.238	C52 H41 N O17	C52 H42 N O17	952.2453	3.04
			951.2321	C59 H37 N O12	C59 H38 N O12	952.2394	-3.13
			951.2316	C72 H29 N3 O	C72 H30 N3 O	952.2389	-3.66
			951.2388	C67 H35 O7	C67 H36 O7	952.2461	3.91
			951.2313	C44 H43 N2 O22	C44 H44 N2 O22	952.2386	-4
			951.2398	C40 H45 N3 O24	C40 H46 N3 O24	952.2471	4.99
47.677	Negative			Noise			
50.007	Negative			Noise			
52.269	Negative			Noise			
55.480	Negative			Noise			
57.161	Negative			Noise			

Chapter 9

Bibliography

Abbas, T., & Dutta, A. (2009). p21 in cancer: intricate networks and multiple activities. *Nature Reviews Cancer, 9*(6), 400-414.

Abbastabar, M., Kheyrollah, M., Azizian, K., Bagherlou, N., Tehrani, S. S., Maniati, M., & Karimian, A. (2018). Multiple functions of p27 in cell cycle, apoptosis, epigenetic modification and transcriptional regulation for the control of cell growth: a double-edged sword protein. *DNA repair, 69*, 63-72.

Abdel-Tawab, M., Werz, O., & Schubert-Zsilavecz, M. (2011). Boswellia serrata. *Clinical pharmacokinetics, 50*(6), 349-369.

Abdoul-latif, F. M., Obame, L.-C., Bassolé, I. H. N., & Dicko, M. H. (2012). Antimicrobial activities of essential oil and methanol extract of Boswellia sacra Flueck. and Boswellia papyrifera (Del.) Hochst from Djibouti. *International Journal of Management, Modern Sciences and Technologies, 1*, 1-10.

Aboelsoud, N. H. (2010). Herbal medicine in ancient Egypt. *Journal of Medicinal Plants Research, 4*(2), 082-086.

Adhikari, S., Hussain, O., Phillips, R. M., Kaminsky, W., & Kollipara, M. R. (2018). Neutral and cationic half-sandwich arene d6 metal complexes containing pyridyl and pyrimidyl thiourea ligands with interesting bonding modes: Synthesis, structural and anti-cancer studies. *Applied Organometallic Chemistry, 32*(9), e4476.

Aggarwal, B. B., & Gehlot, P. (2009). Inflammation and cancer: how friendly is the relationship for cancer patients? *Current opinion in pharmacology, 9*(4), 351-369.

Agrahari, V., Bajpai, M., & Nanda, S. (2013). Essential Concepts of Mobile Phase Selection for Reversed Phase HPLC. *Research Journal of Pharmacy and Technology, 6*(5), 1.

Ahmed, H. H., Abd-Rabou, A. A., Hassan, A. Z., & Kotob, S. E. (2015). Phytochemical analysis and anti-cancer investigation of Boswellia serrata bioactive constituents in vitro. *Asian Pacific Journal of Cancer Prevention, 16*(16), 7179-7188.

AIHW. (2019). Australian Institute of Health and Welfare: Cancer in Australia: In brief 2019. *Cancer series no. 122*.

Al-Dosary, S. K. (2018). Antibacterial effect of Thymus sp. and Boswellia sp. extracts on Streptococcus pneumoniae and Klebsiella pneumoniae isolates. *African Journal of Biotechnology, 17*(5), 133-138.

Al-Harrasi, A., & Al-Saidi, S. (2008). Phytochemical analysis of the essential oil from botanically certified oleogum resin of Boswellia sacra (Omani Luban). *Molecules (Basel, Switzerland), 13*(9), 2181-2189.

Al-Harrasi, A., Hussain, H., Csuk, R., & Khan, H. Y. (2018). *Chemistry and bioactivity of boswellic acids and other terpenoids of the genus boswellia*: Elsevier.

Al-Qubaisi, M., Rozita, R., Yeap, S.-K., Omar, A.-R., Ali, A.-M., & Alitheen, N. B. (2011). Selective cytotoxicity of goniothalamin against hepatoblastoma HepG2 cells. *Molecules (Basel, Switzerland), 16*(4), 2944-2959.

Al-Yasiry, A. R. M., & Kiczorowska, B. (2016). Frankincense-therapeutic properties. *Advances in Hygiene & Experimental Medicine/Postepy Higieny i Medycyny Doswiadczalnej, 70*.

Alfarouk, K. O., Stock, C.-M., Taylor, S., Walsh, M., Muddathir, A. K., Verduzco, D., . . . Harguindey, S. (2015). Resistance to cancer chemotherapy: failure in drug response from ADME to P-gp. *Cancer cell international, 15*(1), 1-13.

Ali, E. N., & Mansour, S. Z. (2011). Boswellic acids extract attenuates pulmonary fibrosis induced by bleomycin and oxidative stress from gamma irradiation in rats. *Chinese Medicine, 6*(1), 1-14.

Alipanah, H., & Zareian, P. (2018). Anti-cancer properties of the methanol extract of Boswellia serrata gum resin: Cell proliferation arrest and inhibition of angiogenesis and metastasis in BALB/c mice breast cancer model. *Physiology and Pharmacology, 22*(3), 183-194.

Alitalo, K., Keski-oja, J., & Vaheri, A. (1981). Extracellular matrix proteins characterize human tumor cell lines. *International journal of cancer, 27*(6), 755-761.

Allemani, C., Weir, H. K., Carreira, H., Harewood, R., Spika, D., Wang, X.-S., . . . Bonaventure, A. (2015). Global surveillance of cancer survival 1995–2009: analysis of individual data for 25 676 887 patients from 279 population-based registries in 67 countries (CONCORD-2). *The Lancet, 385*(9972), 977-1010.

Almoallim, H., Abdulaziz, S., Fallatah, E., Alhazmi, H., Meraiani, N., Bazuhair, T., . . . Fathaldin, O. (2017). Clinical characteristics and outcomes of cancer patients with post-chemotherapy arthritis: a retrospective case series report. *Open access rheumatology: research and reviews, 9*, 111.

Althouse, R., Huff, J., Tomatis, L., & Wilbourn, J. (1979). Chemicals and industrial processes associated with cancer in humans. IARC Monographs, Volumes 1 to 20. *IARC monographs on the evaluation of the carcinogenic risk of chemicals to humans. Supplement*(1), 1-71.

Altmann, A., Poeckel, D., Fischer, L., Schubert-Zsilavecz, M., Steinhilber, D., & Werz, O. (2004). Coupling of boswellic acid-induced Ca2+ mobilisation and MAPK activation to lipid metabolism and peroxide formation in human leucocytes. *British journal of pharmacology, 141*(2), 223-232.

Amin, A., Gali-Muhtasib, H., Ocker, M., & Schneider-Stock, R. (2009). Overview of major classes of plant-derived anticancer drugs. *International journal of biomedical science: IJBS, 5*(1), 1.

Ammon. (2016). Boswellic acids and their role in chronic inflammatory diseases. *Anti-inflammatory Nutraceuticals and Chronic Diseases*, 291-327.

Ammon, Safayhi, H., Mack, T., & Sabieraj, J. (1993). Mechanism of antiinflammatory actions of curcumine and boswellic acids. *Journal of ethnopharmacology, 38*(2-3), 105-112.

Ammon, H. (2006). Boswellic acids in chronic inflammatory diseases. *Planta medica, 72*(12), 1100-1116.

Anderson, K., Lutz, C., Van Delft, F. W., Bateman, C. M., Guo, Y., Colman, S. M., . . . Swansbury, J. (2011). Genetic variegation of clonal architecture and propagating cells in leukaemia. *Nature, 469*(7330), 356-361.

Anthoni, C., Laukoetter, M. G., Rijcken, E., Vowinkel, T., Mennigen, R., Muller, S., . . . Bergmann, J. (2006). Mechanisms underlying the anti-inflammatory actions of boswellic acid derivatives in experimental colitis. *American Journal of Physiology-Gastrointestinal and Liver Physiology, 290*(6), G1131-G1137.

Antwi, C. A., Amisigo, C. M., Adjimani, J. P., & Gwira, T. M. (2019). In vitro activity and mode of action of phenolic compounds on Leishmania donovani. *PLoS neglected tropical diseases, 13*(2), e0007206.

Arnold, M., Leitzmann, M., Freisling, H., Bray, F., Romieu, I., Renehan, A., & Soerjomataram, I. (2016). Obesity and cancer: an update of the global impact. *Cancer epidemiology, 41*, 8-15.

Asad, M., & Alhomoud, M. (2016). Proulcerogenic effect of water extract of Boswellia sacra oleo gum resin in rats. *Pharmaceutical biology, 54*(2), 225-230.

Assefa, M., Dekebo, A., Kassa, H., Habtu, A., Fitwi, G., & Redi-Abshiro, M. (2012). Biophysical and chemical investigations of frankincense of Boswellia papyrifera from North and Northwestern Ethiopia. *Journal of Chemical and Pharmaceutical Research, 4*(2), 1074-1089.

Atanasov, A. G., Zotchev, S. B., Dirsch, V. M., & Supuran, C. T. (2021). Natural products in drug discovery: advances and opportunities. *Nature reviews Drug discovery*, 1-17.

Aubrey, B. J., Kelly, G. L., Janic, A., Herold, M. J., & Strasser, A. (2018). How does p53 induce apoptosis and how does this relate to p53-mediated tumour suppression? *Cell Death & Differentiation, 25*(1), 104-113.

Avendaño, C., & Menendez, J. C. (2015). *Medicinal chemistry of anticancer drugs*: Elsevier.

Backus, H., Pinedo, H., Wouters, D., Kuiper, C., Jansen, G., Van Groeningen, C., & Peters, G. (2001). Differences in the induction of DNA damage, cell cycle arrest, and cell death by 5-fluorouracil and antifolates. *Oncology Research Featuring Preclinical and Clinical Cancer Therapeutics, 12*(5), 231-239.

Badmus, J. A., Ekpo, O. E., Hussein, A. A., Meyer, M., & Hiss, D. C. (2019). Cytotoxic and cell cycle arrest properties of two steroidal alkaloids isolated from Holarrhena floribunda (G. Don) T. Durand & Schinz leaves. *BMC Complementary and Alternative Medicine, 19*(1), 1-9.

Baghel, U. S., Singh, A., Singh, D., & Sinha, M. (2017). Application of mass spectroscopy in pharmaceutical and biomedical analysis. In E. Sharmin & F. Zafar (Eds.), *Spectroscopic Analyses-Developments and Applications*. Retrieved from https://www.intechopen.com/books/spectroscopic-analyses-developments-and-applications/application-of-mass-spectroscopy-in-pharmaceutical-and-biomedical-analysis

Bagnardi, V., Rota, M., Botteri, E., Tramacere, I., Islami, F., Fedirko, V., . . . Pasquali, E. (2015). Alcohol consumption and site-specific cancer risk: a comprehensive dose–response meta-analysis. *British journal of cancer, 112*(3), 580-593.

Baguley, B. (1991). DNA intercalating anti-tumour agents. *Anti-cancer drug design, 6*(1), 1-35.

Bai, J., Li, Y., & Zhang, G. (2017). Cell cycle regulation and anticancer drug discovery. *Cancer biology & medicine, 14*(4), 348.

Balk, S. P., Ko, Y.-J., & Bubley, G. J. (2003). Biology of prostate-specific antigen. *Journal of clinical oncology, 21*(2), 383-391.

Banno, N., Akihisa, T., Yasukawa, K., Tokuda, H., Tabata, K., Nakamura, Y., . . . Suzuki, T. (2006). Anti-inflammatory activities of the triterpene acids from the resin of Boswellia carteri. *Journal of ethnopharmacology, 107*(2), 249-253.

Bardal, S. K., Waechter, J. E., & Martin, D. S. (2011). *Applied pharmacology*: Elsevier Health Sciences.

Barentsz, J., Takahashi, S., Oyen, W., Mus, R., De Mulder, P., Reznek, R., . . . Mali, W. (2006). Commonly used imaging techniques for diagnosis and staging. *Journal of clinical oncology, 24*(20), 3234-3244.

Barkan, N. P., Turan, S. K., Yildizhan, H., Demiralp, F. D. Ö., Uslu, B., & Ozkan, S. A. (2018). Conventional and current imaging techniques in cancer research and clinics. In *Design of Nanostructures for Theranostics Applications* (pp. 493-528): Elsevier.

Bartek, J., & Lukas, J. (2003). Chk1 and Chk2 kinases in checkpoint control and cancer. *Cancer cell, 3*(5), 421-429.

Baudino. (2015). Targeted cancer therapy: the next generation of cancer treatment. *Current drug discovery technologies, 12*(1), 3-20.

Beghelli, D., Isani, G., Roncada, P., Andreani, G., Bistoni, O., Bertocchi, M., . . . Alunno, A. (2017). Antioxidant and ex vivo immune system regulatory properties of Boswellia serrata extracts. *Oxidative medicine and cellular longevity, 2017*.

Bekana, D., Kebede, T., Assefa, M., & Kassa, H. (2014). Comparative phytochemical analyses of resins of Boswellia species (B. papyrifera (Del.) Hochst., B. neglecta S. Moore, and B. rivae Engl.) from northwestern, southern, and southeastern Ethiopia. *International Scholarly Research Notices, 2014*.

Bendris, N., Lemmers, B., & Blanchard, J. M. (2015). Cell cycle, cytoskeleton dynamics and beyond: the many functions of cyclins and CDK inhibitors. *Cell Cycle, 14*(12), 1786-1798.

Berman, H. M., & Young, P. R. (1981). The interaction of intercalating drugs with nucleic acids. *Annual review of biophysics and bioengineering, 10*(1), 87-114.

Bernardini, S., Tiezzi, A., Laghezza Masci, V., & Ovidi, E. (2018). Natural products for human health: an historical overview of the drug discovery approaches. *Natural product research, 32*(16), 1926-1950.

Bertocchi, M., Isani, G., Medici, F., Andreani, G., Tubon Usca, I., Roncada, P., . . . Bernardini, C. (2018). Anti-inflammatory activity of Boswellia serrata extracts: an in vitro study on porcine aortic endothelial cells. *Oxidative medicine and cellular longevity, 2018*.

Bertoli, C., Skotheim, J. M., & De Bruin, R. A. (2013). Control of cell cycle transcription during G1 and S phases. *Nature reviews Molecular cell biology, 14*(8), 518-528.

Bertram, J. S. (2000). The molecular biology of cancer. *Molecular aspects of medicine, 21*(6), 167-223.

Bhutada, S. A., Muneer Farhan, M., & Dahikar, S. B. (2017). Preliminary phytochemical screening and antibacterial activity of resins of Boswellia serrata Roxb. *J Pharmacogn Phytochem, 6*, 182-185.

Biggs, I., Sirdaarta, J., White, A., & Cock, I. E. (2016). GC-MS Analysis of Frankincense Extracts which Inhibit the Growth of Bacterial Triggers of Selected Autoimmune Diseases. *Pharmacognosy Communications, 6*(1).

Bonelli, M., La Monica, S., Fumarola, C., & Alfieri, R. (2019). Multiple effects of CDK4/6 inhibition in cancer: From cell cycle arrest to immunomodulation. *Biochemical pharmacology, 170*, 113676.

Bortner, D. M., & Rosenberg, M. P. (1997). Induction of mammary gland hyperplasia and carcinomas in transgenic mice expressing human cyclin E. *Molecular and cellular biology, 17*(1), 453-459.

Bouchardy, C., Verkooijen, H. M., & Fioretta, G. (2006). Social class is an important and independent prognostic factor of breast cancer mortality. *International journal of cancer, 119*(5), 1145-1151.

Brana, M., Cacho, M., Gradillas, A., Pascual-Teresa, B. d., & Ramos, A. (2001). Intercalators as anticancer drugs. *Current pharmaceutical design, 7*(17), 1745-1780.

Brauchle, E., Thude, S., Brucker, S. Y., & Schenke-Layland, K. (2014). Cell death stages in single apoptotic and necrotic cells monitored by Raman microspectroscopy. *Scientific reports, 4*(1), 1-9.

Bray, F., Ferlay, J., Soerjomataram, I., Siegel, R. L., Torre, L. A., & Jemal, A. (2018). Global cancer statistics 2018: GLOBOCAN estimates of incidence and mortality worldwide for 36 cancers in 185 countries. *CA: a cancer journal for clinicians, 68*(6), 394-424.

Bretones, G., Delgado, M. D., & León, J. (2015). Myc and cell cycle control. *Biochimica et Biophysica Acta (BBA)-Gene Regulatory Mechanisms, 1849*(5), 506-516.

Brown, K. F., Rumgay, H., Dunlop, C., Ryan, M., Quartly, F., Cox, A., . . . Hounsome, L. (2018). The fraction of cancer attributable to modifiable risk factors in England, Wales, Scotland, Northern Ireland, and the United Kingdom in 2015. *British journal of cancer, 118*(8), 1130-1141.

Brusotti, G., Cesari, I., Dentamaro, A., Caccialanza, G., & Massolini, G. (2014). Isolation and characterization of bioactive compounds from plant resources: the role of analysis in the ethnopharmacological approach. *Journal of pharmaceutical and biomedical analysis, 87*, 218-228.

Büchele, B., Zugmaier, W., & Simmet, T. (2003). Analysis of pentacyclic triterpenic acids from frankincense gum resins and related phytopharmaceuticals by high-performance liquid chromatography. Identification of lupeolic acid, a novel pentacyclic triterpene. *Journal of Chromatography B, 791*(1-2), 21-30.

Buchele, B. Z. W., Estrada, A. G. F., Syrovets, T. P. C., & Schneider, B. S. T. (2006). Characterization of-Acetyl-11-keto-boswellic Acid, a Pentacyclic Triterpenoid Inducing Apoptosis in vitro and in vivo. *Planta Medica-Natural Products and Medicinal Plant Research, 72*(14), 1285-1289.

Butler, M. S. (2004). The role of natural product chemistry in drug discovery. *Journal of natural products, 67*(12), 2141-2153.

Cabo-Calvet, E., Ortiz-Bolsico, C., Baeza-Baeza, J. J., & García-Alvarez-Coque, M. C. (2014). Description of the retention and peak profile for chromolith columns in isocratic and gradient elution using mobile phase composition and flow rate as factors. *Chromatography, 1*(4), 194-210.

Camarda, L., Dayton, T., Di Stefano, V., Pitonzo, R., & Schillaci, D. (2007). Chemical composition and antimicrobial activity of some oleogum resin essential oils from Boswellia spp.(Burseraceae). *Annali di Chimica: Journal of Analytical, Environmental and Cultural Heritage Chemistry, 97*(9), 837-844.

Cao, X., Pobezinskaya, Y. L., Morgan, M. J., & Liu, Z. g. (2011). The role of TRADD in TRAIL-induced apoptosis and signaling. *The FASEB Journal, 25*(4), 1353-1358.

Carelle, N., Piotto, E., Bellanger, A., Germanaud, J., Thuillier, A., & Khayat, D. (2002). Changing patient perceptions of the side effects of cancer chemotherapy. *Cancer, 95*(1), 155-163.

Casimiro, M. C., Crosariol, M., Loro, E., Li, Z., & Pestell, R. G. (2012). Cyclins and cell cycle control in cancer and disease. *Genes & cancer, 3*(11-12), 649-657.

Cavalcante, G. C., Schaan, A. P., Cabral, G. F., Santana-da-Silva, M. N., Pinto, P., Vidal, A. F., & Ribeiro-dos-Santos, Â. (2019). A cell's fate: an overview of the molecular biology and genetics of apoptosis. *International journal of molecular sciences, 20*(17), 4133.

Cazzalini, O., Perucca, P., Savio, M., Necchi, D., Bianchi, L., Stivala, L. A., . . . Prosperi, E. (2008). Interaction of p21 CDKN1A with PCNA regulates the histone acetyltransferase activity of p300 in nucleotide excision repair. *Nucleic acids research, 36*(5), 1713-1722.

Celeghini, R., Vilegas, J. H., & Lanças, F. M. (2001). Extraction and quantitative HPLC analysis of coumarin in hydroalcoholic extracts of Mikania glomerata Spreng:(" guaco") leaves. *Journal of the Brazilian Chemical Society, 12*(6), 706-709.

Cha, H. H., Cram, E. J., Wang, E. C., Huang, A. J., Kasler, H. G., & Firestone, G. L. (1998). Glucocorticoids stimulate p21 gene expression by targeting multiple transcriptional elements within a steroid responsive region of the p21 waf1/cip1 promoter in rat hepatoma cells. *Journal of Biological Chemistry, 273*(4).

Chaitanya, G. V., Alexander, J. S., & Babu, P. P. (2010). PARP-1 cleavage fragments: signatures of cell-death proteases in neurodegeneration. *Cell Communication and Signaling, 8*(1), 1-11.

Chao, H. X., Poovey, C. E., Privette, A. A., Grant, G. D., Chao, H. Y., Cook, J. G., & Purvis, J. E. (2017). Orchestration of DNA damage checkpoint dynamics across the human cell cycle. *Cell systems, 5*(5), 445-459.

Chari, R. V. (2008). Targeted cancer therapy: conferring specificity to cytotoxic drugs. *Accounts of chemical research, 41*(1), 98-107.

Checkley, S., MacCallum, L., Yates, J., Jasper, P., Luo, H., Tolsma, J., & Bendtsen, C. (2015). Bridging the gap between in vitro and in vivo: dose and schedule predictions for the ATR inhibitor AZD6738. *Scientific reports, 5*(1), 1-12.

Chemat, F., Abert Vian, M., Ravi, H. K., Khadhraoui, B., Hilali, S., Perino, S., & Fabiano Tixier, A.-S. (2019). Review of alternative solvents for green extraction of food and natural products: Panorama, principles, applications and prospects. *Molecules (Basel, Switzerland), 24*(16), 3007.

Chen. (2016). The cell-cycle arrest and apoptotic functions of p53 in tumor initiation and progression. *Cold Spring Harbor perspectives in medicine, 6*(3), a026104.

Chen, Jia, Y., Song, W., & Zhang, L. (2018). Therapeutic potential of nitrogen mustard based hybrid molecules. *Frontiers in pharmacology, 9*, 1453.

Chen, Peng, C., Sullivan, C., Li, D., & Li, S. (2010). Critical molecular pathways in cancer stem cells of chronic myeloid leukemia. *Leukemia, 24*(9), 1545-1554.

Chen, Yang, T.-Y., Wu, C.-C., Cheng, C.-C., Hsu, S.-L., Hung, H.-W., . . . Chang, G.-C. (2014). Pemetrexed induces S-phase arrest and apoptosis via a deregulated activation of Akt signaling pathway. *Plos one, 9*(5), e97888.

Chen, Zhou, C., Ge, Z., Liu, Y., Liu, Y., Feng, W., . . . Wei, T. (2013). Composition and potential anticancer activities of essential oils obtained from myrrh and frankincense. *Oncology letters, 6*(4), 1140-1146.

Chen, W., Dong, J., Haiech, J., Kilhoffer, M.-C., & Zeniou, M. (2016). Cancer stem cell quiescence and plasticity as major challenges in cancer therapy. *Stem cells international, 2016*.

Chi, J. J., Li, H., Zhou, Z., Izquierdo-Ferrer, J., Xue, Y., Wavelet, C. M., . . . Lu, X. (2019). A novel strategy to block mitotic progression for targeted therapy. *EBioMedicine, 49*, 40-54.

Choudhari, A. S., Mandave, P. C., Deshpande, M., Ranjekar, P., & Prakash, O. (2020). Phytochemicals in cancer treatment: From preclinical studies to clinical practice. *Frontiers in pharmacology, 10*, 1614.

Ciarallo, S., Subramaniam, V., Hung, W., Lee, J.-H., Kotchetkov, R., Sandhu, C., . . . Slingerland, J. M. (2002). Altered p27Kip1 phosphorylation, localization, and function in human epithelial cells resistant to transforming growth factor β-mediated G1 arrest. *Molecular and cellular biology, 22*(9), 2993-3002.

Cilloni, D., & Saglio, G. (2012). Molecular pathways: Bcr-abl. *Clinical Cancer Research, 18*(4), 930-937.

Cinausero, M., Aprile, G., Ermacora, P., Basile, D., Vitale, M. G., Fanotto, V., . . . Sonis, S. T. (2017). New frontiers in the pathobiology and treatment of cancer regimen-related mucosal injury. *Frontiers in pharmacology, 8*, 354.

Clifford, B., Beljin, M., Stark, G. R., & Taylor, W. R. (2003). G2 arrest in response to topoisomerase II inhibitors: the role of p53. *Cancer research, 63*(14), 4074-4081.

Coates, A., Abraham, S., Kaye, S. B., Sowerbutts, T., Frewin, C., Fox, R., & Tattersall, M. (1983). On the receiving end—patient perception of the side-effects of cancer chemotherapy. *European Journal of Cancer and Clinical Oncology, 19*(2), 203-208.

Coley, H. M. (2008). Mechanisms and strategies to overcome chemotherapy resistance in metastatic breast cancer. *Cancer treatment reviews, 34*(4), 378-390.

Conklin. (2004). Chemotherapy-associated oxidative stress: impact on chemotherapeutic effectiveness. *Integrative cancer therapies, 3*(4), 294-300.

Conklin, K. A. (2004). Cancer chemotherapy and antioxidants. *The Journal of nutrition, 134*(11), 3201S-3204S.

Cooper, G. M., & Hausman, R. E. (2019). *The cell: a molecular approach* (8th ed.). USA: Oxford University Press.

Coussens, L. M., & Werb, Z. (2002). Inflammation and cancer. *Nature, 420*(6917), 860-867.

Cox, T. R., & Erler, J. T. (2011). Remodeling and homeostasis of the extracellular matrix: implications for fibrotic diseases and cancer. *Disease models & mechanisms, 4*(2), 165-178.

Cragg, G. M., & Newman, D. J. (2005). Plants as a source of anti-cancer agents. *Journal of ethnopharmacology, 100*(1-2), 72-79.

Cragg, G. M., & Pezzuto, J. M. (2016). Natural products as a vital source for the discovery of cancer chemotherapeutic and chemopreventive agents. *Medical Principles and Practice, 25*(Suppl. 2), 41-59.

CRUK. (2020a). Cancer Research UK: Cancer incidence by age. Retrieved from https://www.cancerresearchuk.org/health-professional/cancer-statistics/incidence/age

CRUK. (2020b). Cancer Research UK: Cancer Statistics for the UK. Retrieved from https://www.cancerresearchuk.org/health-professional/cancer-statistics-for-the-uk

CRUK. (2020c). Cancer Research UK: Worldwide cancer statistics. Retrieved from https://www.cancerresearchuk.org/health-professional/cancer-statistics/worldwide-cancer

CRUK. (2021a). Cancer Research UK: Chemotherapy. Retrieved from https://www.cancerresearchuk.org/about-cancer/cancer-in-general/treatment/chemotherapy

CRUK. (2021b). Cancer treatment statistics. Retrieved from https://www.cancerresearchuk.org/health-professional/cancer-statistics/treatment

Cupit-Link, M. C., Kirkland, J. L., Ness, K. K., Armstrong, G. T., Tchkonia, T., LeBrasseur, N. K., . . . Hashmi, S. K. (2017). Biology of premature ageing in survivors of cancer. *Esmo Open, 2*(5), e000250.

Dai, X., Zhang, J., Arfuso, F., Chinnathambi, A., Zayed, M. E., Alharbi, S. A., . . . Sethi, G. (2015). Targeting TNF-related apoptosis-inducing ligand (TRAIL) receptor by natural products as a potential therapeutic approach for cancer therapy. *Experimental Biology and Medicine, 240*(6), 760-773.

Dailey, A., & Vuong, Q. V. (2015). Effect of extraction solvents on recovery of bioactive compounds and antioxidant properties from macadamia (Macadamia tetraphylla) skin waste. *Cogent Food & Agriculture, 1*(1), 1115646.

Danaei, G., Vander Hoorn, S., Lopez, A. D., Murray, C. J., Ezzati, M., & group, C. R. A. c. (2005). Causes of cancer in the world: comparative risk assessment of nine behavioural and environmental risk factors. *The Lancet, 366*(9499), 1784-1793.

Darzynkiewicz, Z., Juan, G., & Bedner, E. (1999). Determining cell cycle stages by flow cytometry. *Current protocols in cell biology, 1*(1), 8-4.

Davidovich, P., Kearney, C. J., & Martin, S. J. (2014). Inflammatory outcomes of apoptosis, necrosis and necroptosis. *Biological chemistry, 395*(10), 1163-1171.

de Oliveira, P. F., Alves, J. M., Damasceno, J. L., Oliveira, R. A. M., Dias, H. J., Crotti, A. E. M., & Tavares, D. C. (2015). Cytotoxicity screening of essential oils in cancer cell lines. *Revista Brasileira de Farmacognosia, 25*(2), 183-188.

Dean, M., Fojo, T., & Bates, S. (2005). Tumour stem cells and drug resistance. *Nature Reviews Cancer, 5*(4), 275-284.

DeCarlo, A., Johnson, S., Okeke-Agulu, K. I., Dosoky, N. S., Wax, S. J., Owolabi, M. S., & Setzer, W. N. (2019). Compositional analysis of the essential oil of Boswellia dalzielii frankincense from West Africa reveals two major chemotypes. *Phytochemistry, 164*, 24-32.

DeCarlo, A., Johnson, S., Poudel, A., Satyal, P., Bangerter, L., & Setzer, W. N. (2018). Chemical Variation in Essential Oils from the Oleo-gum Resin of Boswellia carteri: A Preliminary Investigation. *Chemistry & biodiversity, 15*(6), e1800047.

Desai, A. G., Qazi, G. N., Ganju, R. K., El-Tamer, M., Singh, J., Saxena, A. K., . . . Bhat, H. K. (2008). Medicinal plants and cancer chemoprevention. *Current drug metabolism, 9*(7), 581-591.

Desgrosellier, J. S., & Cheresh, D. A. (2010). Integrins in cancer: biological implications and therapeutic opportunities. *Nature Reviews Cancer, 10*(1), 9-22.

Dewson, G., & Kluck, R. M. (2009). Mechanisms by which Bak and Bax permeabilise mitochondria during apoptosis. *Journal of cell science, 122*(16), 2801-2808.

Dholwani, K. K., Saluja, A. K., Gupta, A. R., & Shah, D. R. (2008). A review on plant-derived natural products and their analogs with anti-tumor activity. *Indian journal of pharmacology, 40*(2), 49.

Di Rora, A. G. L., Iacobucci, I., & Martinelli, G. (2017). The cell cycle checkpoint inhibitors in the treatment of leukemias. *Journal of hematology & oncology, 10*(1), 1-14.

Dias, D. A., Urban, S., & Roessner, U. (2012). A historical overview of natural products in drug discovery. *Metabolites, 2*(2), 303-336.

Dick, F. A., & Rubin, S. M. (2013). Molecular mechanisms underlying RB protein function. *Nature reviews Molecular cell biology, 14*(5), 297-306.

Dickens, L. S., Boyd, R. S., Jukes-Jones, R., Hughes, M. A., Robinson, G. L., Fairall, L., . . . MacFarlane, M. (2012). A death effector domain chain DISC model reveals a crucial role for caspase-8 chain assembly in mediating apoptotic cell death. *Molecular cell, 47*(2), 291-305.

Ding, L., Cao, J., Lin, W., Chen, H., Xiong, X., Ao, H., . . . Cui, Q. (2020). The roles of cyclin-dependent kinases in cell-cycle progression and therapeutic strategies in human breast cancer. *International journal of molecular sciences, 21*(6), 1960.

DiPaola, R. S. (2002). To arrest or not to G2-M Cell-cycle arrest: commentary re: AK Tyagi et al., Silibinin strongly synergizes human prostate carcinoma DU145 cells to doxorubicin-induced growth inhibition, G2-M arrest, and apoptosis. Clin. Cancer Res., 8: 3512–3519, 2002. *Clinical Cancer Research, 8*(11), 3311-3314.

Dolcet, X., Llobet, D., Pallares, J., & Matias-Guiu, X. (2005). NF-kB in development and progression of human cancer. *Virchows archiv, 446*(5), 475-482.

Dorstyn, L., Akey, C. W., & Kumar, S. (2018). New insights into apoptosome structure and function. *Cell Death & Differentiation, 25*(7), 1194-1208.

Doughari, J. H., Human, I. S., Benadé, A. J., & Ndakidemi, P. A. (2009). Phytochemicals as chemotherapeutic agents and antioxidants: Possible solution to the control of antibiotic resistant verocytotoxin producing bacteria.

Drabløs, F., Feyzi, E., Aas, P. A., Vaagbø, C. B., Kavli, B., Bratlie, M. S., . . . Krokan, H. E. (2004). Alkylation damage in DNA and RNA—repair mechanisms and medical significance. *DNA repair, 3*(11), 1389-1407.

Druker, B. J., Guilhot, F., O'Brien, S. G., Gathmann, I., Kantarjian, H., Gattermann, N., . . . Stone, R. M. (2006). Five-year follow-up of patients receiving imatinib for chronic myeloid leukemia. *New England Journal of Medicine, 355*(23), 2408-2417.

Du, W., & Searle, J. S. (2009). The rb pathway and cancer therapeutics. *Current drug targets, 10*(7), 581-589.

Duffy. (2013). The war on cancer: are we winning? *Tumor Biology, 34*(3), 1275-1284.

Duffy, M. J. (2013). Tumor markers in clinical practice: a review focusing on common solid cancers. *Medical Principles and Practice, 22*(1), 4-11.

Dunn, J. M., Phillips, R. A., Becker, A. J., & Gallie, B. L. (1988). Identification of germline and somatic mutations affecting the retinoblastoma gene. *Science, 241*(4874), 1797-1800.

Dyson, N. J. (2016). RB1: a prototype tumor suppressor and an enigma. *Genes & development, 30*(13), 1492-1502.

Eastman, A. (2017). Improving anticancer drug development begins with cell culture: misinformation perpetrated by the misuse of cytotoxicity assays. *Oncotarget, 8*(5), 8854.

Egger, K., Werner, M., Meining, A., Ott, R., Allescher, H., Höfler, H., . . . Rösch, T. (2003). Biopsy surveillance is still necessary in patients with Barrett's oesophagus despite new endoscopic imaging techniques. *Gut, 52*(1), 18-23.

El-Awady, R., Saleh, E., Hashim, A., Soliman, N., Dallah, A., Elrasheed, A., & Elakraa, G. (2017). The role of eukaryotic and prokaryotic ABC transporter family in failure of chemotherapy. *Frontiers in pharmacology, 7*, 535.

Ellis, L., Canchola, A. J., Spiegel, D., Ladabaum, U., Haile, R., & Gomez, S. L. (2018). Racial and ethnic disparities in cancer survival: the contribution of tumor, sociodemographic, institutional, and neighborhood characteristics. *Journal of clinical oncology, 36*(1), 25.

Elmore, S. (2007). Apoptosis: a review of programmed cell death. *Toxicologic pathology, 35*(4), 495-516.

Engel, B. E., Cress, W. D., & Santiago-Cardona, P. G. (2015). The retinoblastoma protein: a master tumor suppressor acts as a link between cell cycle and cell adhesion. *Cell health and cytoskeleton, 7*, 1.

Eramo, A., Ricci-Vitiani, L., Zeuner, A., Pallini, R., Lotti, F., Sette, G., . . . De Maria, R. (2006). Chemotherapy resistance of glioblastoma stem cells. *Cell Death & Differentiation, 13*(7), 1238-1241.

Ernst, E. (2008). Frankincense: systematic review. *Bmj, 337*.

Ersoy, O. (2005). Very high alpha-fetoprotein in a young man due to concomitant presentation of hepatocellular carcinoma and Sertoli cell testis tumor. *World Journal of Gastroenterology, 11*(44), 7051.

Escalante, J., McQuade, R. M., Stojanovska, V., & Nurgali, K. (2017). Impact of chemotherapy on gastrointestinal functions and the enteric nervous system. *Maturitas, 105*, 23-29.

Eymin, B., & Gazzeri, S. (2010). Role of cell cycle regulators in lung carcinogenesis. *Cell adhesion & migration, 4*(1), 114-123.

Farombi, E. O. (2003). African indigenous plants with chemotherapeutic potentials and biotechnological approach to the production of bioactive prophylactic agents. *African Journal of Biotechnology, 2*(12), 662-671.

Fass, L. (2008). Imaging and cancer: a review. *Molecular oncology, 2*(2), 115-152.

Feeley, K. M., & Wells, M. (2001). Precursor lesions of ovarian epithelial malignancy. *Histopathology, 38*(2), 87-95.

Ferlay, J., Wild, C. P., & Bray, F. (2016). The burden of cancer worldwide: Current and future perspectives. *Holland-Frei Cancer Medicine*, 1-15.

Fernald, K., & Kurokawa, M. (2013). Evading apoptosis in cancer. *Trends in cell biology, 23*(12), 620-633.
Festjens, N., Berghe, T. V., & Vandenabeele, P. (2006). Necrosis, a well-orchestrated form of cell demise: signalling cascades, important mediators and concomitant immune response. *Biochimica et Biophysica Acta (BBA)-Bioenergetics, 1757*(9-10), 1371-1387.
Fink, S. L., & Cookson, B. T. (2005). Apoptosis, pyroptosis, and necrosis: mechanistic description of dead and dying eukaryotic cells. *Infection and immunity, 73*(4), 1907-1916.
Florescu, M., Cinteza, M., & Vinereanu, D. (2013). Chemotherapy-induced cardiotoxicity. *Maedica, 8*(1), 59.
Foster, I. (2008). Cancer: A cell cycle defect. *Radiography, 14*(2), 144-149.
Frank, Yang, Q., Osban, J., Azzarello, J. T., Saban, M. R., Saban, R., . . . Lin, H.-K. (2009). Frankincense oil derived from Boswellia carteri induces tumor cell specific cytotoxicity. *BMC Complementary and Alternative Medicine, 9*(1), 1-11.
Frank, A., & Unger, M. (2006). Analysis of frankincense from various Boswellia species with inhibitory activity on human drug metabolising cytochrome P450 enzymes using liquid chromatography mass spectrometry after automated on-line extraction. *Journal of Chromatography A, 1112*(1-2), 255-262.
Franker, M. A. M., & Hoogenraad, C. C. (2013). Microtubule-based transport–basic mechanisms, traffic rules and role in neurological pathogenesis. *Journal of cell science, 126*(11), 2319-2329.
Fridlender, M., Kapulnik, Y., & Koltai, H. (2015). Plant derived substances with anti-cancer activity: from folklore to practice. *Frontiers in plant science, 6*, 799.
Fridman, J. S., & Lowe, S. W. (2003). Control of apoptosis by p53. *Oncogene, 22*(56), 9030-9040.
Fu, D., Calvo, J. A., & Samson, L. D. (2012). Balancing repair and tolerance of DNA damage caused by alkylating agents. *Nature Reviews Cancer, 12*(2), 104-120.
Fulda, S. (2009). Tumor resistance to apoptosis. *International journal of cancer, 124*(3), 511-515.
Fulda, S., & Debatin, K.-M. (2006). Extrinsic versus intrinsic apoptosis pathways in anticancer chemotherapy. *Oncogene, 25*(34), 4798-4811.
Galluzzi, L., Vitale, I., Aaronson, S. A., Abrams, J. M., Adam, D., Agostinis, P., . . . Andrews, D. W. (2018). Molecular mechanisms of cell death: recommendations of the Nomenclature Committee on Cell Death 2018. *Cell Death & Differentiation, 25*(3), 486-541.
Galmarini, C. M., Mackey, J. R., & Dumontet, C. (2002). Nucleoside analogues and nucleobases in cancer treatment. *The Lancet Oncology, 3*(7), 415-424.
García-Morales, P., Hernando, E., Carrasco-García, E., Menéndez-Gutierrez, M. P., Saceda, M., & Martínez-Lacaci, I. (2006). Cyclin D3 is down-regulated by rapamycin in HER-2-overexpressing breast cancer cells. *Molecular cancer therapeutics, 5*(9), 2172-2181.
García-Reyes, B., Kretz, A.-L., Ruff, J.-P., Von Karstedt, S., Hillenbrand, A., Knippschild, U., . . . Lemke, J. (2018). The emerging role of cyclin-dependent kinases (CDKs) in pancreatic ductal adenocarcinoma. *International journal of molecular sciences, 19*(10), 3219.
Gartung, A., Yang, J., Sukhatme, V. P., Bielenberg, D. R., Fernandes, D., Chang, J., . . . Huang, S. (2019). Suppression of chemotherapy-induced cytokine/lipid mediator surge and ovarian cancer by a dual COX-2/sEH inhibitor. *Proceedings of the National Academy of Sciences, 116*(5), 1698-1703.
Gascoigne, K. E., & Taylor, S. S. (2009). How do anti-mitotic drugs kill cancer cells? *Journal of cell science, 122*(15), 2579-2585.
Gates, K. S. (2009). An overview of chemical processes that damage cellular DNA: spontaneous hydrolysis, alkylation, and reactions with radicals. *Chemical research in toxicology, 22*(11), 1747-1760.
Gerber, D. E. (2008). Targeted therapies: a new generation of cancer treatments. *American family physician, 77*(3), 311-319.
Giacinti, C., & Giordano, A. (2006). RB and cell cycle progression. *Oncogene, 25*(38), 5220-5227.

Gille, L., & Nohl, H. (1997). Analyses of the molecular mechanism of adriamycin-induced cardiotoxicity. *Free radical biology and medicine, 23*(5), 775-782.
Glaser, T., Winter, S., Groscurth, P., Safayhi, H., Sailer, E., Ammon, H., . . . Weller, M. (1999). Boswellic acids and malignant glioma: induction of apoptosis but no modulation of drug sensitivity. *British journal of cancer, 80*(5), 756-765.
Goda, A. E., Erikson, R. L., Ahn, J.-S., & Kim, B.-Y. (2015). Induction of G1 arrest by SB265610 involves cyclin D3 down-regulation and suppression of CDK2 (Thr160) phosphorylation. *Anticancer research, 35*(6), 3235-3243.
Goftar, M. K., Kor, N. M., & Kor, Z. M. (2014). DNA intercalators and using them as anticancer drugs. *Int. J. Adv. Biol. Biomed. Res, 2*(3), 811-822.
Golstein, P., & Kroemer, G. (2007). Cell death by necrosis: towards a molecular definition. *Trends in biochemical sciences, 32*(1), 37-43.
Gonzalez, H., Hagerling, C., & Werb, Z. (2018). Roles of the immune system in cancer: from tumor initiation to metastatic progression. *Genes & development, 32*(19-20), 1267-1284.
Grant, G. D., & Cook, J. G. (2017). The Temporal Regulation of S Phase Proteins During G 1. *DNA Replication*, 335-369.
Greenblatt, M. (1994). Mutations in the p53 tumor suppressor gene: clues to cancer etiology and molecular pathogenesis. *Cancer Res., 54*, 4855-4878.
Greten, F. R., & Grivennikov, S. I. (2019). Inflammation and cancer: triggers, mechanisms, and consequences. *Immunity, 51*(1), 27-41.
Greve, H. L., Kaiser, M., Brun, R., & Schmidt, T. J. (2017). Terpenoids from the oleo-gum-resin of Boswellia serrata and their antiplasmodial effects in vitro. *Planta medica, 83*(14/15), 1214-1226.
Guo, Liu, X., Nishikawa, K., & Plunkett, W. (2007). Inhibition of topoisomerase IIα and G2 cell cycle arrest by NK314, a novel benzo [c] phenanthridine currently in clinical trials. *Molecular cancer therapeutics, 6*(5), 1501-1508.
Guo, Tian, T., Nan, K., & Wang, W. (2010). p57: A multifunctional protein in cancer. *International journal of oncology, 36*(6), 1321-1329.
Gupta, Gupta, V., Parihar, A., Gupta, S., Lüdtke, R., Safayhi, H., & Ammon, H. P. (1998). Effects of Boswellia serrata gum resin in patients with bronchial asthma: results of a double-blind, placebo-controlled, 6-week clinical study. *European journal of medical research, 3*(11), 511-514.
Gupta, Rout, P. K., Misra, L. N., Gupta, P., Singh, N., Darokar, M. P., . . . Bhakuni, R. S. (2017). Chemical composition and bioactivity of Boswellia serrata Roxb. essential oil in relation to geographical variation. *Plant Biosystems-An International Journal Dealing with all Aspects of Plant Biology, 151*(4), 623-629.
Häcker, G. (2000). The morphology of apoptosis. *Cell and tissue research, 301*(1), 5-17.
Hakkim, F. L., Al-Buloshi, M., & Al-Sabahi, J. (2015). Frankincense derived heavy terpene cocktail boosting breast cancer cell (MDA-MB-231) death in vitro. *Asian Pacific Journal of Tropical Biomedicine, 5*(10), 824-828.
Hamm, S., Bleton, J., Connan, J., & Tchapla, A. (2005). A chemical investigation by headspace SPME and GC–MS of volatile and semi-volatile terpenes in various olibanum samples. *Phytochemistry, 66*(12), 1499-1514.
Han, X., Aslanian, A., & Yates III, J. R. (2008). Mass spectrometry for proteomics. *Current opinion in chemical biology, 12*(5), 483-490.
Hanahan, D., & Weinberg, R. A. (2000). The hallmarks of cancer. *Cell, 100*(1), 57-70.
Hanahan, D., & Weinberg, R. A. (2011). Hallmarks of cancer: the next generation. *Cell, 144*(5), 646-674.
Hande, K. R. (2008). Topoisomerase II inhibitors. *Update on cancer therapeutics, 3*(1), 13-26.
Harborne, A. J. (1998). *Phytochemical methods a guide to modern techniques of plant analysis*: springer science & business media.

Hardwick, J. M., & Soane, L. (2013). Multiple functions of BCL-2 family proteins. *Cold Spring Harbor perspectives in biology, 5*(2), a008722.
Hartmann, R. M., Fillmann, H. S., Morgan Martins, M. I., Meurer, L., & Marroni, N. P. (2014). Boswellia serrata has beneficial anti-inflammatory and antioxidant properties in a model of experimental colitis. *Phytotherapy research, 28*(9), 1392-1398.
Hartwell, J. L. (1982). *Plants used against cancer: a survey*: Quarterman Publications.
Harvey, A. L. (2008). Natural products in drug discovery. *Drug discovery today, 13*(19-20), 894-901.
Hassanpour, S. H., & Dehghani, M. (2017). Review of cancer from perspective of molecular. *Journal of Cancer Research and Practice, 4*(4), 127-129.
Haykin, M. E., Gorman, M., Van Hoff, J., Fulbright, R. K., & Baehring, J. M. (2006). Diffusion-weighted MRI correlates of subacute methotrexate-related neurotoxicity. *Journal of neuro-oncology, 76*(2), 153-157.
Hengartner, M. O. (2000). The biochemistry of apoptosis. *Nature, 407*(6805), 770-776.
Henke, E., Nandigama, R., & Ergün, S. (2020). Extracellular matrix in the tumor microenvironment and its impact on cancer therapy. *Frontiers in molecular biosciences, 6*, 160.
Henkel, A., Kather, N., Mönch, B., Northoff, H., Jauch, J., & Werz, O. (2012). Boswellic acids from frankincense inhibit lipopolysaccharide functionality through direct molecular interference. *Biochemical pharmacology, 83*(1), 115-121.
Henley, S. A., & Dick, F. A. (2012). The retinoblastoma family of proteins and their regulatory functions in the mammalian cell division cycle. *Cell division, 7*(1), 1-14.
Hickman, E. S., Moroni, M. C., & Helin, K. (2002). The role of p53 and pRB in apoptosis and cancer. *Current opinion in genetics & development, 12*(1), 60-66.
Hoernlein, R., Orlikowsky, T., Zehrer, C., Niethammer, D., Sailer, E., Simmet, T., . . . Ammon, H. (1999). Acetyl-11-keto-β-boswellic acid induces apoptosis in HL-60 and CCRF-CEM cells and inhibits topoisomerase I. *Journal of Pharmacology and Experimental Therapeutics, 288*(2), 613-619.
Hoesel, B., & Schmid, J. A. (2013). The complexity of NF-κB signaling in inflammation and cancer. *Molecular cancer, 12*(1), 1-15.
Hollenstein, K., Dawson, R. J. P., & Locher, K. P. (2007). Structure and mechanism of ABC transporter proteins. *Current opinion in structural biology, 17*(4), 412-418.
Horn, A., Morild, I., & Dahl, O. (1990). Tumour shrinkage and down staging after preoperative radiation of rectal adenocarcinomas. *Radiotherapy and Oncology, 18*(1), 19-28.
Hou, L., Liu, K., Li, Y., Ma, S., Ji, X., & Liu, L. (2016). Necrotic pyknosis is a morphologically and biochemically distinct event from apoptotic pyknosis. *Journal of cell science, 129*(16), 3084-3090.
Huang, Di Liberto, M., Jayabalan, D., Liang, J., Ely, S., Bretz, J., . . . Randolph, S. (2012). Prolonged early G1 arrest by selective CDK4/CDK6 inhibition sensitizes myeloma cells to cytotoxic killing through cell cycle–coupled loss of IRF4. *Blood, 120*(5), 1095-1106.
Huang, Shen, A., Ding, J., & Geng, M. (2014). Molecularly targeted cancer therapy: some lessons from the past decade. *Trends in pharmacological sciences, 35*(1), 41-50.
Huang, Zhang, L., Greshock, J., Colligon, T. A., Wang, Y., Ward, R., . . . Godwin, A. K. (2011). Frequent genetic abnormalities of the PI3K/AKT pathway in primary ovarian cancer predict patient outcome. *Genes, Chromosomes and cancer, 50*(8), 606-618.
Hustedt, N., & Durocher, D. (2017). The control of DNA repair by the cell cycle. *Nature cell biology, 19*(1), 1-9.
Ibrahim, S., Gao, D., & Sinko, P. J. (2014). Selective cytotoxicity and combined effects of camptothecin or paclitaxel with sodium-R-alpha lipoate on A549 human non-small cell lung cancer cells. *Nutrition and cancer, 66*(3), 492-499.
Igney, F. H., & Krammer, P. H. (2002). Death and anti-death: tumour resistance to apoptosis. *Nature Reviews Cancer, 2*(4), 277-288.
IHME. (2018). Global Burden of Disease Collaborative Network: Global Burden of Disease Study 2017 (GBD 2017) Results. Retrieved from http://ghdx.healthdata.org/gbd-results-tool

Ilan, Y. (2019). Microtubules: From understanding their dynamics to using them as potential therapeutic targets. *Journal of cellular physiology, 234*(6), 7923-7937.
Iqbal, J., Abbasi, B. A., Mahmood, T., Kanwal, S., Ali, B., Shah, S. A., & Khalil, A. T. (2017). Plant-derived anticancer agents: A green anticancer approach. *Asian Pacific Journal of Tropical Biomedicine, 7*(12), 1129-1150.
Isak, N. N. (2018). Challenges of Domestic Revenue Mobilization in Somalia. *International Journal of Economics, Commerce and Management, 6*(9).
Islam, Anggondowati, T., Deviany, P., Ryan, J., Fetrick, A., Bagenda, D., . . . McKean, H. (2019). Patient preferences of chemotherapy treatment options and tolerance of chemotherapy side effects in advanced stage lung cancer. *BMC cancer, 19*(1), 1-9.
Islam, Lustberg, M., Staff, N. P., Kolb, N., Alberti, P., & Argyriou, A. A. (2019). Vinca alkaloids, thalidomide and eribulin-induced peripheral neurotoxicity: From pathogenesis to treatment. *Journal of the Peripheral Nervous System, 24*, S63-S73.
Islami, F., Goding Sauer, A., Miller, K. D., Siegel, R. L., Fedewa, S. A., Jacobs, E. J., . . . Soerjomataram, I. (2018). Proportion and number of cancer cases and deaths attributable to potentially modifiable risk factors in the United States. *CA: a cancer journal for clinicians, 68*(1), 31-54.
Ismail, S. M., Aluru, S., Sambasivarao, K., & Matcha, B. (2014). Antimicrobial activity of frankincense of Boswellia serrata. *Int. J. Curr. Microbiol. App. Sci, 3*(10), 1095-1101.
Jaafari-Ashkavandi, Z., Hamedi, A., Assar, S., & Ebrahimpour, A. (2017). The Effects of Frankincense on Oral Squamous Cell Carcinoma Cell Line. *International Journal of Cancer Management, 10*(5).
Jacobs, I., & Bast Jr, R. C. (1989). The CA 125 tumour-associated antigen: a review of the literature. *Human reproduction, 4*(1), 1-12.
Jain, K. K., & Jain, K. K. (2010). *The handbook of biomarkers*: Springer.
Jemal, A., Center, M. M., DeSantis, C., & Ward, E. M. (2010). Global patterns of cancer incidence and mortality rates and trends. *Cancer Epidemiology and Prevention Biomarkers, 19*(8), 1893-1907.
Ji, X., Lu, Y., Tian, H., Meng, X., Wei, M., & Cho, W. C. (2019). Chemoresistance mechanisms of breast cancer and their countermeasures. *Biomedicine & Pharmacotherapy, 114*, 108800.
Jin, Z., & El-Deiry, W. S. (2005). Overview of cell death signaling pathways. *Cancer biology & therapy, 4*(2), 147-171.
Jin, Z., McDonald Iii, E. R., Dicker, D. T., & El-Deiry, W. S. (2004). Deficient tumor necrosis factor-related apoptosis-inducing ligand (TRAIL) death receptor transport to the cell surface in human colon cancer cells selected for resistance to TRAIL-induced apoptosis. *Journal of Biological Chemistry, 279*(34), 35829-35839.
Jing, Y., Nakajo, S., Xia, L., Nakaya, K., Fang, Q., Waxman, S., & Han, R. (1999). Boswellic acid acetate induces differentiation and apoptosis in leukemia cell lines. *Leukemia research, 23*(1), 43-50.
Johnson, S., DeCarlo, A., Satyal, P., Dosoky, N. S., Sorensen, A., & Setzer, W. N. (2019). Organic certification is not enough: The case of the methoxydecane frankincense. *Plants, 8*(4), 88.
Jordan, M. A., & Wilson, L. (2004). Microtubules as a target for anticancer drugs. *Nature Reviews Cancer, 4*(4), 253-265.
Julien, O., & Wells, J. A. (2017). Caspases and their substrates. *Cell Death & Differentiation, 24*(8), 1380-1389.
Kalogeris, T., Baines, C. P., Krenz, M., & Korthuis, R. J. (2012). Cell biology of ischemia/reperfusion injury. *International review of cell and molecular biology, 298*, 229-317.
Kang, Z.-J., Liu, Y.-F., Xu, L.-Z., Long, Z.-J., Huang, D., Yang, Y., . . . Yan, J.-S. (2016). The Philadelphia chromosome in leukemogenesis. *Chinese journal of cancer, 35*(1), 1-15.
Kasibhatla, S., & Tseng, B. (2003). Why target apoptosis in cancer treatment? *Molecular cancer therapeutics, 2*(6), 573-580.
Kastan, M. B., & Lim, D.-s. (2000). The many substrates and functions of ATM. *Nature reviews Molecular cell biology, 1*(3), 179-186.

Kaufmann. (2007). The Intrinsic Pathway of Apoptosis. In H. S. E. Gewirtz D.A., Grant S. (Ed.), *Apoptosis, Senescence, and Cancer*: Humana Press.

Kaufmann, Desnoyers, S., Ottaviano, Y., Davidson, N. E., & Poirier, G. G. (1993). Specific proteolytic cleavage of poly (ADP-ribose) polymerase: an early marker of chemotherapy-induced apoptosis. *Cancer research, 53*(17), 3976-3985.

Kayl, A. E., & Meyers, C. A. (2006). Side-effects of chemotherapy and quality of life in ovarian and breast cancer patients. *Current Opinion in Obstetrics and Gynecology, 18*(1), 24-28.

Kehm, R. D., Spector, L. G., Poynter, J. N., Vock, D. M., Altekruse, S. F., & Osypuk, T. L. (2018). Does socioeconomic status account for racial and ethnic disparities in childhood cancer survival? *Cancer, 124*(20), 4090-4097.

Kellner, U., Sehested, M., Jensen, P. B., Gieseler, F., & Rudolph, P. (2002). Culprit and victim–DNA topoisomerase II. *The Lancet Oncology, 3*(4), 235-243.

Kerckhove, N., Collin, A., Condé, S., Chaleteix, C., Pezet, D., & Balayssac, D. (2017). Long-term effects, pathophysiological mechanisms, and risk factors of chemotherapy-induced peripheral neuropathies: a comprehensive literature review. *Frontiers in pharmacology, 8*, 86.

Kerr, J. F., Wyllie, A. H., & Currie, A. R. (1972). Apoptosis: a basic biological phenomenon with wideranging implications in tissue kinetics. *British journal of cancer, 26*(4), 239-257.

Khan. (2012). Medicinal properties of frankincense. *International Journal of Nutrition, Pharmacology, Neurological Diseases, 2*(2), 79.

Khan. (2014). Medicinal plants in light of history: recognized therapeutic modality. *Journal of evidence-based complementary & alternative medicine, 19*(3), 216-219.

Khan, Ali, R., Parveen, R., Najmi, A. K., & Ahmad, S. (2016). Pharmacological evidences for cytotoxic and antitumor properties of Boswellic acids from Boswellia serrata. *Journal of ethnopharmacology, 191*, 315-323.

Khan, & Hashim, M. J. (2014). Global burden of deaths from Epstein-Barr virus attributable malignancies 1990-2010. *Infectious agents and cancer, 9*(1), 1-11.

Kim. (2016). Chemotherapy resistance in lung cancer. *Lung Cancer and Personalized Medicine*, 189-209.

Kim, Choi, E.-J., & Joe, C. O. (2000). Activation of death-inducing signaling complex (DISC) by pro-apoptotic C-terminal fragment of RIP. *Oncogene, 19*(39), 4491-4499.

Kim, & Jung, H. C. (2010). The role of serum pepsinogen in the detection of gastric cancer. *Gut and liver, 4*(3), 307.

Kim, Lee, J.-Y., Kim, D.-G., Koo, G.-B., Yu, J.-W., & Kim, Y.-S. (2011). TRADD is critical for resistance to TRAIL-induced cell death through NF-κB activation. *Febs Letters, 585*(14), 2144-2150.

Kim, A. H., Khursigara, G., Sun, X., Franke, T. F., & Chao, M. V. (2001). Akt phosphorylates and negatively regulates apoptosis signal-regulating kinase 1. *Molecular and cellular biology, 21*(3), 893-901.

Kimmatkar, N., Thawani, V., Hingorani, L., & Khiyani, R. (2003). Efficacy and tolerability of Boswellia serrata extract in treatment of osteoarthritis of knee–a randomized double blind placebo controlled trial. *Phytomedicine, 10*(1), 3-7.

Kinch, M. S. (2014). An analysis of FDA-approved drugs for oncology. *Drug discovery today, 19*(12), 1831-1835.

Koeberle, A., & Werz, O. (2018). Natural products as inhibitors of prostaglandin E2 and pro-inflammatory 5-lipoxygenase-derived lipid mediator biosynthesis. *Biotechnology advances, 36*(6), 1709-1723.

Kolben, T., Jeschke, U., Reimer, T., Karsten, N., Schmoeckel, E., Semmlinger, A., . . . Kolben, T. M. (2018). Induction of apoptosis in breast cancer cells in vitro by Fas ligand reverse signaling. *Journal of cancer research and clinical oncology, 144*(2), 249-256.

Kondo, N., Takahashi, A., Ono, K., & Ohnishi, T. (2010). DNA damage induced by alkylating agents and repair pathways. *Journal of nucleic acids, 2010*.

Koparde, A. A., Doijad, R. C., & Magdum, C. S. (2019). Natural products in drug discovery. *Pharmacognosy-medicinal plants*, 1-20.
Kunnumakkara, A. B., Nair, A. S., Sung, B., Pandey, M. K., & Aggarwal, B. B. (2009). Boswellic acid blocks signal transducers and activators of transcription 3 signaling, proliferation, and survival of multiple myeloma via the protein tyrosine phosphatase SHP-1. *Molecular cancer research, 7*(1), 118-128.
Kuo, R.-Y., Qian, K., Morris-Natschke, S. L., & Lee, K.-H. (2009). Plant-derived triterpenoids and analogues as antitumor and anti-HIV agents. *Natural product reports, 26*(10), 1321-1344.
Kupiec, T. (2004). Quality-control analytical methods: High-performance liquid chromatography. *International journal of pharmaceutical compounding, 8*, 223-227.
Kuroda, S., Kagawa, S., & Fujiwara, T. (2014). Selectively replicating oncolytic adenoviruses combined with chemotherapy, radiotherapy, or molecular targeted therapy for treatment of human cancers. In *Gene Therapy of Cancer* (pp. 171-183): Elsevier.
Kurosaka, K., Takahashi, M., Watanabe, N., & Kobayashi, Y. (2003). Silent cleanup of very early apoptotic cells by macrophages. *The Journal of Immunology, 171*(9), 4672-4679.
Lancellotti, P., Zamorano, J. L., & Galderisi, M. (2016). *Anticancer Treatments and Cardiotoxicity: Mechanisms, Diagnostic and Therapeutic Interventions*: Academic Press.
Land, S. R., Kopec, J. A., Cecchini, R. S., Ganz, P. A., Wieand, H. S., Colangelo, L. H., . . . Needles, B. M. (2007). Neurotoxicity from oxaliplatin combined with weekly bolus fluorouracil and leucovorin as surgical adjuvant chemotherapy for stage II and III colon cancer: NSABP C-07. *Journal of clinical oncology, 25*(16), 2205-2211.
Langer, S. W. (2014). Dexrazoxane for the treatment of chemotherapy-related side effects. *Cancer management and research, 6*, 357.
Lapenna, S., & Giordano, A. (2009). Cell cycle kinases as therapeutic targets for cancer. *Nature reviews Drug discovery, 8*(7), 547-566.
Larrea, M. D., Liang, J., Da Silva, T., Hong, F., Shao, S. H., Han, K., . . . Slingerland, J. M. (2008). Phosphorylation of p27Kip1 regulates assembly and activation of cyclin D1-Cdk4. *Molecular and cellular biology, 28*(20), 6462-6472.
Lavrik, I. N., Golks, A., & Krammer, P. H. (2005). Caspases: pharmacological manipulation of cell death. *The Journal of clinical investigation, 115*(10), 2665-2672.
Lazebnik, Y. (2010). What are the hallmarks of cancer? *Nature Reviews Cancer, 10*(4), 232-233.
Lee, & Berger, J. M. (2019). Cell cycle-dependent control and roles of DNA topoisomerase II. *Genes, 10*(11), 859.
Lee, Hokinson, D., Park, S., Elvira, R., Kusuma, F., Lee, J.-M., . . . Han, J. (2019). ER stress induces cell cycle arrest at the G2/M phase through eIF2α phosphorylation and GADD45α. *International journal of molecular sciences, 20*(24), 6309.
Lehnert, M. (1998). Chemotherapy resistance in breast cancer. *Anticancer research, 18*(3C), 2225-2226.
Lemieux, J., Maunsell, E., & Provencher, L. (2008). Chemotherapy-induced alopecia and effects on quality of life among women with breast cancer: a literature review. *Psycho-Oncology: Journal of the Psychological, Social and Behavioral Dimensions of Cancer, 17*(4), 317-328.
Lerman, L. (1961). Structural considerations in the interaction of DNA and acridines. *Journal of molecular biology, 3*(1), 18-IN14.
Letai, A. (2017). Apoptosis and Cancer. *Annual Review of Cancer Biology, 1*(1), 275-294. doi:10.1146/annurev-cancerbio-050216-121933
Leung, K. K., & Shilton, B. H. (2015). Binding of DNA-intercalating agents to oxidized and reduced quinone reductase 2. *Biochemistry, 54*(51), 7438-7448.
Li, & Yuan, J. (2008). Caspases in apoptosis and beyond. *Oncogene, 27*(48), 6194-6206.
Li, Zhou, M., Hu, Q., Bai, X.-c., Huang, W., Scheres, S. H. W., & Shi, Y. (2017). Mechanistic insights into caspase-9 activation by the structure of the apoptosome holoenzyme. *Proceedings of the National Academy of Sciences, 114*(7), 1542-1547.

Lian, Q., Xu, J., Yan, S., Huang, M., Ding, H., Sun, X., . . . Geng, M. (2017). Chemotherapy-induced intestinal inflammatory responses are mediated by exosome secretion of double-strand DNA via AIM2 inflammasome activation. *Cell Research, 27*(6), 784-800.

Lilja, H., Ulmert, D., & Vickers, A. J. (2008). Prostate-specific antigen and prostate cancer: prediction, detection and monitoring. *Nature Reviews Cancer, 8*(4), 268-278.

Lim, S., & Kaldis, P. (2013). Cdks, cyclins and CKIs: roles beyond cell cycle regulation. *Development, 140*(15), 3079-3093.

Liu, Huang, B., & Hooi, S. C. (2006). Acetyl-keto-β-boswellic acid inhibits cellular proliferation through a p21-dependent pathway in colon cancer cells. *British journal of pharmacology, 148*(8), 1099-1107.

Liu, Qu, L., Meng, L., & Shou, C. (2019). Topoisomerase inhibitors promote cancer cell motility via ROS-mediated activation of JAK2-STAT1-CXCL1 pathway. *Journal of experimental & clinical cancer research, 38*(1), 1-12.

Liu, Wang, S.-k., Xu, Q.-q., Yuan, H.-q., Guo, Y.-x., Wang, Q., . . . Wang, R.-m. (2019). Acetyl-11-keto-β-boswellic acid suppresses docetaxel-resistant prostate cancer cells in vitro and in vivo by blocking Akt and Stat3 signaling, thus suppressing chemoresistant stem cell-like properties. *Acta Pharmacologica Sinica, 40*(5), 689-698.

Liu, H., Dibling, B., Spike, B., Dirlam, A., & Macleod, K. (2004). New roles for the RB tumor suppressor protein. *Current opinion in genetics & development, 14*(1), 55-64.

Liu, J.-J., Nilsson, A., Oredsson, S., Badmaev, V., & Duan, R.-D. (2002). Keto-and acetyl-keto-boswellic acids inhibit proliferation and induce apoptosis in Hep G2 cells via a caspase-8 dependent pathway. *International journal of molecular medicine, 10*(4), 501-505.

Liu, J., Willför, S., & Xu, C. (2015). A review of bioactive plant polysaccharides: Biological activities, functionalization, and biomedical applications. *Bioactive Carbohydrates and Dietary Fibre, 5*(1), 31-61.

Loman, B. R., Jordan, K. R., Haynes, B., Bailey, M. T., & Pyter, L. M. (2019). Chemotherapy-induced neuroinflammation is associated with disrupted colonic and bacterial homeostasis in female mice. *Scientific reports, 9*(1), 1-16.

Loos, G., Van Schepdael, A., & Cabooter, D. (2016). Quantitative mass spectrometry methods for pharmaceutical analysis. *Philosophical Transactions of the Royal Society A: Mathematical, Physical and Engineering Sciences, 374*(2079), 20150366.

López-Lázaro, M. (2015). The migration ability of stem cells can explain the existence of cancer of unknown primary site. Rethinking metastasis. *Oncoscience, 2*(5), 467.

Lopez-Mejia, I. C., & Fajas, L. (2015). Cell cycle regulation of mitochondrial function. *Current opinion in cell biology, 33*, 19-25.

Loreto, C., La Rocca, G., Anzalone, R., Caltabiano, R., Vespasiani, G., Castorina, S., . . . Giunta, S. (2014). The role of intrinsic pathway in apoptosis activation and progression in Peyronie's disease. *BioMed research international, 2014*.

Lovly, C. M., & Shaw, A. T. (2014). Molecular pathways: resistance to kinase inhibitors and implications for therapeutic strategies. *Clinical Cancer Research, 20*(9), 2249-2256.

Lu, M., Xia, L., Hua, H., & Jing, Y. (2008). Acetyl-keto-β-Boswellic acid induces apoptosis through a death receptor 5–mediated pathway in prostate cancer cells. *Cancer research, 68*(4), 1180-1186.

Luo, J., Solimini, N. L., & Elledge, S. J. (2009). Principles of cancer therapy: oncogene and non-oncogene addiction. *Cell, 136*(5), 823-837.

Luqmani, Y. (2005). Mechanisms of drug resistance in cancer chemotherapy. *Medical Principles and Practice, 14*(Suppl. 1), 35-48.

Lv, M., Shao, S., Zhang, Q., Zhuang, X., & Qiao, T. (2020). Acetyl-11-Keto-β-Boswellic acid exerts the anti-cancer effects via cell cycle arrest, apoptosis induction and autophagy suppression in non-small cell lung cancer cells. *OncoTargets and therapy, 13*, 733.

Madan, R. A., Pal, S. K., Sartor, O., & Dahut, W. L. (2011). Overcoming chemotherapy resistance in prostate cancer. *Clinical Cancer Research, 17*(12), 3892-3902.
Magge, R. S., & DeAngelis, L. M. (2015). The double-edged sword: neurotoxicity of chemotherapy. *Blood reviews, 29*(2), 93-100.
Malavolta, L., Poletti, E. F., Silva, E. H., Schreier, S., & Nakaie, C. R. (2008). Application of electron paramagnetic resonance spectroscopy for validation of the novel (AN+ DN) solvent polarity scale. *International journal of molecular sciences, 9*(7), 1321-1332.
Malhotra, V., & Perry, M. C. (2003). Classical chemotherapy: mechanisms, toxicities and the therapeutc window. *Cancer biology & therapy, 2*(sup1), 1-3.
Malumbres, M., & Barbacid, M. (2006). Is Cyclin D1-CDK4 kinase a bona fide cancer target? *Cancer cell, 9*(1), 2-4.
Mansilla, S. F., De La Vega, M. B., Calzetta, N. L., Siri, S. O., & Gottifredi, V. (2020). CDK-independent and PCNA-dependent functions of p21 in DNA replication. *Genes, 11*(6), 593.
Mansoori, B., Mohammadi, A., Davudian, S., Shirjang, S., & Baradaran, B. (2017). The different mechanisms of cancer drug resistance: a brief review. *Advanced pharmaceutical bulletin, 7*(3), 339.
Mantovani, F., Collavin, L., & Del Sal, G. (2019). Mutant p53 as a guardian of the cancer cell. *Cell Death & Differentiation, 26*(2), 199-212.
Mariño, G., & Kroemer, G. (2013). Mechanisms of apoptotic phosphatidylserine exposure. *Cell Research, 23*(11), 1247-1248.
Martin, S. J. (2016). Cell death and inflammation: the case for IL-1 family cytokines as the canonical DAMPs of the immune system. *The FEBS journal, 283*(14), 2599-2615.
Martinetz, D., Lohs, K., & Janzen, J. r. (1989). *Weihrauch und Myrrhe*: Wissenschaftliche Verlagsgesellschaft.
Martinez-Ruiz, G., Maldonado, V., Ceballos-Cancino, G., Grajeda, J. P. R., & Melendez-Zajgla, J. (2008). Role of Smac/DIABLO in cancer progression. *Journal of experimental & clinical cancer research, 27*(1), 1-7.
Martinou, J.-C., & Youle, R. J. (2011). Mitochondria in apoptosis: Bcl-2 family members and mitochondrial dynamics. *Developmental cell, 21*(1), 92-101.
McIlwain, D. R., Berger, T., & Mak, T. W. (2013). Caspase functions in cell death and disease. *Cold Spring Harbor perspectives in biology, 5*(4), a008656.
McQuade, R. M., Stojanovska, V., Abalo, R., Bornstein, J. C., & Nurgali, K. (2016). Chemotherapy-induced constipation and diarrhea: pathophysiology, current and emerging treatments. *Frontiers in pharmacology, 7*, 414.
Meegan, M. J., & O'Boyle, N. M. (2019). Special issue "anticancer drugs". *Pharmaceuticals, 12*(3), 134.
Melnik, S., Werth, N., Boeuf, S., Hahn, E.-M., Gotterbarm, T., Anton, M., & Richter, W. (2019). Impact of c-MYC expression on proliferation, differentiation, and risk of neoplastic transformation of human mesenchymal stromal cells. *Stem cell research & therapy, 10*(1), 1-18.
Mickley, L. A., Spengler, B. A., Knutsen, T. A., Biedler, J. L., & Fojo, T. (1997). Gene rearrangement: a novel mechanism for MDR-1 gene activation. *The Journal of clinical investigation, 99*(8), 1947-1957.
Middleton, M. R., & Margison, G. P. (2003). Improvement of chemotherapy efficacy by inactivation of a DNA-repair pathway. *The Lancet Oncology, 4*(1), 37-44.
Mikhaeil, B. R., Maatooq, G. T., Badria, F. A., & Amer, M. M. (2003). Chemistry and immunomodulatory activity of frankincense oil. *Zeitschrift für Naturforschung C, 58*(3-4), 230-238.
Miller, Tadagavadi, R. K., Ramesh, G., & Reeves, W. B. (2010). Mechanisms of cisplatin nephrotoxicity. *Toxins, 2*(11), 2490-2518.
Miller, Thomas, S. D., Islam, A., Muench, D., & Sedoris, K. (2012). c-Myc and cancer metabolism. In: AACR.

Mittnacht, S. (1998). Control of pRB phosphorylation. *Current opinion in genetics & development, 8*(1), 21-27.
Miyatake, S., Nakano, H., Park, S. Y., Yamazaki, T., Takase, K., Matsushime, H., . . . Saito, T. (1995). Induction of G1 arrest by down-regulation of cyclin D3 in T cell hybridomas. *The Journal of experimental medicine, 182*(2), 401-408.
Mladěnka, P., Applová, L., Patočka, J., Costa, V. M., Remiao, F., Pourová, J., . . . Vopršalová, M. (2018). Comprehensive review of cardiovascular toxicity of drugs and related agents. *Medicinal research reviews, 38*(4), 1332-1403.
Moiseeva, T. N., Yin, Y., Calderon, M. J., Qian, C., Schamus-Haynes, S., Sugitani, N., . . . Bakkenist, C. J. (2019). An ATR and CHK1 kinase signaling mechanism that limits origin firing during unperturbed DNA replication. *Proceedings of the National Academy of Sciences, 116*(27), 13374-13383.
Monsuez, J.-J., Charniot, J.-C., Vignat, N., & Artigou, J.-Y. (2010). Cardiac side-effects of cancer chemotherapy. *International journal of cardiology, 144*(1), 3-15.
Montessuit, S., Somasekharan, S. P., Terrones, O., Lucken-Ardjomande, S., Herzig, S., Schwarzenbacher, R., . . . Meda, P. (2010). Membrane remodeling induced by the dynamin-related protein Drp1 stimulates Bax oligomerization. *Cell, 142*(6), 889-901.
Moore, P. S., Beghelli, S., Zamboni, G., & Scarpa, A. (2003). Genetic abnormalities in pancreatic cancer. *Molecular cancer, 2*(1), 1-6.
Mordente, A., Meucci, E., Martorana, G. E., & Silvestrini, A. (2015). Cancer biomarkers discovery and validation: state of the art, problems and future perspectives. *Advances in Cancer Biomarkers*, 9-26.
Morgan, D. O. (2007). *The cell cycle: principles of control*: New science press.
Muramatsu, S., Hirai, K., Tak, Y.-S., Kamimura, Y., & Araki, H. (2010). CDK-dependent complex formation between replication proteins Dpb11, Sld2, Pol ε, and GINS in budding yeast. *Genes & development, 24*(6), 602-612.
Murayama, C., Kimura, Y., & Setou, M. (2009). Imaging mass spectrometry: principle and application. *Biophysical reviews, 1*(3), 131.
Murray, A. (1994). Cell cycle checkpoints. *Current opinion in cell biology, 6*(6), 872-876.
Musgrove, E. A., Swarbrick, A., Lee, C. S., Cornish, A. L., & Sutherland, R. L. (1998). Mechanisms of cyclin-dependent kinase inactivation by progestins. *Molecular and cellular biology, 18*(4), 1812-1825.
Myers, J. S. (2009, 2012). *Chemotherapy-related cognitive impairment: the breast cancer experience*.
Nagpal, M., Singh, S., Singh, P., Chauhan, P., & Zaidi, M. A. (2016). Tumor markers: A diagnostic tool. *National journal of maxillofacial surgery, 7*(1), 17.
Naidu, M. U. R., Ramana, G. V., Rani, P. U., Suman, A., & Roy, P. (2004). Chemotherapy-induced and/or radiation therapy-induced oral mucositis-complicating the treatment of cancer. *Neoplasia, 6*(5), 423-431.
Najafi, M., Mortezaee, K., & Majidpoor, J. (2019). Cancer stem cell (CSC) resistance drivers. *Life sciences, 234*, 116781.
Nakano, K., & Vousden, K. H. (2001). PUMA, a novel proapoptotic gene, is induced by p53. *Molecular cell, 7*(3), 683-694.
Nallanthighal, S., Heiserman, J. P., & Cheon, D.-J. (2019). The role of the extracellular matrix in cancer stemness. *Frontiers in cell and developmental biology, 7*, 86.
Neganova, I., Vilella, F., Atkinson, S. P., Lloret, M., Passos, J. F., Von Zglinicki, T., . . . Armstrong, L. (2011). An important role for CDK2 in G1 to S checkpoint activation and DNA damage response in human embryonic stem cells. *Stem Cells, 29*(4), 651-659.
Nenclares, P., & Harrington, K. J. (2020). The biology of cancer. *Medicine, 48*(2), 67-72.
Newton, H. B. (2012). Neurological complications of chemotherapy to the central nervous system. *Handbook of clinical neurology, 105*, 903-916.

Ni, X., Suhail, M. M., Yang, Q., Cao, A., Fung, K.-M., Postier, R. G., . . . Lin, H.-K. (2012). Frankincense essential oil prepared from hydrodistillation of Boswellia sacra gum resins induces human pancreatic cancer cell death in cultures and in a xenograft murine model. *BMC Complementary and Alternative Medicine, 12*(1), 1-14.

Nicolescu, T. O. (2017). Interpretation of mass spectra. In M. Aliofkhazraei (Ed.), *Mass Spectrometry*. Retrieved from https://www.intechopen.com/books/mass-spectrometry/interpretation-of-mass-spectra

Nigg, E. A. (2001). Mitotic kinases as regulators of cell division and its checkpoints. *Nature reviews Molecular cell biology, 2*(1), 21-32.

Niida, H., Katsuno, Y., Banerjee, B., Hande, M. P., & Nakanishi, M. (2007). Specific role of Chk1 phosphorylations in cell survival and checkpoint activation. *Molecular and cellular biology, 27*(7), 2572-2581.

Nurgali, K., Jagoe, R. T., & Abalo, R. (2018). Adverse effects of cancer chemotherapy: Anything new to improve tolerance and reduce sequelae? *Frontiers in pharmacology, 9*, 245.

O'Brien, S. G., Guilhot, F., Larson, R. A., Gathmann, I., Baccarani, M., Cervantes, F., . . . Hughes, T. (2003). Imatinib compared with interferon and low-dose cytarabine for newly diagnosed chronic-phase chronic myeloid leukemia. *New England Journal of Medicine, 348*(11), 994-1004.

O'Connor, P. M., & Fan, S. (1996). Cell cycle checkpoints and cancer chemotherapy. In *Platinum and other metal coordination compounds in cancer chemotherapy 2* (pp. 293-301): Springer.

Oberst, A., Pop, C., Tremblay, A. G., Blais, V., Denault, J.-B., Salvesen, G. S., & Green, D. R. (2010). Inducible dimerization and inducible cleavage reveal a requirement for both processes in caspase-8 activation. *Journal of Biological Chemistry, 285*(22), 16632-16642.

Obexer, P., & Ausserlechner, M. J. (2014). X-linked inhibitor of apoptosis protein–a critical death resistance regulator and therapeutic target for personalized cancer therapy. *Frontiers in oncology, 4*, 197.

Oke, J. L., O'Sullivan, J. W., Perera, R., & Nicholson, B. D. (2018). The mapping of cancer incidence and mortality trends in the UK from 1980–2013 reveals a potential for overdiagnosis. *Scientific reports, 8*(1), 1-8.

Olshina, M. A., & Sharon, M. (2016). Mass spectrometry: a technique of many faces. *Quarterly reviews of biophysics, 49*.

ONS. (2018). *Cancer registration statistics, England 2017*. United Kingdom Office for National Statistics Retrieved from https://www.ons.gov.uk/peoplepopulationandcommunity/healthandsocialcare/conditionsanddiseases/bulletins/cancerregistrationstatisticsengland/2017

Oronsky, B. T., Reid, T., Knox, S. J., & Scicinski, J. J. (2012). The scarlet letter of alkylation: a mini review of selective alkylating agents. *Translational oncology, 5*(4), 226-229.

Oun, R., Moussa, Y. E., & Wheate, N. J. (2018). The side effects of platinum-based chemotherapy drugs: a review for chemists. *Dalton transactions, 47*(19), 6645-6653.

Ovejero, S., Bueno, A., & Sacristán, M. P. (2020). Working on genomic stability: From the S-phase to mitosis. *Genes, 11*(2), 225.

Owen-Schaub, L. (2001). Soluble Fas and cancer. *Clinical Cancer Research, 7*(5), 1108-1109.

Ozaki, T., & Nakagawara, A. (2011). Role of p53 in cell death and human cancers. *Cancers, 3*(1), 994-1013.

Pabla, & Dong, Z. (2008). Cisplatin nephrotoxicity: mechanisms and renoprotective strategies. *Kidney international, 73*(9), 994-1007.

Pabla, & Dong, Z. (2012). Curtailing side effects in chemotherapy: a tale of PKCδ in cisplatin treatment. *Oncotarget, 3*(1), 107.

Pabla, Murphy, R. F., Liu, K., & Dong, Z. (2009). The copper transporter Ctr1 contributes to cisplatin uptake by renal tubular cells during cisplatin nephrotoxicity. *American Journal of Physiology-Renal Physiology, 296*(3), F505-F511.

Padma, V. V. (2015). An overview of targeted cancer therapy. *Biomedicine, 5*(4).
Pandey, M., Debnath, M., Gupta, S., & Chikara, S. K. (2011). Phytomedicine: An ancient approach turning into future potential source of therapeutics. *Journal of Pharmacognosy and phytotherapy, 3*(1), 113-117.
Pang, X., Yi, Z., Zhang, X., Sung, B., Qu, W., Lian, X., . . . Liu, M. (2009). Acetyl-11-keto-β-boswellic acid inhibits prostate tumor growth by suppressing vascular endothelial growth factor receptor 2–mediated angiogenesis. *Cancer research, 69*(14), 5893-5900.
Panzarini, E., Inguscio, V., & Dini, L. (2011). Timing the multiple cell death pathways initiated by Rose Bengal acetate photodynamic therapy. *Cell death & disease, 2*(6), e169-e169.
Paré, J. J., & Yaylayan, V. (1997). Mass spectrometry: Principles and applications. In *Techniques and instrumentation in analytical chemistry* (Vol. 18, pp. 239-266): Elsevier.
Park, Kim, J., Elghiaty, A., & Ham, W. S. (2018). Recent global trends in testicular cancer incidence and mortality. *Medicine, 97*(37).
Park, B., Prasad, S., Yadav, V., Sung, B., & Aggarwal, B. B. (2011). Boswellic acid suppresses growth and metastasis of human pancreatic tumors in an orthotopic nude mouse model through modulation of multiple targets. *Plos one, 6*(10), e26943.
Parkin. (2011). 11. Cancers attributable to infection in the UK in 2010. *British journal of cancer, 105*(2), S49-S56.
Parkin, Boyd, L., & Walker, L. (2011). 16. The fraction of cancer attributable to lifestyle and environmental factors in the UK in 2010. *British journal of cancer, 105*(2), S77-S81.
Partheen, K., Kristjansdottir, B., & Sundfeldt, K. (2011). Evaluation of ovarian cancer biomarkers HE4 and CA-125 in women presenting with a suspicious cystic ovarian mass. *Journal of gynecologic oncology, 22*(4), 244.
Partridge, A. H., Burstein, H. J., & Winer, E. P. (2001). Side effects of chemotherapy and combined chemohormonal therapy in women with early-stage breast cancer. *JNCI Monographs, 2001*(30), 135-142.
Patwardhan, B., Vaidya, A. D., & Chorghade, M. (2004). Ayurveda and natural products drug discovery. *Current science*, 789-799.
Peña-Morán, O. A., Villarreal, M. L., Álvarez-Berber, L., Meneses-Acosta, A., & Rodríguez-López, V. (2016). Cytotoxicity, post-treatment recovery, and selectivity analysis of naturally occurring podophyllotoxins from Bursera fagaroides var. fagaroides on breast cancer cell lines. *Molecules (Basel, Switzerland), 21*(8), 1013.
Penna, L. S., Henriques, J. A. P., & Bonatto, D. (2017). Anti-mitotic agents: Are they emerging molecules for cancer treatment? *Pharmacology & therapeutics, 173*, 67-82.
Perez, E. A. (2009). Impact, mechanisms, and novel chemotherapy strategies for overcoming resistance to anthracyclines and taxanes in metastatic breast cancer. *Breast cancer research and treatment, 114*(2), 195-201.
Perri, F., Pisconti, S., & Scarpati, G. D. V. (2016). P53 mutations and cancer: a tight linkage. *Annals of translational medicine, 4*(24).
Peter, M. E., Hadji, A., Murmann, A. E., Brockway, S., Putzbach, W., Pattanayak, A., & Ceppi, P. (2015). The role of CD95 and CD95 ligand in cancer. *Cell Death & Differentiation, 22*(4), 549-559.
Pezzani, R., Salehi, B., Vitalini, S., Iriti, M., Zuñiga, F. A., Sharifi-Rad, J., . . . Martins, N. (2019). Synergistic effects of plant derivatives and conventional chemotherapeutic agents: An update on the cancer perspective. *Medicina, 55*(4), 110.
Pfeffer, C. M., & Singh, A. T. K. (2018). Apoptosis: a target for anticancer therapy. *International journal of molecular sciences, 19*(2), 448.
Phi, L. T. H., Sari, I. N., Yang, Y.-G., Lee, S.-H., Jun, N., Kim, K. S., . . . Kwon, H. Y. (2018). Cancer stem cells (CSCs) in drug resistance and their therapeutic implications in cancer treatment. *Stem cells international, 2018*.
Planas-Silva, M. D., & Weinberg, R. A. (1997). The restriction point and control of cell proliferation. *Current opinion in cell biology, 9*(6), 768-772.

Pobezinskaya, Y. L., & Liu, Z. (2012). The role of TRADD in death receptor signaling. *Cell Cycle, 11*(5), 871-876.
Poon, I. K. H., Lucas, C. D., Rossi, A. G., & Ravichandran, K. S. (2014). Apoptotic cell clearance: basic biology and therapeutic potential. *Nature Reviews Immunology, 14*(3), 166-180.
Pozarowski, P., & Darzynkiewicz, Z. (2004). Analysis of cell cycle by flow cytometry. In *Checkpoint controls and cancer* (pp. 301-311): Springer.
Prieto-Vila, M., Takahashi, R.-u., Usuba, W., Kohama, I., & Ochiya, T. (2017). Drug resistance driven by cancer stem cells and their niche. *International journal of molecular sciences, 18*(12), 2574.
Pritchett, J. C., Naesens, L., & Montoya, J. (2014). Treating HHV-6 infections: The laboratory efficacy and clinical use of ati-HHV-6 agents.
Prives, C., & Gottifredi, V. (2008). The p21 and PCNA partnership: a new twist for an old plot. *Cell Cycle, 7*(24), 3840-3846.
Pugachev, M. V., Nguyen, T. T. N., Bulatov, T. M., Pavelyev, R. S., Iksanova, A. G., Bondar, O. V., . . . Shtyrlin, Y. G. (2017). Synthesis and Antitumor Activity of Novel Pyridoxine-Based Bioisosteric Analogs of trans-Stilbenes. *Journal of Chemistry, 2017*.
Puyo, S., Montaudon, D., & Pourquier, P. (2014). From old alkylating agents to new minor groove binders. *Critical reviews in oncology/hematology, 89*(1), 43-61.
Qi, C., Wang, X., Shen, Z., Chen, S., Yu, H., Williams, N., & Wang, G. (2018). Anti-mitotic chemotherapeutics promote apoptosis through TL1A-activated death receptor 3 in cancer cells. *Cell Research, 28*(5), 544-555.
Qin, S., Yang, C., Zhang, B., Li, X., Sun, X., Li, G., . . . Huang, G. (2016). XIAP inhibits mature Smac-induced apoptosis by degrading it through ubiquitination in NSCLC. *International journal of oncology, 49*(4), 1289-1296.
Quaresma, M., Coleman, M. P., & Rachet, B. (2015). 40-year trends in an index of survival for all cancers combined and survival adjusted for age and sex for each cancer in England and Wales, 1971–2011: a population-based study. *The Lancet, 385*(9974), 1206-1218.
Rådmark, O., & Samuelsson, B. (2009). 5-Lipoxygenase: mechanisms of regulation. *Journal of lipid research, 50*, S40-S45.
Raguz, S., & Yagüe, E. (2008). Resistance to chemotherapy: new treatments and novel insights into an old problem. *British journal of cancer, 99*(3), 387-391.
Rai, N. K., Tripathi, K., Sharma, D., & Shukla, V. K. (2005). Apoptosis: a basic physiologic process in wound healing. *The international journal of lower extremity wounds, 4*(3), 138-144.
Raja, A. F., Ali, F., Khan, I. A., Shawl, A. S., Arora, D. S., Shah, B. A., & Taneja, S. C. (2011). Antistaphylococcal and biofilm inhibitory activities of acetyl-11-keto-β-boswellic acid from Boswellia serrata. *BMC microbiology, 11*(1), 1-9.
Rakoff-Nahoum, S. (2006). Cancer issue: why cancer and inflammation? *The Yale journal of biology and medicine, 79*(3-4), 123.
Ralhan, R., & Kaur, J. (2007). Alkylating agents and cancer therapy. *Expert Opinion on Therapeutic Patents, 17*(9), 1061-1075.
Ranjbarnejad, T., Saidijam, M., Moradkhani, S., & Najafi, R. (2017). Methanolic extract of Boswellia serrata exhibits anti-cancer activities by targeting microsomal prostaglandin E synthase-1 in human colon cancer cells. *Prostaglandins & other lipid mediators, 131*, 1-8.
Rao, A. S., & Camilleri, M. (2010). metoclopramide and tardive dyskinesia. *Alimentary pharmacology & therapeutics, 31*(1), 11-19.
Rasul, M. G. (2018). Extraction, isolation and characterization of natural products from medicinal plants. *Int. J. Basic Sci. Appl. Comput, 2*, 1-6.
Rawla, P., Sunkara, T., & Gaduputi, V. (2019). Epidemiology of pancreatic cancer: global trends, etiology and risk factors. *World journal of oncology, 10*(1), 10.
Reichardt, C., & Welton, T. (2011). *Solvents and solvent effects in organic chemistry*: John Wiley & Sons.

Ren, R. (2005). Mechanisms of BCR–ABL in the pathogenesis of chronic myelogenous leukaemia. *Nature Reviews Cancer, 5*(3), 172-183.
Rescifina, A., Zagni, C., Varrica, M. G., Pistarà, V., & Corsaro, A. (2014). Recent advances in small organic molecules as DNA intercalating agents: Synthesis, activity, and modeling. *European journal of medicinal chemistry, 74*, 95-115.
Reuter, S., Gupta, S. C., Chaturvedi, M. M., & Aggarwal, B. B. (2010). Oxidative stress, inflammation, and cancer: how are they linked? *Free radical biology and medicine, 49*(11), 1603-1616.
Riley, Quarato, G., Cloix, C., Lopez, J., O'Prey, J., Pearson, M., . . . Passos, J. F. (2018). Mitochondrial inner membrane permeabilisation enables mt DNA release during apoptosis. *The EMBO journal, 37*(17), e99238.
Riley, T., Sontag, E., Chen, P., & Levine, A. (2008). Transcriptional control of human p53-regulated genes. *Nature reviews Molecular cell biology, 9*(5), 402-412.
Riva, G., Baronchelli, S., Paoletta, L., Butta, V., Biunno, I., Lavitrano, M., . . . Bentivegna, A. (2014). In vitro anticancer drug test: A new method emerges from the model of glioma stem cells. *Toxicology reports, 1*, 188-199.
Rochat, B. (2005). Role of cytochrome P450 activity in the fate of anticancer agents and in drug resistance. *Clinical pharmacokinetics, 44*(4), 349-366.
Rock, K. L., & Kono, H. (2008). The inflammatory response to cell death. *Annu. Rev. Pathol. Mech. Dis., 3*, 99-126.
Rock, K. L., Lai, J. J., & Kono, H. (2011). Innate and adaptive immune responses to cell death. *Immunological reviews, 243*(1), 191-205.
Rodriguez-Antona, C., & Ingelman-Sundberg, M. (2006). Cytochrome P 450 pharmacogenetics and cancer. *Oncogene, 25*(11), 1679-1691.
Roh, J. S., & Sohn, D. H. (2018). Damage-associated molecular patterns in inflammatory diseases. *Immune network, 18*(4).
Roth, W., Isenmann, S., Nakamura, M., Platten, M., Wick, W., Kleihues, P., . . . Weller, M. (2001). Soluble decoy receptor 3 is expressed by malignant gliomas and suppresses CD95 ligand-induced apoptosis and chemotaxis. *Cancer research, 61*(6), 2759-2765.
Rowinsky, E. K., Onetto, N., Canetta, R., & Arbuck, S. (1992). *Taxol: the first of the taxanes, an important new class of antitumor agents.* Paper presented at the Seminars in oncology.
Roy, N. K., Parama, D., Banik, K., Bordoloi, D., Devi, A. K., Thakur, K. K., . . . Sethi, G. (2019). An update on pharmacological potential of boswellic acids against chronic diseases. *International journal of molecular sciences, 20*(17), 4101.
Rubin, S. M. (2013). Deciphering the retinoblastoma protein phosphorylation code. *Trends in biochemical sciences, 38*(1), 12-19.
Rusdi, M., Alam, G., & Manggau, M. A. (2013). Selective Cytotoxicity evaluation in Anticancer drug screening of Boehmeria virgata (Forst) Guill leaves to several human cell lines: HeLa, WiDr, T47D and Vero. *Dhaka University Journal of Pharmaceutical Sciences, 12*(2), 87-90.
Saadatmand, S., Bretveld, R., Siesling, S., & Tilanus-Linthorst, M. M. A. (2015). Influence of tumour stage at breast cancer detection on survival in modern times: population based study in 173 797 patients. *Bmj, 351*.
Safayhi, H., Mack, T., Sabieraj, J., Anazodo, M. I., Subramanian, L. R., & Ammon, H. P. (1992). Boswellic acids: novel, specific, nonredox inhibitors of 5-lipoxygenase. *Journal of Pharmacology and Experimental Therapeutics, 261*(3), 1143-1146.
Safayhi, H., Sailer, E.-R., & Ammon, H. P. (1995). Mechanism of 5-lipoxygenase inhibition by acetyl-11-keto-beta-boswellic acid. *Molecular pharmacology, 47*(6), 1212-1216.
Salazar-Roa, M., & Malumbres, M. (2017). Fueling the cell division cycle. *Trends in cell biology, 27*(1), 69-81.
Samatar, A. A., & Poulikakos, P. I. (2014). Targeting RAS–ERK signalling in cancer: promises and challenges. *Nature reviews Drug discovery, 13*(12), 928-942.

Samuelsson, Dahlen, S.-E., Lindgren, J. A., Rouzer, C. A., & Serhan, C. N. (1987). Leukotrienes and lipoxins: structures, biosynthesis, and biological effects. *Science, 237*(4819), 1171-1176.
Samuelsson, G., & Bohlin, L. (2017). *Drugs of natural origin: a treatise of pharmacognosy*: CRC Press Inc.
Saraiya, M., Unger, E. R., Thompson, T. D., Lynch, C. F., Hernandez, B. Y., Lyu, C. W., . . . Hopenhayn, C. (2015). US assessment of HPV types in cancers: implications for current and 9-valent HPV vaccines. *JNCI: Journal of the National Cancer Institute, 107*(6).
Saraste, A., & Pulkki, K. (2000). Morphologic and biochemical hallmarks of apoptosis. *Cardiovascular research, 45*(3), 528-537.
Sarkar, S., Horn, G., Moulton, K., Oza, A., Byler, S., Kokolus, S., & Longacre, M. (2013). Cancer development, progression, and therapy: an epigenetic overview. *International journal of molecular sciences, 14*(10), 21087-21113.
Sarker, S. D., Latif, Z., & Gray, A. I. (2006). Natural product isolation: an overview. *Methods in Biotechnology, 20*, 1.
Sasidharan, Chen, Y., Saravanan, D., Sundram, K. M., & Latha, L. Y. (2011). Extraction, isolation and characterization of bioactive compounds from plants' extracts. *African Journal of Traditional, Complementary and Alternative Medicines, 8*(1).
Sasidharan, S., Chen, Y., Saravanan, D., Sundram, K., & Latha, L. Y. (2011). Extraction, isolation and characterization of bioactive compounds from plants' extracts. *African Journal of Traditional, Complementary and Alternative Medicines, 8*(1).
Savill, J., & Fadok, V. (2000). Corpse clearance defines the meaning of cell death. *Nature, 407*(6805), 784-788.
Sawyers, C. (2004). Targeted cancer therapy. *Nature, 432*(7015), 294-297.
Sayed, A. S., Gomaa, I. E. O., Bader, M., & El Sayed, N. S. E. D. (2018). Role of 3-acetyl-11-keto-beta-boswellic acid in counteracting LPS-induced neuroinflammation via modulation of miRNA-155. *Molecular neurobiology, 55*(7), 5798-5808.
Schellinger, A. P., & Carr, P. W. (2006). Isocratic and gradient elution chromatography: a comparison in terms of speed, retention reproducibility and quantitation. *Journal of Chromatography A, 1109*(2), 253-266.
Schimmel, K. J. M., Richel, D. J., van den Brink, R. B. A., & Guchelaar, H.-J. (2004). Cardiotoxicity of cytotoxic drugs. *Cancer treatment reviews, 30*(2), 181-191.
Schmiech, M., Lang, S. J., Werner, K., Rashan, L. J., Syrovets, T., & Simmet, T. (2019). Comparative Analysis of Pentacyclic Triterpenic Acid Compositions in Oleogum Resins of Different Boswellia Species and Their In Vitro Cytotoxicity against Treatment-Resistant Human Breast Cancer Cells. *Molecules (Basel, Switzerland), 24*(11), 2153. doi:10.3390/molecules24112153
Scholler, N., & Urban, N. (2007). CA125 in ovarian cancer. *Biomarkers In Medicine, 1*(4).
Segawa, K., & Nagata, S. (2015). An apoptotic 'eat me'signal: phosphatidylserine exposure. *Trends in cell biology, 25*(11), 639-650.
Sengupta, K., Alluri, K. V., Satish, A. R., Mishra, S., Golakoti, T., Sarma, K. V. S., . . . Raychaudhuri, S. P. (2008). A double blind, randomized, placebo controlled study of the efficacy and safety of 5-Loxin® for treatment of osteoarthritis of the knee. *Arthritis research & therapy, 10*(4), 1-11.
Seo, J.-H., Kim, J.-E., Shim, J.-H., Yoon, G., Bang, M., Bae, C.-S., . . . Cho, S.-S. (2016). HPLC analysis, optimization of extraction conditions and biological evaluation of Corylopsis coreana Uyeki Flos. *Molecules (Basel, Switzerland), 21*(1), 94.
Shah, B. A., Qazi, G. N., & Taneja, S. C. (2009). Boswellic acids: a group of medicinally important compounds. *Natural product reports, 26*(1), 72-89.
Shangguan, W.-J., Li, H., & Zhang, Y.-H. (2014). Induction of G2/M phase cell cycle arrest and apoptosis by ginsenoside Rf in human osteosarcoma MG‐63 cells through the mitochondrial pathway. *Oncology reports, 31*(1), 305-313.
Sharma, Bhardwaj, V., Singh, S., Ali, S. A., Gupta, D., Paul, S., . . . Verma, M. K. (2016). Simultaneous quantification of triterpenoic acids by high performance liquid chromatography method in

the extracts of gum resin of Boswellia serrata obtained by different extraction techniques. *Chemistry Central Journal, 10*(1), 1-10.
Sharma, Boise, L. H., & Shanmugam, M. (2019). Cancer metabolism and the evasion of apoptotic cell death. *Cancers, 11*(8), 1144.
Sheaff, R. J., Groudine, M., Gordon, M., Roberts, J. M., & Clurman, B. E. (1997). Cyclin E-CDK2 is a regulator of p27Kip1. *Genes & development, 11*(11), 1464-1478.
Sherr, C. J., & Bartek, J. (2017). Cell cycle–targeted cancer therapies.
Shi. (2002). Mechanisms of caspase activation and inhibition during apoptosis. *Molecular cell, 9*(3), 459-470.
Shi. (2004). Caspase activation: revisiting the induced proximity model. *Cell, 117*(7), 855-858.
Shi, & Mitchison, T. J. (2017). Cell death response to anti-mitotic drug treatment in cell culture, mouse tumor model and the clinic. *Endocrine-related cancer, 24*(9), T83.
Shi, Z., Azuma, A., Sampath, D., Li, Y.-X., Huang, P., & Plunkett, W. (2001). S-Phase arrest by nucleoside analogues and abrogation of survival without cell cycle progression by 7-hydroxystaurosporine. *Cancer research, 61*(3), 1065-1072.
Shin, M. S., Kim, H. S., Lee, S. H., Park, W. S., Kim, S. Y., Park, J. Y., . . . Jung, S. S. (2001). Mutations of tumor necrosis factor-related apoptosis-inducing ligand receptor 1 (TRAIL-R1) and receptor 2 (TRAIL-R2) genes in metastatic breast cancers. *Cancer research, 61*(13), 4942-4946.
Siddiqui, M. Z. (2011a). Boswellia serrata, a potential antiinflammatory agent: an overview. *Indian journal of pharmaceutical sciences, 73*(3), 255.
Siddiqui, M. Z. (2011b). Boswellia Serrata, A Potential Antiinflammatory Agent: An Overview. *Indian Journal of Pharmaceutical Sciences, 73*(3), 255-261. doi:10.4103/0250-474X.93507
Siegel, R. L., Miller, K. D., & Jemal, A. (2016). Cancer statistics, 2016. *CA: a cancer journal for clinicians, 66*(1), 7-30.
Singh, R., Letai, A., & Sarosiek, K. (2019). Regulation of apoptosis in health and disease: the balancing act of BCL-2 family proteins. *Nature reviews Molecular cell biology, 20*(3), 175-193.
Sinha, B. K. (1995). Topoisomerase inhibitors. *Drugs, 49*(1), 11-19.
Sisinni, L., & Landriscina, M. (2015). The role of human chorionic gonadotropin as tumor marker: biochemical and clinical aspects. *Advances in Cancer Biomarkers*, 159-176.
Slee, E. A., Adrain, C., & Martin, S. J. (2001). Executioner caspase-3,-6, and-7 perform distinct, non-redundant roles during the demolition phase of apoptosis. *Journal of Biological Chemistry, 276*(10), 7320-7326.
Smith, A. K., Xu, Y., Ropella, G. E. P., & Hunt, C. A. (2018). A model mechanism-based explanation of an in vitro-in vivo disconnect for improving extrapolation and translation. *Journal of Pharmacology and Experimental Therapeutics, 365*(1), 127-138.
Snyder. (1978). Classification off the solvent properties of common liquids. *Journal of Chromatographic Science, 16*(6), 223-234.
Snyder, Kirkland, J. J., & Glajch, J. L. (2012). *Practical HPLC method development*: John Wiley & Sons.
Solanki, R., & Nagori, B. P. (2012). New method for extracting phytoconstituents from plants. *Int J Biomed Adv Res, 3*(10), 770-774.
Sonneveld, P., & List, A. F. (2001). Chemotherapy resistance in acute myeloid leukaemia. *Best Practice & Research Clinical Haematology, 14*(1), 211-233.
Sordet, O., Khan, Q. A., Kohn, K. W., & Pommier, Y. (2003). Apoptosis induced by topoisomerase inhibitors. *Current Medicinal Chemistry-Anti-Cancer Agents, 3*(4), 271-290.
Soussi, T., & Wiman, K. (2015). TP53: an oncogene in disguise. *Cell Death & Differentiation, 22*(8), 1239-1249.
Stamey, T. A., Yang, N., Hay, A. R., McNeal, J. E., Freiha, F. S., & Redwine, E. (1987). Prostate-specific antigen as a serum marker for adenocarcinoma of the prostate. *New England Journal of Medicine, 317*(15), 909-916.

Su, S., Duan, J., Chen, T., Huang, X., Shang, E., Yu, L., . . . Guo, S. (2015). Frankincense and myrrh suppress inflammation via regulation of the metabolic profiling and the MAPK signaling pathway. *Scientific reports, 5*(1), 1-15.

Suber, T., & Rosen, A. (2009). Apoptotic cell blebs–repositories of autoantigens and contributors to immune context. *Arthritis and rheumatism, 60*(8), 2216.

Suhail, M. M., Wu, W., Cao, A., Mondalek, F. G., Fung, K.-M., Shih, P.-T., . . . Lin, H.-K. (2011). Boswellia sacra essential oil induces tumor cell-specific apoptosis and suppresses tumor aggressiveness in cultured human breast cancer cells. *BMC Complementary and Alternative Medicine, 11*(1), 1-14.

Sun, Wei, Q., Zhou, Y., Wang, J., Liu, Q., & Xu, H. (2017). A systematic analysis of FDA-approved anticancer drugs. *BMC systems biology, 11*(5), 1-17.

Sun, C. C., Bodurka, D. C., Weaver, C. B., Rasu, R., Wolf, J. K., Bevers, M. W., . . . Rubenstein, E. B. (2005). Rankings and symptom assessments of side effects from chemotherapy: insights from experienced patients with ovarian cancer. *Supportive Care in Cancer, 13*(4), 219-227.

Sundar, R., Bandla, A., Tan, S. S. H., Liao, L.-D., Kumarakulasinghe, N. B., Jeyasekharan, A. D., . . . Lim, J. S. J. (2017). Limb hypothermia for preventing paclitaxel-induced peripheral neuropathy in breast cancer patients: a pilot study. *Frontiers in oncology, 6*, 274.

Swamy, M. K., Purushotham, B., & Sinniah, U. R. (2021). Camptothecin: Occurrence, Chemistry and Mode of Action. In *Bioactive Natural Products for Pharmaceutical Applications* (pp. 311-327): Springer.

Syrovets, T., Büchele, B., Gedig, E., Slupsky, J. R., & Simmet, T. (2000). Acetyl-boswellic acids are novel catalytic inhibitors of human topoisomerases I and IIα. *Molecular pharmacology, 58*(1), 71-81.

Syrovets, T., Gschwend, J. E., Büchele, B., Laumonnier, Y., Zugmaier, W., Genze, F., & Simmet, T. (2005). Inhibition of IκB kinase activity by acetyl-boswellic acids promotes apoptosis in androgen-independent PC-3 prostate cancer cells in vitro and in vivo. *Journal of Biological Chemistry, 280*(7), 6170-6180.

Tait, S. W., Ichim, G., & Green, D. R. (2014). Die another way–non-apoptotic mechanisms of cell death. *Journal of cell science, 127*(10), 2135-2144.

Takahashi, M., Sung, B., Shen, Y., Hur, K., Link, A., Boland, C. R., . . . Goel, A. (2012). Boswellic acid exerts antitumor effects in colorectal cancer cells by modulating expression of the let-7 and miR-200 microRNA family. *Carcinogenesis, 33*(12), 2441-2449.

Tang, D., Kang, R., Berghe, T. V., Vandenabeele, P., & Kroemer, G. (2019). The molecular machinery of regulated cell death. *Cell Research, 29*(5), 347-364.

Tao, J. J., Visvanathan, K., & Wolff, A. C. (2015). Long term side effects of adjuvant chemotherapy in patients with early breast cancer. *The Breast, 24*, S149-S153.

Tausch, L., Henkel, A., Siemoneit, U., Poeckel, D., Kather, N., Franke, L., . . . Geisslinger, G. (2009). Identification of human cathepsin G as a functional target of boswellic acids from the anti-inflammatory remedy frankincense. *The Journal of Immunology, 183*(5), 3433-3442.

Technologies, A. (2016). *The LC Handbook: Guide to LC Columns and Method Development*. Retrieved from https://www.agilent.com/cs/library/primers/Public/LC-Handbook-Complete-2.pdf

Testa, U., Pelosi, E., & Castelli, G. (2018). Colorectal cancer: genetic abnormalities, tumor progression, tumor heterogeneity, clonal evolution and tumor-initiating cells. *Medical Sciences, 6*(2), 31.

Thu, K., Soria-Bretones, I., Mak, T., & Cescon, D. (2018). Targeting the cell cycle in breast cancer: towards the next phase. *Cell Cycle, 17*(15), 1871-1885.

Tischer, J., & Gergely, F. (2019). Anti-mitotic therapies in cancer. *Journal of Cell Biology, 218*(1), 10-11.

Toden, S., Okugawa, Y., Buhrmann, C., Nattamai, D., Anguiano, E., Baldwin, N., . . . Goel, A. (2015). Novel evidence for curcumin and boswellic acid–induced chemoprevention through

regulation of miR-34a and miR-27a in colorectal cancer. *Cancer Prevention Research, 8*(5), 431-443.
Todoric, J., Antonucci, L., & Karin, M. (2016). Targeting inflammation in cancer prevention and therapy. *Cancer Prevention Research, 9*(12), 895-905.
Tonnus, W., Meyer, C., Paliege, A., Belavgeni, A., von Mässenhausen, A., Bornstein, S. R., . . . Linkermann, A. (2019). The pathological features of regulated necrosis. *The Journal of pathology, 247*(5), 697-707.
Tourneur, L., & Chiocchia, G. (2010). FADD: a regulator of life and death. *Trends in immunology, 31*(7), 260-269.
Truong, D.-H., Nguyen, D. H., Ta, N. T. A., Bui, A. V., Do, T. H., & Nguyen, H. C. (2019). Evaluation of the use of different solvents for phytochemical constituents, antioxidants, and in vitro anti-inflammatory activities of Severinia buxifolia. *Journal of food quality, 2019*.
Tseng, H.-H., & He, B. (2013). Molecular markers as therapeutic targets in lung cancer. *Chinese journal of cancer, 32*(2), 59.
Umar, S., Umar, K., Sarwar, A. H. M. G., Khan, A., Ahmad, N., Ahmad, S., . . . Khan, H. A. (2014). Boswellia serrata extract attenuates inflammatory mediators and oxidative stress in collagen induced arthritis. *Phytomedicine, 21*(6), 847-856.
Vaidyanathan, R., Soon, R. H., Zhang, P., Jiang, K., & Lim, C. T. (2019). Cancer diagnosis: from tumor to liquid biopsy and beyond. *Lab on a Chip, 19*(1), 11-34.
Van Cruchten, S., & Van Den Broeck, W. (2002). Morphological and biochemical aspects of apoptosis, oncosis and necrosis. *Anatomia, histologia, embryologia, 31*(4), 214-223.
Van Elswijk, D., & Irth, H. (2002). Analytical tools for the detection and characterization of biologically active compounds from nature. *Phytochemistry Reviews, 1*(3), 427-439.
Van Vuuren, S. F., Kamatou, G. P., & Viljoen, A. M. (2010). Volatile composition and antimicrobial activity of twenty commercial frankincense essential oil samples. *South African Journal of Botany, 76*(4), 686-691.
Verstappen, C. C., Heimans, J. J., Hoekman, K., & Postma, T. J. (2003). Neurotoxic complications of chemotherapy in patients with cancer. *Drugs, 63*(15), 1549-1563.
Villanueva, J., Yung, Y., Walker, J. L., & Assoian, R. K. (2007). ERK activity and G1 phase progression: identifying dispensable versus essential activities and primary versus secondary targets. *Molecular biology of the cell, 18*(4), 1457-1463.
Vinogradov, S., & Wei, X. (2012). Cancer stem cells and drug resistance: the potential of nanomedicine. *Nanomedicine, 7*(4), 597-615.
Viola-Magni, M., Cataldi, S., & Marocco, D. . (2017). Bladder Cancer Markers and Recent Innovations, Bladder Cancer. In M. Hammad (Ed.), *Management of NMI and Muscle-Invasive Cancer*. Retrieved from https://www.intechopen.com/books/bladder-cancer-management-of-nmi-and-muscle-invasive-cancer/bladder-cancer-markers-and-recent-innovations
Visht, S., & Chaturvedi, S. (2012). Isolation of natural products. *Journal of Current Pharma Research, 2*(3), 584.
Voelkel-Johnson, C. (2011). TRAIL-mediated signaling in prostate, bladder and renal cancer. *Nature Reviews Urology, 8*(8), 417.
Vuddanda, P. R., Singh, S., & Velaga, S. (2016). Boswellic acid–Medicinal use of an ancient herbal remedy. *Journal of Herbal Medicine, 6*(4), 163-170.
Vyas, D., Laput, G., & Vyas, A. K. (2014). Chemotherapy-enhanced inflammation may lead to the failure of therapy and metastasis. *OncoTargets and therapy, 7*, 1015.
Wajant, H., & Siegmund, D. (2019). TNFR1 and TNFR2 in the control of the life and death balance of macrophages. *Frontiers in cell and developmental biology, 7*, 91.
Wakeel, A., Jan, S. A., Ullah, I., Shinwari, Z. K., & Xu, M. (2019). Solvent polarity mediates phytochemical yield and antioxidant capacity of Isatis tinctoria. *PeerJ, 7*, e7857.
Walker, C., Mojares, E., & del Río Hernández, A. (2018). Role of extracellular matrix in development and cancer progression. *International journal of molecular sciences, 19*(10), 3028.

Wallach, D., & Kovalenko, A. (2014). Apoptosis: Keeping inflammation at bay. *Elife, 3*, e02583.
Walsby, E. J., Coles, S. J., Knapper, S., & Burnett, A. K. (2011). The topoisomerase II inhibitor voreloxin causes cell cycle arrest and apoptosis in myeloid leukemia cells and acts in synergy with cytarabine. *Haematologica, 96*(3), 393.
Wang, Wang, H., Sun, B., Li, D., Wu, J., Li, J., . . . Liu, Y. (2020). Acetyl-11-keto-β-boswellic acid triggers premature senescence via induction of DNA damage accompanied by impairment of DNA repair genes in hepatocellular carcinoma cells in vitro and in vivo. *Fundamental & clinical pharmacology, 34*(1), 65-76.
Wang, & Weller, C. L. (2006). Recent advances in extraction of nutraceuticals from plants. *Trends in Food Science & Technology, 17*(6), 300-312.
Wang, Zhang, H., & Chen, X. (2019). Drug resistance and combating drug resistance in cancer. *Cancer Drug Resistance, 2*(2), 141-160.
Wang, Zhang, M., Sun, W., Yang, S., Su, Y., Zhang, H., . . . Kim, S. (2013). Reduction of decoy receptor 3 enhances TRAIL-mediated apoptosis in pancreatic cancer. *Plos one, 8*(10), e74272.
Wang, D., Ge, S., Bai, J., & Song, Y. (2018). Boswellic acid exerts potent anticancer effects in HCT-116 human colon cancer cells mediated via induction of apoptosis, cell cycle arrest, cell migration inhibition and inhibition of PI3K/AKT signalling pathway. *J. BUON, 23*(2), 340-345.
Wang, D., Montgomery, R. B., Schmidt, L. J., Mostaghel, E. A., Huang, H., Nelson, P. S., & Tindall, D. J. (2009). Reduced Tumor Necrosis Factor Receptor–Associated Death Domain Expression Is Associated with Prostate Cancer Progression. *Cancer research, 69*(24), 9448-9456.
Wang, M., Zhang, C., Song, Y., Wang, Z., Wang, Y., Luo, F., . . . Xu, Y. (2017). Mechanism of immune evasion in breast cancer. *OncoTargets and therapy, 10*, 1561.
Wang, X., Fu, Z., Chen, Y., & Liu, L. (2017). Fas expression is downregulated in gastric cancer. *Molecular medicine reports, 15*(2), 627-634.
Webersik, C., Hansen, S. J., & Egal, A. (2018). Somalia: A Political Economy Analysis.
Weiderpass, E. (2010). Lifestyle and cancer risk. *Journal of preventive medicine and public health, 43*(6), 459-471.
Wenzel, E. S., & Singh, A. T. K. (2018). Cell-cycle checkpoints and aneuploidy on the path to cancer. *in vivo, 32*(1), 1-5.
Wheate, N. J., Brodie, C. R., Collins, J. G., Kemp, S., & Aldrich-Wright, J. R. (2007). DNA intercalators in cancer therapy: organic and inorganic drugs and their spectroscopic tools of analysis. *Mini reviews in medicinal chemistry, 7*(6), 627-648.
White, M. C., Holman, D. M., Boehm, J. E., Peipins, L. A., Grossman, M., & Henley, S. J. (2014). Age and cancer risk: a potentially modifiable relationship. *American journal of preventive medicine, 46*(3), S7-S15.
WHO. (2021, 26.03.2021). IARC monographs on the identification of carcinogenic hazards to Humans. Retrieved from https://monographs.iarc.who.int/cards_page/publications-monographs/
Wickman, G., Julian, L., & Olson, M. F. (2012). How apoptotic cells aid in the removal of their own cold dead bodies. *Cell Death & Differentiation, 19*(5), 735-742.
Wilkens, S. (2015). Structure and mechanism of ABC transporters. *F1000prime reports, 7*.
Williams, G. H., & Stoeber, K. (2012). The cell cycle and cancer. *The Journal of pathology, 226*(2), 352-364.
Wiman, K., & Zhivotovsky, B. (2017). Understanding cell cycle and cell death regulation provides novel weapons against human diseases. *Journal of internal medicine, 281*(5), 483-495.
Winking, M., Sarikaya, S., Rahmanian, A., Jödicke, A., & Böker, D. K. (2000). Boswellic acids inhibit glioma growth: a new treatment option? *Journal of neuro-oncology, 46*(2), 97-103.
Winterstein, A., & Stein, G. (1932). Untersuchungen in der Saponinreihe. X. Mitteilung. Zur Kenntnis der Mono-oxy-triterpensäuren. *Biological chemistry, 208*(1-3), 9-25.
Wong, R. S. Y. (2011). Apoptosis in cancer: from pathogenesis to treatment. *Journal of experimental & clinical cancer research, 30*(1), 1-14.

Woolley, C. L., Suhail, M. M., Smith, B. L., Boren, K. E., Taylor, L. C., Schreuder, M. F., . . . Lin, H.-K. (2012). Chemical differentiation of Boswellia sacra and Boswellia carterii essential oils by gas chromatography and chiral gas chromatography–mass spectrometry. *Journal of Chromatography A, 1261*, 158-163.

Wroblewski, L. E., Peek, R. M., & Wilson, K. T. (2010). Helicobacter pylori and gastric cancer: factors that modulate disease risk. *Clinical microbiology reviews, 23*(4), 713-739.

WSP. (2001). *WSP Somali Program: Rebuilding Somalia: Issues and Possibilities for Puntland*. London, United Kingdom: Haan Publishing.

Wu, N., Wu, X.-W., Agama, K., Pommier, Y., Du, J., Li, D., . . . An, L.-K. (2010). A novel DNA topoisomerase I inhibitor with different mechanism from camptothecin induces G2/M phase cell cycle arrest to K562 cells. *Biochemistry, 49*(47), 10131-10136.

Xia, Chen, D., Han, R., Fang, Q., Waxman, S., & Jing, Y. (2005). Boswellic acid acetate induces apoptosis through caspase-mediated pathways in myeloid leukemia cells. *Molecular cancer therapeutics, 4*(3), 381-388.

Xia, Lou, W., Fung, K.-M., Wolley, C. L., Suhail, M. M., & Lin, H.-K. (2017). Cancer chemopreventive effects of Boswellia sacra gum resin hydrodistillates on invasive urothelial cell carcinoma: report of a case. *Integrative cancer therapies, 16*(4), 605-611.

Xing, R., Zhang, H., Yuan, J., Zhang, K., Li, L., Guo, H., . . . Gao, T. (2017). Novel 6-substituted benzoyl and non-benzoyl straight chain pyrrolo [2, 3-d] pyrimidines as potential antitumor agents with multitargeted inhibition of TS, GARFTase and AICARFTase. *European journal of medicinal chemistry, 139*, 531-541.

Yang, Jiang, G., Zhang, P., & Fan, J. (2015). Programmed cell death and its role in inflammation. *Military Medical Research, 2*(1), 1-12.

Yang, Müller, C., Huynh, V., Fung, Y. K., Yee, A. S., & Koeffler, H. P. (1999). Functions of cyclin A1 in the cell cycle and its interactions with transcription factor E2F-1 and the Rb family of proteins. *Molecular and cellular biology, 19*(3), 2400-2407.

Yang, Ren, J., & Wang, A. (2018). Isolation, characterization, and hepatoprotective activities of terpenes from the gum resin of Boswellia carterii Birdw. *Phytochemistry Letters, 23*, 73-77.

Yang, Villani, R. M., Wang, H., Simpson, M. J., Roberts, M. S., Tang, M., & Liang, X. (2018). The role of cellular reactive oxygen species in cancer chemotherapy. *Journal of experimental & clinical cancer research, 37*(1), 1-10.

Yang, Xu, Z.-P., Huang, Y., Hamrick, H. E., Duerksen-Hughes, P. J., & Yu, Y.-N. (2004). ATM and ATR: sensing DNA damage. *World Journal of Gastroenterology, 10*(2), 155.

Yang, Yin, K., Zhong, D., Liao, Q., & Li, K. (2015). Inhibition of osteosarcoma cell progression by MacroH2A via the downregulation of cyclin D and cyclindependent kinase genes. *Molecular medicine reports, 11*(3), 1905-1910.

Yardley, D. A. (2013). Drug resistance and the role of combination chemotherapy in improving patient outcomes. *International journal of breast cancer, 2013*.

Yazdanpanahi, N., Behbahani, M., & Yektaeian, A. (2014). Effect of Boswellia thurifera gum methanol extract on cytotoxicity and p53 gene expression in human breast cancer cell line. *Iranian journal of pharmaceutical research: IJPR, 13*(2), 719.

Yu, J.-Q., Geng, Y.-L., Wang, D.-J., Zhao, H.-W., Guo, L., & Wang, X. (2018). Terpenes from the gum resin of Boswellia carterii and their NO inhibitory activies. *Phytochemistry Letters, 28*, 59-63.

Yuan, & Akey, C. W. (2013). Apoptosome structure, assembly, and procaspase activation. *Structure, 21*(4), 501-515.

Yuan, Gajan, A., Chu, Q., Xiong, H., Wu, K., & Wu, G. S. (2018). Developing TRAIL/TRAIL death receptor-based cancer therapies. *Cancer and Metastasis Reviews, 37*(4), 733-748.

Yuan, Kong, F., Wang, X.-L., Young, C. Y. F., Hu, X.-Y., & Lou, H.-X. (2008). Inhibitory effect of acetyl-11-keto-β-boswellic acid on androgen receptor by interference of Sp1 binding activity in prostate cancer cells. *Biochemical pharmacology, 75*(11), 2112-2121.

Zhang, Aguilera, D., Das, C., Vasquez, H., Zage, P., Gopalakrishnan, V., & Wolff, J. (2007). Measuring cytotoxicity: a new perspective on LC50. *Anticancer research, 27*(1A), 35-38.
Zhang, Biggs, I., Sirdaarta, J., White, A., & Cock, I. E. (2016). Antibacterial and Anticancer properties of boswellia carteri birdw. And commiphora molmol engl. Oleo-resin solvent extractions. *Pharmacogn. Commn, 6*(3), 120-136.
Zhang, & Fang, B. (2005). Mechanisms of resistance to TRAIL-induced apoptosis in cancer. *Cancer gene therapy, 12*(3), 228-237.
Zhang, Lei, W. E. N., Chen, X., Wang, S., & Qian, W. (2018). Oxidative stress response induced by chemotherapy in leukemia treatment. *Molecular and clinical oncology, 8*(3), 391-399.
Zhang, Ramesh, G., Norbury, C., & Reeves, W. (2007). Cisplatin-induced nephrotoxicity is mediated by tumor necrosis factor-α produced by renal parenchymal cells. *Kidney international, 72*(1), 37-44.
Zhang, & Zhang, B. (2008). TRAIL resistance of breast cancer cells is associated with constitutive endocytosis of death receptors 4 and 5. *Molecular cancer research, 6*(12), 1861-1871.
Zhang, X., Tang, N., Hadden, T. J., & Rishi, A. K. (2011). Akt, FoxO and regulation of apoptosis. *Biochimica et Biophysica Acta (BBA)-Molecular Cell Research, 1813*(11), 1978-1986.
Zhang, Y., & Hunter, T. (2014). Roles of Chk1 in cell biology and cancer therapy. *International journal of cancer, 134*(5), 1013-1023.
Zhao, Entschladen, F., Liu, H., Niggemann, B., Fang, Q., Zaenker, K. S., & Han, R. (2003). Boswellic acid acetate induces differentiation and apoptosis in highly metastatic melanoma and fibrosarcoma cells. *Cancer Detection and prevention, 27*(1), 67-75.
Zhao, Shi, W., Deng, X.-q., Xie, G., Mao, Y.-q., Li, Z.-g., . . . Wei, Y.-q. (2008). Cell growth inhibition, G2/M cell cycle arrest, and apoptosis induced by chloroquine in human breast cancer cell line Bcap-37. *Cellular Physiology and Biochemistry, 22*(5-6), 431-440.
Zheng, H.-C. (2017). The molecular mechanisms of chemoresistance in cancers. *Oncotarget, 8*(35), 59950.
Zhou, L. L., Zhou, L. Y., Luo, K. Q., & Chang, D. C. (2005). Smac/DIABLO and cytochrome c are released from mitochondria through a similar mechanism during UV-induced apoptosis. *Apoptosis, 10*(2), 289-299.
Zhu, W., Giangrande, P. H., & Nevins, J. R. (2004). E2Fs link the control of G1/S and G2/M transcription. *The EMBO journal, 23*(23), 4615-4626.
Ziegler, U., & Groscurth, P. (2004). Morphological features of cell death. *Physiology, 19*(3), 124-128.
Zilfou, J. T., & Lowe, S. W. (2009). Tumor suppressive functions of p53. *Cold Spring Harbor perspectives in biology, 1*(5), a001883.
Zong, W.-X., & Thompson, C. B. (2006). Necrotic death as a cell fate. *Genes & development, 20*(1), 1-15.
Zu, Y., Yang, Z., Tang, S., Han, Y., & Ma, J. (2014). Effects of P-glycoprotein and its inhibitors on apoptosis in K562 cells. *Molecules (Basel, Switzerland), 19*(9), 13061-13075.